

Durham E-Theses

Mechanistic studies of copper and thiolate ion induced s-nitrosothiol decompositions

Dicks, Andrew P.

How to cite:

Dicks, Andrew P. (1997) *Mechanistic studies of copper and thiolate ion induced s-nitrosothiol decompositions*, Durham theses, Durham University. Available at Durham E-Theses Online: <http://etheses.dur.ac.uk/4703/>

Use policy

The full-text may be used and/or reproduced, and given to third parties in any format or medium, without prior permission or charge, for personal research or study, educational, or not-for-profit purposes provided that:

- a full bibliographic reference is made to the original source
- a [link](#) is made to the metadata record in Durham E-Theses
- the full-text is not changed in any way

The full-text must not be sold in any format or medium without the formal permission of the copyright holders.

Please consult the [full Durham E-Theses policy](#) for further details.

**MECHANISTIC STUDIES OF COPPER AND THIOLATE ION INDUCED
S-NITROSTHIOL DECOMPOSITIONS**

by

Andrew P. Dicks, B.Sc. (Hons.)

(Graduate Society)

A thesis submitted for the degree of Doctor of Philosophy in the
Department of Chemistry, University of Durham

September 1997

The copyright of this thesis rests
with the author. No quotation
from it should be published
without the written consent of the
author and information derived
from it should be acknowledged.



20 NOV 1997

MECHANISTIC STUDIES OF COPPER AND THIOLATE ION INDUCED S-NITROSTHIOL DECOMPOSITIONS

by Andrew P. Dicks

A thesis submitted for the degree of Doctor of Philosophy in the Department of Chemistry, University of Durham, September 1997.

ABSTRACT

A detailed study concerning the aqueous decomposition characteristics of S-nitrosothiols in both the presence and absence of cupric ions was undertaken. Spectrophotometric measurements established that the true catalytic species generating nitric oxide from S-nitrosothiols is Cu^+ , formed by the reduction of copper(II) ions by thiolate, which is present as an impurity in solution. Introduction of the specific cuprous ion chelator neocuproine inhibited reaction, with the concentration of thiol *in situ* having a significant influence on the absorbance/time traces obtained. Under certain conditions thiolate ions clearly promoted S-nitrosothiol decomposition, whereas at times an opposite effect was noted. These results have been correlated with the reductive ability and chelation properties towards Cu^{2+} of each thiol in question. Structure/reactivity studies were extended further to include a range of S-nitrosated aromatic and heterocyclic thiols which generated the corresponding disulfides in distilled water yet reformed the appropriate thione at pH 7.4, along with nitric oxide in both media. A mechanism has been proposed which accounts for these observations.

The reaction of S-nitrosothiols with cupric ions bound to biologically significant molecules such as amino acids, peptides and proteins was followed. Despite Cu^{2+} being chelated in this manner, S-nitrosothiol decomposition was apparent, albeit at a slower rate than that seen when copper(II) sulfate pentahydrate was utilised. Thiolate ions were capable of reducing $\text{Cu}^{2+} \rightarrow \text{Cu}^+$ which was bound to such molecules suggesting a possible mechanism for nitric oxide formation from S-nitrosothiols *in vivo*. The blue copper protein ceruloplasmin also promoted NO generation under physiological conditions. A brief investigation into the direct reaction of thiolate ion with its corresponding S-nitrosothiol was also carried out. It was discovered that the major reaction product in this instance is ammonia and not nitric oxide, suggesting that a different copper-ion independent process is occurring involving direct interaction between the two species.

ACKNOWLEDGEMENTS

I would like to express my thanks to my supervisor, Professor D. Lyn H. Williams for his time, friendship and advice throughout the course of this research. I am also indebted to my fellow associates Alex, Helen, Simon, Gaynor, Yurii, Pablo, Ian, Andy, Kathryn and E for all their encouragement and support. Special thanks are due to Mr. Colin Greenhalgh for his patient help with the computer software and upkeep of machines.

I would also like to take this opportunity to thank Dr. Richard Knowles, for his advice on biological matters and Rick, Tony, Caroline, Neil, Jo, Fiona and everyone else at the Department of Enzyme Pharmacology, Glaxo-Wellcome Research Laboratories, Stevenage for making my three month period there both enjoyable and fruitful.

My thanks also go to the Graduate Society Football Club and all its members for some great times and to InterChem for two fantastic campaigns.

Finally, I would like to indicate my gratitude towards all of my family and to Gill, who have always been there for me.

I acknowledge the financial support provided by EPSRC and Glaxo-Wellcome.

DECLARATION

The material in this thesis is the result of research carried out in the Department of Chemistry, University of Durham, between October 1994 and September 1997. It has not been submitted for any other degree and is the authors own work, except where acknowledged by reference.

STATEMENT OF COPYRIGHT

The copyright of this thesis lies with the author. No quotation from it should be published without his prior written consent and information derived from it should be acknowledged.

In memory of my father, John

CONTENTS

Chapter 1: Introduction	1
1.1 Chemistry of Nitric Oxide	2
1.1.1 Introduction	2
1.1.2 Preparation	2
1.1.3 Physical Properties	3
1.1.4 Selected Chemical Properties	4
1.2 Physiological Roles of Nitric Oxide	8
1.2.1 Vasodilation	8
1.2.2 Biosynthesis of NO	11
1.2.3 Neurotransmission	12
1.2.4 Inhibition of Platelet Aggregation	13
1.2.5 Macrophage Cytotoxicity	14
1.2.6 Further New Roles of Nitric Oxide	15
1.3 S-Nitrosation	16
1.3.1 Introduction	16
1.3.2 Nitrous Acid HNO ₂	16
1.3.3 Other Nitrosating Agents	17
1.3.4 Kinetics of Nitrosation	22
1.3.5 Nitrosation of Thiocarbonyl Compounds	27
1.4 Properties and Reactions of S-Nitrosothiols	29
1.4.1 Physical Properties	29
1.4.2 Thermal and Photochemical Decomposition	30
1.4.3 Metal Ion Induced Decomposition	30

1.4.3.1 Copper Ion Catalysis	30
1.4.3.2 Silver and Mercury Ion Induced Reaction	34
1.4.3.3 Ferrous Ion Catalysis	35
1.4.4 Acid Catalysed Decomposition	35
1.4.5 Transnitrosation	37
1.5 Nitric Oxide Donor and Acceptor Compounds	40
1.5.1 Introduction	40
1.5.2 Nitrovasodilators	40
1.5.2.1 S-Nitrosothiols	40
1.5.2.2 Organic Nitrates and Nitrites	41
1.5.2.3 Heterocyclic Nitric Oxide Donors	43
1.5.2.4 Metal Nitrosyls	46
1.5.3 Nitric Oxide Acceptor Compounds	47
References	49
Chapter 2: Mechanistic Studies of Copper Catalysed Nitric Oxide Formation from S-Nitrosothiols	55
2.1 Introduction	56
2.2 Synthesis of a Stable S-Nitrosothiol	56
2.3 Metal Ion Chelation Studies	57
2.3.1 Neocuproine Chelation	57
2.3.2 Cuprizone Chelation	62
2.4 Detection of Thiolate in S-Nitrosothiol Solutions	64
2.5 Addition of Reducing Agents to S-Nitrosothiols in the Presence of Cu ²⁺	67

2.5.1 Effect of Adding N-Acetylpenicillamine to SNAP	67
2.5.2 Effect of Adding Penicillamine to S-Nitrosopenicillamine	71
2.5.3 Further Examples	78
2.6 Time Dependent Reactions	82
2.7 Proposed Mechanism of S-Nitrosothiol Decomposition	84
2.8 Conclusion	86
References	88
Chapter 3: Nitric Oxide Generation from S-Nitrosothiols using Amino Acid, Peptide and Protein Bound Forms of Cu²⁺	91
3.1 Introduction	92
3.2 GlycylGlycylHistidine (GGH)	93
3.2.1 GGH as a Cu ²⁺ Binding Model	93
3.2.2 Reaction of GGH:Cu ²⁺ with NAP	94
3.2.3 Decomposition of SNAP in the Presence of GGH:Cu ²⁺	98
3.2.4 Detection of Reaction Products	105
3.3 Human Serum Albumin (HSA)	108
3.3.1 HSA as a Transport Molecule for Cu ²⁺	108
3.3.2 Reaction of HSA:Cu ²⁺ with NAP	109
3.3.3 S-Nitrosothiol Decomposition in the Presence of HSA:Cu ²⁺	112
3.4 Histidine (HIS)	115
3.4.1 Importance of Amino Acids as Binding Agents	115
3.4.2 Reaction of 2HIS:Cu ²⁺ with NAP	117
3.4.3 S-Nitrosothiol Decomposition in the Presence of 2HIS:Cu ²⁺	118

3.5 Summary of "Transport Cu ²⁺ " Results	122
3.6 Ceruloplasmin	123
3.6.1 Properties and Physiological Roles of Ceruloplasmin	123
3.6.2 Reaction of S-Nitrosocysteine with Ceruloplasmin	125
3.6.3 Addition of L-Cysteine to Ceruloplasmin	130
3.6.4 Effect of Peroxynitrite	132
3.7 Superoxide Dismutase (SOD) and Metallothionein	133
3.7.1 Biological Relevance	133
3.7.2 Effect of SOD on the Stability of S-Nitrosothiols	135
3.7.3 Influence of Metallothionein	137
3.8 Conclusion	137
References	138
Chapter 4: Stability of Novel Aliphatic, Heterocyclic and Aromatic S-Nitrosated Thiols	141
4.1 Introduction	142
4.2 Generation and Reactivity of New Aliphatic S-Nitrosothiols	143
4.3 Heterocyclic and Aromatic S-Nitrosated Thiols	151
4.3.1 Spectral Characteristics	151
4.3.2 S-Nitrosated 2-aminothiophenol	152
4.3.3 S-Nitrosated 2-mercaptopyridine and S-Nitrosated 2-mercaptopyrimidine	153
4.3.3.1 Nitrosation of 2-mercaptopyridine	153

4.3.3.2 Reaction in pH 7.4 Buffer	159
4.3.3.3 Use of a Nitric Oxide Electrode to Detect Reaction Products	164
4.3.3.4 Reaction in Distilled Water	165
4.3.4 S-Nitrosated 2-mercaptoimidazole and Related Derivatives	168
4.3.4.1 Reaction in pH 7.4 Buffer	168
4.3.4.2 Reaction in Distilled Water	171
4.4 Mechanism of Heterocyclic and Aromatic S-Nitrosated Decompositions	175
4.5 Conclusion	176
References	177
Chapter 5: Thiolate Ion Induced S-Nitrosothiol Decompositions	179
5.1 Introduction	180
5.2 Structure/Reactivity Studies	181
5.3 Product Detection	188
5.3.1 Detection of Nitrite	188
5.3.2 Detection of Ammonia	189
5.3.3 Detection of Nitrous Oxide and Disulfide	193
5.4 Reaction under Anaerobic Conditions	193
5.5 Possible Reaction Mechanism	194
5.6 Conclusion	197
References	198

Chapter 6: Experimental Details	199
6.1 Experimental Techniques	200
6.1.1 Ultraviolet/Visible Spectrophotometry	200
6.1.2 Stopped-Flow Spectrophotometry	202
6.2 pH Measurements	204
6.3 Nitric Oxide Electrode Calibration	204
6.4 Reagents	204
6.5 Analysis	205
APPENDIX	206

Chapter 1

Introduction

Chapter 1: Introduction

1.1 Chemistry of Nitric Oxide

1.1.1 Introduction

In the 1960's it was claimed by Vasu¹ that "from an industrial point of view, nitric oxide is probably the most important oxide of nitrogen". Until the beginning of the last decade, nitric oxide was merely considered to be a toxic molecule and a contributor to atmospheric pollution.

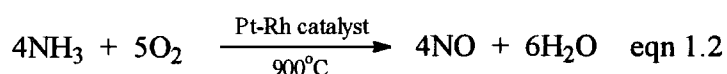
However, more recently it has been shown that NO is involved in many fundamental biochemical processes, indeed in 1992 it achieved status as "Molecule of the Year" in the journal *Science*². Its many essential biological roles include smooth muscle vasodilation, neurotransmission, immune regulation and inhibition of platelet aggregation. The last decade has seen over fifteen thousand journal articles published on some aspect of the physiology or biochemistry of nitric oxide. Many reviews have been written and recent papers by Fontecave and Pierre³ and Ainscough and Brodie⁴ discuss the chemical and biological properties of NO respectively in great detail.

1.1.2 Preparation

Nitric oxide can be prepared in the laboratory via the reduction of nitric acid using copper metal as an electron donor (equation 1.1).



The extremely efficient commercial route to NO is by means of the catalytic oxidation of ammonia (equation 1.2).

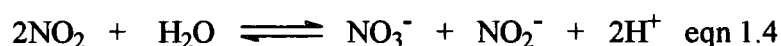


Aerial oxidation of the product gases leads to brown NO₂ being formed (equation 1.3).



This reaction leads to air pollution and the build up of photochemical smogs in cities such as Tokyo and Los Angeles.

Aqueous dissolution of nitrogen dioxide produces nitrite and nitrate ion in a disproportionation reaction, as shown by equation 1.4.

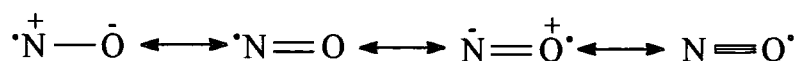


Ostwald was awarded the Nobel Prize in 1909 for his work in this area. Large scale productions of fertilisers and explosives (NH_4NO_3) were developed as a consequence.

1.1.3 Physical Properties

Nitric oxide is a colourless gas at room temperature, with a boiling point of -151°C and a melting point of -163°C ⁵. Both the liquid and the solid are also colourless. Its aqueous solubility is quite low ($1.8 \times 10^{-3} \text{ mol dm}^{-3}$ at standard temperature and pressure) which is similar to that of both dioxygen and carbon monoxide. Thus, it cannot be generated in high concentrations in water.

Nitric oxide is a neutral molecule with an unpaired π^* electron, rendering it paramagnetic. It has a low tendency to dimerise in solution, a feature that can partly be explained by the delocalisation of the lone electron. About 60% of the spin density is located on the nitrogen atom⁶, with various canonical forms representing its structure.



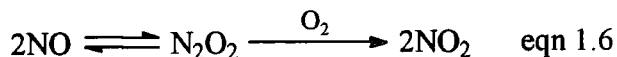
The unpaired electron reduces the bond order to ~ 2.5 . Removal of this electron forms the nitrosonium ion, NO^+ , with the N-O bond order now three (isoelectronic with nitrogen). Another explanation as to the reluctance of dimerisation is that the bond order would be virtually unchanged in the dimer.

1.1.4 Selected Chemical Properties

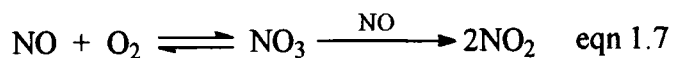
The oxidation of nitric oxide to nitrogen dioxide (section 1.1.2) was first studied kinetically by Bodenstein⁷. It has become established as a classical termolecular gas phase reaction over a wide range of experimental conditions.

$$\frac{-d[\text{NO}]}{dt} = k[\text{NO}]^2[\text{O}_2] \quad \text{eqn 1.5}$$

Equation 1.5 indicates that the reaction is first order in oxygen and second order in nitric oxide. An unusual feature of this reaction is the observed *decrease* in rate constant with increasing temperature. One possible mechanism is detailed in equation 1.6.



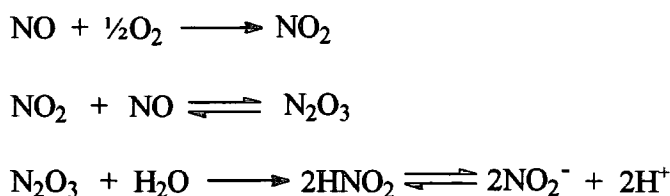
The initial dimerisation of NO to N₂O₂ has a negative ΔH° value and thus increasing the temperature should decrease the equilibrium constant for the first step. However, another equilibrium between O₂ and NO could exist, forming the peroxy nitrite radical (equation 1.7) which then reacts further with another NO molecule to give the product.



The third order nature of the reaction means that the rate of NO₂ formation is only fast at high concentrations, and that NO exists in the gas phase in the air at 10⁻⁶ mol dm⁻³ for around a minute.

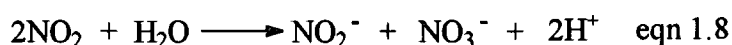
The oxidation of NO has also been studied kinetically in aqueous solution. In contrast to the gaseous reaction the observed product is solely nitrite ion or nitrous acid, depending on the pH. Somewhat surprisingly, no NO₃⁻ can be detected⁸. The proposed mechanism (scheme 1.1) postulates the initial rate limiting oxidation of nitric oxide to NO₂. This reacts with further NO to form the anhydride of nitrous

acid, N_2O_3 . Hydrolysis of this species gives nitrous acid itself which will dissociate to form nitrite ion at $pH > 4$.



Scheme 1.1

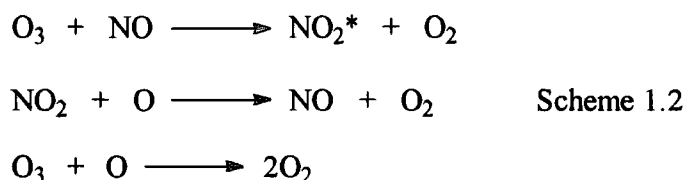
Under these conditions the usual hydrolysis product of NO_2 is an equimolar mixture of nitrate and nitrite (equation 1.8), as described in section 1.1.2.



Thus, the reaction of nitric oxide with NO_2 must be much faster than the hydrolysis of nitrogen dioxide. However, recent work by Akiyama *et al*⁹ has demonstrated the oxidative products of NO to be NO_2^- and NO_3^- in the plasma of dead rabbits. The rate law for reaction of NO in water is found to be the same as that for gaseous reaction.

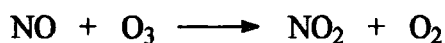
Dinitrogen trioxide, formed by the union of NO and NO_2 (scheme 1.1), exists as an unstable blue liquid at $-20^\circ C$. It can act as an effective nitrosating agent (section 1.3.3) and is responsible for some literature reports ascribing a blue colour to samples of nitric oxide.

Nitric oxide is present in the stratosphere (between 10 and 50 km from the Earth's surface). Problems may occur when ozone reacts with NO forming NO_2 which may combine with atomic oxygen to regenerate NO and oxygen (scheme 1.2).



Nitric oxide is therefore acting as a catalyst increasing the rate of ozone decomposition in the atmosphere. O_3 protects Earth from incoming solar radiation with wavelength less than 300nm. There is increasing concern about NO emission levels from supersonic aircraft which could reduce the stratospheric ozone concentration.

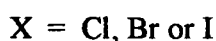
The initial reaction of ozone with NO can be used as an extremely sensitive assay for nitric oxide (detection limit $\geq 10^{-9}$ mol dm^{-3})¹⁰. The basis for detection is chemiluminescence, as some NO_2 molecules are produced in an excited state (scheme 1.3). When these decay to a ground state the luminescence produced is proportional to the concentration of NO_2 in the excited state (and hence the concentration of nitric oxide).



Scheme 1.3

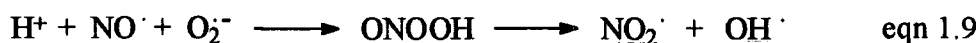


A similar reaction has been noted with halogen atoms (scheme 1.4).



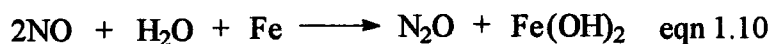
The nitrosyl halides¹¹ formed are gaseous and are widely used as nitrosating agents in organic solvents (section 1.3.3).

NO combines with superoxide anion to give peroxyxynitrite which is an important reaction in biological systems¹² (equation 1.9).



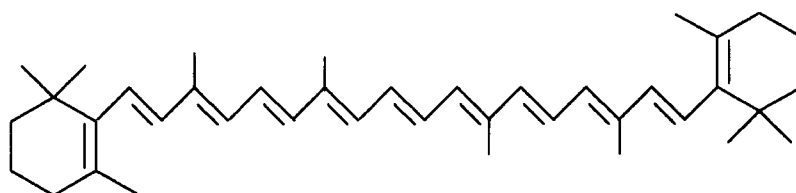
Hydroxyl radicals (OH^\bullet) are known to be extremely destructive towards lipid membranes and DNA, and may act as a reagent in cellular defence mechanisms (section 1.2.5).

A typical example of nitrogen becoming reduced in NO is given by the reaction of nitric oxide with moist iron filings (equation 1.10).



The product nitrous oxide is relatively unreactive and was initially used by Davey as the first anaesthetic. It is currently more widely utilised as an aerosol propellant due to its good lipid solubility, which is similar to that of NO.

Recently, a novel reaction between nitric oxide and a conjugated diene has been reported, which may have important physiological relevance^{13,14}. Polyunsaturated molecules such as β -carotene (1.1) can react with a number of NO molecules to form a lesser conjugated system.



1.1

Precise structures of the derivatives formed have not been established, but it is thought that stable nitroxyl radicals ($\text{R}_2\text{NO}^\bullet$) may be produced. Such conjugated dienes are widespread *in vivo*, especially in fatty acyl chains, where reactions with NO would be favoured due to its high lipid solubility.

Nitric oxide is an extremely powerful ligand and can coordinate to many metal centres both free and in complex form. It may act as a one or three electron donor (utilising the lone pair of electrons on nitrogen) and will give a bent or linear structure respectively (figure 1.1).

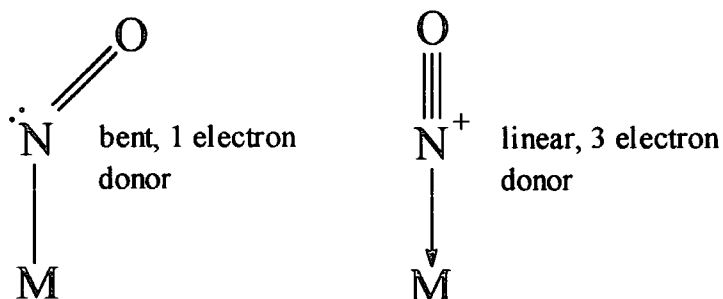


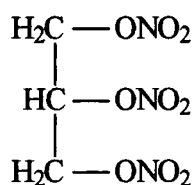
Figure 1.1

A synergistic mechanism allows electron density from the nitric oxide molecule to be donated (forming a σ bond to the metal) in addition to back donation of electron density from metal d-orbitals to the empty π^* antibonding orbital on NO^{15} . Biologically relevant metal nitrosyls will be discussed later (section 1.5).

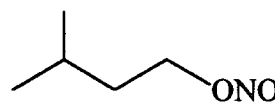
1.2 Physiological Roles of Nitric Oxide

1.2.1 Vasodilation

Glyceryl trinitrate (GTN) (1.2) and other organic nitrates and nitrites such as amyl nitrite (1.3) have been used in medical treatments for over a century.



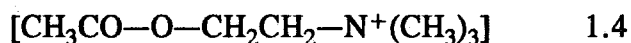
1.2



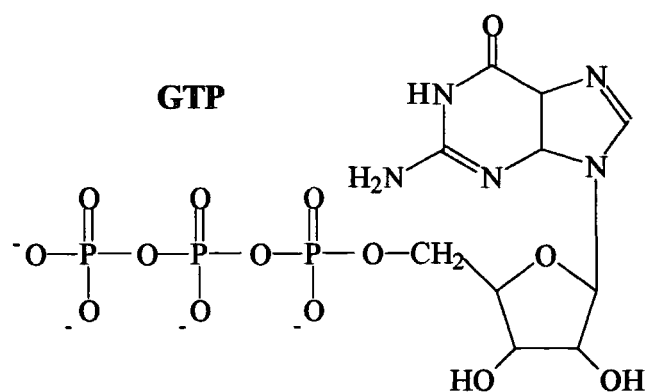
1.3

The use of amyl nitrite was discovered in 1867¹⁶ while the benefits of GTN were noted after girls who worked packing explosives during World War I had abnormally low blood pressure¹⁷. Such compounds relieve the symptoms of angina pectoris (narrowing of the arteries of the heart). However, their mode of action has not been clearly understood until recently, when results were published independently by Palmer *et al*¹⁸ and Ignarro *et al*¹⁹. Until twenty years ago it was believed that the vasodilatory properties of GTN were due to its conversion to nitrite, which is known to act as a vasodilator, albeit slowly²⁰. In 1977, Katsuki *et al*²¹ noted that blood

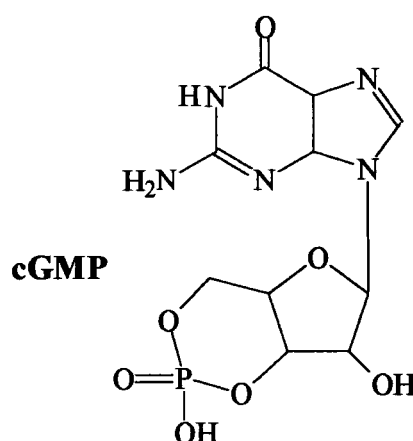
vessel enlargement occurred after metabolism to NO, and not NO₂⁻. It took much painstaking work by Furchgott and Zawadzki²² relating to muscle relaxation to make sense of many experimental observations. They examined the effect of acetylcholine (1.4) on pre-contracted rings of rabbit aorta.



Unusually, the vasodilatory action of this material was not apparent during every set of tests. It became clear that acetylcholine was not effective if the endothelial cells (lining the inside of the aorta) had been removed or accidentally damaged in some way. The conclusion drawn was that acetylcholine was in fact not acting directly upon the muscle cells but instead upon the endothelium which, in turn, produces a "messenger" molecule. This species then diffuses into the muscle cells, activating the enzyme guanylate cyclase (GC). Intracellular levels of cyclic guanosine monophosphate (cGMP) are subsequently increased by the transformation of guanosine triphosphate (GTP), inducing muscular relaxation²³ (scheme 1.5).



Scheme 1.5

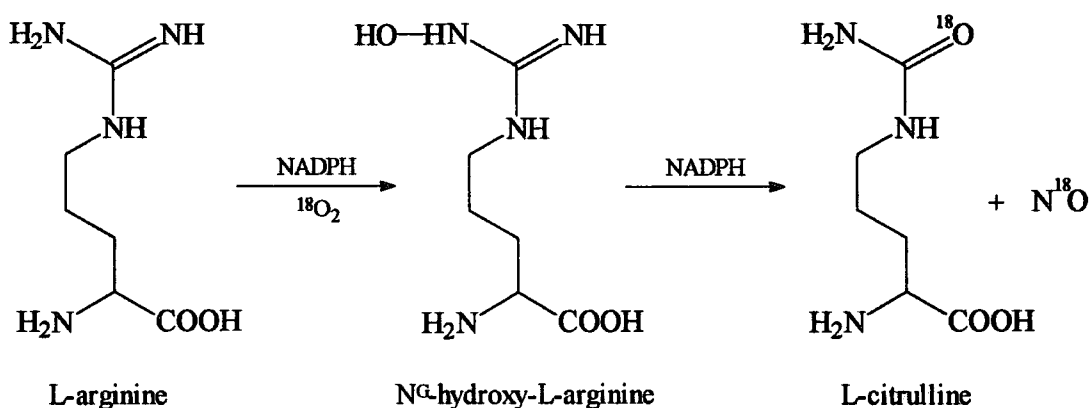


The messenger molecule produced by the endothelium became known as the EDRF, or "endothelium-derived relaxing factor". The chemical identity of the EDRF quickly became a matter of intense speculation. It was clear that the EDRF had a half life of only a few seconds²³ under physiological conditions. In addition, its activity was inhibited by haemoglobin, yet prolonged by the enzyme superoxide dismutase (SOD). Results previously mentioned^{18,19} suggested that nitric oxide was the EDRF as they behaved identically in terms of vascular relaxation. Haemoglobin binds NO very strongly and hence destroys the action of the EDRF, but SOD promotes catalytic O_2^- destruction thus eliminating the reaction of nitric oxide with superoxide (equation 1.9). Guanylate cyclase is thought to be activated by NO binding to the iron of the enzymic haem component²⁴, moving it out of the plane of the porphyrin ring. This leads to an accumulation of cGMP and eventual muscle relaxation.

Although there is overwhelming evidence that the EDRF is nitric oxide, the actual identity is as yet unknown. Even though it appears to be an unstable radical, NO is sufficiently stable to act as a messenger molecule. It has been proposed that the EDRF could be a dinitrosyl iron complex, hydroxylamine, nitroxyl radical or an S-nitrosothiol such as S-nitrosocysteine. Feelisch *et al*²⁵ have recently demonstrated that NO is still the most likely candidate, with the possibility existing that it is formed from a precursor compound before mediating its effects.

1.2.2 Biosynthesis of NO

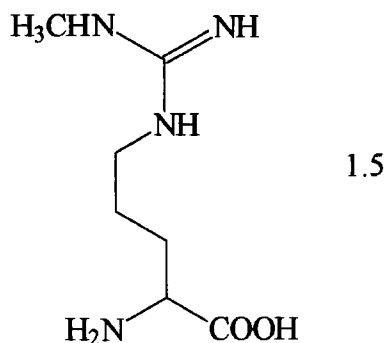
Mammals are known to generate nitric oxide *in vivo* by utilising an enzyme known as nitric oxide synthase (NOS). It has been shown that the essential amino acid L-arginine and dioxygen are the reactive substrates²⁶. NOS cleaves nitric oxide from one of the terminal guanidino groups of L-arginine, forming L-citrulline as a by-product. Isotopic labelling experiments²⁷ with ¹⁸O₂ have indicated that the enzyme incorporates molecular oxygen into both NO and L-citrulline (scheme 1.6).



Scheme 1.6

This discovery eliminated a number of previously proposed pathways. The intermediate NG-hydroxy-L-arginine is a known vasodilator. The production of NO in this manner is very substrate specific, indeed both D-arginine and L-homoarginine will not effect NO formation. Compounds having a similar chemical structure to

arginine (for example, N-monomethyl-L-arginine) (1.5) are powerful inhibitors of NO-synthase and their usage has proved very significant as a diagnostic tool in investigating the biochemistry of NO.



There are two, or possibly three, distinct NOS enzymes which can effect nitric oxide formation. NO-synthase found in endothelial cells is known as a constitutive enzyme, meaning it is consistently present and will respond rapidly to activation if vasodilation is required. This type of NOS will only release picomoles of NO²⁸ and thus no cytotoxic effects are observed when guanylate cyclase is activated in muscle cells. The enzyme is dependent on NADPH, tetrahydrobiopterin (BH₄), Ca²⁺ and calmodulin (a calcium binding protein). Komori *et al*²⁹ have recently undertaken work on the role of thiols in the activation of NOS. It has been found that thiols are required during enzymic turnover for maximum activity. They may serve as reducing agents for the regeneration of BH₄ from dihydrobiopterins (BH₂). Another NO-synthase is expressed by macrophages, and will be discussed in section 1.2.5.

1.2.3 Neurotransmission

There is very good evidence that NO can function as a neurotransmitter in both the peripheral and the central nervous system. Signals are sent along nerve cells as electrical impulses until they reach the gaps between cells (synapses) whereupon a chemical messenger is released (known as a neurotransmitter). Within the central nervous system enhanced levels of cGMP have been noted, analogous to the

possible "overclotting" of platelets which if occurred in a coronary vessel could lead to a heart attack. Gordge *et al*³⁴ has demonstrated the ability of S-nitrosothiols to act as aggregation inhibitors, presumably following the release of nitric oxide. There is an enzyme mechanism within the platelets themselves which acts on L-arginine to produce the required release of NO, which is also made available from nearby endothelial cells.

1.2.5 Macrophage Cytotoxicity

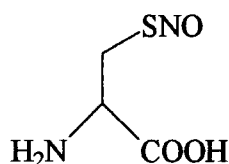
It has been shown that nitric oxide is involved in the immune response, particularly with respect to "non-specific" host defence, linked to macrophage activation. Macrophages are cells found in all tissues and, on encountering an alien microbe, are stimulated to engulf it and kill it (phagocytosis). Such invaders can also be destroyed without coming into contact with the macrophages. It is in the latter sense that NO can act as a cytotoxic agent. Marletta *et al*³⁵ noticed that activated macrophages in cultures produced nitrite and nitrate in the supernatant fluid. In addition, it was discovered that L-arginine was required for the killing action of the macrophages. These results suggest a process occurring which parallels that taking place in endothelial cells.

As previously mentioned (section 1.2.2), macrophages contain NOS which is dissimilar to the enzyme found in the vasculature. The macrophage NOS is inducible (it is not always present), it has longer lasting release of NO in higher quantities (nanomoles) and it is Ca²⁺ and calmodulin independent. There is much doubt as to whether nitric oxide is sufficiently cytotoxic itself to be responsible for killing foreign cells, even though as a free radical it may be capable of destroying the cell membrane. NO can combine with iron containing moieties in key enzymes of the respiratory cycle³⁶, or alternatively react with superoxide to produce highly toxic hydroxyl radicals (section 1.1.4). The onset of infection will lead to much macrophage activity with the consequence that over-production of NO may occur and septic shock could take place, which is often fatal due to a huge fall in blood pressure.

Selective inducible NOS inhibitors could be used to counter this condition. It is clear that nitric oxide is involved in specific immunity, however its precise role has not yet been defined.

1.2.6 Further New Roles of Nitric Oxide

Recently, nitric oxide has been implicated in physiological processes where it forms S-nitrosothiol compounds. Firstly, the formation of S-nitrosohaemoglobin (Hb-SNO) has been detected³⁷ in the human lung. Haemoglobin is composed of two α and two β subunits, with the latter having highly reactive -SH groups present (Cys β 93). Transnitrosation³⁸ was noted from S-nitrosocysteine (1.8) to haemoglobin with the consequence that arterial blood contained significant quantities of Hb-SNO (~300nM) whereas venous levels were virtually undetectable.



1.8

Haemoglobin bound to NO appears to act as a nitric oxide donor in the circulatory system but the question arises as to how Hb-SNO can relax blood vessels when any free NO released would be scavenged instantaneously by Hb itself³⁹. These studies certainly suggest new sensory and regulatory roles for haemoglobin and may have therapeutic value.

Secondly, it has been reported⁴⁰ that nitric oxide can bind to transcription factor proteins that turn genes on or off. During macrophage induced bacterial destruction, NO binds to thiol groups within the bacterium forming S-nitrosothiols which can change the function of the proteins that carry them. Whilst a bacterium tries to repair its altered proteins, the immune system can destroy it. However, bacteria have developed transcription factors which, when NO binds to them, switch on a large number of genes that make defence proteins. It is thought that the same

situation may exist for humans, and if so the door may be opened to new medical treatments for diseases linked to abnormalities in the function of nitric oxide.

1.3 S-Nitrosation

1.3.1 Introduction

S-nitrosation describes the electrophilic addition of "NO⁺" to a sulfur atom. It is a reaction that has been much less studied than the analogous O-nitrosation which consequently has led to a smaller literature referring to S-nitroso compounds. This is also partially due to the greater susceptibility of the S-N bond to homolytic fission, making such compounds unstable. The increase in nucleophilicity encountered when moving from oxygen to an equivalent sulfur atom leads to a greater reactivity of sulfur compounds with respect to nitrosation. The current interest in nitric oxide donor drugs has promoted much research activity related to the mechanism of S-nitrosation *in vivo* and subsequent decomposition of the relevant species formed.

1.3.2 Nitrous Acid HNO₂

It is possible to add NO⁺ to a sulfur-containing substrate in many ways, the most popular reagent utilised being that derived from nitrous acid. HNO₂ will be formed on the acidification of sodium nitrite, with solutions being used immediately due to the decomposition reaction (equation 1.11) occurring.



Nitrous acid is a weak acid (pK_A value of 3.1)⁴¹. Its structure has been determined by infrared studies⁴² and is known to exist in both *cis* and *trans* forms, with the *trans* form prevalent in solution (figure 1.2).

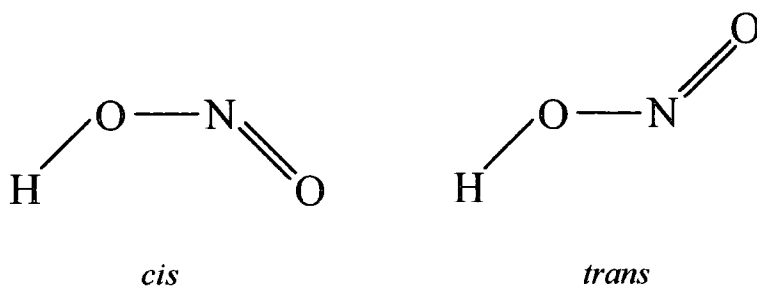
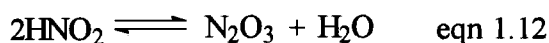


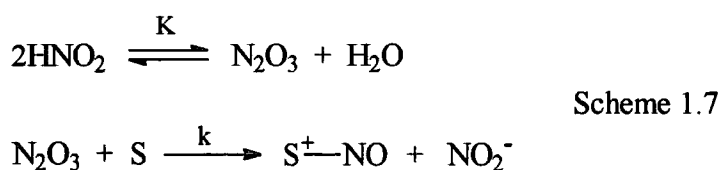
Figure 1.2

1.3.3 Other Nitrosating Agents

Another common reagent used to effect nitrosation is dinitrogen trioxide, N_2O_3 . It is formed from high concentrations of nitrous acid due to the existence of an equilibrium (equation 1.12).

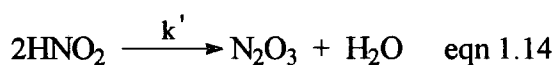


At $[\text{HNO}_2] = 0.1 \text{ mol dm}^{-3}$ the blue colour of dinitrogen trioxide is detectable visually (section 1.1.4). Reaction of N_2O_3 with substrates has been observed generally to involve rate-limiting attack of the substrate (S) by dinitrogen trioxide⁴³ (scheme 1.7).



$$\text{Rate} = k[\text{N}_2\text{O}_3][\text{S}] = kK[\text{HNO}_2]^2[\text{S}] \quad \text{eqn 1.13}$$

The expected rate equation thus predicts a second order dependence upon the nitrous acid concentration and a first order dependence upon the substrate concentration (equation 1.13). However, for extremely reactive substrates, or for substrates at high concentration, reaction of S with N_2O_3 may become faster than the hydrolysis of N_2O_3 to nitrous acid. In this instance, the rate determining step is now the formation of dinitrogen trioxide (equation 1.14).



The rate equation now becomes zero order in substrate yet remains second order in nitrous acid (equation 1.15).

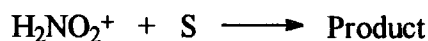
$$\text{Rate} = k'[\text{HNO}_2]^2 \quad \text{eqn 1.15}$$

N_2O_3 readily dissolves in a large number of organic solvents and these solutions can be used to nitrosate a range of nucleophilic centres.

At higher acidities and lower nitrous acid concentration than is normally used for dinitrogen trioxide, other mechanisms become significant. The effective nitrosating agent is not now N_2O_3 as the rate equation (1.16) indicates. The reaction is now first order in free hydrogen ion concentration and first order in both nitrous acid and substrate.

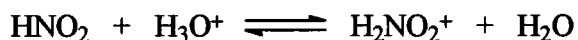
$$\text{Rate} = k[\text{HNO}_2][\text{H}_3\text{O}^+][\text{S}] \quad \text{eqn 1.16}$$

There has been some speculation as to the mechanistic interpretation of this rate equation. Two possible situations could exist which are consistent with the observed experimental data. Hughes *et al*⁴⁴ initially proposed rate limiting attack on the substrate by the nitrous acidium ion (H_2NO_2^+) (scheme 1.8).



Scheme 1.8

It is possible that the nitrosonium ion (NO^+) may act as the reactive species (scheme 1.9).



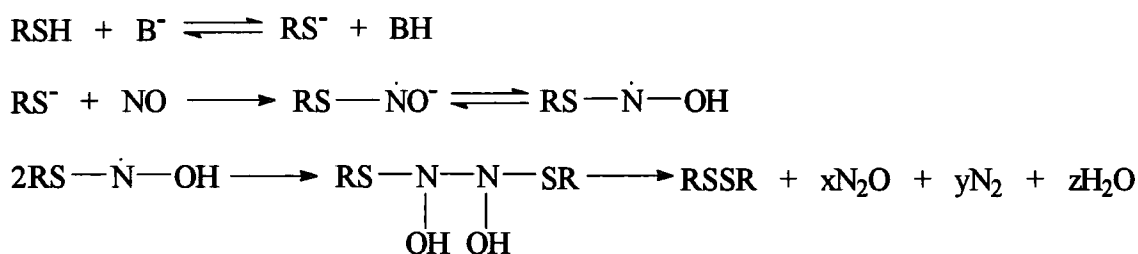
Scheme 1.9

^{18}O exchange experiments⁴⁵ between nitrous acid and water have shown that rate equation 1.17 holds, with a value for k of $230 \text{ mol}^{-1} \text{ dm}^3 \text{ s}^{-1}$ at 0°C .

$$\text{Rate} = k[\text{HNO}_2][\text{H}^+] \quad \text{eqn 1.17}$$

If NO^+ is involved (scheme 1.9) then the exchange of one O atom in nitrous acid occurs for each nitrosonium ion formed which is rehydrated to form H_2NO_2^+ . This process must be faster than the reaction between the substrate and nitrosating species to be in accordance with equation 1.16. However, for reaction of azide ion (and other anions) there is a limiting third order rate constant value of $\sim 2500 \text{ mol}^{-2} \text{ dm}^6 \text{ s}^{-1}$ at 0°C . Under certain experimental conditions the reaction of anion + $\text{NO}^+ \rightarrow$ products is faster than the formation of the nitrosonium ion, suggesting a zero order dependence on the anion concentration. This is at variance with equation 1.16. The nitrous acidium ion has never been detected spectrophotometrically but it is likely that it is the effective nitrosating agent in dilute aqueous acid solution. NO^+ has an extremely short lifetime ($t_{1/2} \sim 3 \times 10^{-10} \text{ s}$) so rehydration will probably be very rapid, possibly taking place with the same water molecule that it was previously bound to, thus not allowing ^{18}O exchange.

Other oxides of nitrogen which can be employed in the formation of S-nitroso compounds are dinitrogen tetroxide and nitric oxide. Many of the reactions of N_2O_4 are best interpreted in terms of an ionic structure NO^+NO_3^- which is thought to exist in sulfuric and perchloric acids. It is an effective nitrosating agent at many nucleophilic sites. It is likely that N_2O_4 (or dinitrogen trioxide) is the nitrosating species present formed by the aerial oxidation of nitric oxide, casting doubt over the effectiveness of NO as a nitrosation agent in its own right. However, when oxygen is excluded, nitric oxide can react with thiols in basic media⁴⁶. The reaction is dissimilar to conventional electrophilic nitrosation and is outlined in scheme 1.10.



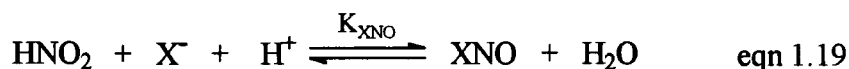
Scheme 1.10

Reaction proceeds via the thiolate ion attacking NO, followed by protonation and radical coupling. The dihydroxyhydrazine product is unstable and will eliminate hyponitrous acid (HON=NOH) to form the corresponding disulfide. Subsequent decomposition of $\text{H}_2\text{N}_2\text{O}_2$ will create nitrogen and nitrous oxide as by-products. Further mechanistic details behind the nitrosation of thiols by nitric oxide *in vitro* and *in vivo* are discussed in section 1.3.4.

Nitrosyl halides¹¹ (scheme 1.4) can be conveniently dissolved in many organic solvents (for example, toluene, ether or chloroform) and used as effective nitrosating agents. This is advantageous for substrates which have a low water solubility, rendering the nitrous acid method unproductive. Such compounds are generally prepared by reaction of nitric oxide with the appropriate halogen (equation 1.18).

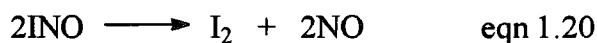


Nitrosyl fluoride, chloride and bromide are all well-known compounds which are gaseous at room temperature and pressure. They are commonly utilised as nitrosating agents following *in situ* generation from halide ion and acidic nitrous acid solution. An equilibrium exists (equation 1.19) where the nitrosyl halide formed can react with any substrate present.

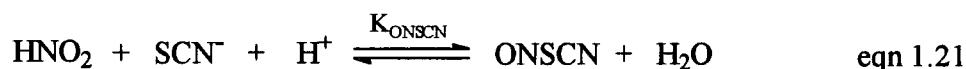


Equilibrium constants have been measured for nitrosyl chloride ($5.6 \times 10^{-4} \text{ mol}^{-2} \text{ dm}^6$) and nitrosyl bromide ($2.2 \times 10^{-2} \text{ mol}^{-2} \text{ dm}^6$) at 0°C ⁴⁷. The faster hydrolysis of NOCl leads to a larger K_{XNO} value for NOBr. Catalytic effects are observed on adding halide ion to both aqueous and organic solvent nitrosations. This is because addition of X^- makes the nitrogen of the nitrosating agent more electrophilic. Nitrosyl chloride is seen to be more reactive than nitrosyl bromide due to the electronegativity difference between chlorine and bromine. Despite this, bromide ion catalysis is always greater due to the difference in K_{XNO} values being so large. Fluoride ion

catalysis is as yet unknown, and although iodide ion catalysis is significant, K_{INO} has not been measured due to the instability with respect to iodine formation (equation 1.20).



Thiocyanate ion (SCN^-) can also act as a good catalyst. Nitrosyl thiocyanate exists as a red unstable species in solution at low temperature. ONSCN has been identified as the nitrosating agent when reactions using acidic nitrous acid solutions containing SCN^- have been carried out. Generally, thiocyanate ion will catalyse the same reactions as halide ion but catalysis is invariably more pronounced in the case of SCN^- . This can be explained by the equilibrium constant (K_{ONSCN}) value (equation 1.21) of $30 \text{ mol}^{-2} \text{ dm}^6$ at 25°C^{48} , analogous to the situation with halide ion.



However, nitrosyl thiocyanate is less reactive than the corresponding nitrosyl halides with respect to nitrosation. The general trend observed is that the greater the nucleophilicity of the anion (X^-), the lower the reactivity of the nitrosyl compound (XNO). The equilibrium values of XNO formation seem to be more significant than the intrinsic reactivity when considering anion catalysis.

Nitrosonium salts NO^+X^- can be prepared by adding dinitrogen trioxide, dinitrogen tetroxide or nitrosyl chloride to a strongly acidic reaction medium (equation 1.22).



Generally such compounds are crystalline, reasonably stable materials. They have to be used under completely anhydrous conditions due to their ready hydrolysis, forming nitrous acid. As expected, they are extremely effective nitrosating species and have been widely used in a synthetic manner.

1.3.4 Kinetics of Nitrosation

The nitrosation of thiol compounds to form S-nitrosothiols is probably the best example of S-nitrosation, having a history dating back to 1837⁴⁹. Both aromatic and aliphatic thiols undergo facile nitrosation with the range of nitrosating agents previously described (section 1.3.2 - 1.3.3). The reaction can be undertaken in both organic and aqueous solvents (equation 1.23).

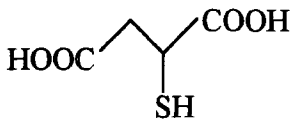
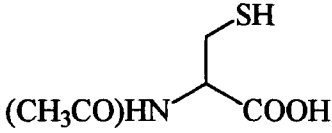
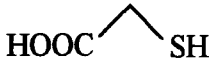


Kinetics have been carried out on the nitrosation reaction and for aqueous systems, under pseudo-first order conditions ($[\text{RSH}] \gg [\text{HNO}_2]$), the following rate equation deduced (equation 1.24).

$$\text{Rate} = k_3[\text{HNO}_2][\text{H}^+][\text{RSH}] \quad \text{eqn 1.24}$$

The reaction is seen to be first order in terms of nitrous acid, thiol and acid concentration. Third order rate constants (k_3) measured for the nitrosation of structurally different thiols⁵⁰ are similar and are usually obtained by stopped-flow spectrophotometry (table 1.1). For the most reactive thiols, k_3 approaches 7000 $\text{mol}^{-2} \text{dm}^6 \text{s}^{-1}$, which is thought to be the diffusion controlled limit.

Table 1.1

Substrate	k_3 ($\text{mol}^{-2} \text{dm}^6 \text{s}^{-1}$)
	1000
	1590
	2630

It is clear that the nitrosation of these thiols is extremely favourable. The N-acetylated derivative of L-cysteine (table 1.1) is almost four times as reactive as L-cysteine which can be explained by the positive charge on sulfur developed in the transition state being stabilised by interaction with the oxygen atom of the N-acetyl group (figure 1.3).

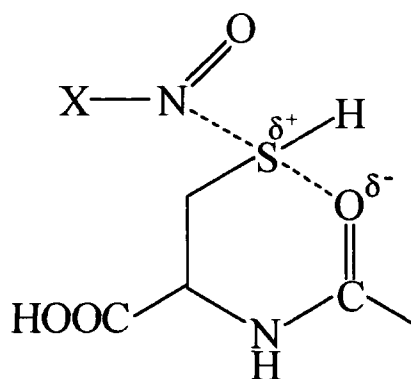
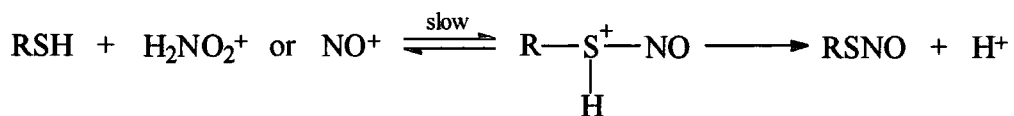


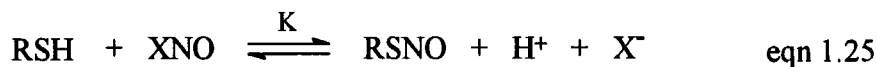
Figure 1.3

This forms a six membered ring which will be sterically favourable. The rate law is consistent with rate limiting attack of the nitrosonium ion or nitrous acidium ion at sulfur (scheme 1.11).



Scheme 1.11

As sulfur atoms are more nucleophilic than corresponding oxygen atoms, the nitrosation reaction is observed to be more rapid for thiols than alcohols. Plots of pseudo-first order rate constants against [RSH] do not show significant intercepts, suggesting that the reaction is irreversible. However, O-nitrosation has been noted to be significantly reversible. This can be rationalised by the fact that oxygen is much more basic than sulfur ($\Delta pK_A \sim 5$) in organic molecules and thus can accept a proton much more readily, which is the first step in the reverse reaction. It can be seen therefore that the forward reaction is governed by differing nucleophilicities ($S > O$) whereas the reverse reaction is determined by the difference in basicities ($O > S$). Herves Beloso and Williams⁵¹ have shown that the kinetic method of measuring the reversibility of S-nitrosothiol formation is not sufficiently sensitive but that a colorimetric technique can be employed. Indeed, it is more appropriate to express equation 1.23 as a reversible process (equation 1.25).

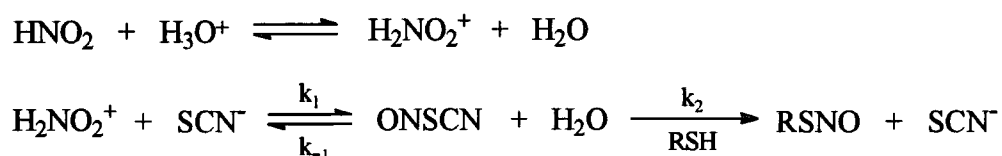


The equilibrium constant, K has been measured as $3 \times 10^5 \text{ mol}^{-1} \text{ dm}^3$ using penicillamine as the substrate. Typical corresponding K values for alcohols are 3.5 and $1.2 \text{ mol}^{-1} \text{ dm}^3$ for CH_3OH and $\text{C}_2\text{H}_5\text{OH}$ respectively⁵², illustrating the vast difference in reversibility of alcohol and thiol nitrosation.

The nitrosation of thiols is catalysed by halide or thiocyanate ion as predicted. The rate equation for thiol reaction with nitrous acid in the presence of such nucleophiles has been determined (equation 1.26).

$$\text{Rate} = k_2[\text{RSH}][\text{XNO}] \quad \text{eqn 1.26}$$

The familiar order of reactivity $\text{NOCl} > \text{NOBr} > \text{ONSCN}$ is observed. For the majority of thiols, the reaction is first order in $[\text{RSH}]$ as the rate equation suggests. However, the reaction of mercaptoacetic acid in the presence of thiocyanate or bromide ion produces plots of pseudo-first order rate constants against $[\text{RSH}]$ which are linear initially but eventually level off at high $[\text{RSH}]$, suggesting a zero order dependence on thiol. This experimental observation can be explained in terms of the mechanism postulated in scheme 1.12.

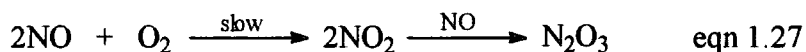


Scheme 1.12

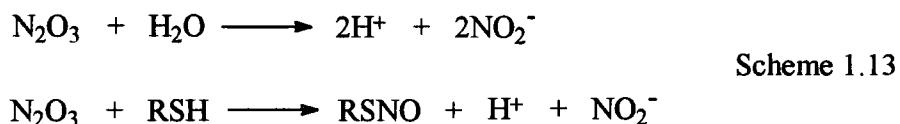
The nitrous acidium ion is formed in the usual manner during the initial step. An equilibrium exists between this species, added nucleophile (SCN^- in this case) and the corresponding nitrosyl compound. ONSCN is then capable of attacking the thiol in the rate determining step. The zero order dependence is rationalised by the fact that at higher $[\text{RSH}]$, the rate of formation of nitrosyl thiocyanate (k_1) becomes rate limiting and is achieved when $k_2[\text{RSH}] \gg k_{-1}[\text{H}_2\text{O}]$.

There have been several recent literature reports proposing new mechanisms for the nitrosation of thiol species, with a view to predicting the situation *in vivo*. As mentioned previously (scheme 1.10), nitric oxide can react with $-\text{SH}$ groups forming S-nitrosothiols under alkaline conditions in the complete absence of oxygen. However, NO is not thought to be able to perform this reaction at physiological pH (7.4) unless oxygen is present. Kharitonov *et al*⁵³ have demonstrated this to be the case, suggesting that the effective nitrosating species is N_2O_3 , formed via the aerial oxidation of NO . A first order dependence on oxygen and second order dependence

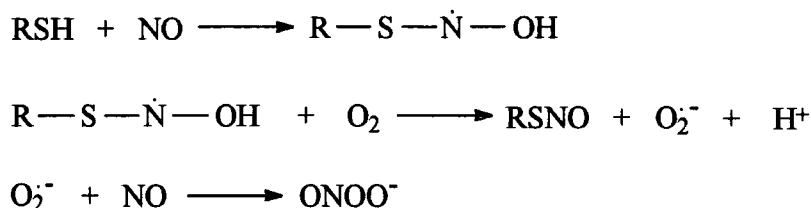
on nitric oxide is observed, consistent with the rate determining formation of nitrogen dioxide (equation 1.27).



Two competing reactions are thought to subsequently occur (scheme 1.13).



Potentially, N_2O_4 could be acting as the nitrosating agent in this system. As nitrite is the other remaining reaction product, and no nitrate detected, dinitrogen trioxide is in fact favoured as both reagents act as a source of NO^+ for electrophilic nitrosation. Goldstein and Czapski⁵⁴ have since verified this mechanism but postulate that it is unlikely to occur *in vivo* as a biosynthetic pathway for S-nitrosothiol formation as the half-life of the reaction will be greater than seven minutes under physiological conditions. From these results it can be concluded that S-nitrosothiols cannot act as carrier molecules of nitric oxide as NO will react with other substrates such as haemoglobin³⁹. However, a novel mechanism⁵⁵ proposes direct reaction of nitric oxide with reduced thiol in the presence of an electron acceptor (scheme 1.14).

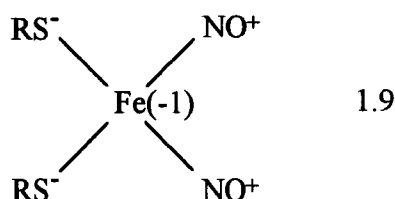


Scheme 1.14

The overall mechanism can therefore be represented by equation 1.28.



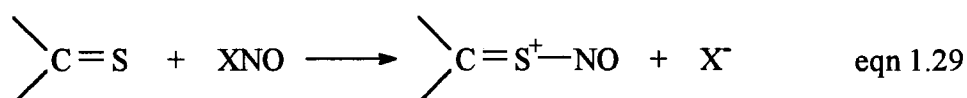
Under aerobic conditions, oxygen can act as the electron acceptor forming superoxide which is converted to hydrogen peroxide in the presence of superoxide dismutase. It has also been shown that reaction may occur under anaerobic conditions using NAD^+ as an electron acceptor. Dinitrosyl iron complexes (DNIC's) (1.9) have been implicated in the nitrosation of thiols under physiological conditions⁵⁶.



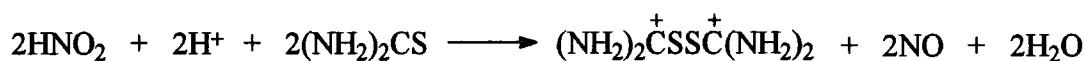
Such species act as a source of the nitrosonium ion. It is clear that there are several mechanisms that exist which could account for the *in vivo* formation of S-nitrosothiols.

1.3.5 Nitrosation of Thiocarbonyl Compounds

Thiocarbonyl compounds (such as thioureas) are nitrosated by XNO to initially form the S-nitrososulfonium ion (equation 1.29).

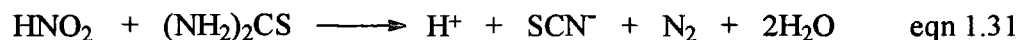


Such species are unstable, and generally decompose to form the corresponding disulfide or disulfide dication. When thiourea (H_2NCSNH_2) is the substrate two reactions can occur depending on the acidity⁵⁷. At high acid concentration nitric oxide is released and the disulfide dication is formed (equation 1.30).

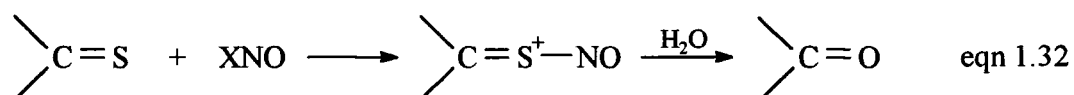


eqn 1.30

During nitrosation a red or yellow colour is observed, characteristic of the formation of an S-nitroso species. At low $[H^+]$, N-nitrosation is apparent with the products being thiocyanate ion and nitrogen (equation 1.31).



Under certain circumstances urea is the final product of the nitrosation of thiourea⁵⁸. This is seen at higher $[H^+]$ and hence may occur via nucleophilic attack of water on the S-nitrososulfonium ion (equation 1.32).



This is an extremely useful method of converting a thiocarbonyl compound into the corresponding carbonyl compound. The equilibrium constant K has been calculated (equation 1.33) to be $5000 \text{ mol}^{-2} \text{ dm}^6$ for the formation of the yellow species derived from nitrous acid and thiourea⁵⁹.



This relatively large value explains the marked nitrosation catalysis seen by thiourea which is analogous to that observed to that observed by halide ion and thiocyanate ion. This is to be expected when taking into account the greater nucleophilicity of H_2NCSNH_2 . The rate equation (equation 1.34) is similar to that seen for the nitrosation of thiols.

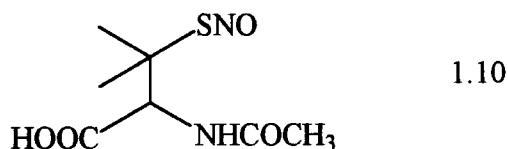
$$\text{Rate} = k_3[(NH_2)_2CS][HNO_2][H^+] \quad \text{eqn 1.34}$$

For thiourea, $k_3 = 6960 \text{ mol}^{-2} \text{ dm}^6 \text{ s}^{-1}$ at 25°C ⁶⁰ which is considered to be that of the encounter controlled reaction between the thiourea molecule and the effective nitrosating species.

1.4 Properties and Reactions of S-Nitrosothiols

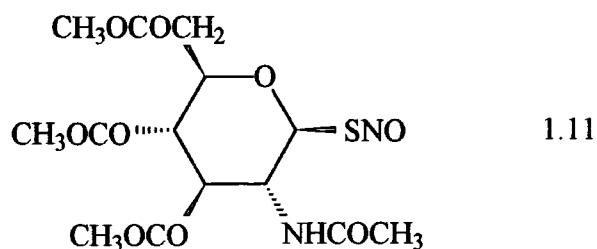
1.4.1 Physical Properties

S-nitrosothiols (or thionitrites) are of the general formula RSNO and are the sulfur analogues of the much more widely studied alkyl nitrites. A comprehensive study of the chemistry of such compounds is reviewed by Oae and Shinhama⁶¹. Primary and secondary nitrosothiols are orange or red in colour, whereas more sterically hindered tertiary nitrosothiols are green, such as S-nitroso-N-acetyl penicillamine (SNAP) (1.10).



This compound is indefinitely stable in its solid form, having a melting point of 152-154°C and a molar extinction coefficient value at 340nm of 980 mol⁻¹ dm³ cm⁻¹. This is typical of most aliphatic nitrosothiols which have an ultraviolet absorption maxima between 330 - 350nm with a corresponding ϵ value of the order of 10³ mol⁻¹ dm³ cm⁻¹. In addition, primary and secondary compounds exhibit a characteristic visible absorbance at 540nm whereas tertiary nitrosothiols absorb at around 590nm, ($\epsilon \sim 10 - 20$ mol⁻¹ dm³ cm⁻¹), these bands leading to the compounds being coloured. The electronic transitions responsible for ultraviolet/visible absorption have been assigned by Barrett et al⁶² so that the absorption at 330 - 350nm is due to the $n_o \rightarrow \pi^*$ transition and at 540/590nm the $n_N \rightarrow \pi^*$ transition is observed.

More recently the S-nitrosothiol derived from 2-acetamido-2-deoxy-1-thio- β -D-glucopyranose 3,4,6-triacetate has been synthesised and isolated⁶³ (1.11).



1.4.2 Thermal and Photochemical Decomposition

Almost all primary and secondary S-nitrosothiols are unstable at room temperature and will decompose according to equation 1.35, the same reaction also occurring photochemically.



The thiyl radical has been detected as an intermediate in this reaction⁶⁴, formed by the homolytic fission of the S-N bond. The nitrosation of thiols has in fact been utilised as a synthetic method for making symmetrical disulfides.

1.4.3 Metal Ion Induced Decomposition

1.4.3.1 Copper Ion Catalysis

It has become well documented that the release of nitric oxide from S-nitrosothiols at pH 7.4 in aqueous buffer solutions is a copper catalysed process⁶⁵. Essentially, the reaction occurs with the same stoichiometry as the thermal and photolytic decomposition reactions (equation 1.36).

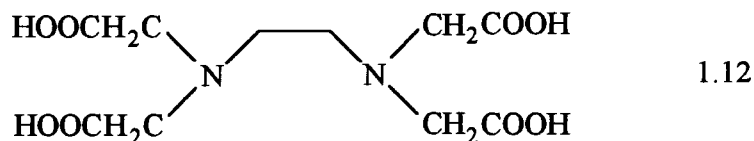


The nitric oxide produced will become oxidised prior to hydrolysis at pH 7.4 (scheme 1.1), forming nitrite which has been detected quantitatively⁶⁵. If oxygen is excluded then it is possible to detect NO itself using an NO-specific electrode. Concentrated solutions (0.1 mol dm⁻³) of S-nitrosocysteine will decompose to form the corresponding disulfide (cystine) in > 90% yield. Non-stoichiometric quantities of

copper ions are required to effect reaction, indeed there is often enough present as an impurity in buffer or distilled water solutions. The rate law (which applies for a range of copper ion concentrations) is given by equation 1.37.

$$\text{Rate} = k_2[\text{Cu}^{2+}][\text{RSNO}] + k'[\text{RSNO}] \quad \text{eqn 1.37}$$

A first order dependence on S-nitrosothiol and Cu^{2+} is observed. The term k' represents the portion of the rate due to the presence of adventitious copper ions as well as the spontaneous thermal reaction. Indeed, when the non-specific metal ion chelator EDTA (ethylenediaminetetraacetic acid, 1.12) is added to the reaction of copper ions and SNAP, decomposition is completely suppressed⁶⁶.

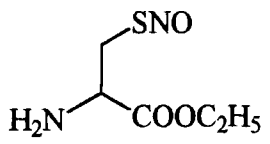
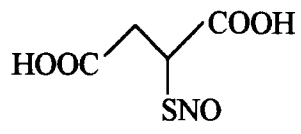
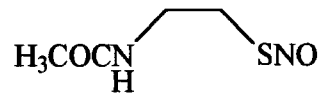


The catalysis due to "impurity" copper ions being present is apparent when a plot of pseudo-first order rate constant, k_{obs} (defined by equation 1.38) against $[\text{Cu}^{2+}]$ is constructed. A linear relationship is revealed with a small intercept, as predicted.

$$\frac{-d}{dt} [\text{RSNO}] = k_{\text{obs}}[\text{RSNO}] \quad k_{\text{obs}} = k_2[\text{Cu}^{2+}] + k' \quad \text{eqn 1.38}$$

Therefore, the slope of such a plot is equal to k_2 , the second order rate constant for reaction (equation 1.37). The value of k_2 depends greatly on the nature of R^{66} (table 1.2).

Table 1.2

Substrate	k_2 ($\text{mol}^{-1} \text{dm}^3 \text{s}^{-1}$)
	270,000
	1100
	0

The most reactive structures are for the S-nitrosothiols derived from cysteine, cysteamine and penicillamine, where the added copper can be complexed with both the nitrogen atom of the nitroso group and the nitrogen atom of the amino group (figure 1.4).

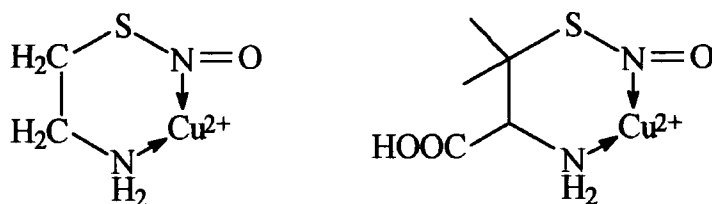
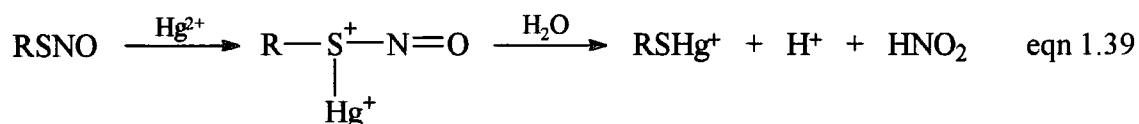


Figure 1.4

Co-ordination can also be envisaged at the carboxylate group in compounds such as S-nitrosomercaptoacetic acid (figure 1.5).

1.4.3.2 Silver and Mercury Ion Induced Reaction

Mercuric ion also promotes the decomposition of S-nitrosothiols in aqueous solution (equation 1.39).



The reaction differs to that of copper ion catalysis in that stoichiometric amounts of Hg^{2+} are required (2:1 $\text{RSNO}:\text{Hg}^{2+}$ in order to obtain complete nitrosothiol decomposition), indicating a non-catalytic reaction. Also, nitric oxide was not detected as a product⁶⁹ using an NO-specific electrode suggesting a different reaction mechanism. Saville⁷⁰ proposed that Hg^{2+} co-ordinates to the sulfur atom of the nitrosothiol and causes heterolytic N-S bond fission, forming RSHg^+ and NO^+ . Use has been made of this reaction in the quantification of thiols⁷⁰. It is found to be first order in both nitrosothiol and mercuric ion (equation 1.40).

$$\text{Rate} = k_2[\text{Hg}^{2+}][\text{RSNO}] \quad \text{eqn 1.40}$$

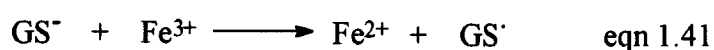
In direct contrast to results obtained for Cu^{2+} catalysis, k_2 values do not vary greatly in terms of altering the environment around the S-nitroso group. This implies that co-ordination of mercuric ion occurs only to the sulfur atom and not to any other functional group in the molecule. This is to be expected as the affinity of Hg^{2+} for thiol species is greater than for any other ligand, leading to the -SH functionality being termed "mercapto". The formation of such stable complexes leads to large values for k_2 (of the order of 10^3 - $10^4 \text{ mol}^{-1} \text{ dm}^3 \text{ s}^{-1}$)⁶⁹, generally greater than that noted for copper ion catalysis.

Silver(I) also has a high affinity for -SH groups. Product analysis of the reaction between Ag^+ and S-nitrosoglutathione indicated that RSAg and nitrous acid were formed⁶⁹. The timescale of the reaction between S-nitrosothiols and silver(I) is

similar to that of Cu^{2+} . However, due to the insolubility of the product RSAg complexes limiting kinetic studies, a structure/reactivity analysis is difficult to undertake.

1.4.3.3 Ferrous Ion Catalysis

It has also been noted that ferrous ion (Fe^{2+}) is capable of acting as a catalyst for the release of nitric oxide from S-nitrosothiols⁶⁵. Due to the instability of ferrous ion with respect to aerial oxidation, any kinetic studies have to be performed under completely anaerobic conditions. The reaction between SNAP and Fe^{2+} was examined and pseudo-first order rate constants varied from $1.5\text{-}9.4 \times 10^{-3} \text{ s}^{-1}$ utilising the same reactant concentrations for 14 separate experiments⁶⁹. This irreproducibility of results may be partly due to the nitrogen purging method of producing an oxygen-free environment not being completely effective, thus allowing the oxidation of Fe^{2+} to catalytically inactive ferric ion. An additional problem is that of copper catalysis interfering with the ferrous ion reaction. There is a literature report⁷¹ that S-nitrosoglutathione will decompose in the presence of glutathione (GSH) and added Fe^{3+} , suggesting the possibility of reduction by thiolate to ferrous ion and subsequent reaction catalysis (equation 1.41).



Such a mechanism may prove to be of physiological significance *in vivo*.

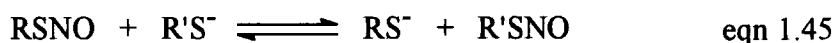
1.4.4 Acid Catalysed Decomposition

As mentioned in section 1.3.4, nitrosation of thiols is essentially an irreversible process, which can be explained by the lower basicity of the sulfur atom compared with an analogous oxygen atom. However, denitrosation is observed⁷² at high acidities ($1\text{-}4 \text{ mol dm}^{-3} \text{ H}_2\text{SO}_4$) in the presence of added nucleophiles and a nitrous acid trap (such as N_3^-) to prevent the reverse reaction. Scheme 1.15 details the proposed reaction mechanism.

is found to be less reactive than thiocyanate ion even though it is a better nucleophile. Steric reasons have been proposed to explain this observation.

1.4.5 Transnitrosation

Transnitrosation describes the transfer of the NO group from an S-nitrosothiol (or other nitroso-containing molecule) to a suitable nucleophile. If the nucleophile is thiolate ion then a new S-nitrosothiol is formed (equation 1.45).



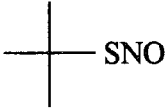
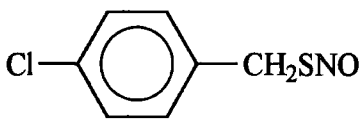
The reaction occurs readily in aqueous solution at $\text{pH} > 8$ and has been found to be first order in both nitrosothiol and thiolate⁷³ (equation 1.46).

$$\text{Rate} = k_2[\text{RSNO}][\text{R}'\text{S}^-] \quad \text{eqn 1.46}$$

The question arises as to whether a direct reaction takes place between the S-nitrosothiol and thiol (or thiolate) or if prior release of nitric oxide occurs. A pH dependence study has shown that the reactive species is thiolate as an S-shaped curve of pH against pseudo-first order rate constant is obtained, when $[\text{R}'\text{SH}] \gg [\text{RSNO}]$ ⁷⁴. This suggests that nucleophilic attack is occurring at the nitroso-nitrogen atom. A mechanism where nitric oxide is released and oxidised to form an electrophilic nitrosating agent (such as N_2O_3) can be disregarded, as the rate of NO release from S-nitrosothiols such as SNAP⁶⁶ is an order of magnitude smaller than the measured rate of transnitrosation⁷³.

Structure-reactivity studies using the same thiolate ion (table 1.3) have indicated that a larger second order rate constant (k_2 in equation 1.46) is obtained on introducing electron withdrawing species in the nitrosothiol.

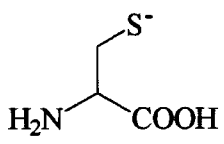
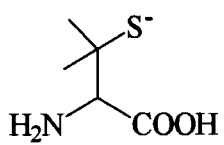
Table 1.3

Substrate	k_2 ($\text{mol}^{-1} \text{dm}^3 \text{s}^{-1}$)
	95
	432
	1016

(for reaction with the thiolate ion derived from N-acetylcysteine)

This reinforces the mechanism of nucleophilic attack previously described. On repeating this work with a particular S-nitrosothiol and nine thiolate anions, little variation in k_2 was noted. However, the reactivity of the anions derived from cysteine and penicillamine are of interest (table 1.4).

Table 1.4

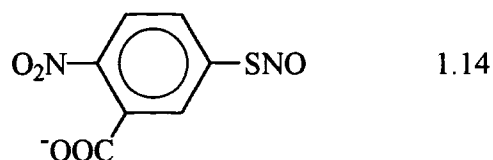
Substrate	k_2 ($\text{mol}^{-1} \text{dm}^3 \text{s}^{-1}$)
	445
	23

(for reaction with S-nitroso-2-hydroxyethanethiol)

The decreased reactivity of the penicillamine thiolate ion is not to be expected on electronic grounds, so a steric effect must be significant in this case. The same trend has been documented by Meyer *et al*⁷⁵. Recent work by Zhang *et al*⁷⁶ has followed the transnitrosation reaction between various S-nitrosothiols and bovine serum albumin (BSA), which has a thiol group (Cys-34) present in a hydrophobic pocket, next to an anionic carboxylate group. Unsurprisingly, cationic nitrosothiols (1.13) are the most reactive ($k_2 = 510 \text{ mol}^{-1} \text{ dm}^3 \text{ s}^{-1}$).



Disulfides were shown to be reasonably unreactive with respect to reaction with Cys-34. The anion derived from S-nitrosothio-2-nitrobenzoic acid (1.14) has been shown⁷⁷ to act as an effective reagent for the nitrosation of thiol groups in human serum albumin (HSA) via a transnitrosation mechanism.



1.5 Nitric Oxide Donor and Acceptor Compounds

1.5.1 Introduction

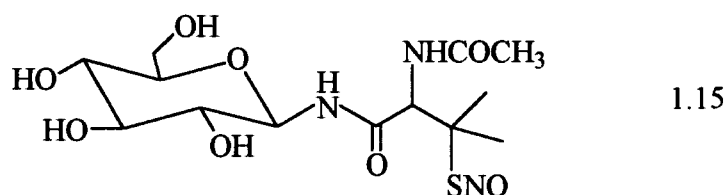
It is clear that nitric oxide is a molecule of profound importance in a physiological sense (section 1.2). Therefore, there is currently unprecedented interest in the design and synthesis of molecules that can deliver NO *in vivo* (nitrovasodilators). Such compounds must be of low toxicity and have controllable distribution characteristics throughout the body, along with harmless byproducts. Very many drugs are now tested for their nitrovasodilatory properties which have vastly differing chemical structures. However, they all seek to act in a similar manner by activating the enzyme guanylate cyclase and raising the levels of cyclic guanosine monophosphate within cells. In addition, the search is now on for compounds which can significantly reduce intracellular nitric oxide levels, either by inhibition of inducible nitric oxide synthase (section 1.2.2) or by binding of NO directly for the treatment of diseases such as septic shock. Future prospects appear to be extremely encouraging in this popular field of research, which will now be discussed in detail.

1.5.2 Nitrovasodilators

1.5.2.1 S-Nitrosothiols

S-nitrosothiols have been implicated in the inhibition of platelet aggregation³⁴ and shown to promote vascular arterial smooth muscle dilation⁷⁸. However, in many cases, the chemical properties of such compounds *in vitro* are not mirrored by their physiological behaviour *in vivo*. At this time it is unresolved as to whether S-nitrosothiols can mediate their effects via prior release of nitric oxide or whether the

molecule remains intact. The *in vitro* decomposition of these materials has been extensively studied (section 1.4.3 - 1.4.5) with the discovery of the copper catalysed reaction⁶⁵ suggesting a plausible mechanism *in vivo*. The possibility exists that more stable nitrosothiols (such as GSNO) act as a "reservoir" of nitric oxide which can be transferred via transnitrosation to form reactive nitrosothiols (such as S-nitrosocysteine) which subsequently decompose, releasing NO. It may be the case that protein molecules (eg HSA) can store nitric oxide before transnitrosation⁷⁹. S-nitrosothiols have the advantage of being less prone to inducing tolerance⁸⁰, a problem associated with glyceryl trinitrate (section 1.5.2.2), with their decomposition products being disulfides which are non-toxic and easily excreted. Recently, Ramirez *et al*⁸¹ has synthesised a range of novel glyco-S-nitrosothiols (for example, 1.15) which have improved water solubility and cell penetration characteristics.

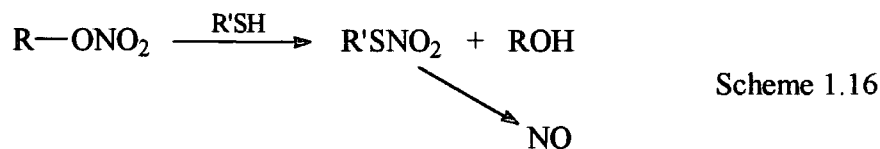


Such materials are hoped to show improved pharmacokinetic properties when compared with well-known nitrovasodilators (eg SNAP).

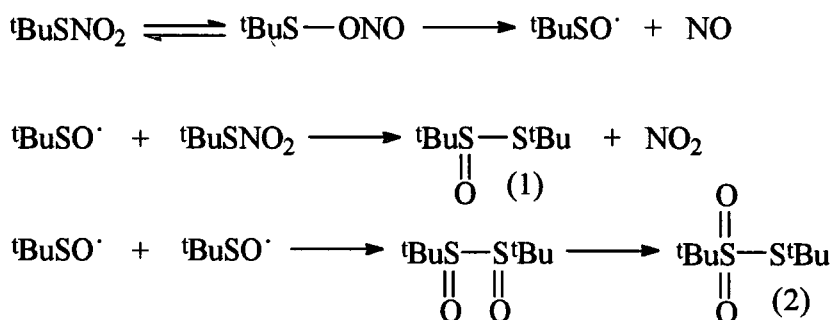
1.5.2.2 Organic Nitrates and Nitrites

As mentioned in section 1.2.1, glyceryl trinitrate (GTN) and amyl nitrite have been used for the treatment of angina pectoris and other circulatory problems for many years. Despite this, a detailed understanding of how these compounds cause vasodilation has only relatively recently come to light. In 1973, it was discovered that GTN had to react with thiols in order to exhibit its nitrovasodilator characteristics⁸², even though it was not known that nitric oxide was released. Ignarro *et al*⁸³ subsequently demonstrated the formation of nitric oxide from GTN in the presence of thiol. However, it is now clear that although thiols such as cysteine and N-acetylcysteine will decompose organic nitrates to form NO, most will react to

form nitrite and nitrate ions⁸⁴. It is believed that nucleophilic attack of thiolate ion takes place at the nitrogen of the organic nitrate, forming a thionitrate which decomposes to release NO (scheme 1.16).



Recent reports⁸⁵ have suggested that thionitrates are indeed intermediates in this reaction. The fate of t-butyl thionitrate (^tBuSNO₂) has been studied at pH 7.4 and the mechanism of decomposition outlined in scheme 1.17.



Scheme 1.17

It can be seen that t-butyl thionitrate dissociates rapidly following rearrangement to form nitric oxide and sulfinyl radical. The observed carbon containing products are (1) and (2), di-t-butyl thiosulfinate and di-t-butyl thiosulfonate respectively. Nitric oxide was detected using an NO-specific electrode. The absence of ^tBuSS^tBu as a product eliminates the possibility of S-nitrosothiol formation and decomposition. Perhaps surprisingly, t-butyl thionitrate did not activate soluble guanylate cyclase, either in the presence or absence of added thiol. This implies that the β-carboxylate group of cysteinyl thionitrate and N-acetylcysteinyl thionitrate are essential for GC activation. The development of tolerance to GTN and other organic nitrates is a big problem that such compounds have as therapeutic drugs. This may be explained by the progressive depletion of intracellular thiol levels due to the formation of

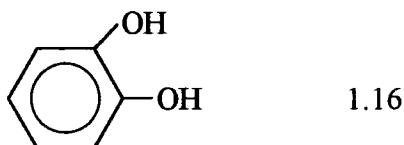
thionitrates. An enzymic mechanism involving the interaction of GTN with glutathione-S-transferase has also been postulated which is again dependent on the presence of a sulfhydryl group.

In comparison, the mechanism of nitric oxide formation from organic nitrites is much more established. A transnitrosation reaction⁸⁶ takes place with thiols producing a nitrosothiol which decomposes to NO (scheme 1.18).



Scheme 1.18

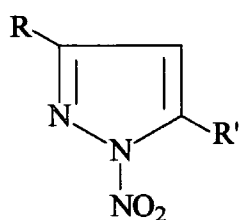
As mentioned in section 1.5.2.1, the release of nitric oxide from S-nitrosothiols *in vivo* is not fully understood. RONO compounds can also react with biologically relevant reducing agents which are conjugation stabilised ene diols (such as catechol, 1.16)⁸⁷.



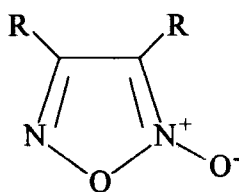
The reaction is thought to proceed via nitrosation of the dianion derived from catechol and homolytic cleavage of the O-NO bond, forming nitric oxide. This may constitute an alternative pathway to the transnitrosation mechanism described previously for the *in vivo* formation of NO from alkyl nitrites.

1.5.2.3 Heterocyclic Nitric Oxide Donors

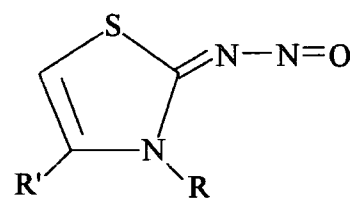
Among the more popular compounds currently being studied as potential NO donors are heterocycles containing a nitrogen (or other) heteroatom. Typical examples are given in figure 1.7.



N-nitropyrazoles



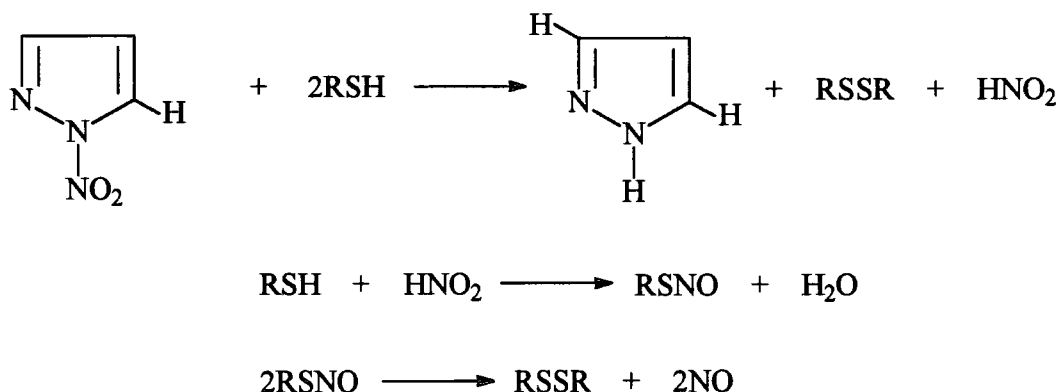
Furoxans



Nitrosimines

Figure 1.7

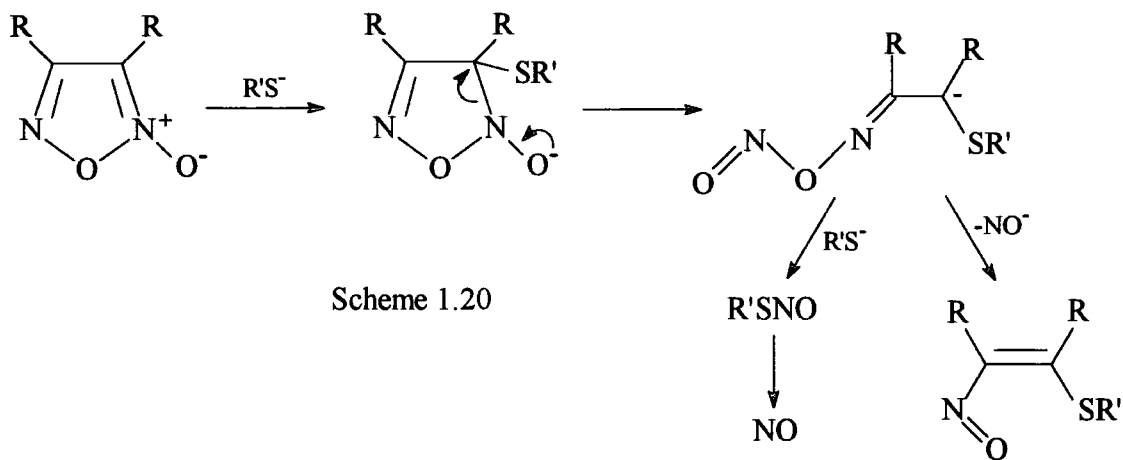
N-nitropyrazoles have been analysed by Grigor'ev *et al*⁸⁸. These compounds have been found to react with cysteine to form nitrous acid which nitrosates the thiol producing S-nitrosocysteine. Subsequent decomposition releases nitric oxide (scheme 1.19).



Scheme 1.19

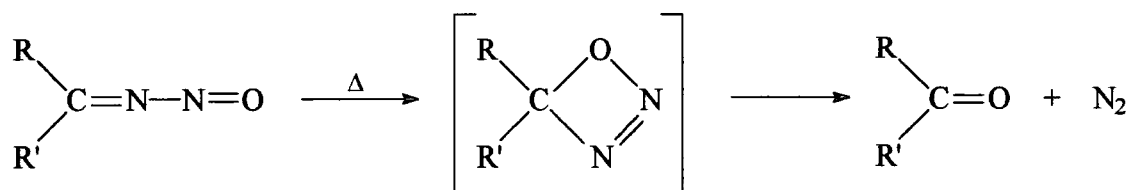
There is an apparent similarity between the participation of cysteine in this instance and in the case of GTN, which has already been discussed. Preliminary data suggests that the N-nitropyrazole ($\text{R} = \text{R}' = \text{CH}_3$) will activate soluble guanylate cyclase.

Furoxans are another type of heterocyclic compound that, in a similar manner to organic nitrites, will react with a thiol to form an unstable S-nitrosothiol, again releasing NO on decomposition⁸⁹. Furoxans will however stimulate soluble guanylate cyclase in the absence of sulfhydryl-containing compounds. Any thiol will release NO from these materials via a nitrosothiol intermediate. A tentative mechanism for this intermediate formation is outlined in scheme 1.20.

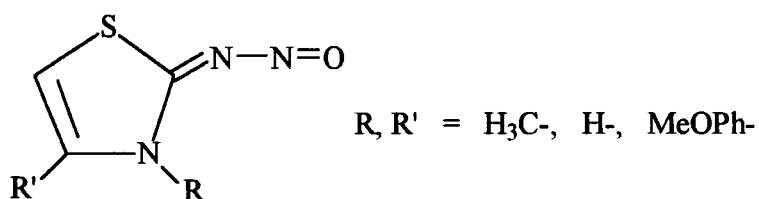


The delocalisation of positive charge on N-2 of the furazan ring makes nucleophilic attack of $R'S^-$ at C-3 likely. Subsequent ring-opening forms the nitroso derivative which reacts with further thiol to form an S-nitrosothiol.

Nitrosimines are normally extremely unstable compounds⁹⁰ which decompose to the corresponding ketones by expulsion of molecular nitrogen (scheme 1.21).



On substituting a heterocyclic ring (eg thiazole), much more stable species are formed (1.17).

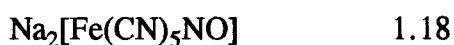


1.17

Thiazole-2-nitrosimine ($R=R'=H$) is susceptible to photolytic N-NO bond cleavage⁹¹ and will activate soluble guanylate cyclase in the presence of thiols.

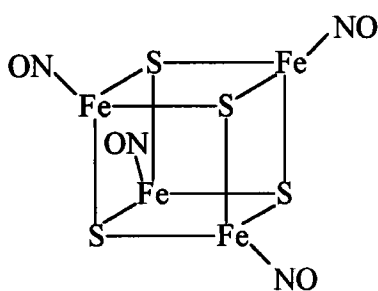
1.5.2.4 Metal Nitrosyls

Other compounds containing nitric oxide as a ligand have the same potential as more commonly known nitrovasodilators to deliver NO *in vivo*. These include metal nitrosyls, which contain one or more M-NO bonds (as described in section 1.1.4). Sodium nitroprusside (1.18) is such a drug which is commonly used to induce low blood pressure during surgery.

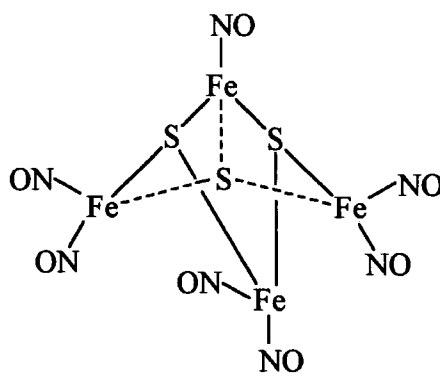


Photolysis of sodium nitroprusside leads to cleavage of the Fe-NO bond⁹². There is also a non-photochemical mechanism of nitric oxide release which is thought to involve thiols⁷⁸.

Other iron-nitrosyl complexes known to be capable of NO mediated vasodilation are Cubane and Roussin's Black Salt (RBS)⁹³, tetranitrosyltetra- μ_3 -sulfidotetrahydro-tetrairon and heptanitrosyl- μ_3 -thioxotetraferate(1-) respectively (1.19).



Cubane



Roussin's Black Salt

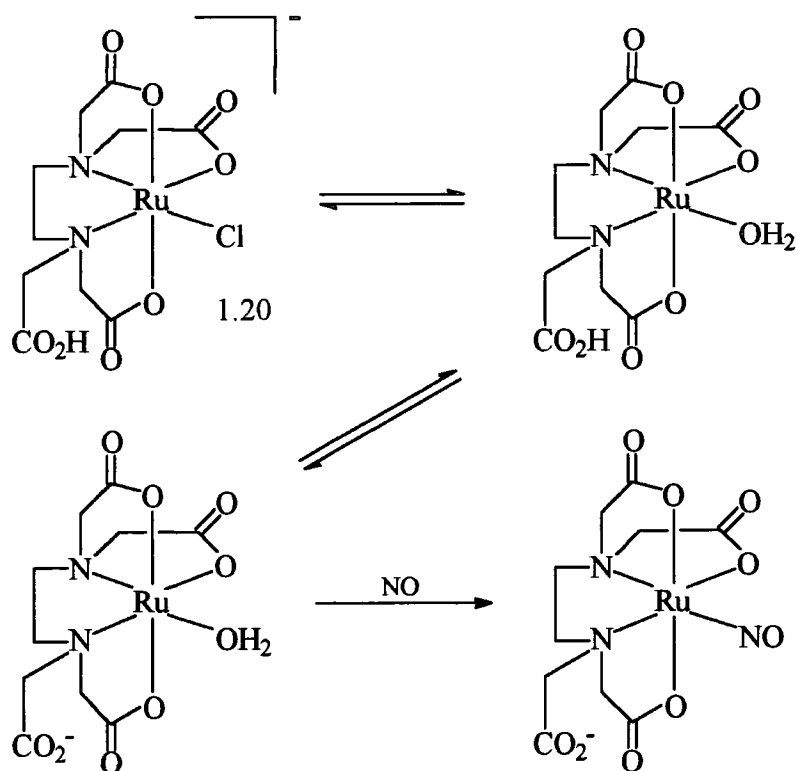
1.19

RBS is made by self-assembly from sulfide, iron(II) and nitrite and converted into Cubane by reaction with elemental sulfur. Solutions of both compounds are intensely black and endothelial cell staining is observed during the measurement of rat tail arterial relaxation⁹⁴. The surprising lipid solubility of RBS (considering its ionic

nature) may explain the long lasting vasodilatory effects observed in this case. Haemoglobin (an NO scavenger) and methylene blue (an inhibitor of soluble guanylate cyclase) both block the action of these compounds *in vivo*. Morlino *et al*⁹⁵ have described nitric oxide release from metalloporphyrin-NO complexes, in particular nitrosylcobalt(II) tetraphenylporphinate, (TPP)-Co^{II}-NO. The NO ligand is released following light absorption in the molecular π system within ~ 30 picoseconds. It is possible that such metalloporphyrins may act as storage and transport systems for nitric oxide.

1.5.3 Nitric Oxide Acceptor Compounds

Septic shock (section 1.2.5) is a disease caused by high levels of bacteria present in the blood circulation. This induces macrophage stimulation and an increase in nitric oxide concentration, leading to vasodilation. The consequence is a severe drop in blood pressure, and eventually vascular collapse. It is fatal in over 50% of cases, and thus the search is on for new drugs that can reduce NO levels. The traditional approach is via organic chemistry with many researchers investigating the use of inhibitors of inducible nitric oxide synthase⁹⁶ (section 1.2.2). However, such compounds (eg N-monomethyl-L-arginine, 1.5) have a number of side-effects, mainly affecting the local blood circulation within organs, particularly the lungs. An alternative method is to remove nitric oxide by use of a specific, high affinity, non-toxic scavenger. Ruthenium readily forms nitrosyl complexes and indeed has a higher affinity for NO than any other metal⁹⁷. Ru(III) will react with NO to form a very stable bond and the presence of other ligands conferring water solubility allows rapid *in vivo* clearance. It has been demonstrated that ruthenium(III) polyaminocarboxylate, K[Ru(Hedta)Cl] (1.20) is a water soluble complex which will reduce nitrite levels in a culture medium of macrophage cells stimulated to produce nitric oxide⁹⁸.



Scheme 1.22

The proposed mechanism for this reaction involves the formation of the aqua species $[\text{Ru}(\text{Hedta})(\text{H}_2\text{O})]$, (scheme 1.22), followed by associative ligand substitution with NO to form the nitrosyl. The pendant carboxylate group may facilitate this substitution⁹⁹ since replacement by an alcohol group leads to a reduction in the observed activity. At pH 7.4 and 7.3°C the second order rate constant for nitric oxide binding is $\sim 2 \times 10^7 \text{ mol}^{-1} \text{ dm}^3 \text{ s}^{-1}$. Such complexes therefore have great potential as NO scavengers in nitric oxide mediated diseases.

References

1. K.I. Vasu, *Mellor's Comprehensive Treatise on Inorganic and Theoretical Chemistry, Nitrogen*, Longmans, London, 1967, **8**, Suppl. 2, Part 2, 628.
2. E. Culotta and D.E. Koshland Jr, *Science*, 1992, **258**, 1862.
3. M. Fontecave and J-L. Pierre, *Bull. Soc. Chim. Fr.*, 1994, **131**, 620.
4. E.W. Ainscough and A.M. Brodie, *J. Chem. Educ.*, 1995, **72**, 686.
5. K. Jones, *Comprehensive Inorganic Chemistry*, Vol. 2, Eds. J.C. Bailar, H.R. Emelius, R. Nyholm and A.F. Trotman-Dickenson, Pergamon Press, New York, 1973, 329.
6. R. Beringer, E. Rawson and A. Henry, *Phys. Rev.*, 1954, **94**, 343.
7. M. Bodenstein, *Helv. Chim. Acta*, 1935, **18**, 743.
8. W.A. Seddon and H.C. Sutton, *Trans. Farad. Soc.*, 1963, **59**, 2323.
9. K. Akiyama, H. Suzuki, P. Grant and R.J. Bing, *J. Mol. Cell. Cardiology*, 1997, **29**, 1.
10. A. Fontijn, A.J. Sabadell and R.J. Ronco, *Anal. Chem.*, 1970, **42**, 575.
11. L.J. Beckmann, W.A. Fessler and M.A. Kise, *Chem. Rev.*, 1951, **48**, 319.
12. J.S. Beckman, T.W. Beckman, J.Chen, P.A. Marshall and B.A. Freeman, *Proc. Natl. Acad. Sci., USA*, 1990, **87**, 1620.
13. I. Gabr, R.P. Patel, M.C.R. Symons and M.T. Wilson, *J. Chem. Soc., Chem. Commun.*, 1995, 915.
14. I. Gabr and M.C.R. Symons, *J. Chem. Soc., Faraday Trans.*, 1996, **92**, 1767.
15. F.A. Cotton and G. Wilkinson, *Advanced Inorganic Chemistry*, Third Edn., Interscience, 1972, 713.
16. T.L. Brunton, *Lancet*, 1867, **2**, 97.
17. A.R. Butler, *Chem. Br.*, 1990, **26**, 419.
18. R.M.J. Palmer, A.G. Ferrige and S. Moncada, *Nature*, 1987, **327**, 524.

19. L.J. Ignarro, G.M. Buga, K.S. Wood, R.E. Byrns and G. Chaudhuri, *Proc. Natl. Acad. Sci., USA*, 1987, **84**, 9265.
20. R.J.P. Williams, *Chem. Soc. Rev.*, 1996, **25**, 77.
21. S. Katsuki, W.P. Arnold, C.K. Mittal and F. Murad, *J. Cyclic Nucleotide Res.*, 1977, **3**, 23.
22. R.F. Furchgott and J.V. Zawadzki, *Nature*, 1980, **288**, 373.
23. F. Murad, C.K. Mittal, W.P. Arnold, S. Katsuki and H. Kimura, *Adv. Cyclic Nucleotide Res.*, 1978, **9**, 145.
24. C.A. Gruetter, D.Y. Gruetter, J.E. Lyon, P.J. Kadowitz and L.J. Ignarro, *J. Pharm. Exp. Ther.*, 1981, **219**, 181.
25. M. Feelisch, M.T. Poel, R. Zamora, A. Deussen and S. Moncada, *Nature*, 1994, **368**, 62.
26. R.M.J. Palmer, D.S. Ashton and S. Moncada, *Nature*, 1988, **333**, 664.
27. A.M. Leone, R.M.J. Palmer, R.G. Knowles, P.L. Francis, D.S. Ashton and S. Moncada, *J. Biol. Chem.*, 1991, **266**, 23790.
28. S. Moncada, R.M.J. Palmer and E.A. Higgs, *Pharmacol. Rev.*, 1991, **43**, 109.
29. Y. Komori, J. Hyun, K. Chiang and J.M. Fukuto, *J. Biochem.*, 1995, **117**, 923.
30. D.S. Bredt and S.H. Snyder, *Proc. Natl. Acad. Sci., USA*, 1989, **86**, 9030.
31. M. Barinaga, *Science*, 1991, **254**, 1296.
32. L.J. Ignarro, P.A. Bush, G.M. Buga, K.S. Wood, J.M. Fukuto and J. Rajfer, *Biochem. Biophys. Res. Commun.*, 1990, **170**, 843.
33. R.M.J. Palmer, S. Moncada and M.W. Radomski, *Brit. J. Pharmacol.*, 1987, **92**, 181.
34. M.P. Gordge, J.S. Hothersall, G.H. Neild and A. Noronha-Dutra, *Brit. J. Pharmacol.*, 1996, **119**, 533.
35. M.A. Marletta, P.S. Yoon, R. Iyengar, C.D. Leaf and J.S. Wishnok, *Biochemistry*, 1988, **27**, 8706.

36. A.R. Butler, C. Glidewell, A.R. Hyde and J.C. Walton, *Polyhedron*, 1985, **4**, 303.
37. L. Jia, C. Bonaventura, J. Bonaventura and J.S. Stamler, *Nature*, 1996, **380**, 221.
38. D.J. Barnett, J. McAninly and D.L.H. Williams, *J. Chem. Soc., Perkin Trans. 2*, 1994, 1131.
39. J.R. Lancaster, *Proc. Natl. Acad. Sci., USA*, 1994, **91**, 8137.
40. A. Hausladen, C.T. Privalle, T. Keng, J. DeAngelo and J.S. Stamler, *Cell*, 1996, **86**, 719.
41. J. Tummavuori and P. Lumme, *Acta Chem. Scand.*, 1968, **22**, 2003, P. Lumme, P. Lahermo and J. Tummavuori, *ibid.*, 1965, **19**, 9, P. Lumme and J. Tummavuori, *ibid.*, 1965, **19**, 617.
42. Reference 5, p. 368.
43. J.H. Ridd, *Quart. Rev.*, 1961, **15**, 418.
44. E.D. Hughes, C.K. Ingold and J.H. Ridd, *J. Chem. Soc.*, 1958, 88.
45. C.A. Bunton and G. Stedman, *J. Chem. Soc.*, 1959, 3466.
46. W.A. Pryor, D.F. Church, C.K. Govindan and G. Crank, *J. Org. Chem.*, 1982, **47**, 156.
47. H. Schmid and E. Hallaba, *Monatsh. Chem.*, 1956, **87**, 560, H. Schmid and M.G. Fouad, *ibid*, 1957, **88**, 631.
48. G. Stedman and P.A.E. Whincup, *J. Chem. Soc.*, 1963, 5796.
49. G. Kresze and U. Ulich, *Chem. Ber.*, 1959, **92**, 1048.
50. P.A. Morris and D.L.H. Williams, *J. Chem. Soc., Perkin Trans. 2*, 1988, 513.
51. P. Herves Beloso and D.L.H. Williams, *J. Chem. Soc., Chem. Commun.*, 1997, 89.
52. J. Casado, F.M. Lorenzo, M. Mosquera and M.F.R. Prieto, *Can. J. Chem.*, 1984, **62**, 136.

53. V.G. Kharitonov, A.R. Sundquist and V.S. Sharma, *J. Biol. Chem.*, 1995, **270**, 28158.
54. S. Goldstein and G. Czapski, *J. Am. Chem. Soc.*, 1996, **118**, 3419.
55. A.J. Gow, D.G. Buerk and H. Ischiropoulos, *J. Biol. Chem.*, 1997, **272**, 2841.
56. M. Boese, P.I. Mordvintcev, A.F. Vanin, R. Busse and A. Mülsch, *J. Biol. Chem.*, 1995, **270**, 29244.
57. A.E. Werner, *J. Chem. Soc.*, 1912, **101**, 2180.
58. J.W. Lown and S.M.S. Chauhan, *J. Org. Chem.*, 1983, **48**, 507.
59. K. Al-Mallah, P. Collings and G. Stedman, *J. Chem. Soc., Dalton Trans.*, 1974, 2469.
60. P. Collings, K. Al-Mallah and G. Stedman, *J. Chem. Soc., Perkin Trans. 2*, 1975, 1734.
61. S. Oae and K. Shinhama, *Org. Prep. Proced. Int.*, 1983, **15**, 165.
62. J. Barrett, D.F. Debenham and J. Glauser, *Chem. Commun.*, 1965, **12**, 248.
63. A.P. Munro and D.L.H. Williams, to be published.
64. R.J. Singh, N. Hogg, J. Joseph and B. Kalyanaraman., *J. Biol. Chem.*, 1996, **271**, 18596.
65. J. McAninly, D.L.H. Williams, S.C. Askew, A.R. Butler and C. Russell, *J. Chem. Soc., Chem. Commun.*, 1993, 1758, B. Roy, A. du Moulinet d'Hardemare and M. Fontecave, *J. Org. Chem.*, 1994, **59**, 7019.
66. S.C. Askew, D.J. Barnett, J. McAninly and D.L.H. Williams, *J. Chem. Soc., Perkin Trans. 2*, 1995, 741.
67. W.P. Jencks, *Catalysis in Chemistry and Enzymology*, Dover Publications Inc., New York, 1987, 12.
68. N. Bainbrigge, A.R. Butler and C.H. Görbitz, *J. Chem. Soc., Perkin Trans. 2*, 1997, 351.
69. H.R. Swift, Ph.D. thesis, University of Durham, 1996.
70. B. Saville, *Analyst*, 1958, **83**, 670.

71. A.C.F. Gorren, A. Schrammel, K. Schmidt and B. Mayer., *Arch. Biochem. Biophys.*, 1996, **330**, 219.
72. S.S. Al-Kaabi, D.L.H. Williams, R. Bonnett and S.L. Ooi, *J. Chem. Soc., Perkin Trans. 2*, 1982, 227.
73. D.J. Barnett, A. Ríos and D.L.H. Williams, *J. Chem. Soc., Perkin Trans. 2*, 1995, 1279.
74. D.J. Barnett, J. McAninly and D.L.H. Williams, *J. Chem. Soc., Perkin Trans. 2*, 1994, 1131.
75. D.J. Meyer, H. Kramer, N. Özer, B. Coles and B. Ketterer, *FEBS Lett.*, 1994, **345**, 117.
76. H. Zhang and G.E. Means, *Anal. Biochem.*, 1996, **237**, 141, H. Zhang and G.E. Means, *FASEB J.*, 1996, **10**, 2299.
77. M.S. Studebaker, H. Zhang and G.E. Means, *Anal. Biochem.*, 1996, **237**, 193.
78. L.J. Ignarro, H. Lippton, J.C. Edwards, W.H. Baricos, A.L. Hyman, P.J. Kadowitz and C.A. Gruetter, *J. Pharm. Exp. Ther.*, 1981, **218**, 739.
79. J.S. Stamler, D.I. Simon, J.A. Osborne, M.E. Mullins, O. Jaraki, T. Michel, D.J. Singel and J. Loscalzo, *Proc. Natl. Acad. Sci., USA*, 1992, **89**, 444.
80. E.A. Kowaluk, R. Poliszczuk and H.L. Fung, *Eur. J. Pharmacol.*, 1987, **144**, 379.
81. J. Ramirez, L. Yu, J. Li, P.G. Braunschweiger and P.G. Wang, *Bioorg. Med. Chem. Lett.*, 1996, **6**, 2575.
82. P. Needleman and E.M. Johnson, *J. Pharmacol. Exp. Ther.*, 1973, **184**, 709.
83. L.J. Ignarro, J.C. Edwards, D.Y. Gruetter, B.K. Barry and C.A. Gruetter, *FEBS Lett.*, 1980, **110**, 275.
84. M. Feelisch and E. Noack, *Eur. J. Pharmacol.*, 1987, **142**, 465.
85. J. D. Artz, K. X. Yang, J. Lock, C. Sanchez, B.M. Bennett and G.R.J. Thatcher, *J. Chem. Soc., Chem. Commun.*, 1996, 927, D.R. Cameron, A.M.P. Borrajo, B.M. Bennett and G.R.J. Thatcher, *Can. J. Chem.*, 1995, **73**, 1627.

86. D.L.H. Williams, *Nitrosation*, Cambridge University Press, Cambridge, 1988, 169.
87. J. Ramón Leis and A. Ríos, *J. Chem. Soc., Chem. Commun.*, 1995, 169.
88. N.B. Grigor'ev, V.I. Levina, S.A. Shevelev, I.L. Dalinger and V.G. Granik, *Mendeleev Commun.*, 1996, 1, 11.
89. M. Feelisch, K. Schönafinger and E. Noack, *Biochem. Pharmacol.*, 1992, **44**, 1149.
90. C.J. Thoman and I.M. Hunsberger, *J. Org. Chem.*, 1968, **33**, 2852.
91. K. Rehse, K.J. Schleifer, E. Ludtke and E. Bohme, *Archiv der Pharmazie*, 1994, **327**, 359.
92. F.W. Flitney and G. Kennovin, *J. Physiol.*, 1987, **392**, 43P.
93. S.S. Sung, C. Glidewell, A.R. Butler and R. Hoffmann, *Inorg. Chem.*, 1985, **24**, 3856.
94. F.W. Flitney, I.L. Megson, D.E. Flitney and A.R. Butler, *Brit. J. Pharmacol.*, 1992, **107**, 842.
95. E.A. Morlino, L.A. Walker II, R.J. Sension and M.A.J. Rodgers, *J. Am. Chem. Soc.*, 1995, **117**, 4429.
96. J.F. Kerwin Jr., J.R. Lancaster Jr. and P.L. Feldman, *J. Med. Chem.*, 1995, **38**, 732.
97. F. Bottomley, *Coord. Chem. Rev.*, 1978, **26**, 7.
98. N.A. Davies, M.T. Wilson, E. Slade, S.P. Fricker, B.A. Murrer, N.A. Powell and G.R. Henderson, *J. Chem. Soc., Chem. Commun.*, 1997, 47.
99. A.A. Diamantis and J.V. Dubrawski, *Inorg. Chem.*, 1981, **20**, 1142.

Chapter 2

Mechanistic Studies of Copper Catalysed Nitric Oxide Formation from S-Nitrosothiols

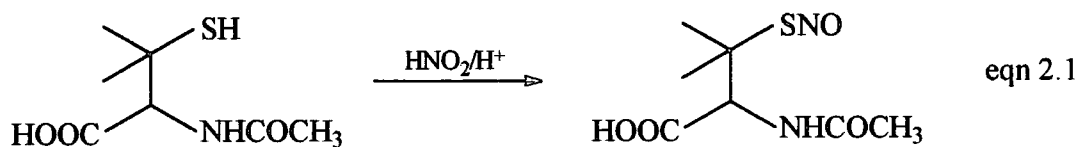
Chapter 2: Mechanistic Studies of Copper Catalysed Nitric Oxide Formation from S-Nitrosothiols

2.1 Introduction

The potential importance of S-nitrosothiols as i) alternative nitric oxide releasing drugs, and ii) storage and transport forms of NO *in vivo* has already been discussed (section 1.5.2.1). It appears that the copper ion mediated decomposition pathway of these compounds is of great significance *in vitro*¹. Askew *et al*² have described in detail the effect of adding Cu²⁺ to S-nitrosothiol solutions and proposed a catalytic mechanism. However, the rate law (given by rate = $k_2[\text{Cu}^{2+}][\text{RSNO}] + k'[\text{RSNO}]$) only appears to apply for a specific range of Cu²⁺ concentrations which may differ from one nitrosothiol to the next. Outside this "window" of copper ion concentrations other kinetic patterns become dominant. At low [Cu²⁺] distinct induction periods are often observed and the reaction appears autocatalytic, whereas on occasions a zero order dependence upon [RSNO] is noted. In addition, a wide range of situations occur where the kinetics are of an intermediate order. Clearly, the mechanism of this reaction has not yet been fully deduced and further work is required to explain all the experimental results collected.

2.2 Synthesis of a Stable S-Nitrosothiol

S-nitroso-N-acetylpenicillamine (SNAP) was prepared (equation 2.1) as described by Field *et al*³ with some slight alteration. 4.78g of N-acetylpenicillamine was dissolved in a 1:1 mixture (300ml) of methanol and 1 mol dm⁻³ HCl with 20ml of concentrated sulfuric acid. The reaction vessel was covered with aluminium foil to minimise disulfide dimer formation by photolysis and cooled to 0°C in an ice bath. A solution of sodium nitrite (3.45g) was added slowly over ten minutes with vigorous stirring. After leaving overnight, a green solid with red reflections was precipitated, filtered and dried thoroughly in a vacuum desiccator.



The yield based on weight of product = 48.2%. Elemental analysis for SNAP requires C = 38.14%, H = 5.45% and N = 12.71%. Obtained: C = 38.12%, H = 5.63% and N = 13.00%.

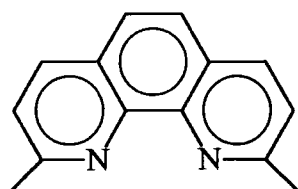
Melting point = 151-152°C dec., literature¹ = 153°C dec.

¹H NMR (Me₂SO-d₆): δ 1.86 (s, 3H), 1.93 (s, 3H), 1.95 (s, 3H), 5.15 (d, J=9Hz, 1H), 8.51 (d, J=9Hz, 1H). SNAP prepared in this manner was used in all subsequent kinetic experiments, unless otherwise stated.

2.3 Metal Ion Chelation Studies

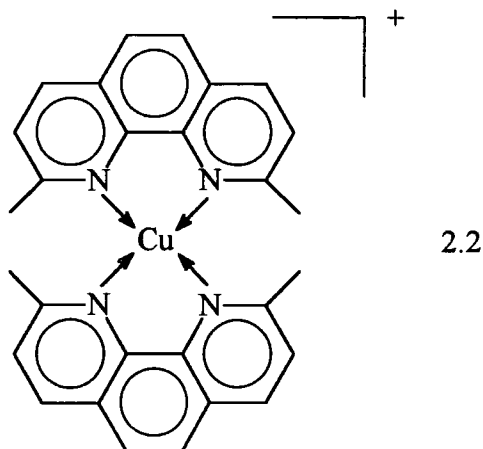
2.3.1 Neocuproine Chelation

As described in section 1.4.3.1, the addition of excess EDTA over Cu²⁺ to the reaction of S-nitrosothiols with copper ions causes inhibition of substrate decomposition³. EDTA favourably binds doubly charged metallic ions such as Cu(II), Ca(II) and Fe(II)⁴ and is also capable of Cu⁺ chelation. The zero order dependence on [nitrosothiol] (section 2.1) could be explained by rate limiting Cu²⁺ → Cu⁺ conversion by reduction. EPR experiments are not in favour of this taking place however as Cu⁺ could not be detected during the course of reaction. The use of a specific copper(I) ion chelator may prove advantageous in this instance. Such a compound is neocuproine⁵ (2,9-dimethyl-1,10-phenanthroline, 2.1).

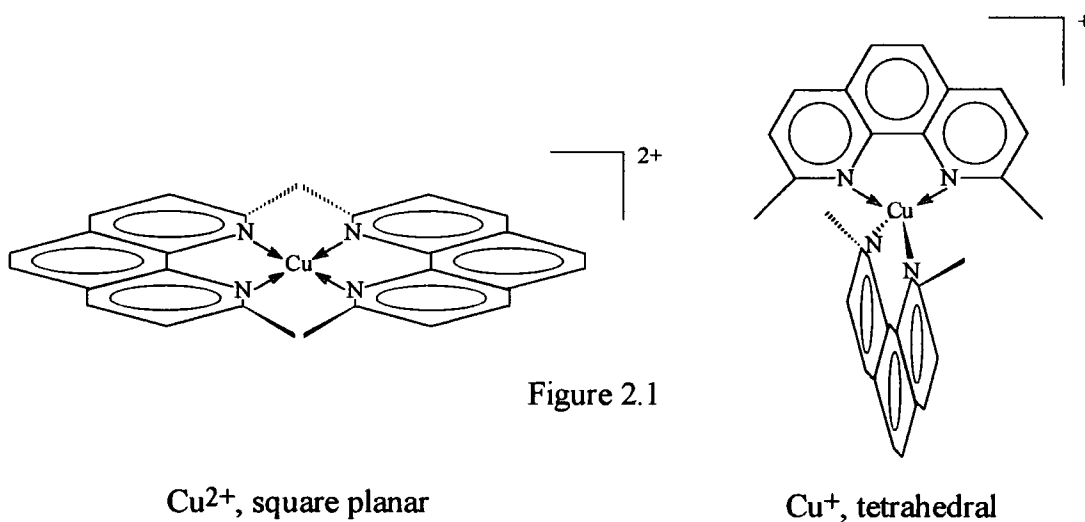


2.1

This chelator was first used for the detection of copper in steel by Smith and McCurdy⁶. It has the benefit of forming an adduct, $\text{Cu}(\text{NC})_2^+$, with Cu^+ (where NC represents neocuproine) which has an absorbance maximum at 453nm ($\epsilon = 7950 \text{ mol}^{-1} \text{ dm}^3 \text{ cm}^{-1}$) (2.2), away from the ultraviolet S-nitrosothiol peak at 330-350nm.

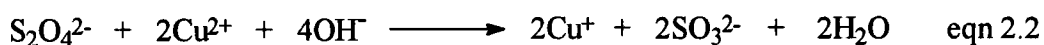


In aqueous solution, the stability constant of structure 2.2 is $1.2 \times 10^{19} \text{ mol}^{-2} \text{ dm}^6$.⁷ Its specificity for Cu^+ can be explained in terms of the electronic configurations of $\text{Cu}(\text{II})$ (d^9) and $\text{Cu}(\text{I})$ (d^{10}) and the resulting preferred geometries of these ions. Cupric complexes are usually square planar (or octahedral with Jahn-Teller distortions), whereas cuprous complexes are more likely to display tetrahedral coordination. The probable geometries exhibited in each instance are shown in figure 2.1.



Steric hindrance is considerable in the four coordinate Cu^{2+} complex due to the interaction of methyl groups whereas no such destabilisation is expected in the cuprous ion case.

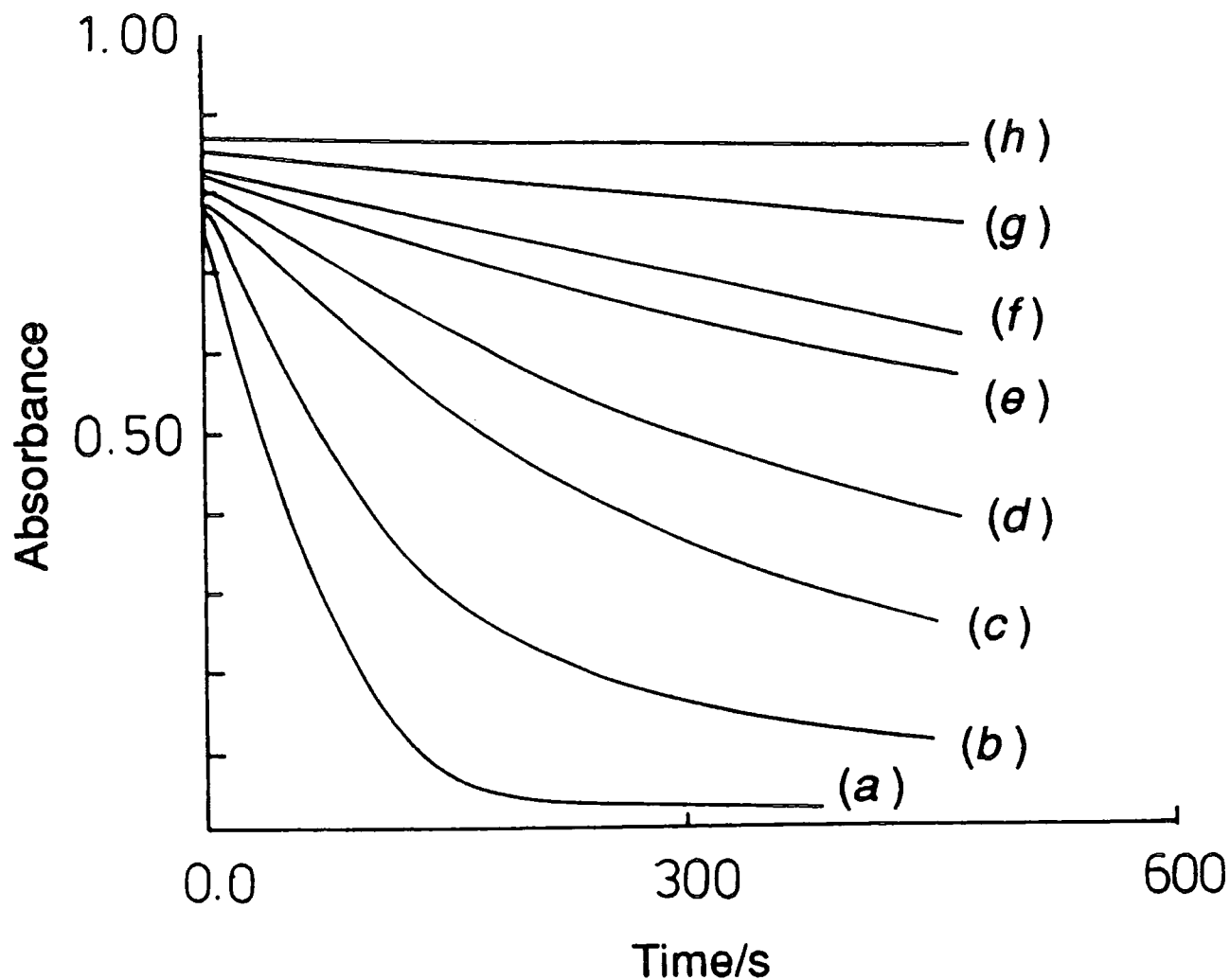
The uv/visible spectrum of $2 \times 10^{-5} \text{ mol dm}^{-3} \text{ Cu}^{2+}$ (added as $\text{CuSO}_4 \cdot 5\text{H}_2\text{O}$) and $4 \times 10^{-5} \text{ mol dm}^{-3}$ neocuproine hydrochloride trihydrate in 0.12 mol dm^{-3} phosphate buffer (pH 7.4) was no different to the equivalent spectrum of neocuproine alone. This indicates the reluctance of neocuproine to chelate Cu^{2+} under these experimental conditions. On adding sodium dithionite, $\text{Na}_2\text{S}_2\text{O}_4$ to the initial copper(II) containing solution an immediate pale yellow colour was noted, along with a new absorbance maximum at 453nm, suggesting the formation of adduct 2.2. Dithionite acts as a reducing agent⁸ (equation 2.2) in this case, forming Cu^+ which becomes trapped by neocuproine.



Having demonstrated the specificity of neocuproine towards copper(I) ions, the decomposition of SNAP ($1 \times 10^{-3} \text{ mol dm}^{-3}$) at pH 7.4 was followed spectrophotometrically at 340nm by monitoring the decrease in absorbance as a function of time. Initially Cu^{2+} ($2 \times 10^{-5} \text{ mol dm}^{-3}$) alone was added and trace (a) (figure 2.2) obtained. Following this varying concentrations of neocuproine were added in the range $4 \times 10^{-5} - 1 \times 10^{-3} \text{ mol dm}^{-3}$. Initial observations indicated that the addition of neocuproine slowed the denitrosation reaction until complete inhibition is attained at $> 10^{-3} \text{ mol dm}^{-3}$. The reduction in rate was accompanied by an increase in absorbance at 453nm, indicative of Cu^+ /neocuproine adduct formation. There must be a competitive complexation effect occurring between copper(I), SNAP and neocuproine. It is only when $[\text{neocuproine}] > [\text{SNAP}]$ that the reaction is entirely prevented.

Figure 2.2

Traces showing the decomposition of SNAP ($1 \times 10^{-3} \text{ mol dm}^{-3}$) in the presence of $2 \times 10^{-5} \text{ mol dm}^{-3} \text{ Cu}^{2+}$ and varying neocuproine concentrations



- (a) no added neocuproine; (b) $4 \times 10^{-5} \text{ mol dm}^{-3}$ neocuproine;
(c) $5 \times 10^{-5} \text{ mol dm}^{-3}$ neocuproine; (d) $6 \times 10^{-5} \text{ mol dm}^{-3}$ neocuproine;
(e) $8 \times 10^{-5} \text{ mol dm}^{-3}$ neocuproine; (f) $1 \times 10^{-4} \text{ mol dm}^{-3}$ neocuproine;
(g) $2 \times 10^{-4} \text{ mol dm}^{-3}$ neocuproine; (h) $1 \times 10^{-3} \text{ mol dm}^{-3}$ neocuproine.

Similar experiments over a smaller range of neocuproine concentrations utilising a different solid sample of SNAP (with a different concentration of thiol impurity present) allowed quantification of this effect. Good first order exponentials

were obtained in each case and rate constants measured. The results are summarised in table 2.1 and figure 2.3.

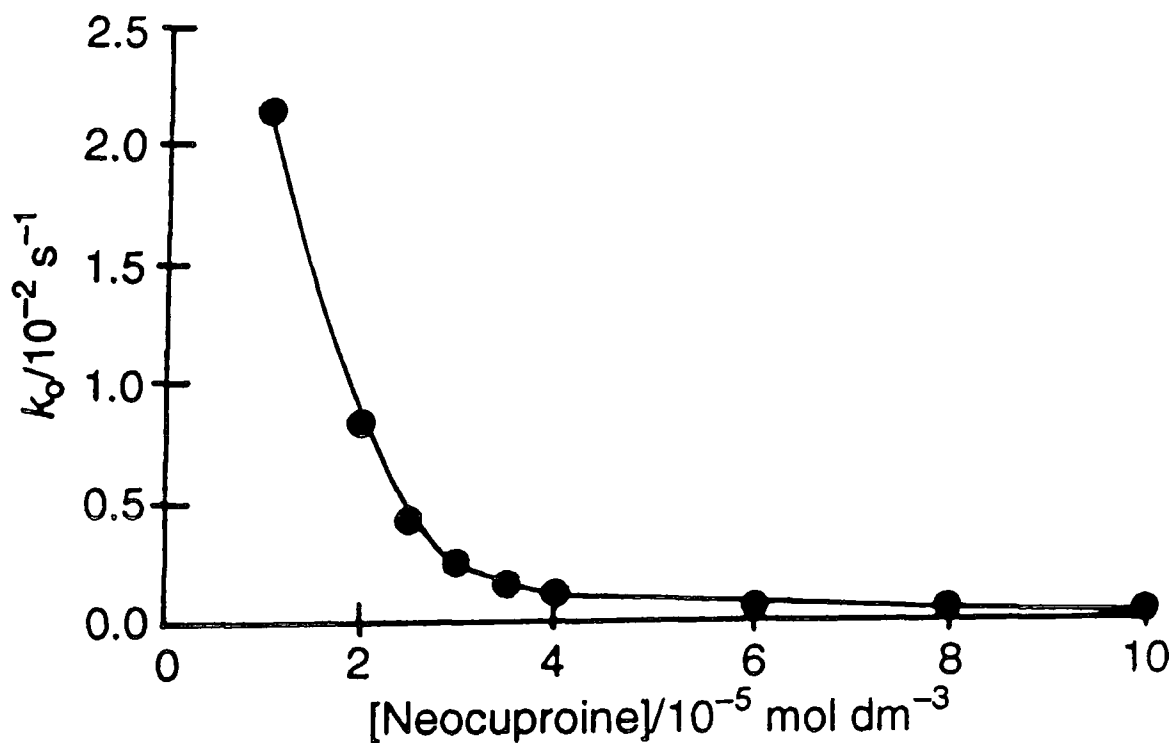
Table 2.1

Kinetic data for the effect of neocuproine on the decomposition of SNAP
($1 \times 10^{-3} \text{ mol dm}^{-3}$) in the presence of Cu^{2+} ($2 \times 10^{-5} \text{ mol dm}^{-3}$)

[neocuproine]/ $10^{-5} \text{ mol dm}^{-3}$	$k_{\text{obs}}/10^{-4} \text{ s}^{-1}$
1.0	214 ± 2
2.0	83 ± 1
2.5	43 ± 1
3.0	26 ± 0.9
3.5	16 ± 0.5
4.0	12 ± 0.4
6.0	6 ± 0.08
8.0	4 ± 0.04
10.0	3 ± 0.03

Figure 2.3

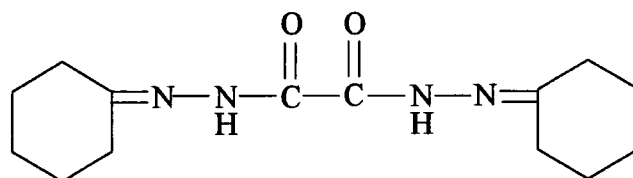
Plot of k_{obs} against added neocuproine concentration for the reaction of SNAP
($1 \times 10^{-3} \text{ mol dm}^{-3}$) in the presence of Cu^{2+} ($2 \times 10^{-5} \text{ mol dm}^{-3}$)



It is clear that cuprous copper is being generated throughout the reaction, with the possibility arising that it may be acting as the true catalytic species. The same trends were observed for other nitrosothiols, namely S-nitroso-2-(mercaptopropionyl)glycine and S-nitroso-2-N,N-dimethylaminoethanethiol. Having detected Cu^+ the use of a further metal ion chelator was employed as a mechanistic probe.

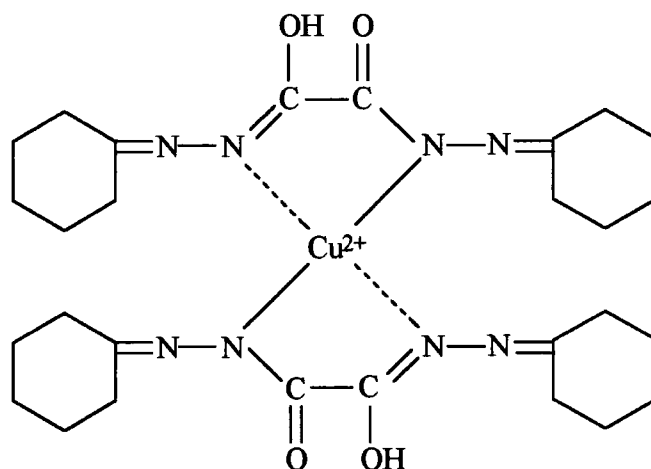
2.3.2 Cuprizone Chelation

Cuprizone (biscyclohexanoneoxalyldihydrazone, 2.3) is a specific Cu^{2+} chelator^{9,10}.



2.3

It is an extremely useful reagent under the required experimental conditions as the blue copper(II):cuprizone complex formed has a molar extinction coefficient of $16,000 \text{ mol}^{-1} \text{ dm}^3 \text{ cm}^{-1}$ at 600nm, meaning that micromolar quantities of Cu^{2+} can be detected. The chelator is soluble in most organic solvents and forms a 2:1 cuprizone: Cu^{2+} complex (2.4), but does not give a colour with any other cations or anions.

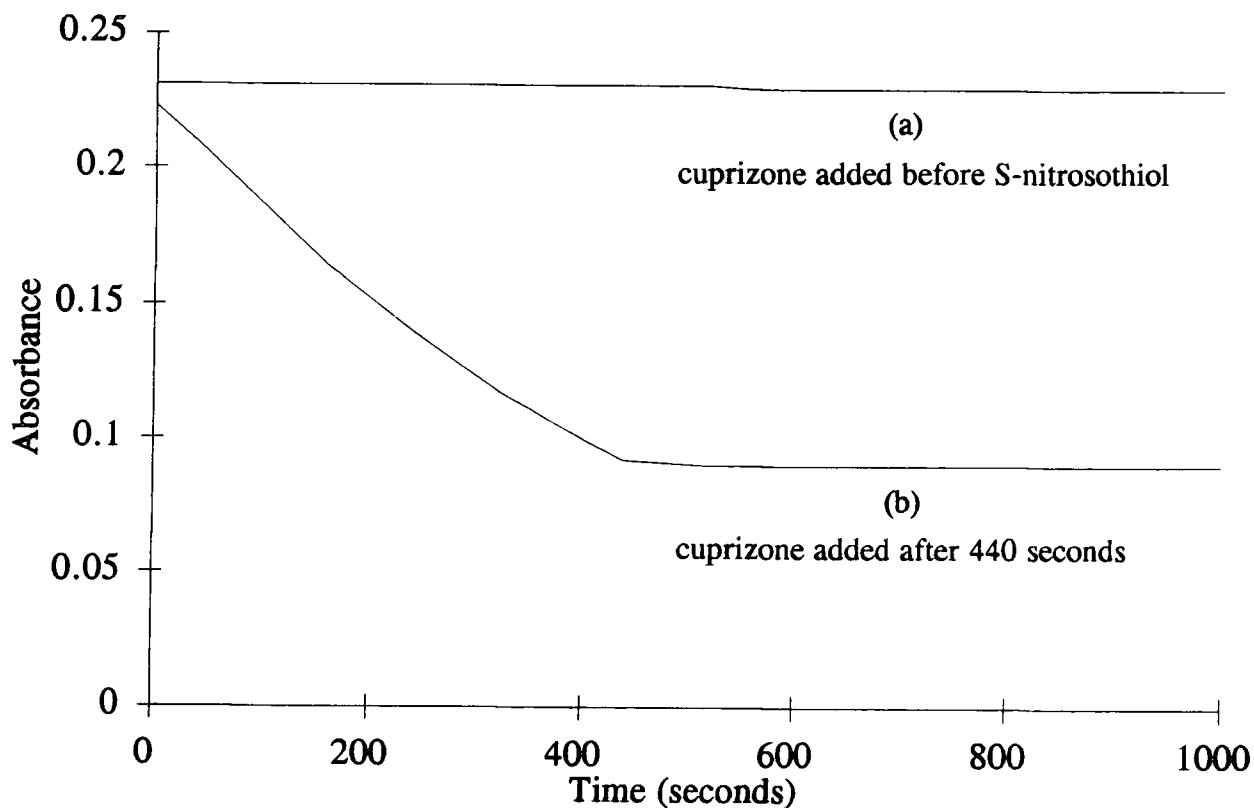


2.4

The specificity of this compound towards Cu^{2+} had been tested by addition of sodium dithionite (x 50 excess) to an aqueous solution of copper(II) sulfate pentahydrate and subsequent addition of cuprizone (x 4 excess)¹¹. No blue colouration or absorbance at 600nm was noted, due to the lack of chelation of cuprous copper. When SNAP ($1 \times 10^{-3} \text{ mol dm}^{-3}$) was allowed to decompose in the presence of Cu^{2+} ($2 \times 10^{-6} \text{ mol dm}^{-3}$), good first order kinetics were observed at 390nm, which is a more convenient wavelength at which to follow the reaction when cuprizone is added. Addition of this chelator ($2 \times 10^{-5} \text{ mol dm}^{-3}$) to the same system before the S-nitrosothiol is introduced leads to complete inhibition of reaction (figure 2.4, trace (a)). When decomposition is allowed to proceed for 440 seconds and then cuprizone added at the same concentration as before, reaction is again halted (figure 2.4, trace (b)).

Figure 2.4

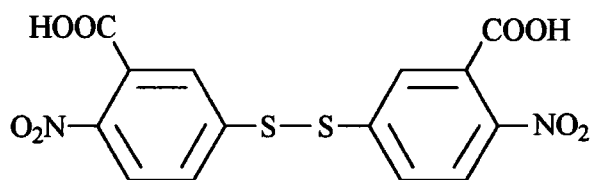
Traces showing the decomposition at 390nm of SNAP ($1 \times 10^{-3} \text{ mol dm}^{-3}$) in the presence of $2 \times 10^{-6} \text{ mol dm}^{-3} \text{ Cu}^{2+}$ and cuprizone ($2 \times 10^{-5} \text{ mol dm}^{-3}$)



During the acquisition of trace (b), the characteristic peak at $\lambda_{\text{max}} = 600\text{nm}$ is observed. This implies that during the decomposition of S-nitrosothiols such as SNAP, a redox mechanism is occurring where the interconversion of Cu^{2+} and Cu^{+} is taking place. Both these ions have now been detected during the course of reaction. The question now arises as to how cuprous ion can be generated *in situ*, and what reducing agents may be present to effect reduction of Cu^{2+} .

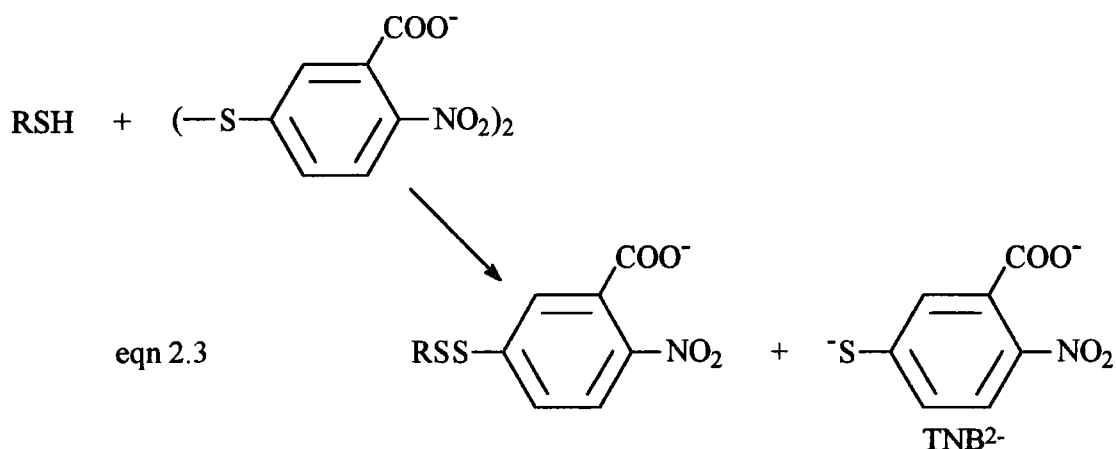
2.4 Detection of Thiolate in S-Nitrosothiol Solutions

In 1959, Ellman described the use of 5,5'-dithiobis(2-nitrobenzoic acid) (DTNB) (2.5) for quantitatively estimating free thiol groups in solution¹².



2.5

The method outlined is based on reaction of the thiol in question with DTNB to produce a mixed disulfide and 2-nitro-5-mercaptobenzoate dianion (TNB^{2-}) (equation 2.3).



Like all nitrothiophenolate dianions, TNB^{2-} has a deep colour (yellow in this instance) which can be used as a measurement of thiol concentration by noting the absorbance at 412nm. The molar extinction coefficient for TNB^{2-} at this wavelength¹³ has to be recorded using authentic thiol prior to analysis. This was performed by mixing

$5 \times 10^{-5} \text{ mol dm}^{-3}$ methanolic DTNB with $1 - 5 \times 10^{-5} \text{ mol dm}^{-3}$ N-acetylpenicillamine (NAP) at pH 7.4. Under these conditions a maximum absorbance at 412nm is attained after fifteen minutes so each solution was left for this period of time (table 2.2).

Table 2.2

Measured absorbance (412nm) for the reaction of N-acetylpenicillamine with DTNB ($5 \times 10^{-5} \text{ mol dm}^{-3}$), pH 7.4

[N-acetylpenicillamine]/ $10^{-5} \text{ mol dm}^{-3}$	Absorbance _{412nm}
1.0	0.150
2.0	0.285
3.0	0.412
4.0	0.554
5.0	0.697

From these results, $\epsilon_{412\text{nm}} = 13,630 \pm 180 \text{ mol}^{-1} \text{ dm}^3 \text{ cm}^{-1}$. This is in excellent agreement with Ellman's original publication¹² which quotes a value of $13,600 \text{ mol}^{-1} \text{ dm}^3 \text{ cm}^{-1}$. Following this, the amount of thiol precursor present in a solid sample of SNAP was quantified by the addition of $5 \times 10^{-5} \text{ mol dm}^{-3}$ DTNB to $1.2 \times 10^{-3} \text{ mol dm}^{-3}$ nitrosothiol. This was repeated three more times with fresh SNAP solutions made up from the same solid preparation. The final absorbance at 412nm in each case was 0.249, 0.247, 0.251 and 0.252. $1.2 \times 10^{-3} \text{ mol dm}^{-3}$ SNAP has a residual absorbance of 0.110 at 412nm as does DTNB (0.01) which has to be subtracted (table 2.3) to give the absorbance due to TNB²⁻ alone.

Table 2.3

Measured and corrected absorbances (412nm) for the determination of [N-acetylpenicillamine] in a solid SNAP sample ($1.2 \times 10^{-3} \text{ mol dm}^{-3}$)

Measured absorbance	Corrected absorbance	[NAP]/ $10^{-6} \text{ mol dm}^{-3}$
0.249	0.129	9.46
0.247	0.127	9.31
0.251	0.131	9.61
0.252	0.132	9.68

The average [NAP] is therefore $9.51 \times 10^{-6} \text{ mol dm}^{-3}$ which represents 0.79% thiol present in the S-nitrosothiol solid sample. This experiment was conducted again under identical conditions using an *in situ* sample of SNAP which was generated as follows. Solid N-acetylpenicillamine and sodium nitrite were placed in a volumetric flask (1:1 molar ratio) and 5ml $0.4 \text{ mol dm}^{-3} \text{ HClO}_4$ added, followed by dilution with distilled water to the required concentration. In comparison, 0.47% NAP was detected in the *in situ* SNAP preparation, less than was present in the solid material. Repetition with a similar *in situ* preparation of S-nitroso-2-(mercaptopropionyl)glycine (SMPG) afforded 0.52% contaminant 2-(mercaptopropionyl)glycine (MPG). These results are summarised in table 2.4.

Table 2.4

Thiolate levels detected by Ellman's reagent in $1.2 \times 10^{-3} \text{ mol dm}^{-3}$ S-nitrosothiol solutions

S-nitrosothiol	% thiolate detected
SNAP (solid)	0.79
SNAP (<i>in situ</i>)	0.47
SMPG (<i>in situ</i>)	0.52

From these results it is clear that however the nitrosothiol is prepared there is always a trace amount of thiolate precursor present in solution. This suggests an element of reversibility when considering the mechanism of S-nitrosation. Recent work by Herves Beloso and Williams¹⁴ utilising Ellman's reagent (section 1.3.4) has demonstrated this in more detail. In the case of S-nitrosocysteine, 7.8% L-cysteine remains at equilibrium from a 1:1 ratio of reactants. This thiol level is reduced on standing, probably due to aerial oxidation and disulfide formation. As the [RSH]:[HNO₂] ratio is altered from 1:1 towards 1:2, the amount of thiol present at equilibrium is again decreased, as expected. A thorough investigation into the generality of this situation is currently in progress¹⁵. Gorren *et al*¹⁶ have reported the problems in synthesising stable solid S-nitrosothiols which are totally thiol-free. In conclusion, it appears that a reducing agent (namely thiolate) will be present in nitrosothiol samples i) made up in acidic solution *in situ* and ii) prepared by dissolution and dilution of solid material such as SNAP. This may have great significance in terms of possible mechanisms of nitrosothiol decomposition.

2.5 Addition of Reducing Agents to S-Nitrosothiols in the Presence of Cu²⁺

2.5.1 Effect of Adding N-Acetylpenicillamine to SNAP

Section 2.3.1 describes the detection of cuprous copper during the course of the decomposition of S-nitrosothiols. It remains to be established how the apparent reduction of copper(II) can take place. It is not thought that nitrosothiols themselves are capable of performing this process, but it has been determined that thiolate is present in micromolar quantities in various nitrosothiol samples (section 2.4). These anions are themselves oxidised to thiyl radicals on reduction of Cu²⁺¹⁷ (equation 2.4).



There are three possibilities for the effect the thiol group may have on the copper ion mediated reaction:

i) there will be no kinetically observable effect.

ii) the added thiol will competitively complex Cu^{2+} and/or Cu^+ , thus slowing the rate of decomposition.

iii) the added thiol will reduce copper(II) to copper(I), presumably increasing the rate of reaction.

Initially, work was undertaken with SNAP, adding the corresponding thiol N-acetylpenicillamine. Use of a different thiol would complicate matters due to the rapid transfer of the NO group from RSNO to R'SH (transnitrosation) leading to the formation of R'SNO as the product¹⁸. SNAP ($1 \times 10^{-3} \text{ mol dm}^{-3}$) was firstly reacted with Cu^{2+} ($1 \times 10^{-5} \text{ mol dm}^{-3}$) alone at physiological pH. Then NAP was added over the range $1 \times 10^{-6} - 1 \times 10^{-3} \text{ mol dm}^{-3}$. Reactions were all kinetically first order, with the rate constants listed in table 2.5 and displayed more clearly in figures 2.5 and 2.6.

Table 2.5

Kinetic data for the decomposition of SNAP ($1 \times 10^{-3} \text{ mol dm}^{-3}$) in the presence of Cu^{2+} ($1 \times 10^{-5} \text{ mol dm}^{-3}$) and added NAP at pH 7.4

$[\text{NAP}]_{\text{added}}/10^{-6} \text{ mol dm}^{-3}$	$k_{\text{obs}}/10^{-3} \text{ s}^{-1}$
0	4.97 ± 0.02
1.0	5.63 ± 0.01
2.0	6.25 ± 0.01
3.0	8.35 ± 0.01
4.0	10.4 ± 0.02
5.0	11.9 ± 0.02
6.0	12.8 ± 0.02
7.0	14.0 ± 0.02
8.0	15.3 ± 0.02
9.0	16.6 ± 0.02
10	17.4 ± 0.03
20	21.7 ± 0.04
30	18.7 ± 0.07
40	14.5 ± 0.06
50	10.9 ± 0.05
90	6.79 ± 0.02
200	4.14 ± 0.01
300	3.37 ± 0.01
500	2.67 ± 0.01
1000	2.12 ± 0.01

Figure 2.5

Plot of k_{obs} against added NAP concentration (4×10^{-6} - 9×10^{-6} mol dm $^{-3}$) for the reaction of SNAP (1×10^{-3} mol dm $^{-3}$) in the presence of Cu $^{2+}$ (1×10^{-5} mol dm $^{-3}$)

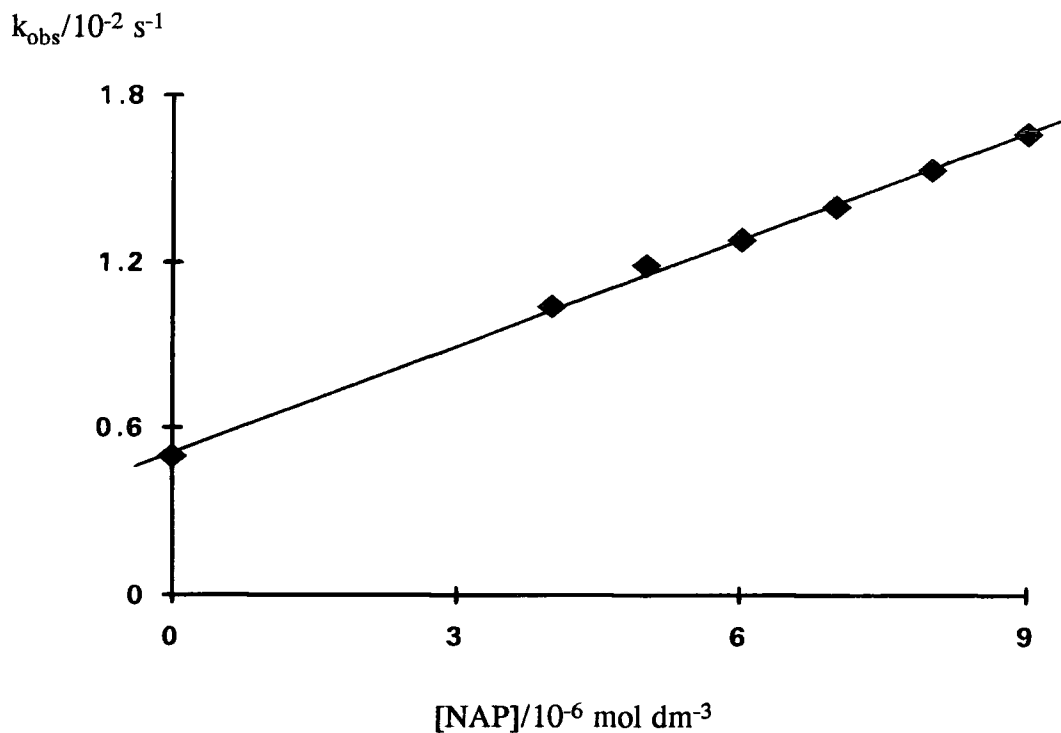
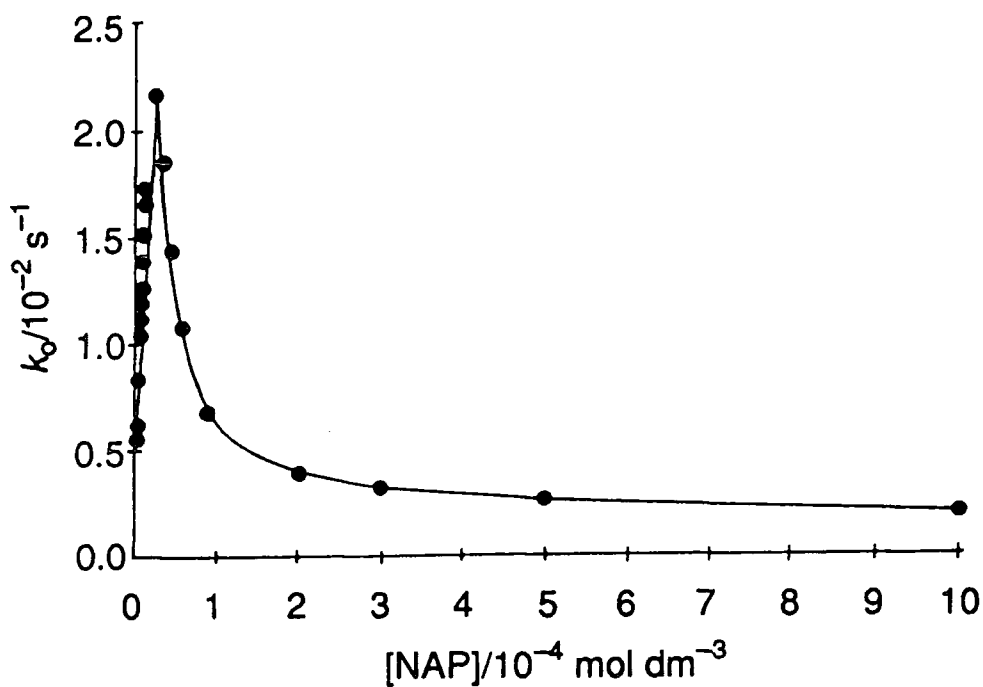
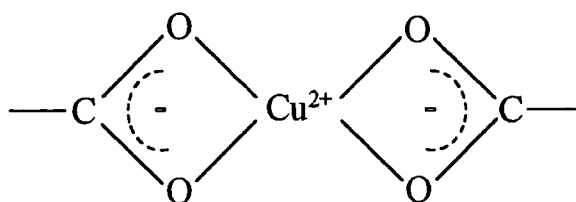


Figure 2.6

Plot of k_{obs} against added NAP concentration (1×10^{-6} - 1×10^{-3} mol dm $^{-3}$) for the reaction of SNAP (1×10^{-3} mol dm $^{-3}$) in the presence of Cu $^{2+}$ (1×10^{-5} mol dm $^{-3}$)

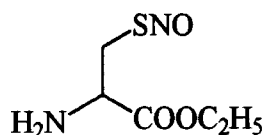


From figure 2.6 two general trends are observable for the addition of NAP to SNAP. When $[\text{Cu}^{2+}]_{\text{added}} > [\text{NAP}]_{\text{added}}$ (figure 2.5) the reaction is distinctly catalysed and a linear increase in the rate constant is apparent. At these concentrations NAP cannot act as a competitive chelator and is acting solely as a reducing agent, generating Cu^+ which appears to be acting as the true reaction catalyst. At higher $[\text{NAP}]$ however ($> 3 \times 10^{-5} \text{ mol dm}^{-3}$) there is a sharp decrease in the observed rate constant which eventually moves towards zero. This can be explained by the subsequent complexation of Cu^{2+} and/or Cu^+ by NAP, which effectively makes these ions unavailable for catalysis. Chelation may possibly occur at the carboxylate group of NAP (2.6) at these high concentrations, such complexes have previously been structurally analysed and isolated¹⁹.



2.6

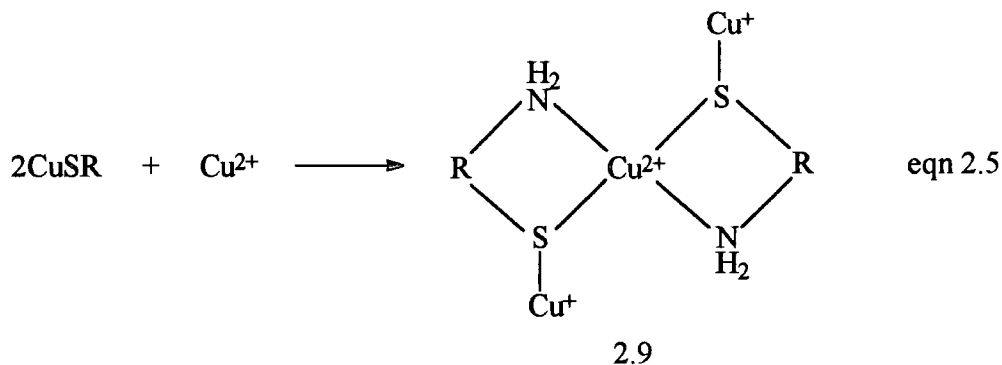
These results indicate that a large problem exists when attempting to interpret literature rate constant values which have been measured relating to S-nitrosothiol decomposition. Arnelle and Stamler²⁰ have reported half lives for the nitrosothiol derived from L-cysteine ethyl ester (2.7) as being 17 seconds, 122 minutes and 6.7 hours as measured by three separate assays.



2.7

This enormous discrepancy can now be seen to be in part due to the varying amount of thiol present in each nitrosothiol sample. Not only is the copper ion concentration of great significance but also [thiolate ion]²¹ when nitric oxide release from these compounds is under scrutiny.

Under experimental conditions where $[\text{PEN}] > [\text{Cu}^{2+}]$, the pale yellow cuprous complex CuSR is formed. However, when $[\text{Cu}^{2+}] \geq [\text{PEN}]$ an intense violet complex ($\lambda_{\text{max}} = 520\text{nm}$, $\epsilon_{520\text{nm}} \sim 10^3 \text{ mol}^{-1} \text{ dm}^3 \text{ cm}^{-1}$)²⁶ is observed. This can be explained by equation 2.5.



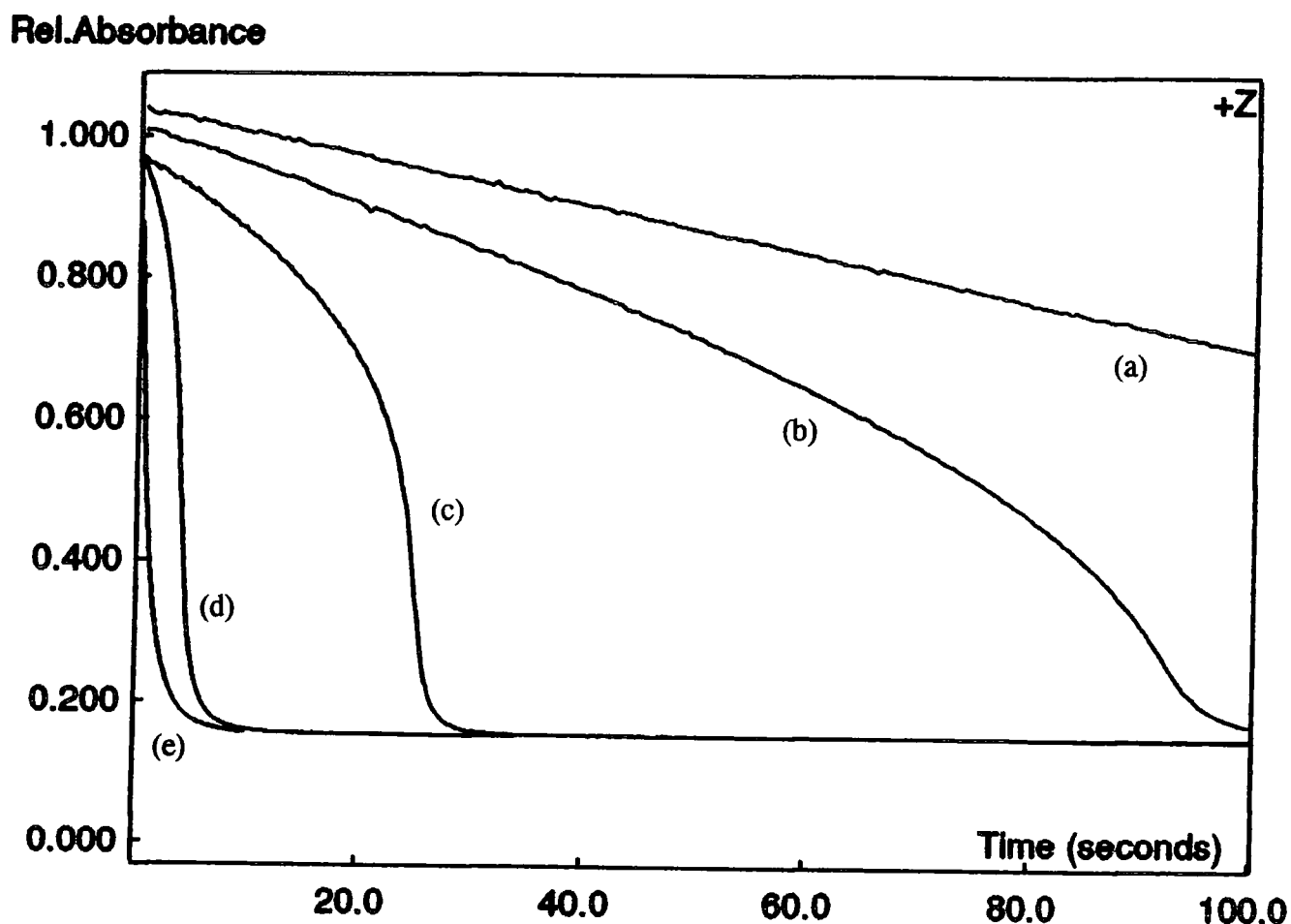
The violet species 2.9 is presumed to be a mixed valence complex whose visible absorbance is intensified by a charge transfer mechanism via sulfide bridges. The infrared spectrum of 2.9 shows the absence of a mercapto group stretching band near 2500 cm^{-1} and a band of coordinated amino group at 3400 cm^{-1} . This implies the presence of mercapto and amino group coordination in the mixed valence complex. Similar thiomalate:copper(I,II) species have been described in the literature²⁷. It appears that the gem methyl groups exert great stability on the violet complex as L-cysteine will not form such a chelate. It is evident that there is an extremely delicate balance between the ability to chelate and the ability to reduce Cu^{2+} where thiols are concerned, which will have a large bearing on S-nitrosothiol reactivity *in situ*.

With these concepts in mind, it is apparent that the penicillamine/S-nitrosopenicillamine system should be more complex in nature both in the presence and absence of added copper ions. Experiments were undertaken utilising S-nitrosopenicillamine ($1 \times 10^{-3} \text{ mol dm}^{-3}$) generated by the *in situ* nitrosation of PEN. In each instance five nitrosothiol solutions were made up, ranging from those containing an excess of NO_2^- to those containing an excess of PEN. Initially the $[\text{Cu}^{2+}]$ introduced was $1 \times 10^{-5} \text{ mol dm}^{-3}$. A large variation in the kinetic traces was

apparent (recorded on a stopped-flow spectrophotometer) according to which of the nitrosothiol solutions was reacted with copper(II) (figure 2.7).

Figure 2.7

Traces showing the decomposition of S-nitrosopenicillamine ($1 \times 10^{-3} \text{ mol dm}^{-3}$) in the presence of $1 \times 10^{-5} \text{ mol dm}^{-3} \text{ Cu}^{2+}$ and excess PEN or NO_2^-



- (a) $1.6 \times 10^{-4} \text{ mol dm}^{-3}$ excess PEN; (b) $8.0 \times 10^{-5} \text{ mol dm}^{-3}$ excess PEN;
(c) no excess PEN or NO_2^- ; (d) $9.0 \times 10^{-5} \text{ mol dm}^{-3}$ excess NO_2^- ;
(e) $1.8 \times 10^{-4} \text{ mol dm}^{-3}$ excess NO_2^- .

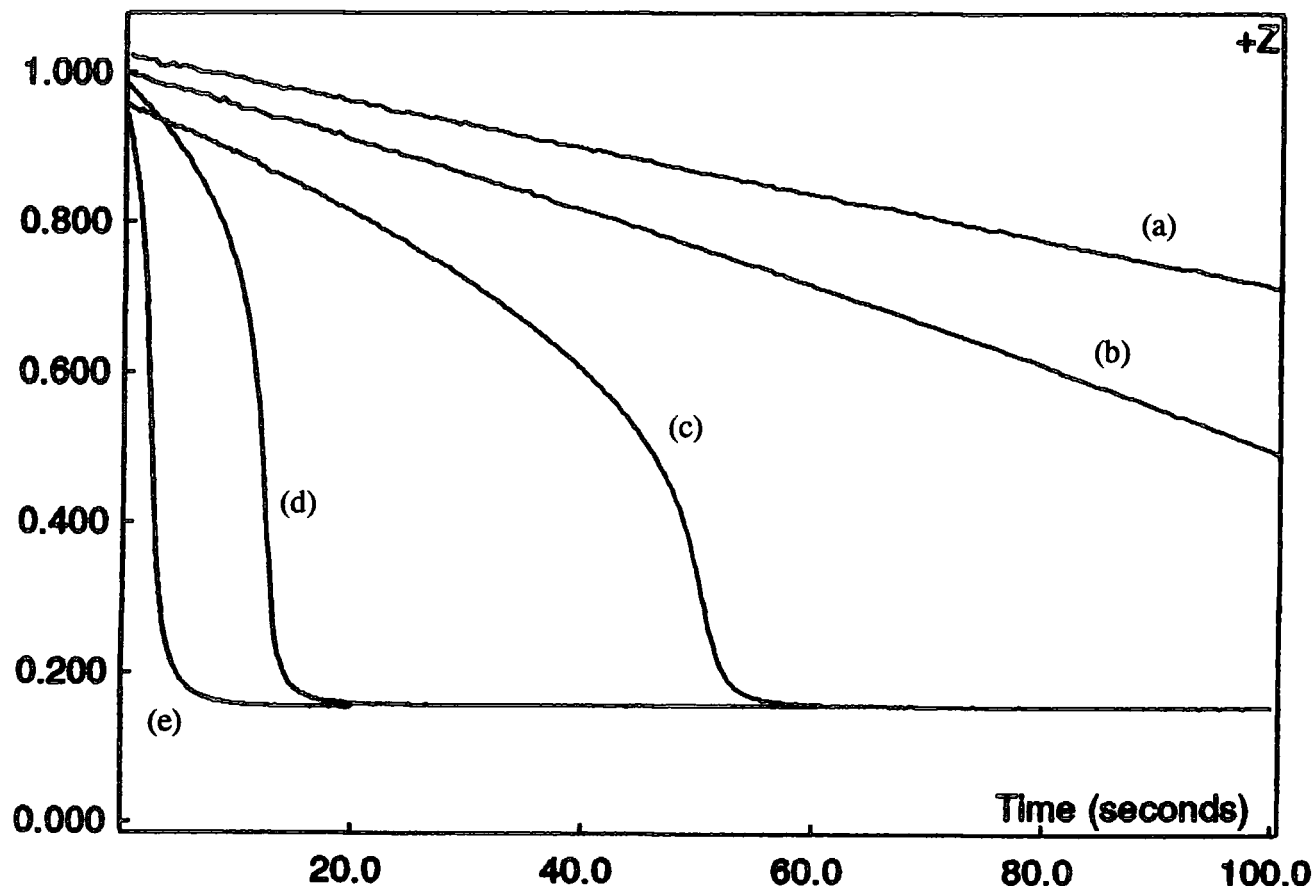
All kinetic runs were performed 20 minutes after initial thiol nitrosation.

When there is an excess of PEN (firstly $1.6 \times 10^{-4} \text{ mol dm}^{-3}$), reaction appears to be taking place very slowly. An induction period is apparent which is decreased on reducing the excess [PEN] to $8.0 \times 10^{-5} \text{ mol dm}^{-3}$. The presence of nitrite in a slight excess leads to even faster reactions where the induction period becomes less noticeable still, with reasonable first order kinetics being obeyed. These results, although seemingly unusual in character, can be explained if the complexing nature of PEN is taken into account. When PEN is present in excess, chelation of Cu^{2+} will take place which makes Cu^+ formation less possible. Eventually some copper(I) will be produced which will effect reaction and, as S-nitrosopenicillamine will bind Cu^+ particularly well, decomposition occurs readily. As the nitrite ion concentration is increased (and hence [PEN] decreased) the reaction becomes quicker due to less cupric ion chelation leading to more Cu^{2+} being available for Cu^+ formation. When this set of experiments was repeated under identical conditions (figure 2.8) but with S-nitrosothiol solutions used fifteen minutes after nitrosation the same kinetic trends were observed. However, the reactions in figure 2.8 are slower in comparison with their counterparts in figure 2.7, and thus an element of time dependence (or age of nitrosothiol solution) becomes significant, which is discussed in more detail in section 2.6.

Figure 2.8

Traces showing the decomposition of S-nitrosopenicillamine ($1 \times 10^{-3} \text{ mol dm}^{-3}$) in the presence of $1 \times 10^{-5} \text{ mol dm}^{-3} \text{ Cu}^{2+}$ and excess PEN or NO_2^-

Rel.Absorbance



- (a) $1.6 \times 10^{-4} \text{ mol dm}^{-3}$ excess PEN; (b) $8.0 \times 10^{-5} \text{ mol dm}^{-3}$ excess PEN;
(c) no excess PEN or NO_2^- ; (d) $9.0 \times 10^{-5} \text{ mol dm}^{-3}$ excess NO_2^- ;
(e) $1.8 \times 10^{-4} \text{ mol dm}^{-3}$ excess NO_2^- .

All kinetic runs were performed 15 minutes after initial thiol nitrosation.

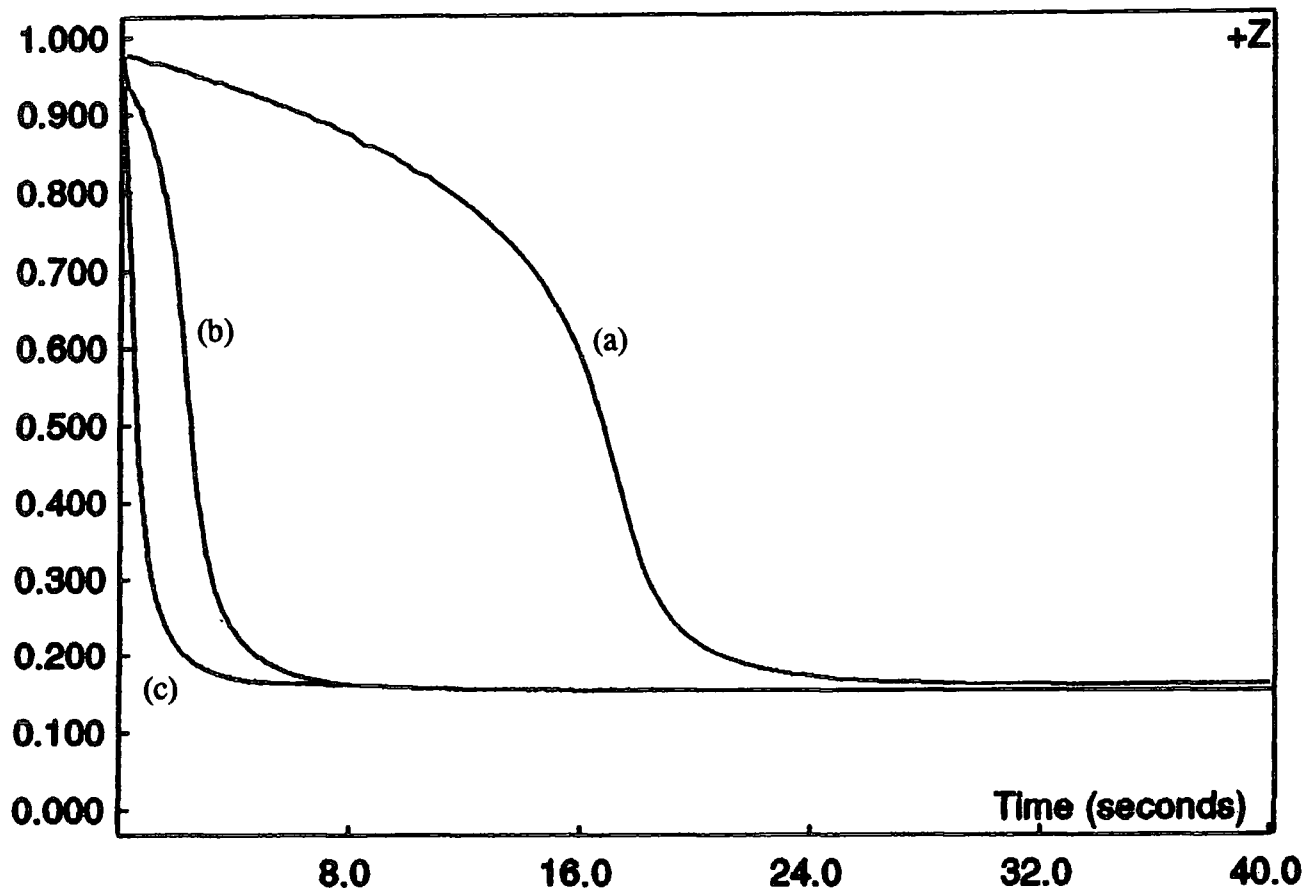
Figure 2.9 demonstrates the effect on reaction of altering the copper(II) ion concentration. As $[\text{Cu}^{2+}]$ is increased from $5 \times 10^{-6} - 2 \times 10^{-5} \text{ mol dm}^{-3}$ the rate of reaction increases with a clear depletion in the induction period. This suggests that

the formation of Cu^+ ions rather than cupric ion complexation with thiolate is favoured on increasing the $[\text{Cu}^{2+}]$.

Figure 2.9

Traces showing the effect of $[\text{Cu}^{2+}]$ on the decomposition of S-nitrosopenicillamine ($1 \times 10^{-3} \text{ mol dm}^{-3}$) in the presence of $1.8 \times 10^{-4} \text{ mol dm}^{-3}$ excess NO_2^-

Rel.Absorbance



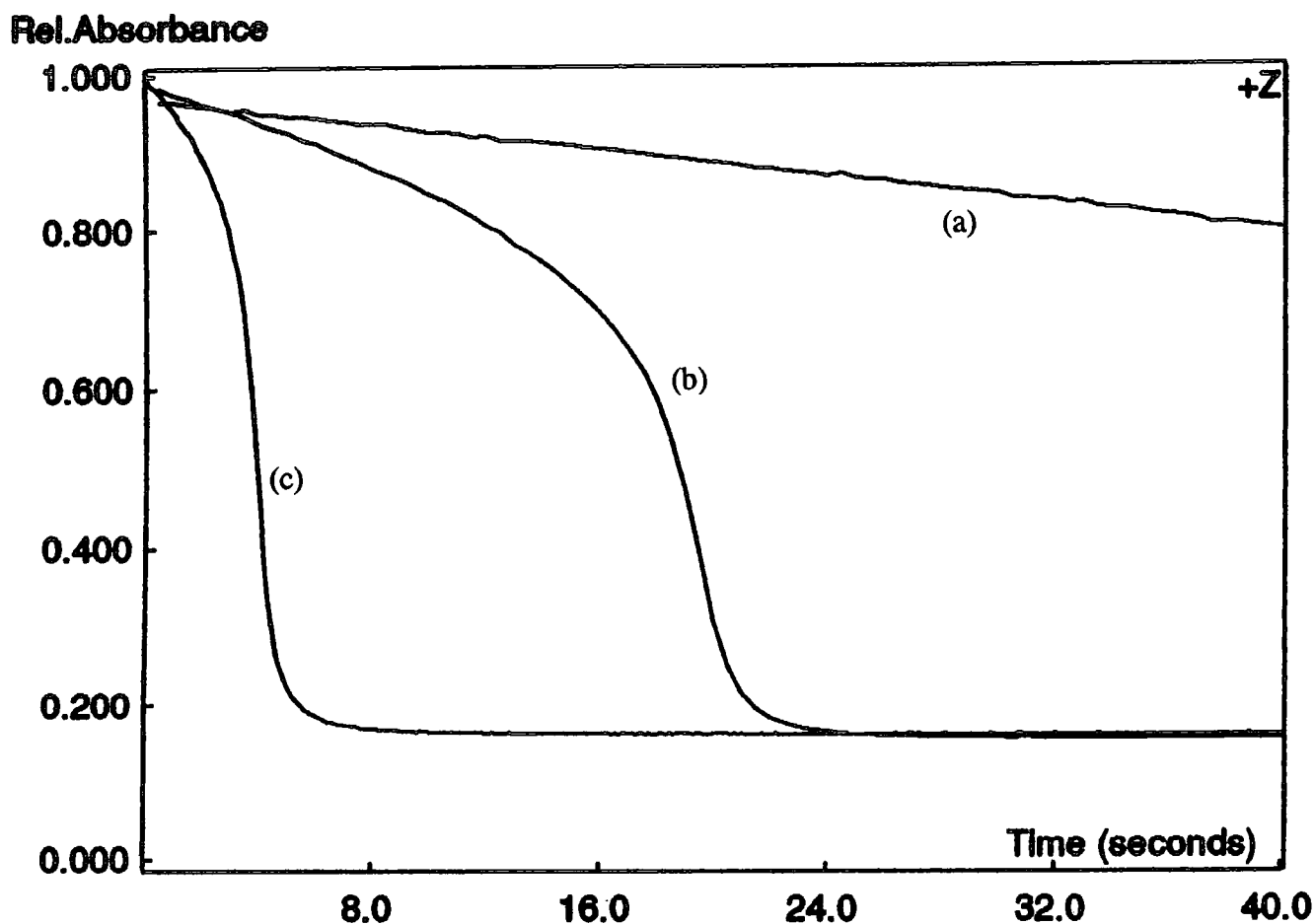
(a) $5 \times 10^{-6} \text{ mol dm}^{-3} \text{ Cu}^{2+}$; (b) $1 \times 10^{-5} \text{ mol dm}^{-3} \text{ Cu}^{2+}$; (c) $2 \times 10^{-5} \text{ mol dm}^{-3} \text{ Cu}^{2+}$.

All kinetic runs were performed 15 minutes after initial thiol nitrosation.

Figure 2.10 indicates the same trend noted previously (rate of reaction dependent on nitrosothiol solution age) when each solution was left for 10 minutes after S-nitrosothiol formation instead of for 15 minutes.

Figure 2.10

Traces showing the effect of $[\text{Cu}^{2+}]$ on the decomposition of S-nitrosopenicillamine ($1 \times 10^{-3} \text{ mol dm}^{-3}$) in the presence of $1.8 \times 10^{-4} \text{ mol dm}^{-3}$ excess NO_2^-



(a) $5 \times 10^{-6} \text{ mol dm}^{-3} \text{ Cu}^{2+}$; (b) $1 \times 10^{-5} \text{ mol dm}^{-3} \text{ Cu}^{2+}$; (c) $2 \times 10^{-5} \text{ mol dm}^{-3} \text{ Cu}^{2+}$.

All kinetic runs were performed 10 minutes after initial thiol nitrosation.

An interpretation of these results is that the dimercaptide complex (2.8) is formed reversibly whilst Cu^+ is formed in a parallel reaction of cupric copper with one thiolate anion (scheme 2.2).



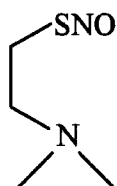
Scheme 2.2



It is clear from this scheme that the reaction profile is extremely dependent on [PEN], in that at high [PEN] complexation of cupric ions will be dominant and the rate of Cu^+ formation lowered, whereas at much lower [PEN] cuprous ion generation will be favoured and chelation of Cu^{2+} less significant. Addition of neocuproine to a solution of Cu^{2+} and PEN leads to the characteristic Cu^+ complex being formed at 453nm. The experimental data in this section confirms and extends previous work defining the role of Cu^+ in nitric oxide release from S-nitrosothiols but also implicates the corresponding thiol as an integral component of the reaction mechanism.

2.5.3 Further Examples

The S-nitrosothiol (2.10) derived from 2-N,N-dimethylaminoethanethiol (DMAET) was readily generated *in situ* and utilised in several kinetic experiments.

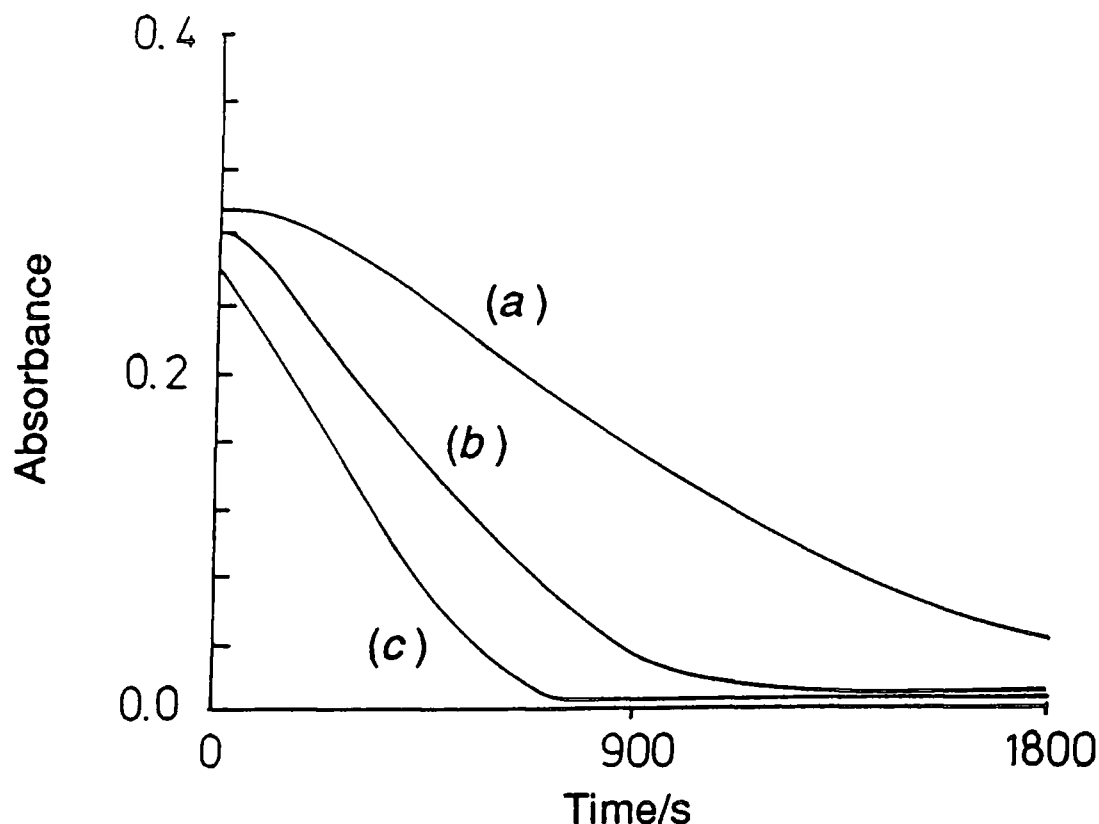


2.10

DMAET is known to be an extremely good metal complexing agent^{28,29} and hence it may be expected that adding this thiol to a solution of corresponding S-nitrosothiol should produce similar results to those obtained for S-nitrosopenicillamine. Indeed, on introducing DMAET (1×10^{-6} - 3×10^{-6} mol dm⁻³) to S-nitroso-2-N,N-dimethylaminoethanethiol (5×10^{-4} mol dm⁻³) and Cu^{2+} (1×10^{-6} mol dm⁻³), a progressive reduction of the apparent induction period is noted (figure 2.11).

Figure 2.11

Traces showing the reaction of S-nitroso-2-N,N-dimethylaminoethanethiol ($5 \times 10^{-4} \text{ mol dm}^{-3}$) in the presence of $1 \times 10^{-6} \text{ mol dm}^{-3} \text{ Cu}^{2+}$ and added DMAET

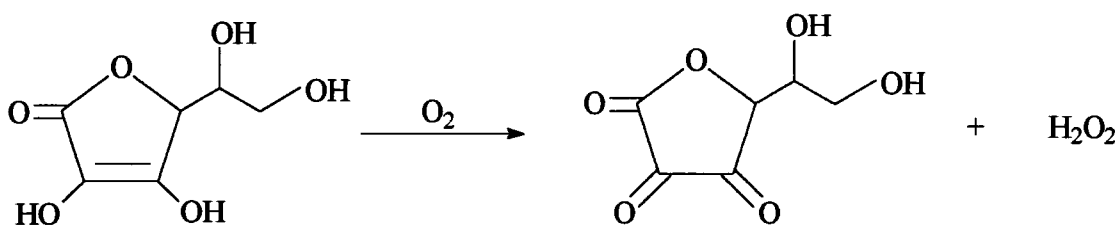


(a) no added thiol; (b) $1 \times 10^{-6} \text{ mol dm}^{-3}$ DMAET; (c) $3 \times 10^{-6} \text{ mol dm}^{-3}$ DMAET.

In accordance with this, increasing the copper(II) ion concentration in the absence of added DMAET produced a shorter induction period due to more Cu^+ being formed. Figure 2.11 clearly shows the appearance of a zero order dependence upon [RSNO]. This suggests that for a more reactive S-nitrosothiol such as S-nitroso-2-N,N-dimethylaminoethanethiol the rate of $\text{Cu}^{2+} \rightarrow \text{Cu}^+$ becomes rate limiting. It is likely that DMAET will chelate Cu^{2+} and hence produce an initial time period of no reaction (induction). When cuprous copper is generated (more quickly at higher [DMAET]) reaction can proceed as is usually observed. The reaction outlined in figure 2.11 was repeated under anaerobic conditions with all solutions rigorously

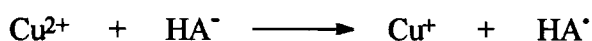
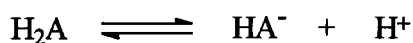
purged with nitrogen gas for thirty minutes prior to mixing, with identical results being afforded. This implies that any oxidation reaction (such as Cu^+ reforming Cu^{2+} by reaction with dissolved oxygen) is not significant under these experimental conditions. It has been demonstrated¹¹ that with more slowly reacting nitrosothiols such as S-nitroso-N-acetylcysteine the competing oxidation of Cu^+ is of much greater importance.

The effect of adding a different reducing agent (ascorbic acid) to the decomposition reaction of S-nitrosothiols was also investigated. Ascorbic acid (H_2A) is a reductant which will become oxidised to dehydroascorbic acid (A) in the presence of oxygen (equation 2.6)³⁰.



eqn 2.6

Xu and Jordan³¹ have more recently postulated the following mechanism for the direct reaction between Cu^{2+} and ascorbic acid (scheme 2.3).



Scheme 2.3

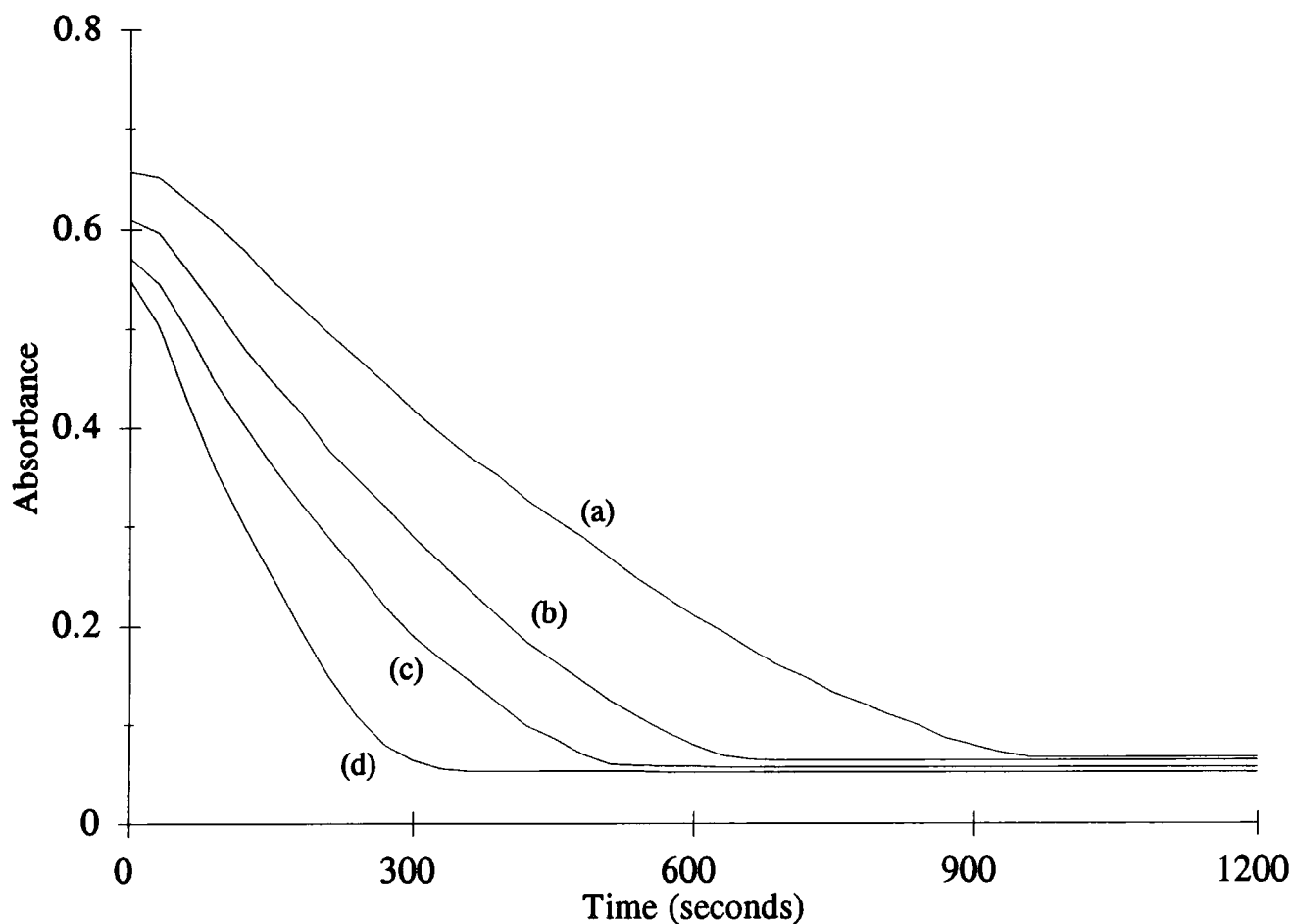


Copper(I) is generated initially by reduction of Cu^{2+} with the semiquinone ion HA^\bullet . The usage of ascorbic acid as a reducing agent in this instance is advantageous as, unlike PEN and DMAET, there are no complications associated with the chelation of metal ions. Ascorbic acid was therefore added to S-nitroso-2-N,N-dimethylaminoethanethiol ($1 \times 10^{-3} \text{ mol dm}^{-3}$) in the presence of $1 \times 10^{-6} \text{ mol dm}^{-3}$

Cu^{2+} (figure 2.12). Again, the reaction becomes faster in the presence of H_2A with a concomitant reduction in the induction period, as predicted.

Figure 2.12

Traces showing the reaction of S-nitroso-2-N,N-dimethylaminoethanethiol ($1 \times 10^{-3} \text{ mol dm}^{-3}$) in the presence of $1 \times 10^{-6} \text{ mol dm}^{-3} \text{ Cu}^{2+}$ and ascorbic acid



(a) no added ascorbic acid; (b) $1 \times 10^{-6} \text{ mol dm}^{-3}$ ascorbic acid;
(c) $5 \times 10^{-6} \text{ mol dm}^{-3}$ ascorbic acid; (d) $1 \times 10^{-5} \text{ mol dm}^{-3}$ ascorbic acid.

A more systematic study³² has indicated that NAP and ascorbic acid possess approximately equal reducing capabilities as the addition of both of these compounds to SNAP *in situ* (over the same range of concentration) leads to extremely similar kinetic traces. Scorza *et al*³³ have discussed the role of ascorbate in the release of nitric oxide from S-nitrosoalbumin and S-nitrosoglutathione present in human plasma.

This reductant was able to induce NO formation from these stable nitrosothiols, as was L-cysteine. It is suggested that metal ion dependent reactions are improbable in plasma due to the lack of availability of transition metals. Therefore, the mechanism of ascorbate mediated S-nitrosothiol decomposition is proposed to be via direct reductive activation (equation 2.7).



This reaction leads to the formation of ascorbyl radical and reduced thiol, which is at variance with the observed disulfide product detected *in vitro*. Although metal ions such as Cu^{2+} are not "freely" present in biological systems, their availability as peptide and protein chelates makes copper catalysed nitric oxide release a distinct possibility *in vivo*, which will be discussed in more detail in Chapter Three.

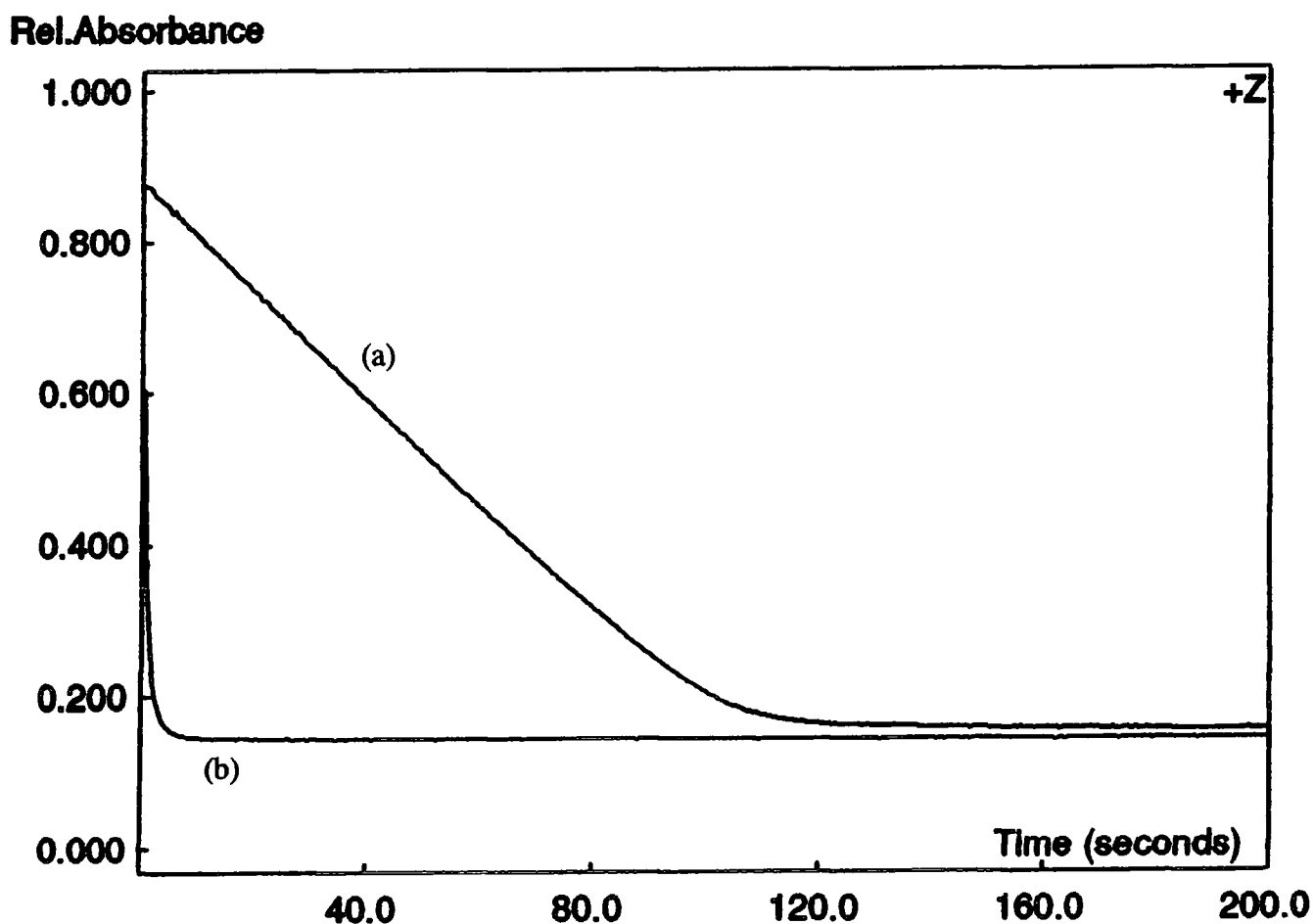
2.6 Time Dependent Reactions

As mentioned in section 2.5.2, the age of the S-nitrosothiol solution used for reaction is of great importance when interpreting kinetic results. S-nitrosopenicillamine ($1 \times 10^{-3} \text{ mol dm}^{-3}$) was generated *in situ* from a 1:1 ratio of PEN:nitrite. Cu^{2+} ($2 \times 10^{-5} \text{ mol dm}^{-3}$) in pH 7.4 buffer was introduced three minutes after initial thiol nitrosation and trace (a), figure 2.13 obtained. The nitrosothiol solution was left to stand for a further thirty-six minutes and the same kinetic run repeated (trace (b)). The absorbance/time plots indicate the initial observation of good zero order kinetics when the S-nitrosopenicillamine had just been made up, to reasonable first order traces as the nitrosothiol solution aged. These results make sense if, on standing, the thiol impurity present becomes oxidised to the disulfide. In effect this represents the same experiment as is described by figure 2.7, with decreasing PEN concentration having a significant rate enhancing effect. A possible interpretation is that after three minutes the concentration of thiol present is still relatively high leading to significant Cu^{2+} chelation. There is however a small concentration of cuprous ions available for reaction due to reduction of Cu^{2+} with the

rate determining step being the conversion of $\text{Cu}^{2+} \rightarrow \text{Cu}^+$ (and hence zero order kinetics). As the [PEN] is reduced a change in the rate determining step occurs as there is more cupric copper available for reaction, the slow step now involving RSNO ($\text{RSNO} + \text{Cu}^+ \rightarrow \text{RS}^- + \text{NO} + \text{Cu}^{2+}$). Work recently undertaken³² has shown the decrease of [PEN] in an S-nitrosopenicillamine solution as a function of time to be very substantial. This means that the kinetics noted now are first order in character. Exactly the same trend was attained for the decomposition of S-nitrosocysteine even though L-cysteine is a poorer chelator of Cu^{2+} than is PEN.

Figure 2.13

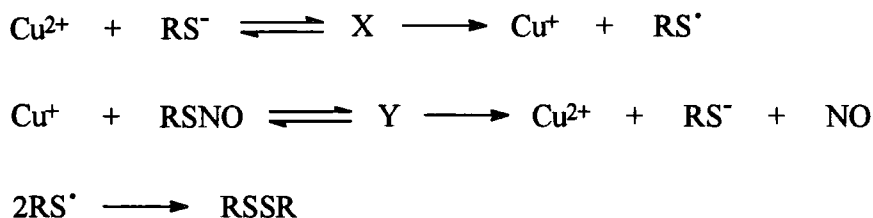
Traces showing the decomposition of S-nitrosopenicillamine ($1 \times 10^{-3} \text{ mol dm}^{-3}$) in the presence of $2 \times 10^{-5} \text{ mol dm}^{-3} \text{ Cu}^{2+}$ as a function of nitrosothiol solution age



(a) acquired three minutes after nitrosation; (b) acquired thirty-nine minutes after nitrosation.

2.7 Proposed Mechanism of S-Nitrosothiol Decomposition

From the results discussed, derived from chelation studies, thiolate detection and the effect of reducing agents on S-nitrosothiols, it is possible to postulate a general mechanism which will account for all the experimental kinetic data obtained. Four limiting absorbance/time traces are observed under varying conditions, they are (a) first order reaction with no induction period, (b) first order reaction with an induction period, (c) zero order reaction with no induction period, and (d) zero order reaction with an induction period. A general scheme (2.4) describes the mechanism in a broad manner.



Scheme 2.4

Following this mechanism, cupric copper is initially reduced by thiolate (detected using Ellman's reagent) via intermediate X (possibly RSCu^+) to generate Cu^+ and thiyl radical. Cu^+ subsequently binds to the S-nitrosothiol forming intermediate Y and thus is acting as the true catalytic species. Cu^{2+} is reformed as is RS^- , with nitric oxide also being released. Probable structures for intermediate Y are shown below (figure 2.14) with additional coordination to two water molecules in each case likely.

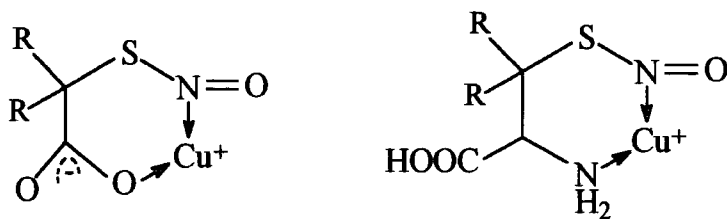
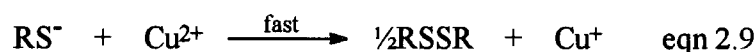


Figure 2.14

Two situations exist which relate to the formation of Cu^+ (trapped by neocuproine), which shall be considered in detail.

i) Rapid formation of Cu^+

If, as in most circumstances, thiolate, RSNO and Cu^{2+} are present prior to reaction then scheme 2.4 can be represented by equations 2.8 and 2.9.



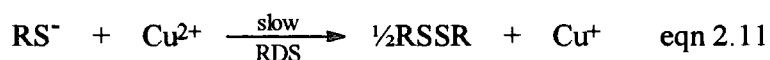
A first order rate equation will ensue (equation 2.10) as cuprous copper is quickly generated via thiolate reduction of Cu^{2+} (equation 2.9).

$$\frac{-d[\text{RSNO}]}{dt} = k_{\text{obs}}[\text{RSNO}] \quad \text{eqn 2.10}$$

Copper(I) rapidly becomes reformed after complexation with RSNO and subsequent re-reduction of Cu^{2+} , so that $[\text{Cu}^+]$ remains constant at any time during a kinetic run. This behaviour is exhibited by S-nitrosothiols (and corresponding thiolates) which do not coordinate copper ions particularly well (such as SNAP and NAP). If however only RSNO and Cu^{2+} are initially available and the thiolate concentration is very low, an induction period will exist which represents the time it takes to form Cu^+ after which decomposition may proceed.

ii) Rate limiting formation of Cu^+

In this instance, scheme 2.4 may be reduced to equations 2.11 and 2.12.



If thiolate, cupric ion and RSNO are all initially present then a zero order reaction will be observed due to rate limiting cuprous ion formation (as seen in the case of S-nitrosopenicillamine). However, if only nitrosothiol and Cu^{2+} are available initially then an induction period will again be apparent before reduction of copper(II) takes place. The results of S-nitroso-2-N,N-dimethylaminoethanethiol decomposition *in situ* indicate this to good effect. In general terms zero order behaviour is noted when studying compounds which chelate copper ions rather strongly, such as S-nitrosopenicillamine and PEN.

It is clear from the kinetic evidence obtained and the use of selective chelating agents that Cu^+ is in fact the effective species implicated in nitric oxide formation from S-nitrosothiols. The mechanism outlined in scheme 2.4 accounts for data collected and reported from several sources^{2,16,20}. Details such as the decomposition of intermediate Y still have to be established, as does the reactivity pattern of such compounds in the presence of other biological forms of Cu^{2+} .

2.8 Conclusion

These experimental results could feasibly have important implications for the decomposition of S-nitrosothiols *in vivo*. It has been well documented (section 1.5.2.1) that these compounds are linked to the inhibition of platelet aggregation³⁴, vasodilation³⁵ and other physiological processes. Gorge *et al*³⁶ have proposed the role of a copper(I) dependent enzyme in the anti-platelet action of S-nitrosoglutathione (GSNO) based on the specific binding of bathocuproine sulfonate (BPS) to a structure on the platelet surface. BPS (a specific Cu^+ chelator) causes a parallel reduction in

platelet aggregation inhibition by GSNO. This suggests that GSNO generates nitric oxide via a mechanism involving copper(I) in the biological milieu. Ioannidis *et al*³⁷ have noted the increased potency of SNAP under hypoxic (oxygen depleted) conditions in terms of cytotoxic effects towards other cells. This phenomenon has been attributed to the anaerobic environment maintaining the presence of more Cu⁺ which acts as the active catalyst for NO formation *in vivo*, as there is no competing oxidation of Cu⁺ → Cu²⁺. The role of copper ions is also postulated to be of great significance when examining the effects of an S-nitrosothiol as a NANC neurotransmitter^{38,39}. In contrast, another publication⁴⁰ attributes the bronchodilatory effects of GSNO and other nitrosothiols to the intact parent compound, without the need for prior release of NO. Therefore, there is some *in vivo* evidence to support the proposed *in vitro* mechanism of NO production from nitrosothiols but there is also a degree of uncertainty as to their precise mode of action at this time. Interestingly, GSNO has recently been used clinically⁴¹ as a treatment of pre-eclampsia, which is a high blood pressure condition suffered by some pregnant women. The possibility of such a Cu⁺ mediated reaction existing *in vivo* depends on the ability of thiolate to reduce copper(II) (present in a bound form with peptides and proteins) to produce a catalytically active species. This would provide greater mechanistic credibility than has been discussed thus far.

References

1. J. McAninly, D.L.H. Williams, S.C. Askew, A.R. Butler and C. Russell, *J. Chem. Soc., Chem. Commun.*, 1993, 1758.
2. S.C. Askew, D.J. Barnett, J. McAninly and D.L.H. Williams, *J. Chem. Soc., Perkin Trans. 2*, 1995, 741.
3. L. Field, R.V. Dilts, R. Ravichandran, P.G. Lenhert and G.E. Carnahan, *J. Chem. Soc., Chem. Commun.*, 1978, 249.
4. A. Vogel, *Textbook of Quantitative Inorganic Analysis*, Fourth Edn., Longman, 1978, 263.
5. A.R. Gahler, *Anal. Chem.*, 1954, **26**, 577, B.G. Stephens, H.L. Felkel Jr. and W.M. Spinelli, *ibid.*, 1974, **46**, 692.
6. G.F. Smith and W.H. McCurdy, *Anal. Chem.*, 1952, **24**, 371.
7. B.R. James and R.J.P. Williams, *J. Chem. Soc.*, 1961, 2007.
8. F.A. Cotton and G. Wilkinson, *Advanced Inorganic Chemistry*, Fourth Edn., Interscience, 1980, 535.
9. R.E. Peterson and M.E. Bollier, *Anal. Chem.*, 1955, **27**, 1195.
10. E. Jacobsen, F.J. Langmyhr and A.R. Selmer-Olsen, *Anal. Chim. Acta*, 1961, **24**, 579.
11. H.R. Swift, Ph.D. thesis, University of Durham, 1996.
12. G.L. Ellman, *Arch. Biochem. Biophys.*, 1959, **82**, 70.
13. P.W. Riddles, R.L. Blakeley and B. Zerner, *Anal. Biochem.*, 1979, **94**, 75.
14. P. Herves Beloso and D.L.H. Williams, *J. Chem. Soc., Chem. Commun.*, 1997, 89.
15. E. Li and D.L.H. Williams, unpublished results.
16. A.C.F. Gorren, A. Schrammel, K. Schmidt and B. Mayer., *Arch. Biochem. Biophys.*, 1996, **330**, 219.
17. F.J. Davis, B.C. Gilbert, R.O.C. Norman and M.C.R. Symons, *J. Chem. Soc., Perkin Trans. 2*, 1983, 1763.

18. D.J. Meyer, H. Kramer, N. Özer, B. Coles and B. Ketterer, *FEBS Lett.*, 1994, **345**, 117.
19. R.J. Doedens, *Prog. Inorg. Chem.*, 1976, **21**, 209.
20. D.R. Arnelle and J.S. Stamler, *Arch. Biochem. Biophys.*, 1995, **318**, 279.
21. D.L.H. Williams, *Tran. Met. Chem.*, 1996, **21**, 189.
22. D. Cavallini, C. De Marco, S. Dupre and G. Rotilio, *Arch. Biochem. Biophys.*, 1969, **130**, 354.
23. J.M. Walshe, *Am. J. Med.*, 1956, **21**, 487.
24. Y. Sugiura and H. Tanaka, *Chem. Pharm. Bull.*, 1970, **18**, 368.
25. J. Peisach and W.E. Blumberg, *Mol. Pharmacol.*, 1969, **5**, 200.
26. P. Day and D.W. Smith, *J. Chem. Soc. (A)*, 1967, 1045.
27. I.M. Klotz, G.H. Czerlinski and H.A. Fiess, *J. Am. Chem. Soc.*, 1958, **80**, 2920.
28. M.L. Mittal, R.S. Saxena and A.V. Pandey, *J. Inorg. Nucl. Chem.*, 1973, **35**, 1691.
29. P.C. Jain, D.K. Rastogi and H.L. Nigain, *Indian. J. Chem.*, 1971, **9**, 1308.
30. A. Weissberger and J.E. LuValle, *J. Am. Chem. Soc.*, 1944, **66**, 700.
31. J. Xu and R.B. Jordan, *Inorg. Chem.*, 1990, **29**, 2933.
32. P. Herves Beloso and D.L.H. Williams, to be published.
33. G. Scorza, D. Pietraforte and M. Minetti, *Free Rad. Biol. Med.*, 1997, **22**, 633.
34. M.W. Radomski, D.D. Rees, A. Noronha-Dutra and S. Moncada, *Brit. J. Pharmacol.*, 1992, **107**, 745.
35. L.J. Ignarro, H. Lipton, J.C. Edwards, W.H. Baricos, A.L. Hyman, P.J. Kadowitz and C.A. Gruetter, *J. Pharm. Exp. Ther.*, 1981, **218**, 739.
36. M.P. Gordge, J.S. Hothersall, G.H. Neild and A. Noronha-Dutra, *Brit. J. Pharmacol.*, 1996, **119**, 533.

37. I. Ioannidis, M. Bätz, T. Paul, H-G. Korth, R. Sustmann and H. DeGroot, *Biochem. J.*, 1996, **318**, 789.
38. J.G. DeMan, B.Y. DeWinter, G.E. Boeckxstaens, A.G. Herman and P.A. Pelckmans, *Gastroenterology*, 1996, **110**, A655.
39. J.G. DeMan, B.Y. DeWinter, G.E. Boeckxstaens, A.G. Herman and P.A. Pelckmans, *Brit. J. Pharmacol.*, 1996, **119**, 990.
40. G. Bannenberg, J. Xue, L. Engman, I. Cotgreave, P. Moldéus and Å. Ryrfeldt, *J. Pharmacol. Exp. Ther.*, 1995, **272**, 1238.
41. A. deBelder, C. Lees, J. Martin, S. Moncada and S. Campbell, *Lancet*, 1995, **345**, 124.

Chapter 3

Nitric Oxide Generation from S-Nitrosothiols using Amino Acid, Peptide and Protein Bound Forms of Cu²⁺

Chapter 3: Nitric Oxide Generation from S-Nitrosothiols using Amino Acid, Peptide and Protein Bound Forms of Cu²⁺

3.1 Introduction

The most common use of copper within biological systems is as an electron transfer component of oxidative enzymes. An example of such a species is galactose oxidase, which catalyses the oxidation of primary alcohols to aldehydes in sugars¹. Ionic copper is ideally suited to perform this task as Cu²⁺ is readily reduced and re-oxidised. In contrast, little signalling is thought to be undertaken by copper due to slow exchange rates existing, this being a response to strong Cu(I) and Cu(II) ligand binding. Indeed, a binding constant at pH 7 of 10¹⁵ is predicted for many copper complexes. The adult human body contains approximately 100mg of copper², with the highest concentrations being found in the liver, brain, heart and kidneys. Absorption of Cu(II) initially occurs in the gastrointestinal tract from where it enters the plasma (which has 1µg copper per ml present). Within the plasma 93 - 95% is bound to the glycoprotein ceruloplasmin, which is not in equilibrium with the tiny amount of ionic copper available. The remaining Cu(II) is bound to albumin and is in rapid exchange with tissue copper. The albumin:Cu(II) complex is therefore considered to be the immediate transport form of copper in plasma. In addition, an amino acid (mainly L-histidine) bound fraction exists which is in equilibrium with copper bound to albumin³. The concentration of ligands (both amino acids and albumin) by far exceeds the plasma Cu(II) concentration. Within one hour of reaching the plasma, the absorbed copper is removed from the circulatory system by the liver where it is processed via two routes. Some, which is not reabsorbed, is excreted in bile into the gastrointestinal tract. Patients with Wilson's disease (section 2.5.2) have an impaired ability of the liver to perform biliary excretion of Cu(II). The second metabolic pathway is copper incorporation into ceruloplasmin, which shall be discussed further (section 3.6.1).

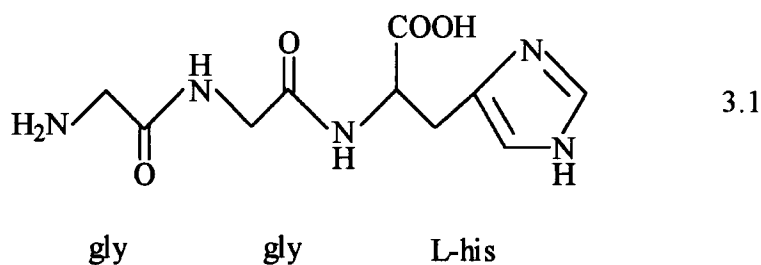
It is therefore apparent that if the copper mediated reaction outlined in Chapter Two is to be considered as an *in vivo* source of nitric oxide, it must be established

whether complexed forms of Cu(II) (bound to albumin, amino acids and ceruloplasmin) may effect S-nitrosothiol decomposition.

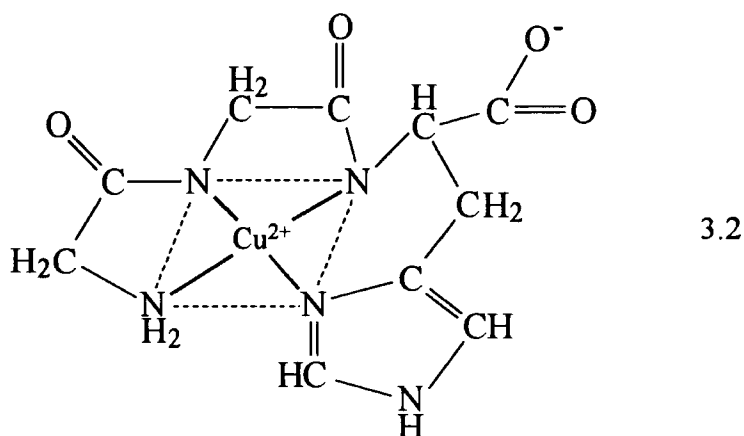
3.2 GlycylGlycylHistidine (GGH)

3.2.1 GGH as a Cu²⁺ Binding Model

As discussed in section 3.1, the polypeptide human serum albumin (HSA) is considered to be the major molecule responsible for reversible binding of Cu(II) within blood plasma. It became established almost forty years ago that HSA had one specific copper chelation site, which has subsequently become well-characterised^{4,5,6} and is outlined in more detail in section 3.3.1. It became clear that the design and synthesis of a model molecule which could mimick the specific Cu(II) transport site of HSA would allow simplification of an already complex system. To this end, Lau *et al*⁷ synthesised a tripeptide, glycylglycylhistidine (GGH) (3.1) and studied its interaction with Cu²⁺ under physiological conditions.



Their results indicate that one major species exists in the GGH:Cu²⁺ system (3.2).



Cu^{2+} exhibits square planar geometry with the tripeptide utilising the same ligand atoms for coordination as does HSA. These are the α -amino nitrogen of the NH_2 terminal glycine residue, two intervening deprotonated peptide nitrogens and the imidazole pyridine nitrogen of the L-histidine residue. The $\text{GGH}:\text{Cu}^{2+}$ formed is deep purple in colour and has a molar extinction coefficient (pH 8.0) of $103 \text{ mol}^{-1} \text{ dm}^3 \text{ cm}^{-1}$ at $\lambda_{\text{max}} = 525 \text{ nm}$. The dissociation constant for this complex can be expressed by equation 3.1.



Equilibrium dialysis measurements utilising $^{67}\text{Cu(II)}$ as an isotopic tracer have calculated K_D to be 1.18×10^{-16} .⁷ A subsequent report⁸ has demonstrated that at 1:1 ligand to metal ratios the purple complex is essentially 100% abundant above pH 7. A small tripeptide species such as GGH may thus be able to mobilise copper *in vivo* and aid its excretion. Wilson's disease has commonly been treated with penicillamine, but due to its lack of specificity and tolerance induction⁹ in certain patients is not entirely satisfactory. GGH could have an important biomedical application in this particular field.

3.2.2 Reaction of $\text{GGH}:\text{Cu}^{2+}$ with NAP

Before the decomposition characteristics of S-nitrosothiols in the presence of $\text{GGH}:\text{Cu}^{2+}$ could be determined, it was necessary to analyse any possible reaction between thiolate and the tripeptide:copper(II) complex. Of specific interest is the formation of Cu^+ from this bound form of Cu^{2+} by reduction. A $1 \times 10^{-2} \text{ mol dm}^{-3}$ solution of $\text{GGH}:\text{Cu}^{2+}$ was prepared by adding an equivalent amount of copper(II) sulfate pentahydrate to the solid tripeptide. On dilution with pH 7.4 buffer a purple colouration was noted and a uv/visible spectrum of this solution recorded ($\lambda_{\text{max}} = 525 \text{ nm}$, $\epsilon = 89 \text{ mol}^{-1} \text{ dm}^3 \text{ cm}^{-1}$). Following this, NAP was added to the same $\text{GGH}:\text{Cu}^{2+}$ solution in the concentration range $2.5 \times 10^{-3} - 1 \times 10^{-2} \text{ mol dm}^{-3}$. An

immediate and substantial reduction in the absorbance at 525nm was observed (table 3.1), along with a visual bleaching of the reactant solution.

Table 3.1

Measured absorbance (525nm) against added [N-acetylpenicillamine] for the reaction of GGH:Cu²⁺ (1 x 10⁻² mol dm⁻³) with NAP, pH 7.4

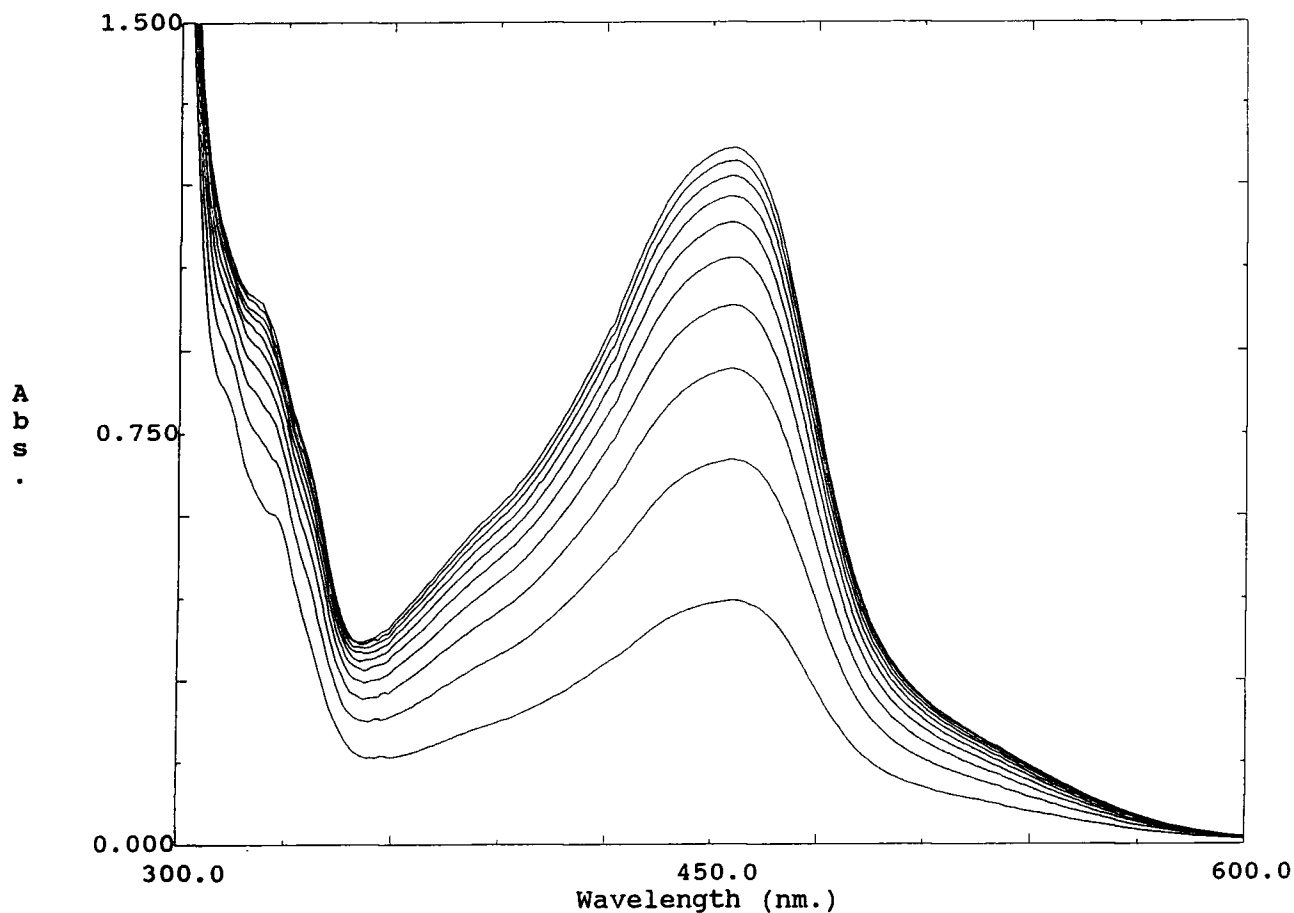
[N-acetylpenicillamine]/10 ⁻³ mol dm ⁻³	Absorbance _{525nm}
0	0.890
2.5	0.798
5.0	0.720
7.5	0.621
10	0.515

Each spectrum obtained remained unchanged for at least two hours after mixing the reaction solutions.

The largest decrease in measured absorbance is obtained when equimolar quantities of GGH:Cu²⁺ and NAP are reacted. This experiment was repeated, under slightly differing conditions, in the presence of neocuproine. When GGH:Cu²⁺ (2 x 10⁻⁴ mol dm⁻³) was treated with an equivalent amount of NAP, and neocuproine (4 x 10⁻⁴ mol dm⁻³) added there was a steady increase in concentration of the characteristic Cu⁺-chelate with $\lambda_{\max} = 453\text{nm}$, as observed previously (section 2.3.1). The spectra recorded are plotted in figure 3.1.

Figure 3.1

Traces showing the absorbance increase at 453nm for the reaction of equimolar GGH:Cu²⁺ with NAP (2×10^{-4} mol dm⁻³) and added neocuproine (4×10^{-4} mol dm⁻³)



Scans acquired every minute.

Very similar results were afforded when L-cysteine and 2-(mercaptopropionyl)glycine were used as the thiol.

In an attempt to quantify the Cu⁺ formed during the course of this reaction, several consecutive spectra were run measuring the absorbance increase at 453nm. Then, on assuming the extinction coefficient of Cu(NC)₂⁺ to be 7950 mol⁻¹ dm³ cm⁻¹ at this wavelength, the percentage Cu⁺ trapped can be estimated and compared with the amount of cuprous ion formed by thiolate reduction of hydrated Cu²⁺ (table 3.2).

Table 3.2

% Cu⁺ chelated by neocuproine (1 x 10⁻³ mol dm⁻³) in the presence of equimolar thiol (2 x 10⁻⁴ mol dm⁻³) and either GGH:Cu²⁺ or hydrated Cu²⁺

Thiol	% Cu ⁺ chelated ^a	
	Hydrated Cu ²⁺ ^b	GGH:Cu ²⁺
NAP	81 ± 3	53 ± 2
L-cysteine	80 ± 3	68 ± 2
MPG	93 ± 3	60 ± 2

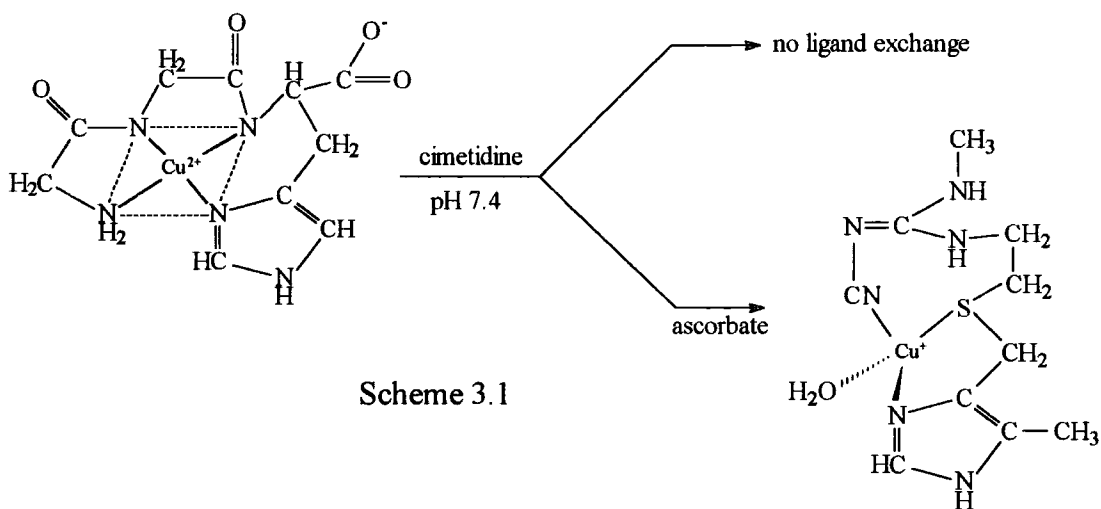
^aPercentages calculated as an average of three experiments measuring the maximum absorbance at 453nm.

^bHydrated Cu²⁺ = CuSO₄·5H₂O.

Two features of this table are of particular note. Firstly, there is incomplete reduction of Cu²⁺ → Cu⁺ by thiolate in the hydrated ion case under these experimental conditions, although > 80% cuprous ion was generated with each thiol. It remains to be seen whether quantitative reduction will occur when [thiol] >> [Cu²⁺]. Secondly, although less Cu⁺ is formed than when CuSO₄·5H₂O is added, substantial cupric ion reduction is induced by thiolate even when Cu²⁺ is chelated to GGH. This is in keeping with results published by Uchida *et al*¹⁰ who noted that the characteristic absorbance due to GGH:Cu²⁺ was completely diminished by ascorbate, implying a one electron reduction of the complex to the colourless GGH:Cu⁺ species (equation 3.2).



Similar effects have also been observed by Kimura *et al*¹¹. In this instance Cu²⁺ bound to GGH becomes reduced by ascorbate and trapped by cimetidine, a compound in current worldwide clinical use for the treatment of peptic ulcers (scheme 3.1). These results suggest that Cu⁺ can be generated from GGH:Cu²⁺ in the presence of a suitable reductant and chelated by another available molecule, which leads to the possibility that such complexes can initiate S-nitrosothiol decomposition.



3.2.3 Decomposition of SNAP in the Presence of GGH:Cu²⁺

After ascertaining that thiolate mediated reduction of tripeptide-bound copper(II) ions can take place, the stability of S-nitrosothiols in the presence of hydrated Cu²⁺ and GGH:Cu²⁺ was examined. SNAP (1 x 10⁻³ mol dm⁻³) was the first nitrosothiol to be kinetically analysed on addition of increasing amounts of CuSO₄·5H₂O (1 - 5 x 10⁻⁶ mol dm⁻³) at pH 7.4. Good first order plots were obtained under these conditions, the appropriate rate constants being quoted in table 3.3.

Table 3.3

Kinetic data for the decomposition of SNAP (1 x 10⁻³ mol dm⁻³) in the presence of added copper(II) ions

[Cu ²⁺]/10 ⁻⁶ mol dm ⁻³	k _{obs} /10 ⁻³ s ⁻¹
1.0	1.12 ± 0.02
2.0	2.55 ± 0.04
3.0	4.02 ± 0.09
4.0	5.21 ± 0.09
5.0	6.12 ± 0.11

As discussed in section 1.4.3.1, equation 1.38 predicts a linear relationship between the observed pseudo-first order rate constant and the [Cu²⁺] which is introduced. The second order rate constant k₂ (equation 1.37) can be calculated from

the gradient of a plot of k_{obs} against $[\text{Cu}^{2+}]_{\text{added}}$ and is equal to $1260 \pm 60 \text{ mol}^{-1} \text{ dm}^3 \text{ s}^{-1}$ in this instance. This result is vastly different to the previous literature value reported¹² of $20 \pm 1 \text{ mol}^{-1} \text{ dm}^3 \text{ s}^{-1}$. This is due to a different solid sample of SNAP being utilised with (crucially) a differing quantity of thiolate impurity present (section 2.4). Published data relating to this reaction will therefore be extremely variable, making quantitative comparisons almost impossible. However, it is more realistic to compare rate constants collected using the same solid batch of SNAP and varying sources of Cu^{2+} . Therefore, this work was repeated under identical conditions but using GGH: Cu^{2+} as the form of copper(II) ions (table 3.4).

Table 3.4

Kinetic data for the decomposition of SNAP ($1 \times 10^{-3} \text{ mol dm}^{-3}$) in the presence of added GGH: Cu^{2+}

$[\text{GGH}:\text{Cu}^{2+}]/10^{-6} \text{ mol dm}^{-3}$	$k_{\text{obs}}/10^{-4} \text{ s}^{-1}$
1.0	4.59 ± 0.08
2.0	8.50 ± 0.12
3.0	12.5 ± 0.2
4.0	17.5 ± 0.2
5.0	22.1 ± 0.3

This data indicates that GGH: Cu^{2+} will effect decomposition of SNAP, but not as effectively as hydrated Cu^{2+} . Equations 1.37 and 1.38 can be adapted to describe a more general situation (equations 3.3 and 3.4).

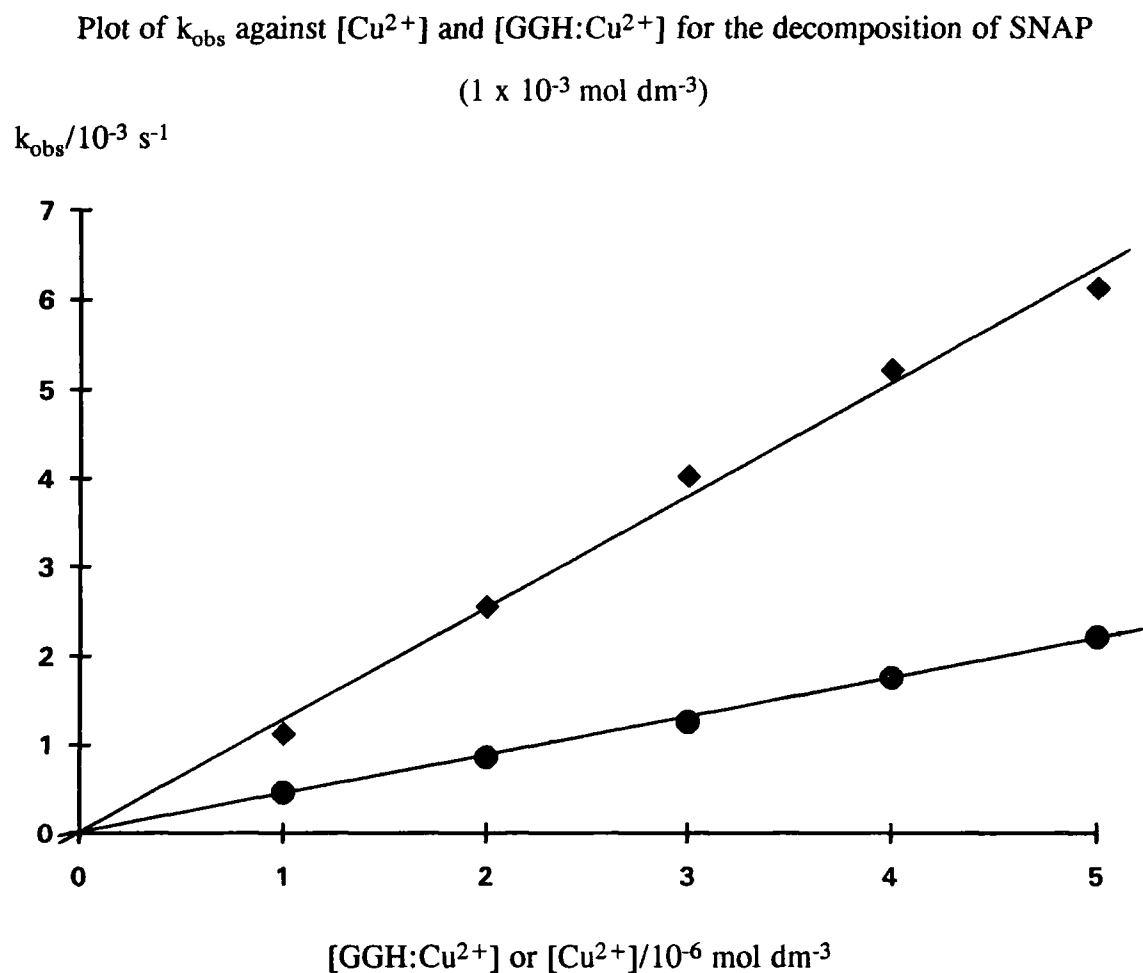
$$\text{Rate} = k_2[\text{copper complex}][\text{RSNO}] + k'[\text{RSNO}] \quad \text{eqn 3.3}$$

$$k_{\text{obs}} = k_2[\text{copper complex}] + k' \quad \text{eqn 3.4}$$

As in the case of hydrated Cu^{2+} , k_2 for reaction of SNAP with GGH: Cu^{2+} can be determined as $440 \pm 13 \text{ mol}^{-1} \text{ dm}^3 \text{ s}^{-1}$, which represents a reduction in reactivity by a factor of three when compared to $1260 \text{ mol}^{-1} \text{ dm}^3 \text{ s}^{-1}$. This is no doubt due to less

Cu⁺ being available for reaction when Cu²⁺ is chelated by GGH (table 3.2). Figure 3.2 displays these results in a clearer manner.

Figure 3.2



◆ = hydrated Cu²⁺

● = GGH:Cu²⁺

To test the generality of this reaction, S-nitrosocysteine (SNC) and S-nitroso-2-(mercaptopropionyl)glycine were separately reacted with CuSO₄·5H₂O and GGH:Cu²⁺ with the respective second order rate constants measured as previously described (tables 3.5 - 3.8).

Table 3.5

Kinetic data for the decomposition of S-nitrosocysteine ($1 \times 10^{-3} \text{ mol dm}^{-3}$) in the presence of added copper(II) ions

$[\text{Cu}^{2+}]/10^{-6} \text{ mol dm}^{-3}$	$k_{\text{obs}}/10^{-2} \text{ s}^{-1}$
0	5.55 ± 0.09
0.25	6.99 ± 0.13
0.50	8.58 ± 0.18
1.0	11.5 ± 0.2
1.5	14.5 ± 0.2

$$k_2 = 60,000 \pm 500 \text{ mol}^{-1} \text{ dm}^3 \text{ s}^{-1}$$

Table 3.6

Kinetic data for the decomposition of S-nitrosocysteine ($1 \times 10^{-3} \text{ mol dm}^{-3}$) in the presence of added GGH: Cu^{2+}

$[\text{GGH}:\text{Cu}^{2+}]/10^{-6} \text{ mol dm}^{-3}$	$k_{\text{obs}}/10^{-2} \text{ s}^{-1}$
1.0	13.3 ± 0.2
1.5	14.0 ± 0.2
2.0	14.5 ± 0.3
3.0	15.5 ± 0.5
4.0	16.9 ± 0.6

$$k_2 = 11,600 \pm 300 \text{ mol}^{-1} \text{ dm}^3 \text{ s}^{-1}$$

Table 3.7

Kinetic data for the decomposition of S-nitroso-2-(mercaptopropionyl)glycine ($1 \times 10^{-3} \text{ mol dm}^{-3}$) in the presence of added copper(II) ions

$[\text{Cu}^{2+}]/10^{-6} \text{ mol dm}^{-3}$	$k_{\text{obs}}/10^{-4} \text{ s}^{-1}$
0.5	4.39 ± 0.13
1.0	6.84 ± 0.19
2.0	11.2 ± 0.3
4.0	17.5 ± 0.4
5.0	20.9 ± 0.5

$$k_2 = 360 \pm 16 \text{ mol}^{-1} \text{ dm}^3 \text{ s}^{-1}$$

Table 3.8

Kinetic data for the decomposition of S-nitroso-2-(mercaptopropionyl)glycine
($1 \times 10^{-3} \text{ mol dm}^{-3}$) in the presence of added GGH: Cu^{2+}

$[\text{GGH}:\text{Cu}^{2+}]/10^{-6} \text{ mol dm}^{-3}$	$k_{\text{obs}}/10^{-4} \text{ s}^{-1}$
0.5	5.88 ± 0.16
1.0	7.26 ± 0.19
3.0	11.6 ± 0.3
4.0	12.8 ± 0.4
5.0	14.1 ± 0.5

$$k_2 = 180 \pm 10 \text{ mol}^{-1} \text{ dm}^3 \text{ s}^{-1}$$

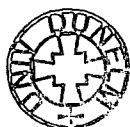
Table 3.9 summarises all results obtained for the reaction of hydrated Cu^{2+} and GGH: Cu^{2+} with these nitrosothiols.

Table 3.9

Second order rate constant (k_2) values for hydrated Cu^{2+} and GGH: Cu^{2+} induced
S-nitrosothiol decomposition

S-nitrosothiol	$k_2 \text{ (mol}^{-1} \text{ dm}^3 \text{ s}^{-1}\text{)}$	
	Hydrated Cu^{2+}	GGH: Cu^{2+}
SNAP	1260 ± 60	440 ± 13
S-nitrosocysteine	$60,000 \pm 500$	$11,600 \pm 300$
SMPG	360 ± 16	180 ± 10

In each instance, GGH: Cu^{2+} can clearly bring about decomposition of the S-nitrosothiol in question but the hydrated form of copper(II) is more reactive, as is to be expected. There does not appear to be a direct correlation between the reduction in k_2 on chelation of Cu^{2+} with GGH and the amount of cuprous copper trapped after thiolate reduction (table 3.2). This is exemplified by L-cysteine appearing to be a very effective reductant of bound copper(II) but S-nitrosocysteine suffering a five-fold decrease in reactivity on changing hydrated Cu^{2+} to GGH: Cu^{2+} . It would appear that the amount of thiolate present in each nitrosothiol sample again exerts a great influence on the observed reactivity of these compounds.



In an attempt to quantify any effect altering the thiol concentration may have on the rate of GGH:Cu²⁺ mediated decomposition, NAP (5 x 10⁻⁵ - 2 x 10⁻⁴ mol dm⁻³) was added to SNAP (1 x 10⁻³ mol dm⁻³) in the presence of 1 x 10⁻⁵ mol dm⁻³ GGH:Cu²⁺. Interestingly, increasing the NAP concentration had very little effect on the pseudo-first order rate constant (table 3.10).

Table 3.10

Kinetic data for the decomposition of SNAP (1 x 10⁻³ mol dm⁻³) in the presence of GGH:Cu²⁺ (1 x 10⁻⁵ mol dm⁻³) and added NAP

[N-acetylpencillamine]/10 ⁻⁵ mol dm ⁻³	k _{obs} /10 ⁻³ s ⁻¹
0	4.33 ± 0.06
5	4.42 ± 0.07
10	4.26 ± 0.07
15	4.40 ± 0.08
20	4.44 ± 0.07

An interpretation of these results is that the maximum possible amount of Cu⁺ has been released from any NAP impurity (~1 x 10⁻⁵ mol dm⁻³) present in the SNAP solution. Thus, increasing the [NAP] will have no observable rate enhancing effect. It might have been thought that introducing higher concentrations of NAP may inhibit reaction somewhat due to competitive chelation between the thiol and nitrosothiol for Cu⁺ (section 2.5.1). This does not however appear to be the case at these NAP levels.

A check was made that decomposition was caused by Cu⁺ and not cupric ion and that the mechanism outlined in section 2.7 holds for GGH:Cu²⁺. Neocuproine was added to SNAP and tripeptide:copper(II) in an analogous fashion to that described by table 2.1 and figure 2.3. As predicted, increasing [neocuproine] progressively decreased the rate constant for the reaction, with decomposition being virtually halted at high neocuproine concentrations (table 3.11). The effect of this cuprous ion chelator on reaction of SNAP with hydrated Cu²⁺ and GGH:Cu²⁺ are compared in figure 3.3.

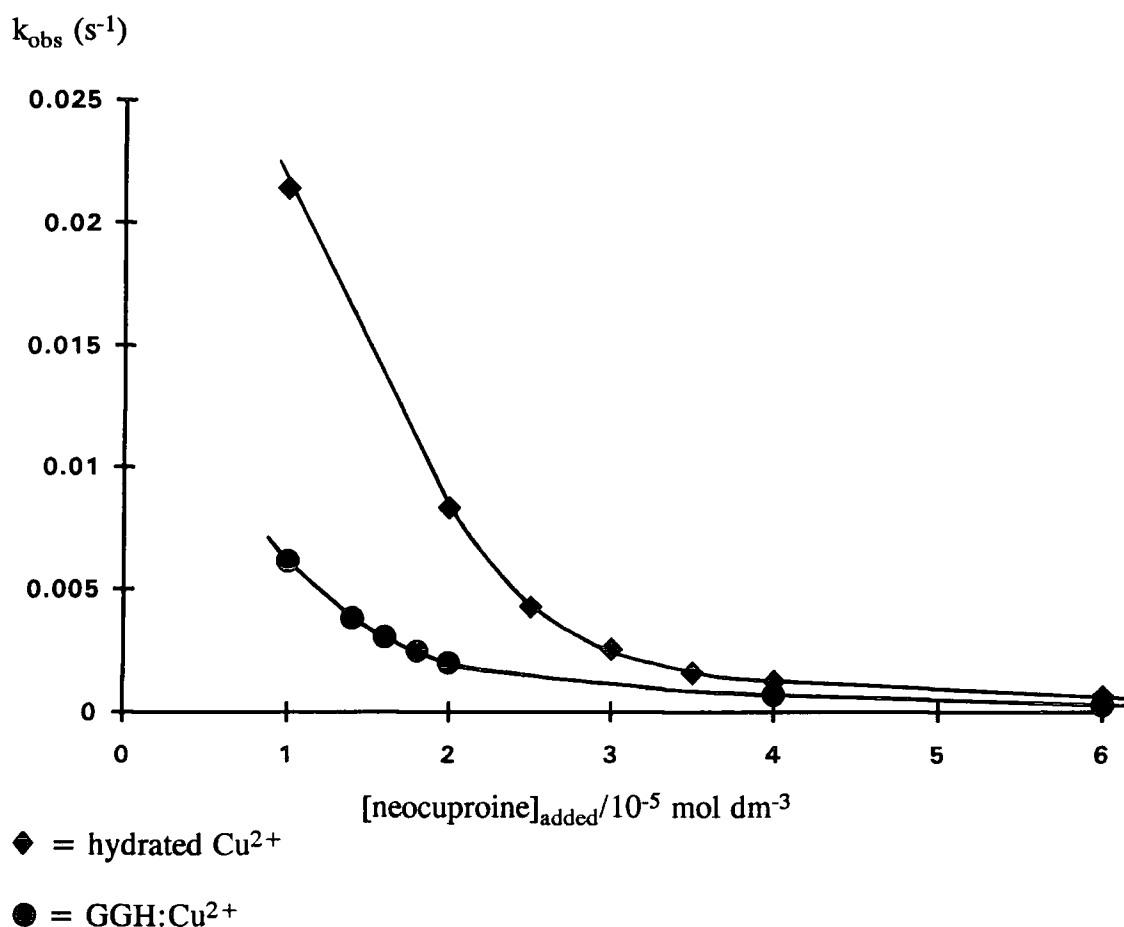
Table 3.11

Kinetic data for the effect of neocuproine on the decomposition of SNAP
($1 \times 10^{-3} \text{ mol dm}^{-3}$) in the presence of GGH: Cu^{2+} ($2 \times 10^{-5} \text{ mol dm}^{-3}$)

[neocuproine]/ $10^{-5} \text{ mol dm}^{-3}$	$k_{\text{obs}}/10^{-4} \text{ s}^{-1}$
1.0	61.4 ± 1.1
1.4	38.1 ± 0.6
1.6	30.6 ± 0.5
1.8	24.6 ± 0.4
2.0	19.8 ± 0.3
4.0	6.86 ± 0.09
6.0	2.64 ± 0.04

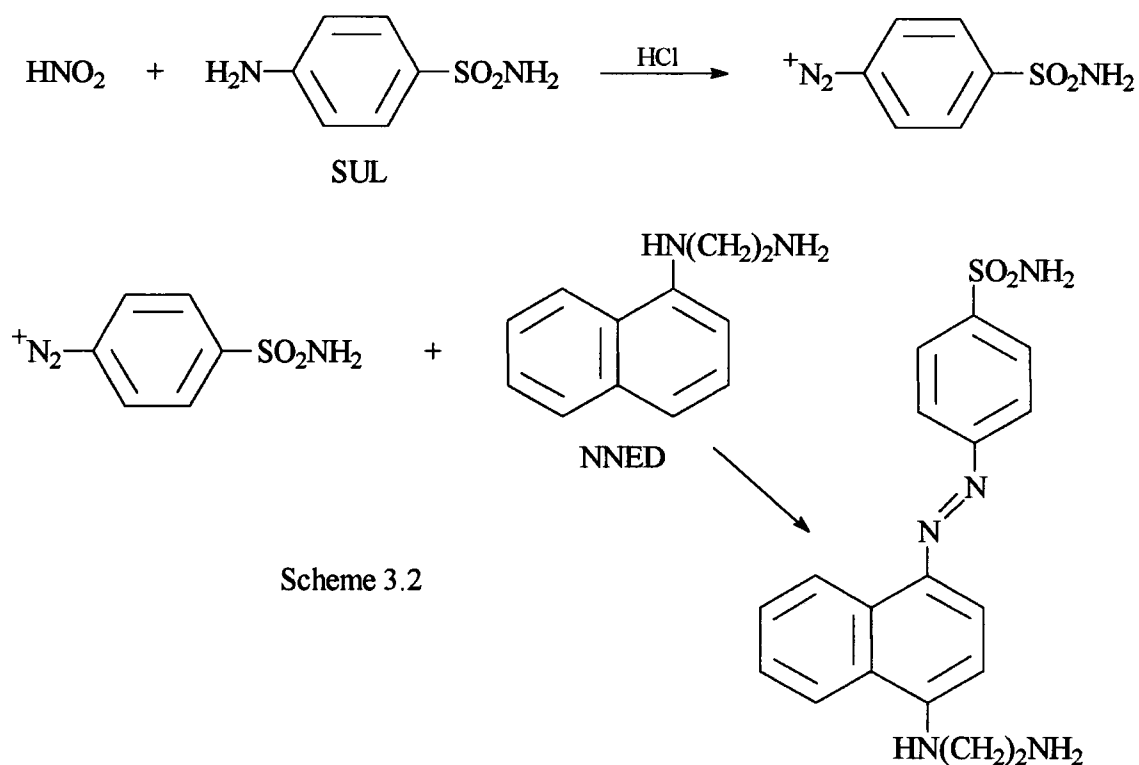
Figure 3.3

Plot of k_{obs} against added neocuproine concentration for the reaction of SNAP
($1 \times 10^{-3} \text{ mol dm}^{-3}$) in the presence of Cu^{2+} or GGH: Cu^{2+} ($2 \times 10^{-5} \text{ mol dm}^{-3}$)



3.2.4 Detection of Reaction Products

It was necessary to determine the nitrogenous product for the bound copper(II) induced decomposition process. The most convenient way to undertake this which would also allow accurate quantification was to perform a Griess reaction¹³. This method will facilitate the measurement of micromolar levels of nitrite ion in solution, thus proving to be a very useful assay in this instance. The reaction is outlined in scheme 3.2.



Scheme 3.2

Any nitrite present will be converted into nitrous acid which in turn diazotises an aryl amine (sulfanilamide, SUL). An aryl coupling agent is then introduced (N-1-naphthylethylenediamine, NNED) which yields a purple azo dye on reaction with diazotised SUL. A calibration curve has to initially be constructed to calculate the molar extinction coefficient at 542nm (λ_{max}) for the dye. The procedure outlined by Vogel¹⁴ was followed with some slight modifications. 10ml SUL (3.4g in 100ml 0.4 mol dm^{-3} HCl) was added to 14ml NNED (0.1g in 100ml 0.4 mol dm^{-3} HCl). A standard sodium nitrite solution was added such that the $[\text{NO}_2^-]$ ranged from

5 - $17.5 \times 10^{-6} \text{ mol dm}^{-3}$ (total solution volume = 50ml) and the absorbance measured at 542nm (table 3.12).

Table 3.12

Calibration data for the detection of nitrite and calculation of $\epsilon_{542\text{nm}}$

$[\text{NO}_2^-]/10^{-6} \text{ mol dm}^{-3}$	Absorbance _{542nm}
5.0	0.297
7.5	0.417
10	0.553
12.5	0.699
15	0.828
17.5	0.926

$$\epsilon_{542\text{nm}} = 53,000 \pm 600 \text{ mol}^{-1} \text{ dm}^3 \text{ cm}^{-1}$$

This value can now be used to calculate nitrite levels in nitrosothiol solutions. A typical decomposition reaction was subsequently set up with $[\text{SNAP}] = 2.5 \times 10^{-4} \text{ mol dm}^{-3}$, and $[\text{GGH}:\text{Cu}^{2+}] = 1 \times 10^{-5} \text{ mol dm}^{-3}$, total reactant volume being 20ml. This mixture was thermostatted at 25°C and a 2ml aliquot removed every five minutes and coupled to SUL/NNED as described previously. The absorbance at 542nm was immediately measured and found to reach a maximum after thirty minutes of 0.952. Using $\epsilon_{542\text{nm}} = 53,000 \text{ mol}^{-1} \text{ dm}^3 \text{ cm}^{-1}$ this corresponds to $1.80 \times 10^{-5} \text{ mol dm}^{-3} \text{ NO}_2^-$ produced. The theoretical maximum amount of nitrite that could be detected is $2.0 \times 10^{-5} \text{ mol dm}^{-3}$ so 90% NO_2^- was formed in this instance which can be assumed to be quantitative.

The next stage was to follow the kinetics of nitrite formation at 542nm. This was performed by reacting SNAP ($2.5 \times 10^{-4} \text{ mol dm}^{-3}$) with GGH: Cu^{2+} ($1 \times 10^{-6} \text{ mol dm}^{-3}$), removing a 2ml sample as before and measuring the absorbance at 542nm after dye formation. Results are tabulated (table 3.13) and are also shown graphically (figure 3.4).

Table 3.13

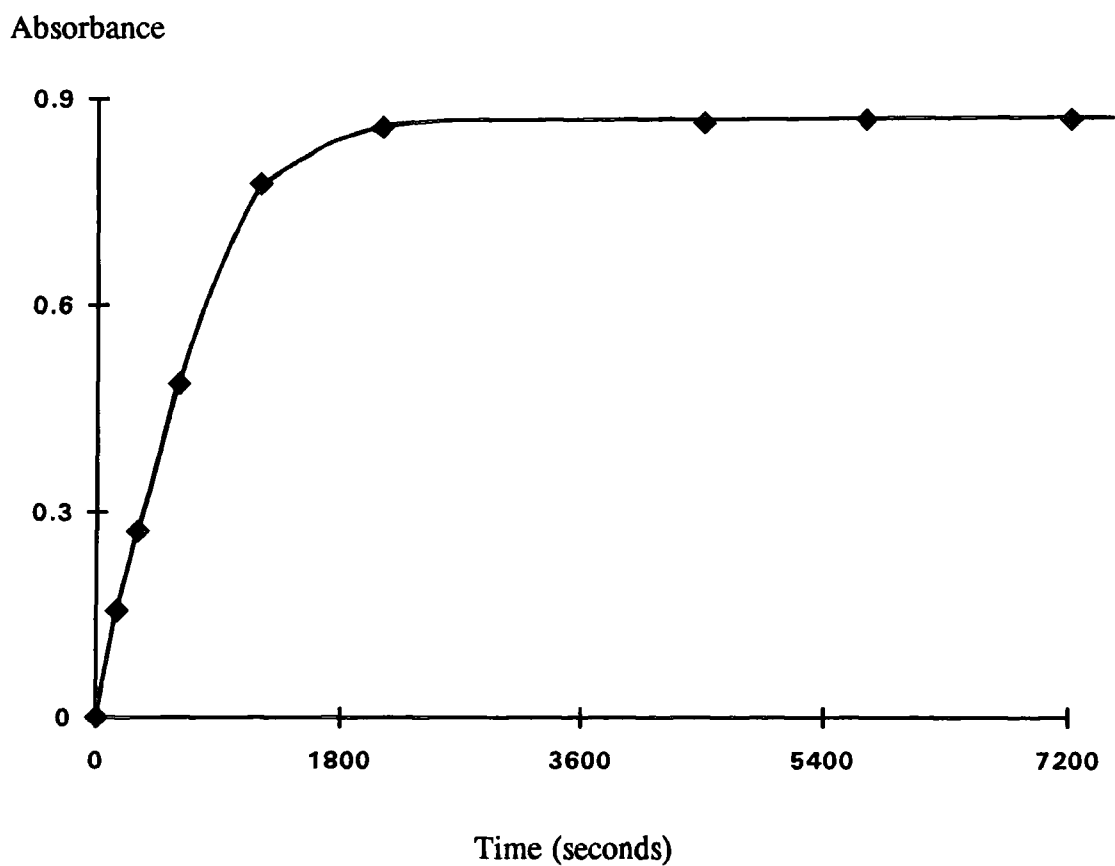
Formation of nitrite from SNAP ($2.5 \times 10^{-4} \text{ mol dm}^{-3}$) in the presence of GGH: Cu^{2+} ($1 \times 10^{-6} \text{ mol dm}^{-3}$) as detected by the Griess test at 542nm

Time (seconds)	Absorbance _{542nm}
0	0.001
150	0.156
300	0.272
600	0.486
1200	0.776
2100	0.858
4500	0.865
5700	0.870
7200	0.870

Infinity taken to be reached after two hours

Figure 3.4

Absorbance/time plot (542nm) for NO_2^- formation from SNAP ($2.5 \times 10^{-4} \text{ mol dm}^{-3}$) in the presence of GGH: Cu^{2+} ($1 \times 10^{-6} \text{ mol dm}^{-3}$)

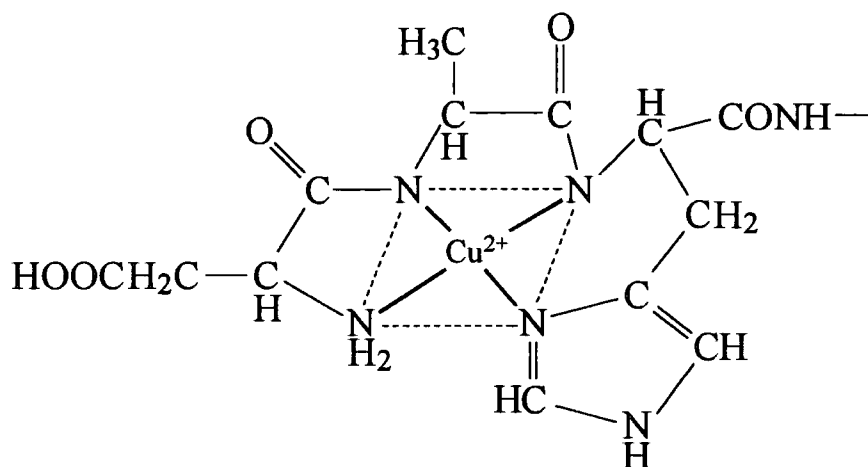


It is apparent from figure 3.4 that good first order kinetics are noted when nitrite formation is considered. This compares favourably with previous results studying the hydrated copper ion reaction with SNAP¹². It is probable that the initial reaction product is therefore nitric oxide, which becomes oxidised to NO₂⁻ (scheme 1.1) in aerated solutions.

3.3 Human Serum Albumin (HSA)

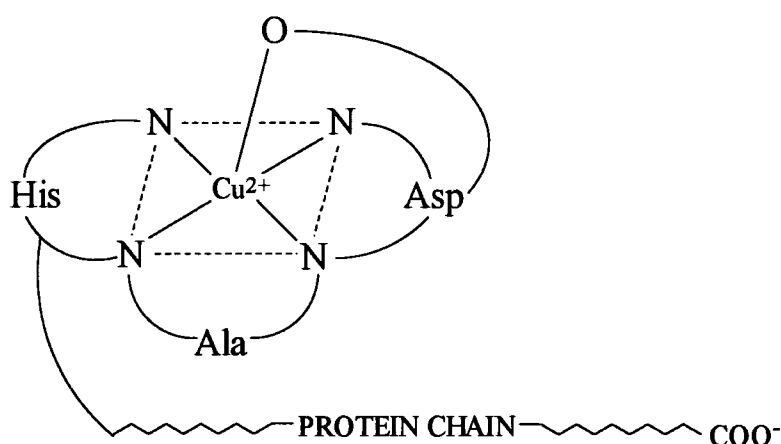
3.3.1 HSA as a Transport Molecule for Cu²⁺

Section 3.2 describes the reaction of thiolate with GGH:Cu²⁺ and subsequent cuprous ion promoted decomposition of S-nitrosothiols. As GGH provides a good model for the specific physiological copper(II) transport binding site it is reasonable to suggest that similar results will be obtained when using human serum albumin (HSA) as a chelant. HSA is a polypeptide synthesised in the liver composed of 585 amino acids in one single chain (with seventeen disulfide linkages), having a molecular weight of 66,500¹⁵. In addition to its role in transporting Cu²⁺ it binds and mobilises other essential materials such as fatty acids, calcium, vitamins and hormones. It is present at a concentration of 35 - 50 grams per litre of blood plasma¹⁶. Some of its ligand binding sites are highly specific and saturable, while others are much less so. The copper(II) binding site has been identified as being particularly strong (K_D in equation 3.1 = 6.61×10^{-17})⁷ and is composed in a similar fashion to GGH (3.3).



3.3

The principal difference between HSA and GGH is the order of amino acids present. Instead of GlyGlyHis making up the tripeptide component, aspartic acid, alanine and L-histidine (AspAlaHis) compose the $-NH_2$ terminus of the polypeptide. ^{13}C and 1H NMR studies¹⁷ have indicated that no other binding group is involved besides those in these first three residues, but that the β -carboxyl side chain of the aspartyl residue may also provide coordination (3.4).



3.4

The ligand atoms are therefore the same in HSA and GGH, with the former binding Cu^{2+} slightly more strongly. Bovine serum albumin has been characterised in a similar way and has threonine present instead of alanine as the second amino acid⁵. HSA: Cu^{2+} exhibits a similar uv/visible spectrum to that of GGH: Cu^{2+} with a peak at $\lambda_{max} = 525nm$ ($\epsilon = 99 \text{ mol}^{-1} \text{ dm}^3 \text{ cm}^{-1}$)⁴. The effect of thiolate on this absorbance was examined.

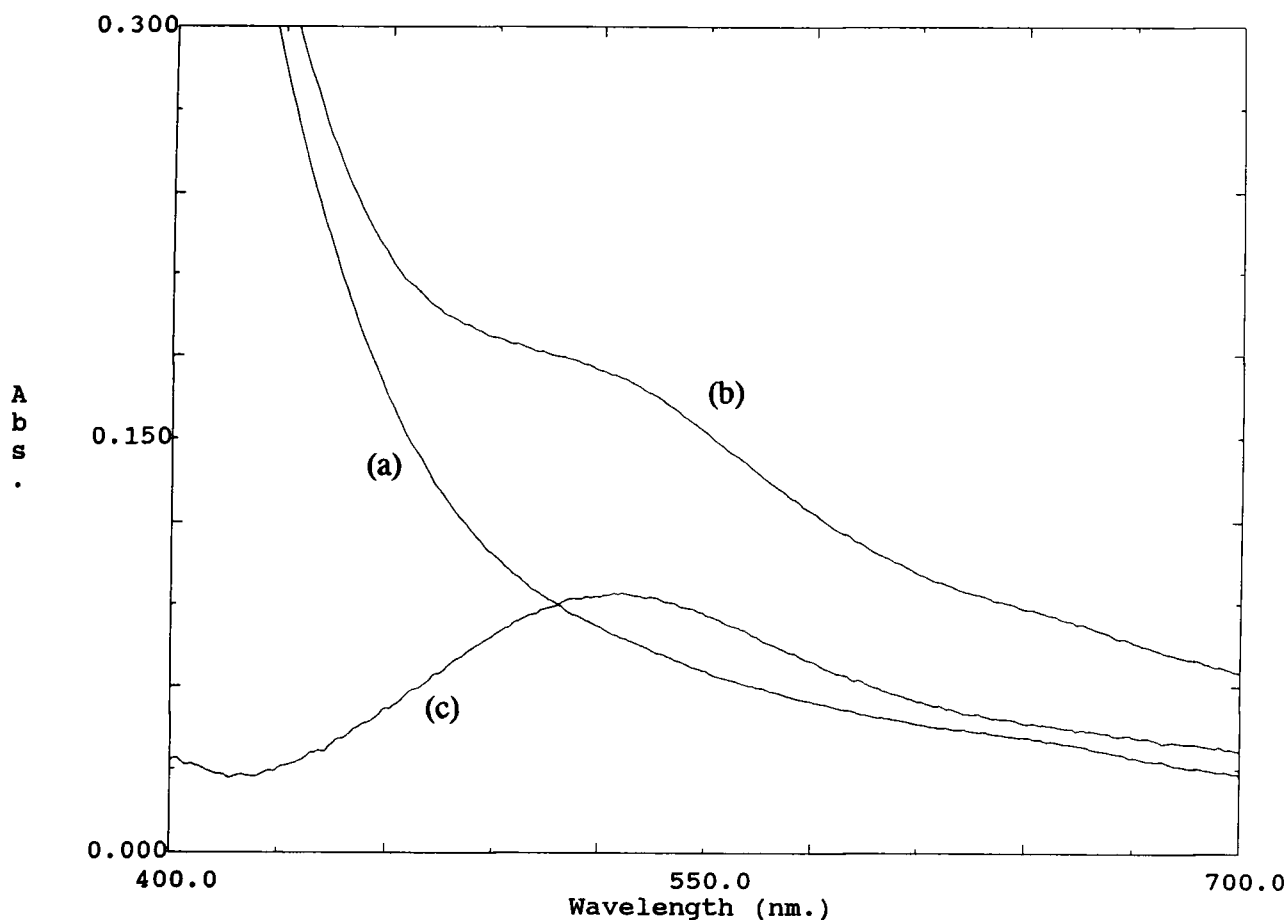
3.3.2 Reaction of HSA: Cu^{2+} with NAP

The interaction between thiolate and HSA: Cu^{2+} was followed in a similar manner to that of the tripeptide:copper(II) complex. A $1 \times 10^{-3} \text{ mol dm}^{-3}$ solution of HSA in pH 7.4 buffer was made up and a uv/visible spectrum run (figure 3.5, trace (a)). One equivalent of Cu^{2+} was added to the solution and the resulting spectrum

recorded (trace (b)). A "difference" spectrum was calculated (trace (c)) which related to the change in absorbance that was observed on adding copper(II) to HSA.

Figure 3.5

Uv/visible spectra of $1 \times 10^{-3} \text{ mol dm}^{-3}$ HSA and $1 \times 10^{-3} \text{ mol dm}^{-3}$ HSA: Cu^{2+}
(pH 7.4)



- (a) $1 \times 10^{-3} \text{ mol dm}^{-3}$ HSA; (b) $1 \times 10^{-3} \text{ mol dm}^{-3}$ HSA: Cu^{2+} ;
(c) difference spectrum ((b) - (a)).

Trace (c) has $\lambda_{\text{max}} = 524\text{nm}$, $\epsilon = 94 \text{ mol}^{-1} \text{ dm}^3 \text{ cm}^{-1}$ and represents the effect of adding Cu^{2+} to HSA. NAP was then introduced ($4 \times 10^{-3} \text{ mol dm}^{-3}$) and the absorbance at 525nm monitored over a period of sixty minutes (table 3.14).

Table 3.14

Change in absorbance (525nm) during the reaction of HSA:Cu²⁺ (1×10^{-3} mol dm⁻³)
with 4×10^{-3} mol dm⁻³ NAP

Time (seconds)	Absorbance _{525nm}
0	0.083
300	0.055
600	0.026
1800	0.019
3600	0.010

The initial measurement (time = 0 seconds) was made immediately after NAP was added to HSA:Cu²⁺. A steady decrease in absorbance is apparent which is in contrast to the reaction of NAP with GGH:Cu²⁺ (section 3.3.2) where an instantaneous reaction is noted. This may in part be due to steric hindrance of the polypeptide chain (in the case of HSA) impeding the action of RS⁻ at the amino terminus where Cu²⁺ is bound. As for GGH:Cu²⁺, this procedure was repeated in the presence of neocuproine under identical experimental conditions. A steady build-up of Cu(NC)₂⁺ at 453nm was discernible, with the amount of cuprous copper generated from HSA:Cu²⁺ on reaction with NAP and L-cysteine summarised in table 3.15.

Table 3.15

% Cu⁺ chelated by neocuproine (1×10^{-3} mol dm⁻³) in the presence of equimolar
HSA:Cu²⁺ and thiol (2×10^{-4} mol dm⁻³)

Thiol	% Cu ⁺ chelated
NAP	53 ± 2
L-cysteine	40 ± 1

These results indicate that NAP is a better reductant than L-cysteine in forming Cu⁺ from HSA:Cu²⁺, which is the opposite trend to that exhibited by GGH:Cu²⁺. It

is not immediately obvious as to why this should be so, but it is clear that only the same quantity (or less) of Cu(I) can be formed when cupric copper is chelated to HSA rather than to GGH.

3.3.3 S-Nitrosothiol Decomposition in the Presence of HSA:Cu²⁺

SNAP ($1 \times 10^{-3} \text{ mol dm}^{-3}$) was firstly reacted with HSA:Cu²⁺ ($5 \times 10^{-7} - 1 \times 10^{-5} \text{ mol dm}^{-3}$) (table 3.16) and the second order rate constant calculated as described in section 3.2.3.

Table 3.16

Kinetic data for the decomposition of SNAP ($1 \times 10^{-3} \text{ mol dm}^{-3}$) in the presence of added HSA:Cu²⁺

[HSA:Cu ²⁺]/10 ⁻⁶ mol dm ⁻³	k _{obs} /10 ⁻⁴ s ⁻¹
0.5	1.70 ± 0.05
1.0	2.58 ± 0.09
3.0	4.95 ± 0.11
4.0	6.17 ± 0.18
5.0	7.12 ± 0.21
10	13.2 ± 0.3

$$k_2 = 120 \pm 2 \text{ mol}^{-1} \text{ dm}^3 \text{ s}^{-1}$$

The k_2 value obtained represents a ten-fold decrease in reactivity when compared to k_2 measured for hydrated Cu²⁺ decomposition. NAP produced the same amount of cuprous ion from both GGH:Cu²⁺ and HSA:Cu²⁺ (tables 3.2 and 3.15) and yet the tripeptide bound form of Cu²⁺ is 3-4 times as reactive towards SNAP. This may be because any cuprous ions that are generated and mobilised by thiolate reduction may become bound to another region of the albumin molecule. Many extra equivalents of Cu²⁺ can become bound to HSA than can be attributed to the specific binding site or to thiol/disulfide groups¹⁸. This would serve to reduce the effective [Cu⁺] available to promote S-nitrosothiol decomposition and hence reduce the value of measured rate constants. HSA added on its own inhibited any decomposition of nitrosothiols, presumably due to complexation of the tiny amount of cupric ions

derived from the buffer, generating a [HSA:Cu²⁺] that is significantly lower than those used in these studies.

The decomposition of SNAP in the presence of HSA bound to two cupric ions (HSA:2Cu²⁺) was also examined (table 3.17).

Table 3.17

Kinetic data for the decomposition of SNAP ($1 \times 10^{-3} \text{ mol dm}^{-3}$) in the presence of added HSA:2Cu²⁺

[HSA:2Cu ²⁺]/10 ⁻⁶ mol dm ⁻³	k _{obs} /10 ⁻⁴ s ⁻¹
0.5	5.11 ± 0.08
1.0	5.88 ± 0.09
2.0	7.68 ± 0.09
3.0	9.00 ± 0.17
4.0	10.4 ± 0.2

$$k_2 = 150 \pm 5 \text{ mol}^{-1} \text{ dm}^3 \text{ s}^{-1}$$

As expected, there is an increase in k_2 on going from HSA:Cu²⁺ to HSA:2Cu²⁺ as the copper ion concentration available is raised. However, the increase from 120 - 150 mol⁻¹ dm³ s⁻¹ may not be as much as would be predicted. Adding an extra equivalent of cupric ion may form peptide:Cu²⁺ complexes which do not allow the ready reduction and formation of Cu⁺, hence the observed small change in reactivity. The introduction of neocuproine to the HSA:Cu²⁺ and HSA:2Cu²⁺ induced decomposition of SNAP firstly slowed and then completely inhibited reaction, as seen previously in section 3.2.3. As with GGH, S-nitrosocysteine and S-nitroso-2-(mercaptopropionyl)glycine were subsequently reacted with HSA:Cu²⁺ to check the effect of altering the nitrosothiol structure (tables 3.18 and 3.19).

Table 3.18

Kinetic data for the decomposition of S-nitrosocysteine ($1 \times 10^{-3} \text{ mol dm}^{-3}$) in the presence of added HSA: Cu^{2+}

$[\text{HSA}:\text{Cu}^{2+}]/10^{-6} \text{ mol dm}^{-3}$	$k_{\text{obs}}/10^{-1} \text{ s}^{-1}$
2.0	9.50 ± 0.17
3.0	10.2 ± 0.2
4.0	11.9 ± 0.2
5.0	13.7 ± 0.3
6.0	15.5 ± 0.3

$$k_2 = 14,600 \pm 900 \text{ mol}^{-1} \text{ dm}^3 \text{ s}^{-1}$$

Table 3.19

Kinetic data for the decomposition of S-nitroso-2-(mercaptopropionyl)glycine ($1 \times 10^{-3} \text{ mol dm}^{-3}$) in the presence of added HSA: Cu^{2+}

$[\text{HSA}:\text{Cu}^{2+}]/10^{-6} \text{ mol dm}^{-3}$	$k_{\text{obs}}/10^{-4} \text{ s}^{-1}$
1.0	8.32 ± 0.18
2.0	11.8 ± 0.2
3.0	14.2 ± 0.3
4.0	16.7 ± 0.3
5.0	18.8 ± 0.4

$$k_2 = 260 \pm 14 \text{ mol}^{-1} \text{ dm}^3 \text{ s}^{-1}$$

For both of these S-nitrosothiols there is a reduction in the value of k_2 when compared with the hydrated copper(II) ion results, but reaction still occurs. It has now been established that such compounds can decompose in the presence of Cu^{2+} which is firmly chelated to peptide molecules composed of many or few amino acids. The question to now be addressed is whether or not amino acid bound Cu^{2+} can effect reaction, as such species make up an important transport form of copper within human plasma.

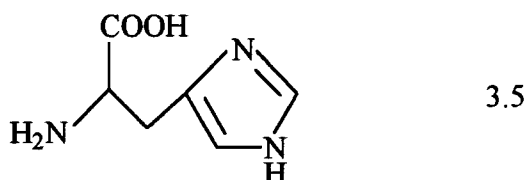
3.4 Histidine (HIS)

3.4.1 Importance of Amino Acids as Binding Agents

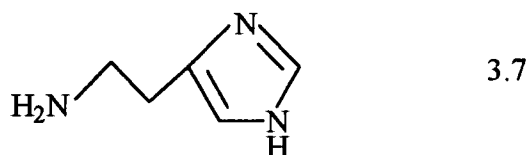
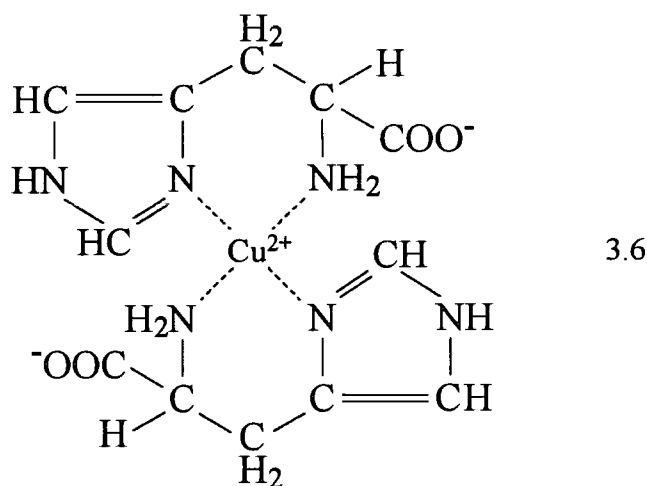
In 1950, Maley and Mellor¹⁹ reported stability constants (defined by equation 3.5) of complexes formed by the interaction of copper(II) with a series of amino acids.



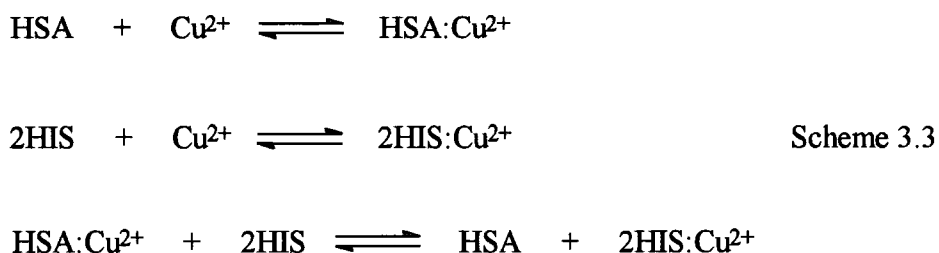
A^{-} represents the ligand amino acid studied (L-histidine, glycine, alanine, valine or leucine). It became apparent that the former substance generated chelates that were significantly more stable than those of the remaining amino acids. Indeed, $\log K$ for the complex $2\text{HIS}:\text{Cu}^{2+}$ was measured as 18.33, some three to four orders of magnitude greater than for the other four ligands. This suggests that L-histidine (3.5) is attached to copper(II) by species different from those involved (amino and carboxylate groups) in the coordination of the other amino acids.



Li *et al*²⁰ subsequently proposed the predominant binding sites of L-histidine to be the pyridine nitrogen of the imidazole group and the amino group. A possible structure was described for $2\text{HIS}:\text{Cu}^{2+}$ which involved copper(II) square planar geometry²¹ and coordination via the atoms as previously discussed²⁰ (3.6). However, it was noted that the analogous stability constant measured for histamine chelation to Cu^{2+} was smaller than that documented for L-histidine. The structure of histamine (3.7) indicates the lack of a carboxylate moiety which could chelate to the metal ion. This would require the formation of a tetragonal arrangement of donor groups with COO^{-} functionalities above and below the plane containing nitrogen atoms and Cu^{2+} .

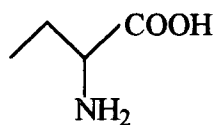


The concentration of L-histidine present in human plasma ranges from 1.1 - 2.1 mg per 100ml²². Neumann *et al*³ investigated the effect of the twenty-three amino acids found in plasma on the binding of copper(II) to HSA. At least half of these species significantly altered Cu²⁺ chelation by the polypeptide with L-histidine having the most marked influence. It seems likely therefore that this amino acid may effectively compete for the binding of copper with albumin with the following equilibria existing (scheme 3.3).



The experimental results obtained are compatible with the third equilibrium expression, that is the transfer of copper(II) from HSA to HIS. Evidence for a ternary coordination complex between HSA, Cu²⁺ and HIS has subsequently been presented^{23,24} which may play a role in the exchange of Cu²⁺ between a

macromolecule and a low molecular weight amino acid which can be transported across the biological membrane. Similar ternary complexes have been reported between 2HIS:Cu²⁺ and amino acids²⁵, particularly 2-aminobutyric acid (3.8) and ornithine (3.9).



3.8



3.9

More recently, 2HIS:Cu²⁺ has been successfully used in the treatment of Menkes' disease, otherwise known as "kinky hair syndrome"²⁶. Patients suffer from an intestinal copper absorption disorder which often leads to death in early childhood if therapy is not commenced at birth. It is clear that an amino acid bound fraction of copper(II) is an important component of Cu²⁺ transport within plasma, especially 2HIS:Cu²⁺ whose interaction with S-nitrosothiols was studied in detail.

3.4.2 Reaction of 2HIS:Cu²⁺ with NAP

As for GGH and HSA, the L-histidine:copper(II) complex was prepared ($1 \times 10^{-2} \text{ mol dm}^{-3}$) by diluting a 2:1 ratio of amino acid:CuSO₄·5H₂O with pH 7.4 buffer. A blue solution ensued which had a maximum absorbance at 640nm and a molar extinction coefficient of $79 \text{ mol}^{-1} \text{ dm}^3 \text{ cm}^{-1}$ at this wavelength (literature = $85 \text{ mol}^{-1} \text{ dm}^3 \text{ cm}^{-1}$, pH 7.5)²³. NAP was then introduced to a similar solution of 2HIS:Cu²⁺ in the concentration range $2.5 \times 10^{-3} - 1 \times 10^{-2} \text{ mol dm}^{-3}$. Increasing amounts of thiolate caused an instantaneous reduction in the measured absorbance at 640nm (table 3.20) which was attributed to disruption of the 2HIS:Cu²⁺ chelate and generation of cuprous ion.

Table 3.20

Measured absorbance (640nm) against added [N-acetylpenicillamine] for the reaction of 2HIS:Cu²⁺ (1 x 10⁻² mol dm⁻³) with NAP, pH 7.4

[N-acetylpenicillamine]/10 ⁻³ mol dm ⁻³	Absorbance _{640nm}
0	0.793
2.0	0.759
4.0	0.682
6.0	0.617
10	0.459

Each spectrum obtained remained unchanged for at least two hours after mixing the reaction solutions.

These results are analogous to those obtained for the reaction of GGH:Cu²⁺ with NAP (section 3.2.2). A linear relationship exists between the amount of thiol added and the decrease in absorbance observed. The formation of Cu⁺ during this reaction was confirmed by the addition of neocuproine (1 x 10⁻³ mol dm⁻³) to equimolar 2HIS:Cu²⁺ and NAP (2 x 10⁻⁴ mol dm⁻³). The absorbance at 453nm (Cu(NC)₂⁺) corresponded to a trapped copper(I) ion concentration of 1.44 x 10⁻⁴ mol dm⁻³, or 72%. This represents a considerable amount of cuprous ion generation and chelation from the reaction of NAP with 2HIS:Cu²⁺. Repetition of this experiment utilising L-cysteine as the reductant afforded 52% copper(I). It is apparent (as has been noted previously) that an amino acid bound form of Cu²⁺ can be reduced *in vitro* by thiolate.

3.4.3 S-Nitrosothiol Decomposition in the Presence of 2HIS:Cu²⁺

The reactions of SNAP, S-nitrosocysteine and S-nitroso-2-(mercaptopropionyl)glycine with added L-histidine:copper(II) were followed kinetically in a similar manner to that outlined in sections 3.2.3 and 3.3.3. In each instance the second order rate constant was calculated (tables 3.21 - 3.23) from a linear plot of [2HIS:Cu²⁺] against pseudo-first order rate constant (figure 3.6).

Table 3.21

Kinetic data for the decomposition of SNAP ($1 \times 10^{-3} \text{ mol dm}^{-3}$) in the presence of added 2HIS:Cu²⁺

[2HIS:Cu ²⁺]/10 ⁻⁶ mol dm ⁻³	k _{obs} /10 ⁻⁴ s ⁻¹
0.25	3.21 ± 0.08
0.50	4.23 ± 0.11
0.75	5.84 ± 0.13
1.0	6.86 ± 0.19
2.0	11.3 ± 0.3

$$k_2 = 460 \pm 15 \text{ mol}^{-1} \text{ dm}^3 \text{ s}^{-1}$$

Table 3.22

Kinetic data for the decomposition of S-nitrosocysteine ($1 \times 10^{-3} \text{ mol dm}^{-3}$) in the presence of added 2HIS:Cu²⁺

[2HIS:Cu ²⁺]/10 ⁻⁷ mol dm ⁻³	k _{obs} /10 ⁻² s ⁻¹
1.6	8.53 ± 0.09
3.2	9.50 ± 0.12
4.0	9.93 ± 0.15
8.0	14.7 ± 0.2
16	22.7 ± 0.3

$$k_2 = 58,000 \pm 1000 \text{ mol}^{-1} \text{ dm}^3 \text{ s}^{-1}$$

Table 3.23

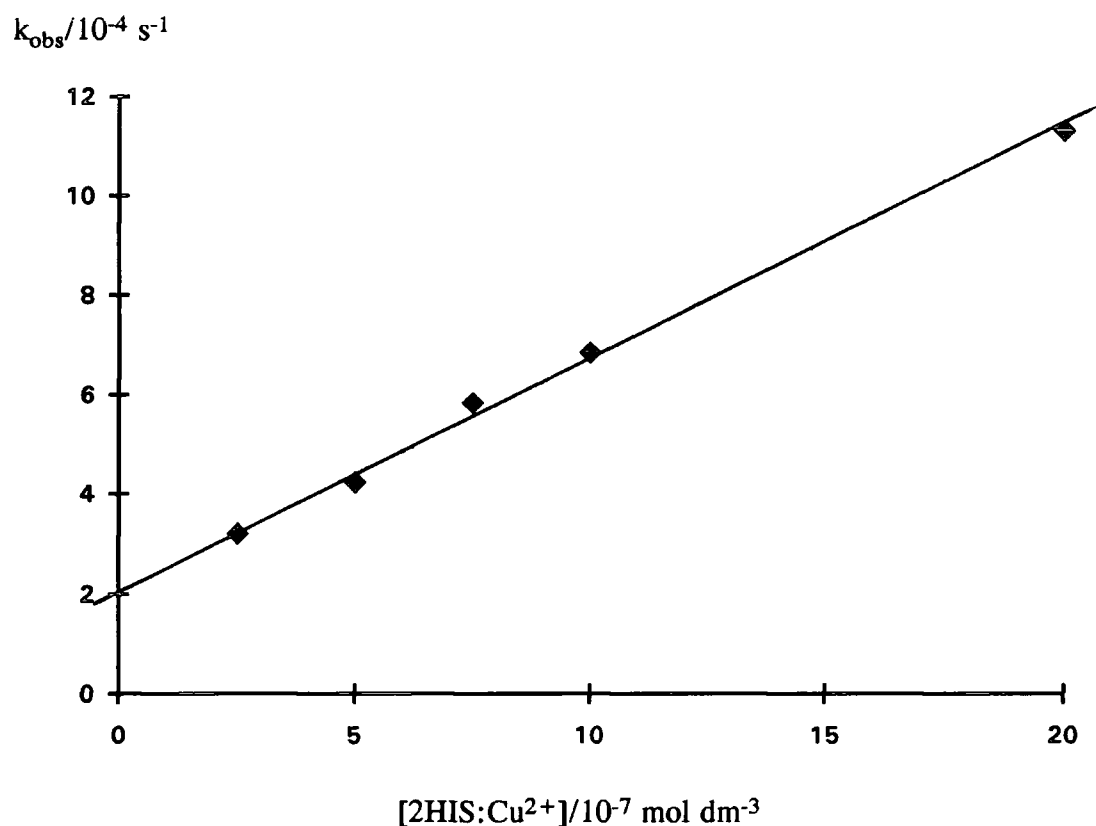
Kinetic data for the decomposition of S-nitroso-2-(mercaptopropionyl)glycine ($1 \times 10^{-3} \text{ mol dm}^{-3}$) in the presence of added 2HIS:Cu²⁺

[2HIS:Cu ²⁺]/10 ⁻⁶ mol dm ⁻³	k _{obs} /10 ⁻⁴ s ⁻¹
1.0	5.14 ± 0.12
2.0	5.69 ± 0.13
3.0	6.02 ± 0.13
4.0	6.48 ± 0.16

$$k_2 = 44 \pm 2 \text{ mol}^{-1} \text{ dm}^3 \text{ s}^{-1}$$

Figure 3.6

Plot of k_{obs} against $[2\text{HIS}:\text{Cu}^{2+}]$ for the decomposition of SNAP ($1 \times 10^{-3} \text{ mol dm}^{-3}$)



It is interesting to note that k_2 for the reaction of S-nitrosocysteine with $2\text{HIS}:\text{Cu}^{2+}$ is $58,000 \text{ mol}^{-1} \text{ dm}^3 \text{ s}^{-1}$ whereas k_2 for the analogous reaction with hydrated copper(II) is $60,000 \text{ mol}^{-1} \text{ dm}^3 \text{ s}^{-1}$. This implies very similar reactivity for the two copper species towards this nitrosothiol. In contrast the second order rate constants obtained for S-nitroso-2-(mercaptopropionyl)glycine are almost an order of magnitude different (360 and $44 \text{ mol}^{-1} \text{ dm}^3 \text{ s}^{-1}$). The effect of changing the amount of thiolate present was followed for a $2\text{HIS}:\text{Cu}^{2+}$ induced decomposition. NAP ($1 \times 10^{-5} - 1 \times 10^{-4} \text{ mol dm}^{-3}$) was added to SNAP ($1 \times 10^{-3} \text{ mol dm}^{-3}$) in the presence of $1 \times 10^{-5} \text{ mol dm}^{-3} 2\text{HIS}:\text{Cu}^{2+}$. An increase in pseudo-first order rate constant was apparent on increasing the $[\text{NAP}]$ (table 3.24).

Table 3.24

Kinetic data for the decomposition of SNAP ($1 \times 10^{-3} \text{ mol dm}^{-3}$) in the presence of 2HIS: Cu^{2+} ($1 \times 10^{-5} \text{ mol dm}^{-3}$) and added NAP

[N-acetylpenicillamine]/ $10^{-5} \text{ mol dm}^{-3}$	$k_{\text{obs}}/10^{-3} \text{ s}^{-1}$
0	1.63 ± 0.04
1.0	1.76 ± 0.04
3.0	2.14 ± 0.05
5.0	2.51 ± 0.06
10	3.61 ± 0.11

This is the opposite effect to that observed when adding NAP to SNAP + GGH: Cu^{2+} under the same conditions (table 3.10) where very little difference in k_{obs} was noted. Increasing [NAP] probably releases more Cu^{+} for catalysis from 2HIS: Cu^{2+} , hence producing a faster rate of S-nitrosothiol decomposition. The thiolate concentration is clearly crucial to the form of the rate profiles recorded as is the concentration of the copper complex introduced.

3.5 Summary of "Transport Cu²⁺" Results

Table 3.25 documents all the second order rate constants obtained for the various sources of copper(II) used for reaction with the three S-nitrosothiols studied.

Table 3.25

Summary of k_2 values obtained for the reaction of SNAP, SNC and SMPG with hydrated Cu²⁺, 2HIS:Cu²⁺, GGH:Cu²⁺ and HSA:Cu²⁺

Copper source	S-nitrosothiol studied		
	SNAP	SNC	SMPG
Hydrated Cu ²⁺	1260 ± 60	60,000 ± 500	360 ± 16
2HIS:Cu ²⁺	460 ± 15	58,000 ± 1000	44 ± 2
GGH:Cu ²⁺	440 ± 13	11,600 ± 300	180 ± 10
HSA:Cu ²⁺	120 ± 2	14,600 ± 900	260 ± 14

Units of k_2 = mol⁻¹ dm³ s⁻¹

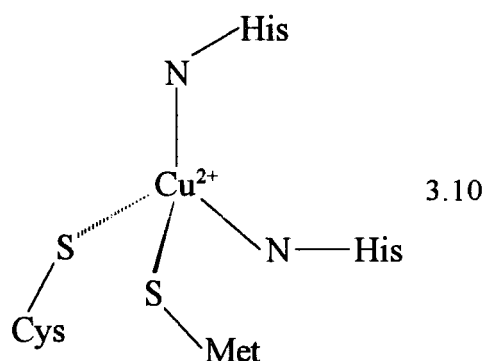
GGH:Cu²⁺, HSA:Cu²⁺ and 2HIS:Cu²⁺ can all be classed as being transport forms of cupric ion as the Cu²⁺ is in rapid exchange with tissue copper *in vivo*. It has been demonstrated that cuprous ion can be formed from each of these species by treatment with a reducing thiol such as NAP. All of the complexes studied catalysed the decomposition of nitrosothiols, releasing NO. In the case of SNAP, the order of reactivity was hydrated Cu²⁺ > 2HIS:Cu²⁺ > GGH:Cu²⁺ > HSA:Cu²⁺ (table 3.25). HSA alone inhibits reaction due to complexation of "impurity" copper, forming an extremely low concentration of HSA:Cu²⁺. In comparison, the reactivity order of these copper sources with SMPG was hydrated Cu²⁺ > HSA:Cu²⁺ > GGH:Cu²⁺ > 2HIS:Cu²⁺. The reaction rates measured are extremely dependent upon the [RS] present in the nitrosothiol solution which will vary from sample to

sample²⁷. As predicted, none of the bound forms of Cu^{2+} is as reactive as hydrated Cu^{2+} but all do display significant reactivity. However, as ~ 95% of plasma copper(II) is bound to ceruloplasmin and is non-exchangeable with tissue Cu^{2+} , the reactivity of this enzyme towards nitrosothiols is of great importance.

3.6 Ceruloplasmin

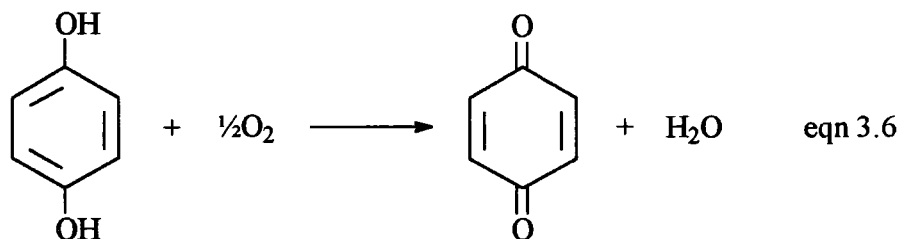
3.6.1 Properties and Physiological Roles of Ceruloplasmin

Ceruloplasmin is an intensely blue coloured, copper-containing glycoprotein existing in the plasma of mammalian blood. It is termed a "blue copper oxidase" which denotes its involvement (along with enzymes such as laccase and ascorbic oxidase) with molecular oxygen in specific catalytic processes. The copper ions in these proteins can easily accommodate electrons from a substrate and readily transfer them to a molecule of O_2 . Ceruloplasmin was first separated and isolated from human serum in 1948 by Holmberg and Laurell²⁸. Its level in plasma ranges between 270 - 370 mg dm^{-3} ¹⁶ but is known to vary significantly in a number of diseases and disorders. It is composed of a single polypeptide chain consisting of 1065 amino acids²⁹ and has a molecular weight of 135,000. This suggests a copper content of seven ions per ceruloplasmin molecule. The different types of copper ions found in copper proteins have been discussed in detail³⁰ but shall now be briefly described. Three classes of Cu are generally recognised, denoted as Type I, II and III. The former relates to the Cu^{2+} ions responsible for the blue colour of these proteins, being characterised by an intense absorption near 600nm with a molar extinction coefficient very much larger than is normally observed for square planar copper(II) complexes. Nearly every possible permutation of ligand type and geometry has been proposed to explain this phenomenon. It is now generally accepted that Cu^{2+} adopts a tetrahedral geometry which involves coordination via two histidine residues and two sulfur atoms from cysteine and methionine residues³¹ (3.10). The $\text{RS}(\sigma) \rightarrow \text{Cu}(\text{d})$ charge transfer explains the abnormally high ϵ value.



Type II Cu ions are often referred to as "non-blue copper(II)" as they display a weak absorption in the visible region ($\epsilon = 100 - 400 \text{ mol}^{-1} \text{ dm}^3 \text{ cm}^{-1}$). An environment of four nitrogen atoms around the Cu^{2+} is thought to exist in a tetragonal arrangement. Type III refers to EPR inactive Cu which has a strong absorption around 310 - 350nm. Great uncertainty exists as to the nature of the oxidation state of copper, hence very little is known about the surrounding environment. Deinum *et al*³² established that two Type I, one Type II and four Type III forms of copper exist in the native ceruloplasmin molecule.

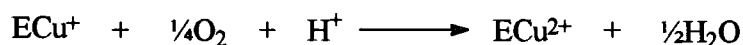
Ceruloplasmin is biosynthesised in the liver, where copper incorporation into the apoprotein also takes place³³. Intravenous injection of $^{64}\text{Cu}(\text{II})$ labelled copper compounds indicate³⁴ that copper undergoes a rapid transfer ($t_{1/2} = 8 - 10$ minutes) from the blood to the liver, with radioactivity re-emerging into the blood as ceruloplasmin-bound Cu^{2+} . The apoprotein can only incorporate copper at the time of its synthesis, and is inactive with respect to oxidase activity. Ceruloplasmin has a broad specificity with the best substrates being *para*-diphenols and related substances, which become oxidised (equation 3.6).



Indeed, all substances which can reduce Cu^{2+} in ceruloplasmin must also be substrates, unless the oxidation product inhibits the reoxidation of copper(I). A general mechanism (scheme 3.4) describes substrate oxidation involving two overall reactions³⁵.



Scheme 3.4



(ECu^{2+} represents the enzyme and AH_2 the substrate)

In instances where the reduction of copper(II) is slow (such as with ascorbic acid) the reducing agent acts as a poor substrate³⁶. Therefore, ceruloplasmin does not significantly catalyse the oxidation of H_2A to A (section 2.5.3, scheme 2.3). Ferrous ion is an excellent substrate however which has led the enzyme to be termed a "ferroxidase". The second order rate constant for reduction of Type I Cu^{2+} (the primary electron acceptor) is about $10^6 \text{ mol}^{-1} \text{ dm}^3 \text{ s}^{-1}$ with Fe^{2+} compared to about $10^3 \text{ mol}^{-1} \text{ dm}^3 \text{ s}^{-1}$ with the best organic substrates³⁷. In general, the oxidase activity of ceruloplasmin is much greater than that of simple Cu(II) salts and complexes, which also differ in that toxic H_2O_2 is the normal product from these as compared to water from ceruloplasmin. Thiols such as L-cysteine³⁸ are known to be able to interact with Type I Cu^{2+} , causing a decrease in absorbance at 610nm with concomitant formation of copper(I). It remains to be seen whether Cu^+ generated in this manner is capable of catalysing nitric oxide formation from S-nitrosothiols.

3.6.2 Reaction of S-Nitrosocysteine with Ceruloplasmin

Human ceruloplasmin (1ml, pH 7.0) was purchased from Sigma-Aldrich Co. Ltd. which had 100 - 150 μg per ml of copper present. The precise copper ion concentration was subsequently calculated using the following procedure. The molar extinction coefficient at λ_{max} (610 nm) was deduced as described by Blumberg *et al*³⁸ who measured the absorbance of a ceruloplasmin solution containing 66.5 μg of

copper per ml to be 1.420 at this wavelength. The concentration can be expressed as $1.04 \times 10^{-3} \text{ mol dm}^{-3}$ copper present, and hence $\epsilon_{610\text{nm}} = 1356 \text{ mol}^{-1} \text{ dm}^3 \text{ cm}^{-1}$. 0.25ml purchased ceruloplasmin was diluted to 5ml with pH 7.4 buffer and the absorbance at 610nm measured as 0.0762. This corresponds to a copper concentration of $5.62 \times 10^{-5} \text{ mol dm}^{-3}$ in the protein. This concentration is lower than the suppliers stated value, and was confirmed when another sample of ceruloplasmin was analysed in a similar manner and found to have $4.31 \times 10^{-5} \text{ mol dm}^{-3}$ copper present. The latter solution was used for all further kinetic experiments.

S-nitrosocysteine was initially studied with respect to its possible interaction with copper ions derived from ceruloplasmin. $1 \times 10^{-3} \text{ mol dm}^{-3}$ nitrosothiol containing $5 \times 10^{-7} \text{ mol dm}^{-3}$ EDTA in order to prolong stability was added to pH 7.4 buffer containing 0 - $3.75 \times 10^{-7} \text{ mol dm}^{-3}$ ceruloplasmin copper bound to the enzyme. The absorbance change at 340nm was followed in the usual way and good first order kinetics observed in each instance both in the presence and absence of ceruloplasmin (figure 3.7). Rate constants were measured at each copper concentration under similar conditions (table 3.26) and the experiment repeated using completely fresh solutions the following day (table 3.27).

Table 3.26

Kinetic data for the decomposition of S-nitrosocysteine ($1 \times 10^{-3} \text{ mol dm}^{-3}$) in the absence and presence of ceruloplasmin

$[\text{Cu}^{2+}_{\text{ceruloplasmin}}]/10^{-7} \text{ mol dm}^{-3}$	$k_{\text{obs}}/10^{-3} \text{ s}^{-1}$
0	2.61 ± 0.04
2.5	7.06 ± 0.15
5.0	11.6 ± 0.2
7.5	16.9 ± 0.3

$$k_2 = 18,900 \pm 560 \text{ mol}^{-1} \text{ dm}^3 \text{ s}^{-1}$$

Table 3.27

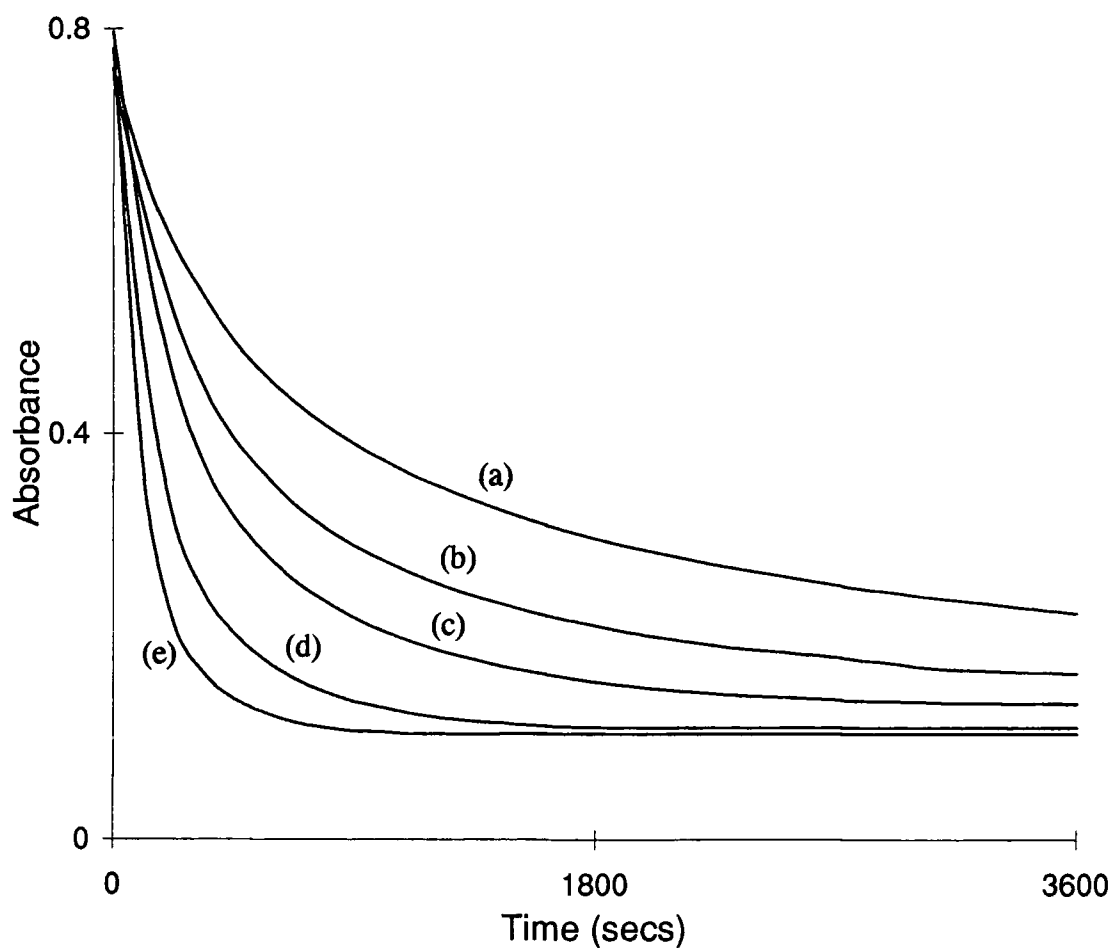
Kinetic data for the decomposition of S-nitrosocysteine ($1 \times 10^{-3} \text{ mol dm}^{-3}$) in the absence and presence of ceruloplasmin

$[\text{Cu}^{2+}_{\text{ceruloplasmin}}]/10^{-7} \text{ mol dm}^{-3}$	$k_{\text{obs}}/10^{-3} \text{ s}^{-1}$
0	2.91 ± 0.05
1.25	5.38 ± 0.11
2.5	7.34 ± 0.18
7.5	16.2 ± 0.3

$$k_2 = 17,600 \pm 260 \text{ mol}^{-1} \text{ dm}^3 \text{ s}^{-1}$$

Figure 3.7

Traces showing the decomposition of S-nitrosocysteine ($1 \times 10^{-3} \text{ mol dm}^{-3}$) in the absence and presence of ceruloplasmin, pH 7.4

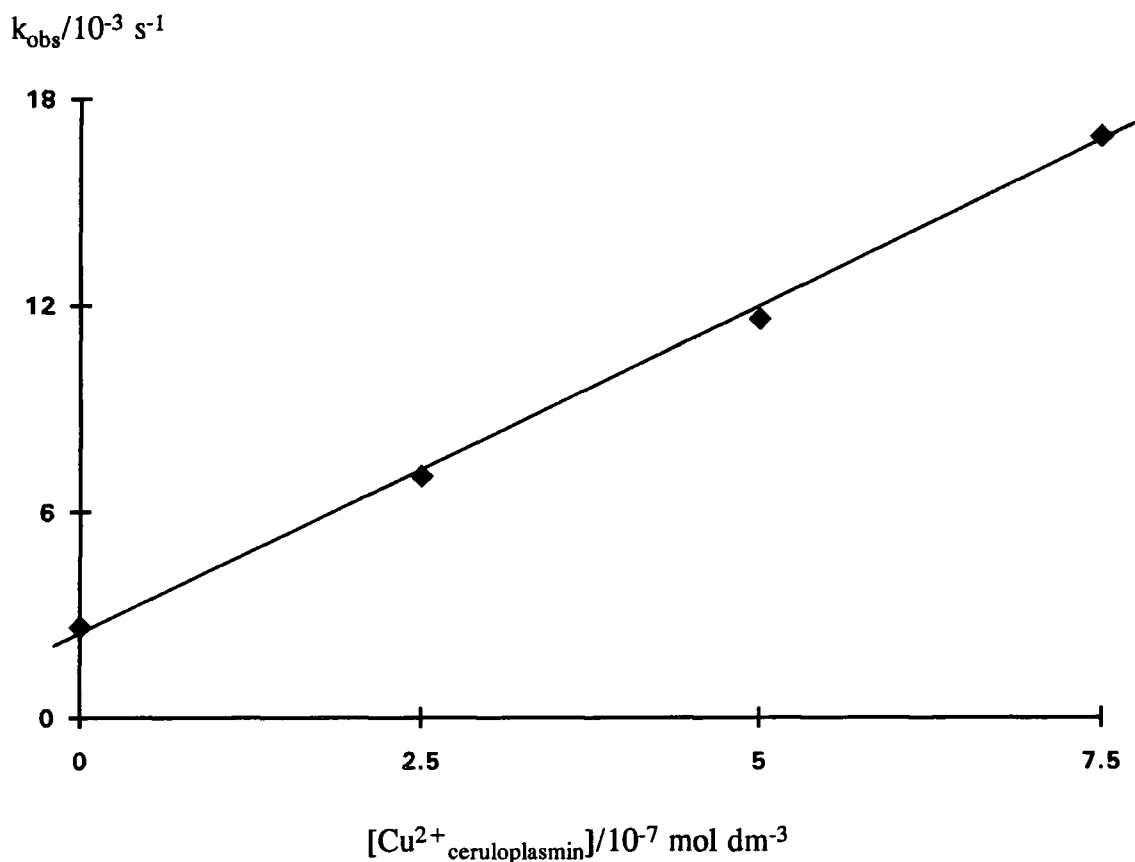


(a) no added ceruloplasmin; (b) $6.25 \times 10^{-8} \text{ mol dm}^{-3}$ ceruloplasmin copper;
 (c) $1.25 \times 10^{-7} \text{ mol dm}^{-3}$ ceruloplasmin copper; (d) $2.5 \times 10^{-7} \text{ mol dm}^{-3}$ ceruloplasmin copper; (e) $3.75 \times 10^{-7} \text{ mol dm}^{-3}$ ceruloplasmin copper.

A plot of the original data (table 3.26) is shown in figure 3.8.

Figure 3.8

Plot of k_{obs} against $[\text{Cu}^{2+}_{\text{ceruloplasmin}}]$ for the decomposition of S-nitrosocysteine
($1 \times 10^{-3} \text{ mol dm}^{-3}$)



Tables 3.26 and 3.27 demonstrate clear decomposition catalysis by ceruloplasmin and indicate the reproducibility of rate constants for this reaction. The second order values for k_2 obtained ($18,900$ and $17,600 \text{ mol}^{-1} \text{ dm}^3 \text{ s}^{-1}$) mean that S-nitrosocysteine has similar reactivity with respect to ceruloplasmin as it does with GGH: Cu^{2+} and HSA: Cu^{2+} (table 3.25). When higher ceruloplasmin concentrations were added the observed pseudo-first order k_{obs} value levelled off and became constant. An explanation for this is that the amount of copper bound to the enzyme may exceed the quantity of thiolate present as an impurity under these conditions meaning that a rate-limiting concentration of Cu^+ can be generated by reduction of copper(II).

The effect of adding reducing agents to the reaction of S-nitrosocysteine with ceruloplasmin was then investigated. L-cysteine and ascorbic acid were separately introduced over the same concentration range (1×10^{-7} - 1×10^{-4} mol dm⁻³) and the pseudo-first order rate constants calculated (table 3.28).

Table 3.28

Kinetic data for the reaction of S-nitrosocysteine (1×10^{-3} mol dm⁻³) and ceruloplasmin (2.5×10^{-7} mol dm⁻³ Cu²⁺_{ceruloplasmin}) with added thiol or ascorbic acid

[thiolate] or [ascorbate]/10 ⁻⁷ mol dm ⁻³	k _{obs} /10 ⁻³ s ⁻¹	
	L-cysteine	ascorbic acid
0	6.92 ± 0.13	6.55 ± 0.13
1	5.95 ± 0.13	5.27 ± 0.12
10	5.92 ± 0.11	5.50 ± 0.13
100	7.38 ± 0.15	5.08 ± 0.11
1000	3.86 ± 0.11	5.50 ± 0.09

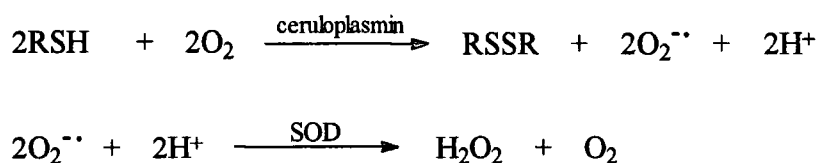
This table indicates that the addition of reducing agents (potential substrates) to ceruloplasmin has little effect on the rate of S-nitrosocysteine decomposition. Indeed, high thiolate concentrations seem to slightly inhibit reaction, probably due to a degree of copper ion chelation. This is at variance with previous results obtained adding L-cysteine to the corresponding nitrosothiol and Cu²⁺.³⁹ At low thiol concentrations (5×10^{-6} mol dm⁻³ - 5×10^{-5} mol dm⁻³) the rate of nitrosothiol decomposition is increased, whereas above [L-cysteine] = 1×10^{-4} mol dm⁻³ the reaction becomes progressively slower. Work undertaken utilising SNAP with added NAP (section 2.5.1) demonstrates an identical trend. As the copper content of ceruloplasmin is so low in this instance (2.5×10^{-7} mol dm⁻³) and the buffer [Cu²⁺] ~ 1×10^{-6} mol dm⁻³ (determined by atomic absorption spectrophotometry), it is likely that the amount of L-cysteine present due to the reversibility of thiol nitrosation²⁷ is greater than the total amount of copper(II) ions available in the system for reduction. If this is the case, increasing the thiol concentration or introducing ascorbic acid will not increase the rate of decomposition significantly. L-cysteine is known to be a good chelator of

Cu^{2+} only above pH 8.0⁴⁰ hence only a small decrease in k_{obs} is apparent when $1 \times 10^{-4} \text{ mol dm}^{-3}$ thiol is present.

Ceruloplasmin also catalysed nitric oxide formation from SNAP and SMPG but to a much lesser extent than for S-nitrosocysteine. Adding the corresponding thiol or ascorbic acid to each reaction again had no observable rate enhancing effect. It appears as if, under certain conditions, thiolate can reduce copper(II) chelated to ceruloplasmin, a theory that could be examined spectrophotometrically.

3.6.3 Addition of L-cysteine to Ceruloplasmin

The possible reaction between ceruloplasmin and L-cysteine was followed using $[\text{Cu}^{2+}_{\text{ceruloplasmin}}] = 5.6 \times 10^{-5} \text{ mol dm}^{-3}$. A solution of protein was added to neocuproine ($1 \times 10^{-3} \text{ mol dm}^{-3}$) in pH 7.4 buffer and thiol ($1 \times 10^{-3} \text{ mol dm}^{-3}$) introduced. A uv/visible spectrum was immediately recorded between 350 - 700nm (figure 3.9, trace (a)) with a further one taken after ten minutes (trace (b)). There is an obvious decrease in absorbance due to Type I Cu at 610nm with a parallel increase at 453nm due to $\text{Cu}(\text{NC})_2^+$ generation. Thus, copper(II) ions that are bound to ceruloplasmin and contribute to the intense blue colour can be reduced in a similar manner to hydrated or chelated Cu^{2+} . A similar effect has been described by Chidambaram *et al*⁴¹ who report a permanent reduction of Type I copper by L-cysteine. However, the authors proposed that superoxide ion is a reaction product as the enzyme superoxide dismutase (SOD) caused a large rate enhancement in thiol oxidation, presumably due to formation of H_2O_2 (scheme 3.5).



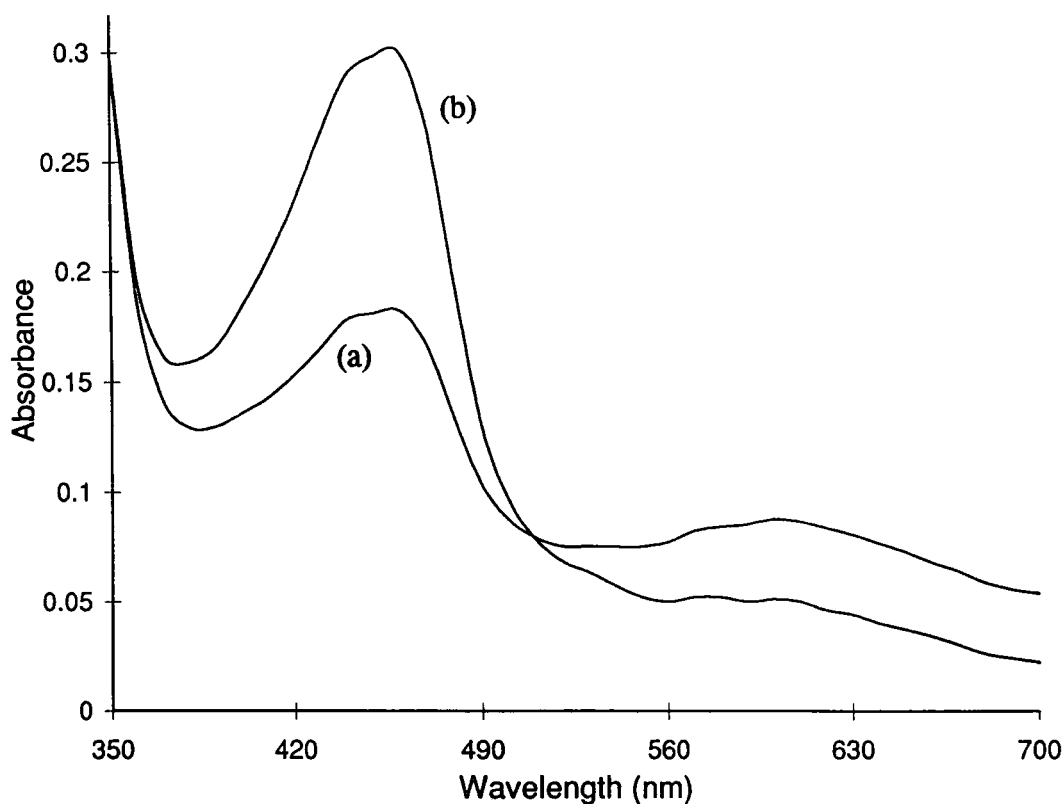
Scheme 3.5

The infinity absorbance at 453nm was measured as 0.305. After subtracting the residual ceruloplasmin absorbance (0.006) at this wavelength, the percentage Cu^+

trapped by neocuproine was calculated as 67% using $\epsilon_{453\text{nm}} = 7950 \text{ mol}^{-1} \text{ dm}^3 \text{ cm}^{-1}$ as before. This seems to be a significant amount of cuprous ion formation. This value cannot be compared with quantities of copper(I) generated from other chelated forms of Cu^{2+} as the [thiol]: $[\text{Cu}^{2+}]$ ratio is approximately 20:1 in this case, whereas for the amino acid, tripeptide and polypeptide bound copper(II) reactions the analogous ratio was 1:1 in every instance. An important point to note is that a tightly bound form of Cu^{2+} can be reduced by thiolate. It is well documented⁴² that ceruloplasmin has a plethora of loose binding sites for divalent metal ions such as Co(II), Ni(II) and Zn(II) as well as for Cu(II). L-cysteine has been shown to interact with Type I copper, which cannot be removed by a metal chelating resin, and is an integral part of the protein structure.

Figure 3.9

Uv/visible spectra of ceruloplasmin ($5.6 \times 10^{-5} \text{ mol dm}^{-3} \text{ Cu}^{2+}_{\text{ceruloplasmin}}$) and equimolar L-cysteine/neocuproine ($1 \times 10^{-3} \text{ mol dm}^{-3}$)



(a) immediate spectrum; (b) spectrum acquired after ten minutes

3.6.4 Effect of Peroxynitrite

Peroxynitrite (ONOO^-) may be generated in the vasculature by the reaction of superoxide with nitric oxide (section 1.1.4, equation 1.9). A recent paper⁴³ has examined the reaction between this ion and ceruloplasmin. It was found that incubation of ONOO^- with the enzyme releases copper ions and reduces ferroxidase activity. A loss of absorbance at 610nm and increase at 460nm is observed, related to redox active copper release which is chelated by 1,10-phenanthroline. The decomposition products of peroxynitrite (nitrate and nitrite ions) have been shown to have no effect on ceruloplasmin. This interesting discovery prompted an investigation into the effect that ONOO^- may have on S-nitrosothiol decomposition in the presence of this enzyme.

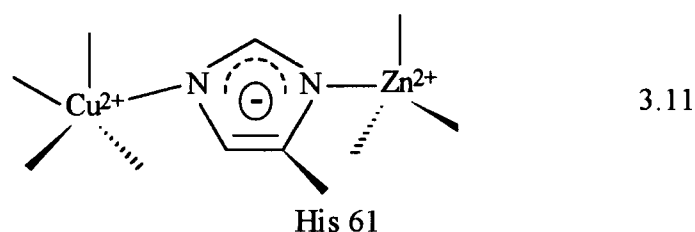
Peroxynitrite was synthesised as its sodium salt by the following procedure. 1.035g NaNO_2 in 25ml water was added to 25ml of acidified hydrogen peroxide ($0.72 \text{ mol dm}^{-3} \text{ H}_2\text{O}_2$ in $0.68 \text{ mol dm}^{-3} \text{ HCl}$) at 0°C under vigorous agitation. Immediately following this, 25ml $1.25 \text{ mol dm}^{-3} \text{ NaOH}$ was introduced to stabilise the mixture. After three minutes the final solution was treated with granulated MnO_2 (to destroy excess peroxide) and filtered. The resulting peroxynitrite was stored frozen at -10°C and its concentration determined by applying a molar extinction coefficient of $1670 \text{ mol}^{-1} \text{ dm}^3 \text{ cm}^{-1}$ at 302nm⁴⁴ against an appropriate blank of "decomposed" ONOO^- in pH 7.4 buffer. The decomposed peroxynitrite contained nitrate, nitrite and chloride ions. S-nitrosocysteine ($1 \times 10^{-3} \text{ mol dm}^{-3}$) was reacted in the presence of ceruloplasmin ($9 \times 10^{-7} \text{ mol dm}^{-3} \text{ Cu}^{2+}_{\text{ceruloplasmin}}$) and the first order rate constant (k_{obs}) measured as $1.73 \pm 0.02 \times 10^{-3} \text{ s}^{-1}$. Subsequently, peroxynitrite was introduced ($1 \times 10^{-3} \text{ mol dm}^{-3}$) and incubated for ten minutes with ceruloplasmin prior to reaction with S-nitrosocysteine ($k_{\text{obs}} = 3.46 \pm 0.05 \times 10^{-2} \text{ s}^{-1}$). This means that there was a 20-fold increase in the rate of nitrosothiol decomposition when ONOO^- was added. The decomposition products of peroxynitrite had little or no effect on the rate of NO formation.

In conclusion, it is clear that various substrates can release cuprous ions from ceruloplasmin *in vitro* which are made available for reaction with nitrosothiols. The biological significance of this should not be understated, as the copper catalysed mechanism of nitric oxide production appears to be even more feasible *in vivo*.

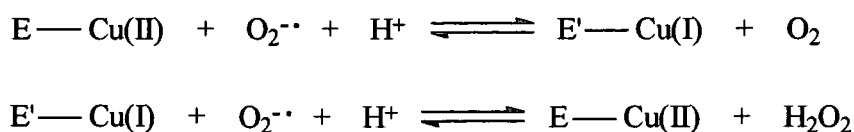
3.7 Superoxide Dismutase (SOD) and Metallothionein

3.7.1 Biological Relevance

Both superoxide dismutase (SOD) and metallothionein are protein molecules which contain copper ions. The former catalyses the rapid two step dismutation of toxic superoxide radical, generating hydrogen peroxide and molecular oxygen (scheme 3.5), via reduction and oxidation of the active site copper. Superoxide is believed to react with thiol groups and tryptophan residues which could prove to be lethal. The structure and mechanism of this enzyme has been reported⁴⁵ with the active site outlined below (3.11).



The main feature of the metal binding region is that copper and zinc ions coordinate to the same imidazole ring of the histidine residue (His-61). Cu^{2+} is coordinated by four histidine residues in total and one water molecule. An important aspect is that the copper ion is located at the bottom of a crevice. This means that Cu^{2+} is accessible to Cl^- and Br^- but not I^- .⁴⁶ During catalysis, copper(II) becomes reversibly oxidised and reduced by successive encounters with O_2^- according to scheme 3.6.



Scheme 3.6

Human SOD has a molecular weight of 31,200 and is composed of two identical subunits, each containing one Cu^{2+} in the oxidised form. The optical spectrum of the enzyme is characterised by a broad absorption band in the visible region between 500 and 900nm with a maximum at about 680nm which is responsible for the bluish-green appearance of concentrated solutions. This band, and another weaker one at 340nm is thought to result from copper. The addition of hydrogen peroxide to a solution of superoxide dismutase results in a bleaching of the 680nm band, which is thought to be due to the reduction of enzymic copper (eqn. 3.7).



Ferrocyanide can also accomplish a bleaching of this band, with the production of ferricyanide indicating that a true reduction of the protein has taken place.

In comparison, the function of metallothionein has been debated ever since its intracellular discovery. This protein contains a high amount of heavy metals which are bound exclusively by clusters of thiolate bonds. Mammalian metallothionein is a 61 or 62 amino acid peptide comprising twenty cysteine residues which bind seven Cu(I) ions. Stability constants range from 10^{19} to 10^{17} for copper, with metallothionein also capable of binding to mercury, cobalt, lead, nickel, cadmium, zinc, silver and gold⁴⁷. Therefore, a role in metal metabolism or detoxification has been proposed. The protein has a random structure in the absence of metal ions, and in certain organisms stimulation of metallothionein synthesis by copper is observed. These two copper containing species provide a potential opportunity for S-nitrosothiol decomposition to occur *in vivo*. The interaction (and possible catalytic effect) of SOD/metallothionein on S-nitrosocysteine was studied.

3.7.2 Effect of SOD on the Stability of S-Nitrosothiols

Superoxide dismutase extracted from bovine erythrocytes was purchased as a lyophilized powder from Sigma-Aldrich Co. Ltd. One mole of SOD is known to contain two moles of Cu^{2+} , so the reaction between S-nitrosocysteine ($1 \times 10^{-3} \text{ mol dm}^{-3}$) and $2 \times 10^{-6} \text{ mol dm}^{-3}$ copper(II) derived from the protein was monitored at 340nm, and compared with an analogous reaction with hydrated cupric ion (table 3.29).

Table 3.29

Kinetic data for the reaction between S-nitrosocysteine ($1 \times 10^{-3} \text{ mol dm}^{-3}$) and hydrated Cu^{2+} or SOD ($[\text{Cu}^{2+}]_{\text{hydrated/SOD}} = 2 \times 10^{-6} \text{ mol dm}^{-3}$)

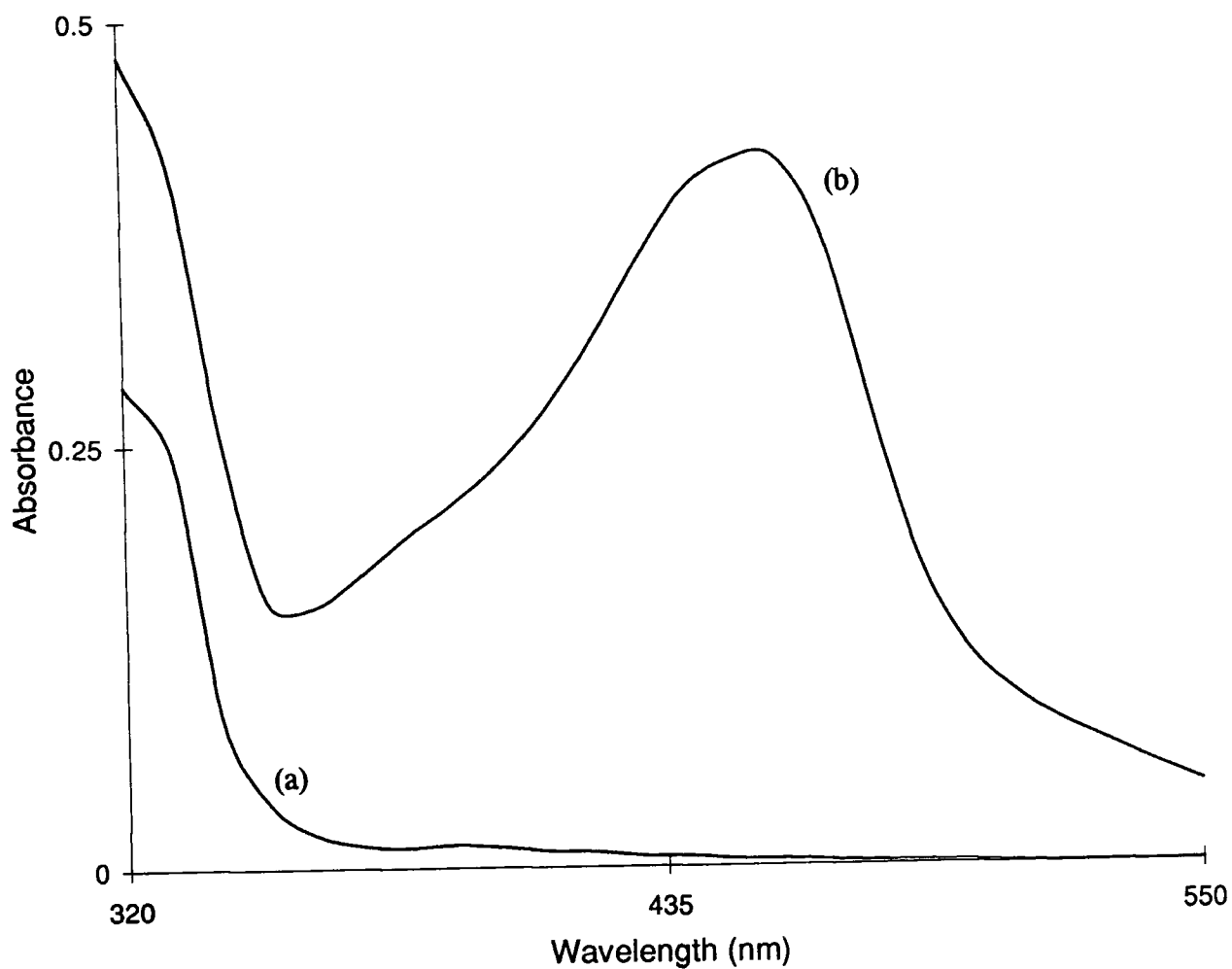
Copper source	$k_{\text{obs}}/10^{-2} \text{ s}^{-1}$
pH 7.4 buffer	9.63 ± 0.21
Hydrated Cu^{2+}	119 ± 7
SOD	9.74 ± 0.23

From these results it is apparent that the rate of reaction is extremely similar both in the presence and absence of added SOD, with decomposition induced by hydrated copper ions some ten times faster as expected. Therefore, this enzyme appears to be having very little effect on nitrosothiol stability, in direct contrast to ceruloplasmin (section 3.6.2). When higher enzyme concentrations were added (up to $[\text{SOD}] = 3 \times 10^{-5} \text{ mol dm}^{-3}$) nitric oxide release was inhibited, presumably due to buffer metal ion chelation by the protein. An experiment was conducted to test whether cupric ions present in superoxide dismutase could be reduced by thiolate and trapped as Cu^+ . SOD ($3 \times 10^{-5} \text{ mol dm}^{-3}$) was added to $1 \times 10^{-4} \text{ mol dm}^{-3}$ L-cysteine in the presence of $3 \times 10^{-4} \text{ mol dm}^{-3}$ neocuproine. No characteristic absorbance increase at 453nm or yellow colouration was noted as was observed for other chelated forms of Cu^{2+} , suggesting that copper(I) cannot be generated in this manner. This is not surprising as the cupric ions are buried within the enzyme structure and can only be reached by small substrates such as $\text{O}_2^{\cdot-}$. It may be the case that the thiolate ion is

too large to reach Cu^{2+} and hence no cuprous ion can be generated from SOD, leading to no rate enhancing effect. When ascorbic acid was utilised as a possible reductant exactly the same results were obtained (figure 3.10). A comparison is made between the amount of copper(I) formed by ascorbate reacting with hydrated Cu^{2+} and that derived from SOD.

Figure 3.10

Uv/visible spectra of $6 \times 10^{-5} \text{ mol dm}^{-3} \text{ Cu}^{2+}$ (derived from SOD or hydrated) in the presence of $1 \times 10^{-4} \text{ mol dm}^{-3}$ ascorbic acid and $3 \times 10^{-4} \text{ mol dm}^{-3}$ neocuproine



(a) Cu^{2+} bound to superoxide dismutase

(b) hydrated Cu^{2+}

Calculations indicate that 88% Cu^+ was chelated by neocuproine following ascorbate induced reduction of hydrated Cu^{2+} whereas no peak at 453nm for SOD is indicative of no cuprous ion formation from the protein molecule. Superoxide dismutase can therefore be discounted as a mediator of S-nitrosothiol decomposition *in vivo*.

3.7.3 Influence of Metallothionein

Horse kidney metallothionein was purchased from Sigma-Aldrich Co. Ltd. and reacted with S-nitrosocysteine. As copper(I) ions are present within the protein structure it was predicted that metallothionein would catalyse nitric oxide formation from this compound, but surprisingly an inhibitory effect was apparent. It appears that the Cu^+ ions are unavailable to bind the nitrosothiol in order to effect reaction. The precise role of this protein within the human body remains a mystery.

3.8 Conclusion

It has clearly been demonstrated that copper(II) ions chelated to either an amino acid, peptide or protein molecule are available for reduction either by thiolate or ascorbate, forming Cu^+ . However, not all bound forms of copper(II) can react in this manner as shown by results pertaining to SOD. Copper(I) which has been generated in this way is readily available to bring about the decomposition of S-nitrosothiols forming NO and the corresponding disulfide by the same mechanism as that outlined in Chapter Two. The significance of these results is that it is now possible to postulate a pathway for the formation of nitric oxide *in vivo* from S-nitrosothiols which utilises chelated copper(II) ions. This particular mode of decomposition could prove to have major importance in explaining the behaviour of these compounds under physiological conditions. The mechanism outlined may account for nitric oxide generation from therapeutically administered nitrosothiols and could lead to the establishment of such compounds as a routinely-used treatment for angina and other circulatory problems.

References

1. J.J.R. Fraústo da Silva and R.J.P. Williams, *The Biological Chemistry of the Elements*, Oxford University Press, 1991, 389.
2. *Harper's Review of Biochemistry*, Twentieth Edn., Lange, 1985, 655.
3. P.Z. Neumann and A. Sass-Kortsak, *J. Clin. Invest.*, 1967, **46**, 646.
4. T. Peters Jr. and F.A. Blumenstock, *J. Biol. Chem.*, 1967, **242**, 1574.
5. W.T. Shearer, R.A. Bradshaw, F.R.N. Gurd and T. Peters Jr., *J. Biol. Chem.*, 1967, **242**, 5451.
6. R.A. Bradshaw, W.T. Shearer and F.R.N. Gurd, *J. Biol. Chem.*, 1968, **243**, 3817.
7. S-J. Lau, T.P.A. Kruck and B. Sarkar, *J. Biol. Chem.*, 1974, **249**, 5878.
8. R.W. Hay, M.M. Hassan and Y.Q. Chen, *J. Inorg. Biochem.*, 1993, **52**, 17.
9. J.M. Walshe, *Quart. J. Med.*, 1973, **42**, 441.
10. K. Uchida and S. Kawakishi, *J. Agric. Food Chem.*, 1989, **37**, 897.
11. E. Kimura, T. Koike, Y. Shimizu and M. Kodama, *Inorg. Chem.*, 1986, **25**, 2242.
12. S.C. Askew, D.J. Barnett, J. McAninly and D.L.H. Williams, *J. Chem. Soc., Perkin Trans. 2*, 1995, 741.
13. J.P. Griess, *Philos. Trans. Roy. Soc.*, 1864, **154**, 667.
14. A. Vogel, *Textbook of Quantitative Inorganic Analysis*, Fourth Edn., Longman, 1978, 755.
15. Geigy Scientific Tables, Vol. 3, *Ciba Geigy, Switzerland*, 137.
16. T.M. Devlin, *Textbook of Biochemistry*, Third Edn., Wiley, 1992, 321.
17. J-P. Laussac and B. Sarkar, *Biochemistry*, 1984, **23**, 2832.
18. P.C. Jocelyn, *Biochemistry of the -SH Group*, Academic Press, 1972, 81.
19. L.E. Maley and D.P. Mellor, *Nature*, 1950, **165**, 453.

20. N.C. Li, E. Doody and J.M. White, *J. Am. Chem. Soc.*, 1957, **79**, 5859.
21. M.A. Doran, S. Chaberek and A.E. Martell, *J. Am. Chem. Soc.*, 1964, **86**, 2129.
22. W.H. Stein and S. Moore, *J. Biol. Chem.*, 1954, **211**, 915.
23. S-J. Lau and B. Sarkar, *J. Biol. Chem.*, 1971, **246**, 5938.
24. M. Tabata and B. Sarkar, *Can. J. Chem.*, 1985, **63**, 3111.
25. M.S. Nair, K. Venkatachalapathi, M. Santappa and P.K. Murugan, *J. Chem. Soc., Dalton Trans.*, 1982, 55.
26. J. Kreuder, A. Otten, H. Fuder, Z. Tumer, T. Tonnesen, N. Horn and D. Dralle, *Eur. J. Pediatrics*, 1993, **152**, 828.
27. P. Herves Beloso and D.L.H. Williams, *J. Chem. Soc., Chem. Commun.*, 1997, 89.
28. C.G. Holmberg and C.B. Laurell, *Acta. Chem. Scand.*, 1948, **2**, 550.
29. L. Ryden and I. Bjork, *Biochemistry*, 1976, **15**, 3411.
30. J.A. Fee, *Struct. Bond.*, 1975, **23**, 1.
31. E.J. Solomon, J.W. Hare and H.B. Gray, *Proc. Natl. Acad. Sci., USA*, 1976, **73**, 1389.
32. J. Deinum and T. Vänngård, *Biochim. Biophys. Acta*, 1973, **310**, 321.
33. C.A. Owen and J.B. Hazelrig, *Am. J. Physiol.*, 1966, **210**, 1059.
34. A. Sass-Kortsak, *Adv. Clin. Chem.*, 1965, **8**, 1.
35. T.P. Singer, *Biological Oxidations*, Interscience, 1968, 431.
36. A.G. Morell, P. Aisen and I.H. Scheinberg, *J. Biol. Chem.*, 1962, **237**, 3455.
37. S. Osaki and O. Walaas, *J. Biol. Chem.*, 1967, **242**, 2653.
38. W.E. Blumberg, J. Eisinger, P. Aisen, A.G. Morell and I.H. Scheinberg, *J. Biol. Chem.*, 1963, **238**, 1675.
39. D.J. Barnett, Ph.D. thesis, University of Durham, 1994.

40. D. Cavallini, C. deMarco, S. Dupre and G. Rotilio, *Arch. Biochem. Biophys.*, 1969, **130**, 354.
41. M.V. Chidambaram, A. Zgirski and E. Frieden, *J. Inorg. Biochem.*, 1984, **21**, 227.
42. D.J. McKee and E. Frieden, *Biochemistry*, 1971, **10**, 3880.
43. J.A. Swain, V. Darley-USmar and J.M.C. Gutteridge, *FEBS Lett.*, 1994, **342**, 49.
44. M.N. Hughes and H.G. Nicklin, *J. Chem. Soc. (A)*, 1968, 450.
45. J.A. Tainer, E.D. Getzoff, J.S. Richardson and D.C. Richardson, *Nature*, 1983, **306**, 284.
46. A. Rigo, R. Stevanato, P. Viglino and G. Rotilio, *Biochem. Biophys. Res. Commun.*, 1977, **79**, 776.
47. D.H. Hamer, *Ann. Rev. Biochem.*, 1986, **55**, 913.

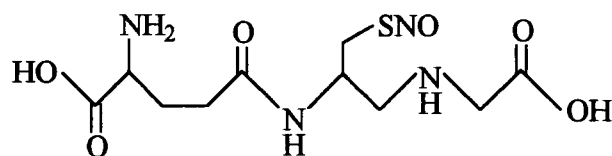
Chapter 4

Stability of Novel Aliphatic, Heterocyclic and Aromatic S-Nitrosated Thiols

Chapter 4: Stability of Novel Aliphatic, Heterocyclic and Aromatic S-Nitrosated Thiols

4.1 Introduction

Since the current interest in S-nitrosothiols as potential nitric oxide donors developed in the late 1980's, many vastly different substrates have been studied and a general structure/reactivity relationship established^{1,2,3}. Much activity has been centred around S-nitrosoglutathione (GSNO, 4.1) as the thiol precursor is the most abundant mercapto compound present within the human body (0.5 - 10 μ mol per gram of fresh tissue)⁴.

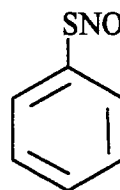


4.1

In addition, many nitrosothiols based on the amino acid L-cysteine have been examined *in vitro*. There remain several thiols which however have not been studied whose S-nitroso derivatives may prove to have an interesting biological profile. To date, nitrosothiols generated from heterocyclic or aromatic starting materials are almost absent in the chemical literature, except for the well-characterised S-nitrosotriphenylmethanethiol (4.2)⁵ and S-nitrosothiophenol (4.3)⁶.



4.2



4.3

Of particular interest are nitrosothiols with an electron donating moiety in close proximity to the -SNO functional group thus providing the capability of bidentately chelating Cu⁺, which appears to be a requirement for decomposition. Therefore, a range of thiols were nitrosated using one equivalent of acidified sodium

nitrite *in situ*. The S-nitrosated species generated were reacted with cupric ions. In all except one instance nitric oxide release in pH 7.4 buffer took place which was a copper ion catalysed process.

4.2 Generation and Reactivity of New Aliphatic S-Nitrosothiols

The S-nitrosothiol compounds under scrutiny were monitored by conventional uv/visible spectrophotometry at 340nm, close to the λ_{\max} value for each material (table 4.1).

Table 4.1

Spectral data obtained for some aliphatic S-nitrosothiols, pH 7.4

S-nitrosothiol	ϵ ($\text{mol}^{-1} \text{dm}^3 \text{cm}^{-1}$)*	λ_{\max} (nm)
S-nitroso-2-N,N-dimethylaminoethanethiol	714 ± 10	332, 541
S-nitroso-2-N,N-diethylaminoethanethiol	623 ± 8	332, 544
S-nitroso-N-carbamylpenicillamine	976 ± 15	340, 588
S-nitroso-N-carbamylcysteine	876 ± 14	337, 544
S-nitroso-2-(mercaptopropionyl)glycine	844 ± 6	334, 546
S-nitrosomercaptoethanesulfonic acid	920 ± 10	329, 546

*All ϵ values measured at 340nm

In each case, a decrease in absorbance at 340nm was exhibited, due to nitrosothiol decomposition and corresponding disulfide formation. A "window" of copper(II) ion concentrations existed (section 2.1), usually between 1×10^{-6} - 5×10^{-5} mol dm^{-3} where good first order kinetics were obtained. Below and above this range traces were collected which had induction periods and were zero order in nature

(section 2.5.2). Interest initially was focused on the $[\text{Cu}^{2+}]$ which allowed first order plots to develop. Tables 4.2 - 4.5 detail the kinetic data relevant to the decomposition of four of these nitrosothiols in the presence of cupric ion.

Table 4.2

Kinetic data for the decomposition of S-nitroso-N-carbamylpenicillamine ($5 \times 10^{-4} \text{ mol dm}^{-3}$) in the presence of added Cu^{2+} , pH 7.4 buffer

$[\text{Cu}^{2+}]/10^{-6} \text{ mol dm}^{-3}$	$k_{\text{obs}}/10^{-3} \text{ s}^{-1}$
3.0	3.00 ± 0.09
4.0	3.72 ± 0.06
5.0	4.81 ± 0.09
7.0	6.17 ± 0.08
8.0	7.12 ± 0.05
9.0	7.47 ± 0.09
10	8.64 ± 0.12

$$k_2 = 780 \pm 30 \text{ mol}^{-1} \text{ dm}^3 \text{ s}^{-1}$$

Percentage thiol impurity in S-nitrosothiol sample = 0.87%

Table 4.3

Kinetic data for the decomposition of S-nitroso-N-carbamylcysteine ($5 \times 10^{-4} \text{ mol dm}^{-3}$) in the presence of added Cu^{2+} , pH 7.4 buffer

$[\text{Cu}^{2+}]/10^{-5} \text{ mol dm}^{-3}$	$k_{\text{obs}}/10^{-3} \text{ s}^{-1}$
1.0	9.80 ± 0.3
2.0	13.9 ± 0.4
3.0	17.2 ± 0.6
4.0	21.5 ± 0.7
5.0	25.1 ± 0.9

$$k_2 = 380 \pm 10 \text{ mol}^{-1} \text{ dm}^3 \text{ s}^{-1}$$

Percentage thiol impurity in S-nitrosothiol sample = 0.54%

Table 4.4

Kinetic data for the decomposition of S-nitroso-2-(mercaptopropionyl)glycine
($5 \times 10^{-4} \text{ mol dm}^{-3}$) in the presence of added Cu^{2+} , pH 7.4 buffer

$[\text{Cu}^{2+}]/10^{-5} \text{ mol dm}^{-3}$	$k_{\text{obs}}/10^{-3} \text{ s}^{-1}$
0.5	2.36 ± 0.06
1.0	3.41 ± 0.09
2.0	6.44 ± 0.17
3.0	8.77 ± 0.19
4.0	10.1 ± 0.3
5.0	14.0 ± 0.2

$$k_2 = 250 \pm 15 \text{ mol}^{-1} \text{ dm}^3 \text{ s}^{-1}$$

Table 4.5

Kinetic data for the decomposition of S-nitroso-2-mercaptoethanesulfonic acid
($1 \times 10^{-3} \text{ mol dm}^{-3}$) in the presence of added Cu^{2+} , pH 7.4 buffer

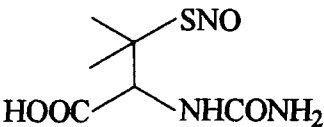
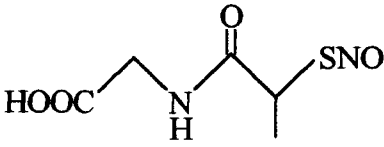
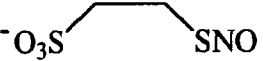
$[\text{Cu}^{2+}]/10^{-5} \text{ mol dm}^{-3}$	$k_{\text{obs}}/10^{-3} \text{ s}^{-1}$
3.0	1.89 ± 0.07
4.0	2.37 ± 0.06
5.0	2.85 ± 0.06
6.0	3.36 ± 0.07
7.0	3.80 ± 0.08
8.0	4.19 ± 0.09
9.0	4.74 ± 0.11

$$k_2 = 47 \pm 2 \text{ mol}^{-1} \text{ dm}^3 \text{ s}^{-1}$$

The second order rate constant, k_2 was obtained from the slope of a plot of k_{obs} against $[\text{Cu}^{2+}]_{\text{added}}$ (section 1.4.3.1). At copper(II) ion concentrations ($1 \times 10^{-4} \text{ mol dm}^{-3}$) higher than those indicated in each table, the linear relationship demonstrated ceased, and very irreproducible results were apparent. Generally, an increase in $[\text{Cu}^{2+}]_{\text{added}}$ did not lead to any significant rate enhancement. A possible reason for this is due to complexation occurring between copper(II) and phosphate buffer, thus making the effective $[\text{Cu}^{2+}]$ available for catalysis unknown. Table 4.6 displays the k_2 values calculated for each compound.

Table 4.6

Values of k_2 for the copper ion catalysed decomposition of aliphatic S-nitrosothiols,
pH 7.4 buffer

S-nitrosothiol	Structure	k_2 ($\text{mol}^{-1} \text{dm}^3 \text{s}^{-1}$)
S-nitroso-N-carbamylpenicillamine (SNCP)		780 ± 30
S-nitroso-N-carbamylcysteine (SNCC)		380 ± 10
S-nitroso-2-(mercaptopropionyl)glycine (SMPG)		250 ± 15
S-nitrosomercaptoethanesulfonic acid		47 ± 2

Two close derivatives of SNAP (S-nitroso-N-carbamylpenicillamine (SNCP) and S-nitroso-N-carbamylcysteine (SNCC)) were formed *in situ* from the thiol precursors generously donated by Glaxo-Wellcome. The first point of interest is a direct comparison between the k_2 values obtained for these two compounds (table 4.6). SNCP is observed to be approximately twice as reactive as SNCC which is similar to the difference in reactivity between S-nitrosopenicillamine and S-nitrosocysteine ($67,000 \text{ mol}^{-1} \text{dm}^3 \text{s}^{-1}$ and $24,700 \text{ mol}^{-1} \text{dm}^3 \text{s}^{-1}$ respectively)¹. This difference can be attributed to the "gem-dimethyl effect" described in section 1.4.3.1. Both SNCP and SNCC are much more susceptible to copper ion catalysed decomposition than is an *in situ* preparation of SNAP (the former forty times, the latter twenty times). Work undertaken by Hudson *et al*⁷ produced second order rate

constants of 18 and 21 mol⁻¹ dm³ s⁻¹ for separate *in situ* samples of SNAP. An explanation for this greater reactivity of SNCP and SNCC concerns the postulated formation of a bidentate intermediate. It is likely that SNAP may react via one of two possible reactive intermediates shown in figure 4.1.

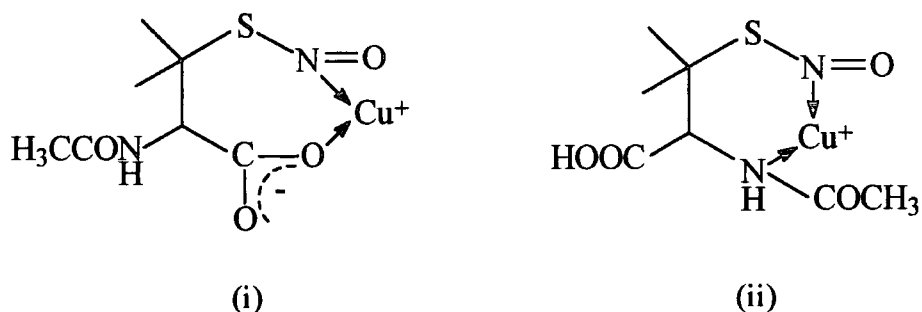


Figure 4.1

If both SNCP and SNCC were to form the seven membered intermediate analogous to (i), it would be likely that these compounds would have a similar second order rate constant to SNAP. Coordination via (ii) in all three substances would instead prove more logical. The presence of the N-carbamyl group (-NH-CO-NH₂) may lead to a greater electron density on the β-amino nitrogen atom than for the N-acetyl group in SNAP (-NH-COCH₃) due to the availability of other electrons on the carbamyl nitrogen atom adjacent to the electron withdrawing carbonyl group in SNCP and SNCC (figure 4.2).

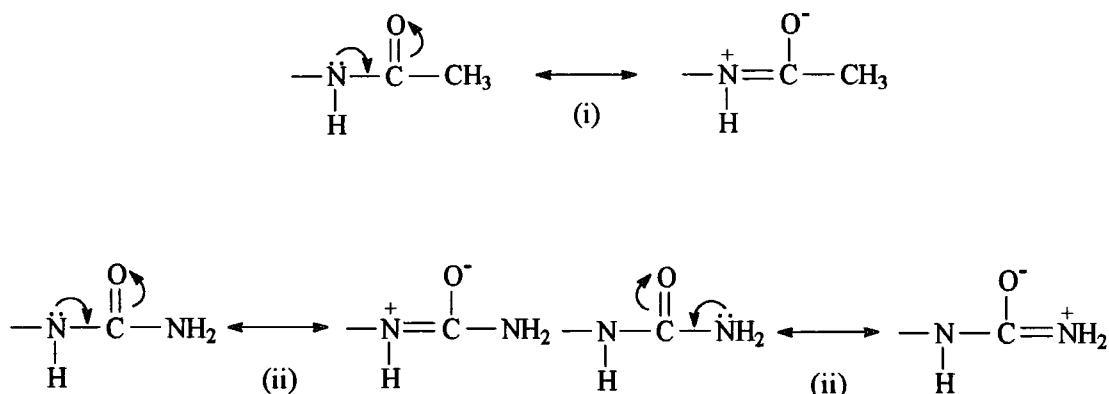
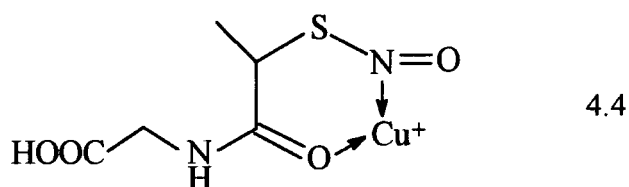


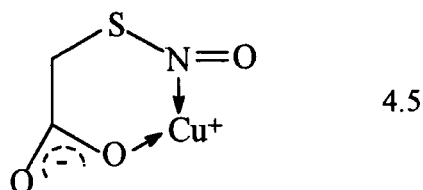
Figure 4.2

There are two possible canonical forms which can be constructed for SNAP (i), whereas three are available for both SNCP and SNCC (ii) with the electron density reduced on the β -amino nitrogen atom in only one of them. Overall, a net higher electron density will exist on this atom in S-nitroso-N-carbamylpenicillamine and S-nitroso-N-carbamylcysteine than for SNAP, explaining these compounds increased reactivity.

S-nitroso-2-(mercaptopropionyl)glycine (SMPG) is also observed to have a moderate reactivity ($k_2 = 250 \pm 15 \text{ mol}^{-1} \text{ dm}^3 \text{ s}^{-1}$) under similar reaction conditions. Examination of the structure of this compound would suggest that bidentate coordination could only occur via the carbonyl oxygen lone pair of electrons, forming a six membered intermediate (4.4).

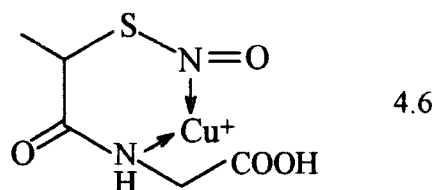


Coordination through oxygen has been previously proposed⁸ in S-nitrosomercaptoacetic acid (4.5), $k_2 = 300 \text{ mol}^{-1} \text{ dm}^3 \text{ s}^{-1}$ but in this instance a full negative charge is associated with the carboxylate group, whereas only a lone pair of electrons is available on the carbonyl oxygen in SMPG. A reduced reactivity is therefore noted for this compound.



The α -methyl moiety may aid reaction by helping to hold the available binding groups in close proximity to Cu^+ . A smaller second order rate constant would thus be expected for S-nitrosomercaptoacetyl glycine. The coordination chemistry of copper(I) is known to be dominated⁹ by binding with N and S groups, due to Cu^+ being a soft

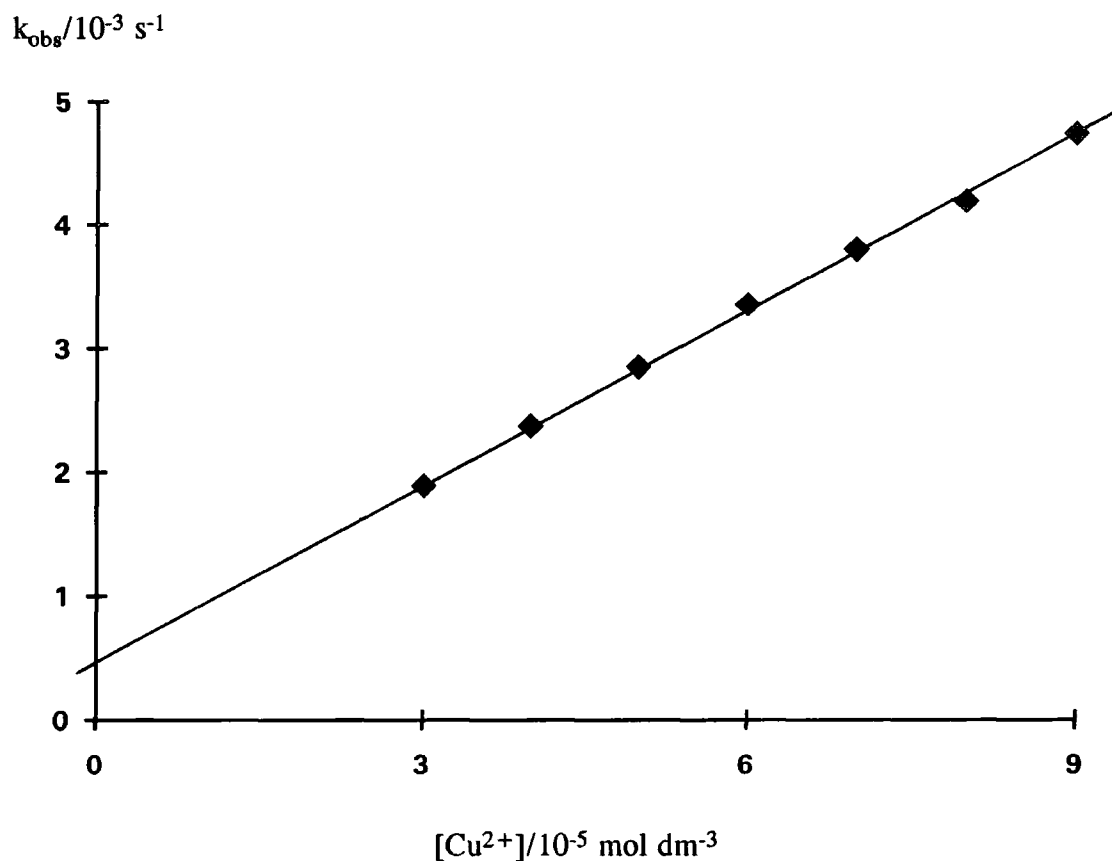
Lewis acid. It is possible (but more unlikely) that in this case coordination will occur through the amide nitrogen atom (4.6).



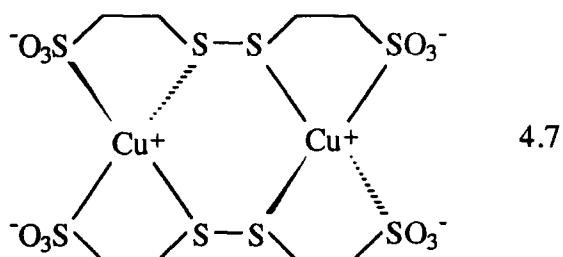
For all of these intermediates it is possible to envisage coordination via the nitrosothiol sulfur atom. However, when Hg^{2+} binds to RSNO in this manner (section 1.4.3.2), the product formed is the nitrosonium ion NO^+ and not nitric oxide, suggesting that nitrogen is the more probable coordinating atom in the case of Cu^+ . There is as yet no direct evidence for the nature of the structural intermediate. It is interesting to note that the second order rate constant for S-nitroso-2-mercaptoethanesulfonic acid is one of the smallest of all the nitrosothiols studied here. Only 50% of the reaction appeared to take place, however a distinct dependence on the copper ion concentration was apparent (figure 4.3) with good first order plots being obtained.

Figure 4.3

Plot of k_{obs} against $[\text{Cu}^{2+}]$ for the decomposition of
S-nitroso-2-mercaptoethanesulfonic acid ($1 \times 10^{-3} \text{ mol dm}^{-3}$)



It may be that the disulfide product generated will preferentially complex catalytic Cu^+ (or Cu^{2+})^{10,11} thus preventing complete reaction by forming a chelate as indicated below (4.7).



Such competitive complexation between the disulfide and S-nitrosothiol for copper(I) could cause inhibition of RSNO decomposition in this instance.

S-nitroso-2-N,N-dimethylaminoethanethiol and its diethyl analogue were thought to be extremely unstable compounds due to an increased electron density on the amino nitrogen atom. However, as has been discussed in section 2.5.3, the corresponding thiol molecules are excellent chelators of copper ions. Subsequently, the expected "window" of $[Cu^{2+}]$ producing first order kinetics could not be found, with clear induction periods present at all copper concentrations. It was therefore not possible to measure k_2 for these species under the current experimental conditions.

4.3 Heterocyclic and Aromatic S-Nitrosated Thiols

4.3.1 Spectral Characteristics

Several heterocyclic and aromatic thiols were readily available for nitrosation in a similar manner to previously discussed aliphatic species (section 4.2). Table 4.7 indicates that the nitroso compounds derived from 2-mercaptoimidazole, 2-mercaptopyridine, 2-mercaptopyrimidine and 2-aminothiophenol do not necessarily exhibit the characteristic absorbance maximum at around 340nm. This meant that reaction kinetics had to be followed at a variety of wavelengths according to the specific compound being studied. The existence of thiol/thione tautomerism in some of these compounds (section 4.3.3) means that it is more relevant to term the nitrosated species "S-nitrosated thiols" rather than "S-nitrosothiols".

Table 4.7

Spectral data obtained for some heterocyclic and aromatic S-nitrosated thiols, pH 7.4

S-nitrosated thiol	λ_{\max} (nm)	ϵ (mol ⁻¹ dm ³ cm ⁻¹)
S-nitrosated 2-aminothiophenol	265 313	4103 ± 60 1940 ± 20
S-nitrosated 2-mercaptopyridine	341 270	1080 ± 30 2110 ± 40
S-nitrosated 2-mercaptopyrimidine	214 234	8900 ± 40 9200 ± 60
S-nitrosated 2-mercaptoimidazole	276	3870 ± 50
S-nitrosated 1-methyl-2-mercaptoimidazole	280	2940 ± 40

It is now necessary to discuss the *in vitro* behaviour of each S-nitrosated thiol separately both in the presence and absence of added copper(II) ions.

4.3.2 S-Nitrosated 2-aminothiophenol

This compound showed no significant decomposition at pH 7.4 after twenty-four hours even in the presence of 5×10^{-5} mol dm⁻³ Cu²⁺. It is well documented¹ that bidentate coordination of the substrate to catalytic copper ions has to occur for the reaction to proceed (section 1.4.3.1) and that the presence of a β -amino group facilitates nitric oxide generation, as in the case of S-nitroso-2-aminoethanethiol (S-nitrosocysteamine), figure 4.4.

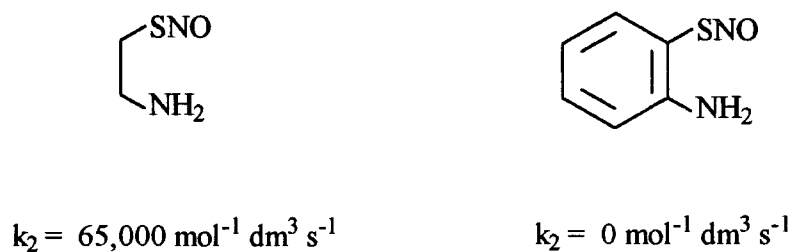


Figure 4.4

However, the lone pair of electrons present on the amino nitrogen atom of S-nitrosated 2-aminothiophenol will become delocalised into the aromatic ring¹² according to figure 4.5.

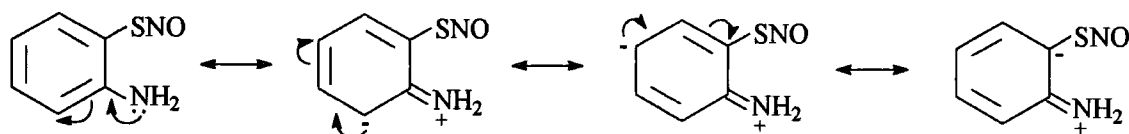


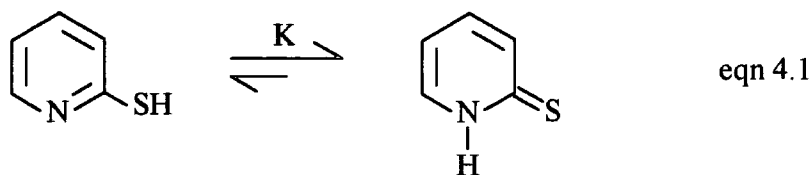
Figure 4.5

This will reduce the electron density available on the nitrogen atom meaning that coordination is very unlikely via the β -amino moiety in this instance. It is not thought that Cu^+ is capable of forming a stable complex with the S-nitroso group alone that will effect nitric oxide release.

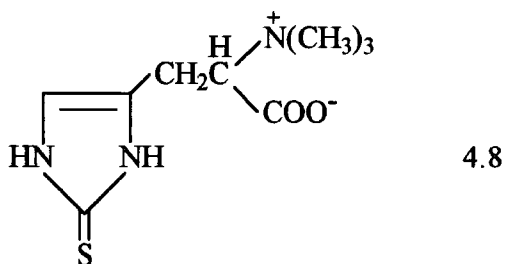
4.3.3 S-Nitrosated 2-mercaptopyridine and S-Nitrosated 2-mercaptopyrimidine

4.3.3.1 Nitrosation of 2-mercaptopyridine

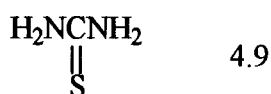
The nitrosation of sulfur-containing compounds has been studied in great detail and summarised within section 1.3. To date, the kinetics of NO^+ attack at sulfur in heterocyclic and aromatic thiols have however not been measured. Such substances are of great mechanistic interest as it is known that thiol/thione tautomerisation exists, for example considering 2-mercaptopyridine (equation 4.1)-



From extensive ultraviolet studies Albert and Barlin¹³ quoted the equilibrium constant K to be 49,000 suggesting that the thione form is predominant in aqueous solution. The biologically relevant thiol ergothioneine (4.8) which has been implicated in brain function is also thought to reside chiefly in this state¹⁴.



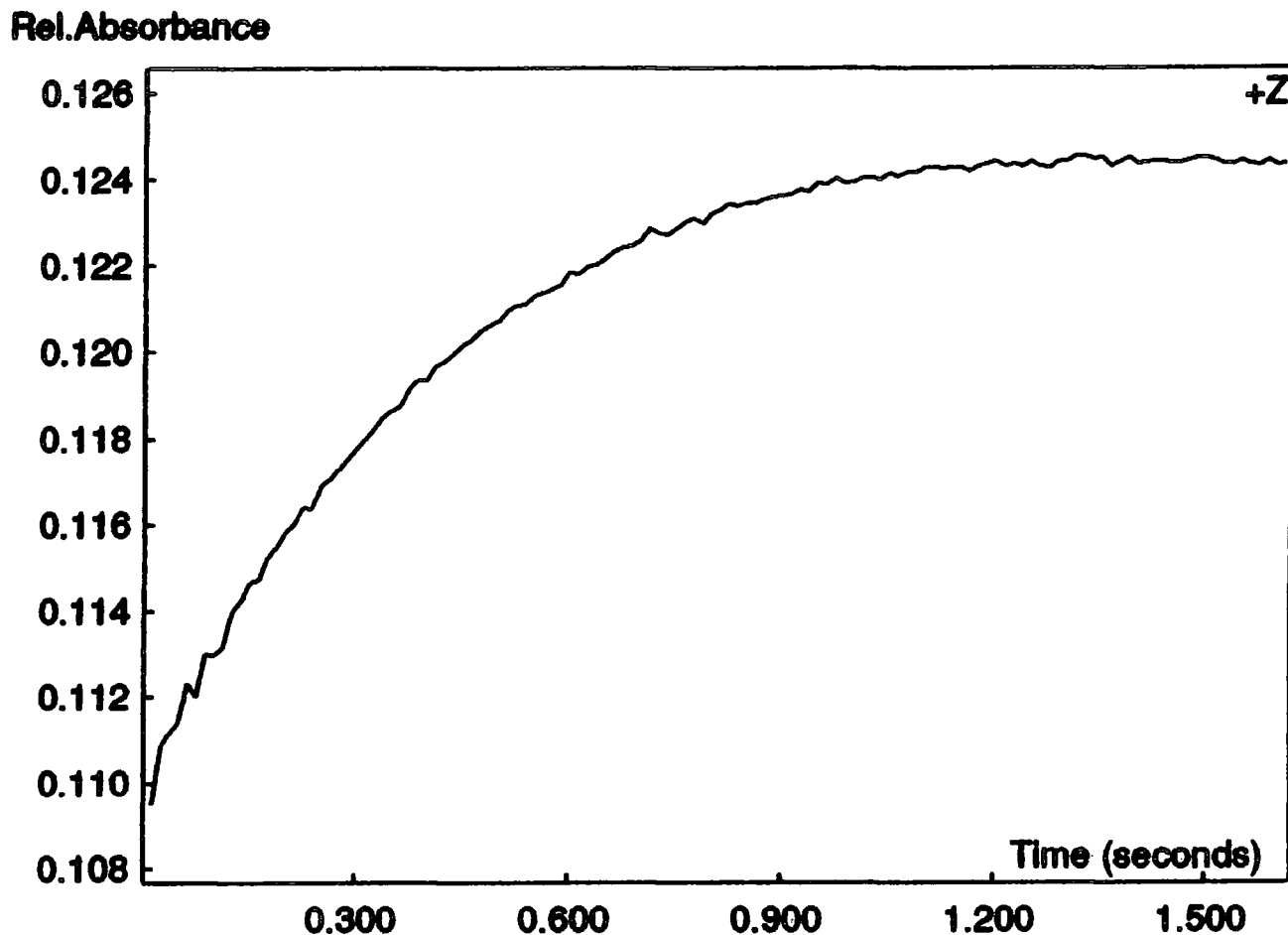
The aqueous nitrosation of analogous thiocarbonyl compounds such as thiourea (4.9) leads to the formation of an S-nitrososulfonium ion¹⁵ ($\text{R}=\text{S}^+-\text{N}=\text{O}$) (section 1.3.5).



Therefore, it may be expected that a similar intermediate species will be generated on reaction between acidified sodium nitrite and 2-mercaptopyridine (ArSH). The absorbance change at 415nm was followed when this thiol ($3 \times 10^{-3} \text{ mol dm}^{-3}$) was reacted with $1 \times 10^{-4} \text{ mol dm}^{-3}$ nitrous acid in 0.1 mol dm^{-3} perchloric acid. A typical kinetic trace is shown in figure 4.6.

Figure 4.6

Kinetic trace showing the nitrosation of 2-mercaptopyridine ($3 \times 10^{-3} \text{ mol dm}^{-3}$) in the presence of $1 \times 10^{-4} \text{ mol dm}^{-3}$ nitrous acid and 0.1 mol dm^{-3} perchloric acid



The concentration of thiol was initially varied at constant acidity and a linear plot of $[\text{ArSH}]$ against pseudo-first order rate constant, k_{obs} constructed. After this the acid concentration was altered at constant $[\text{ArSH}]$ in order to quantify any effect of H^+ . The k_{obs} values obtained are collected in table 4.8 and shown graphically in figure 4.7.

Table 4.8

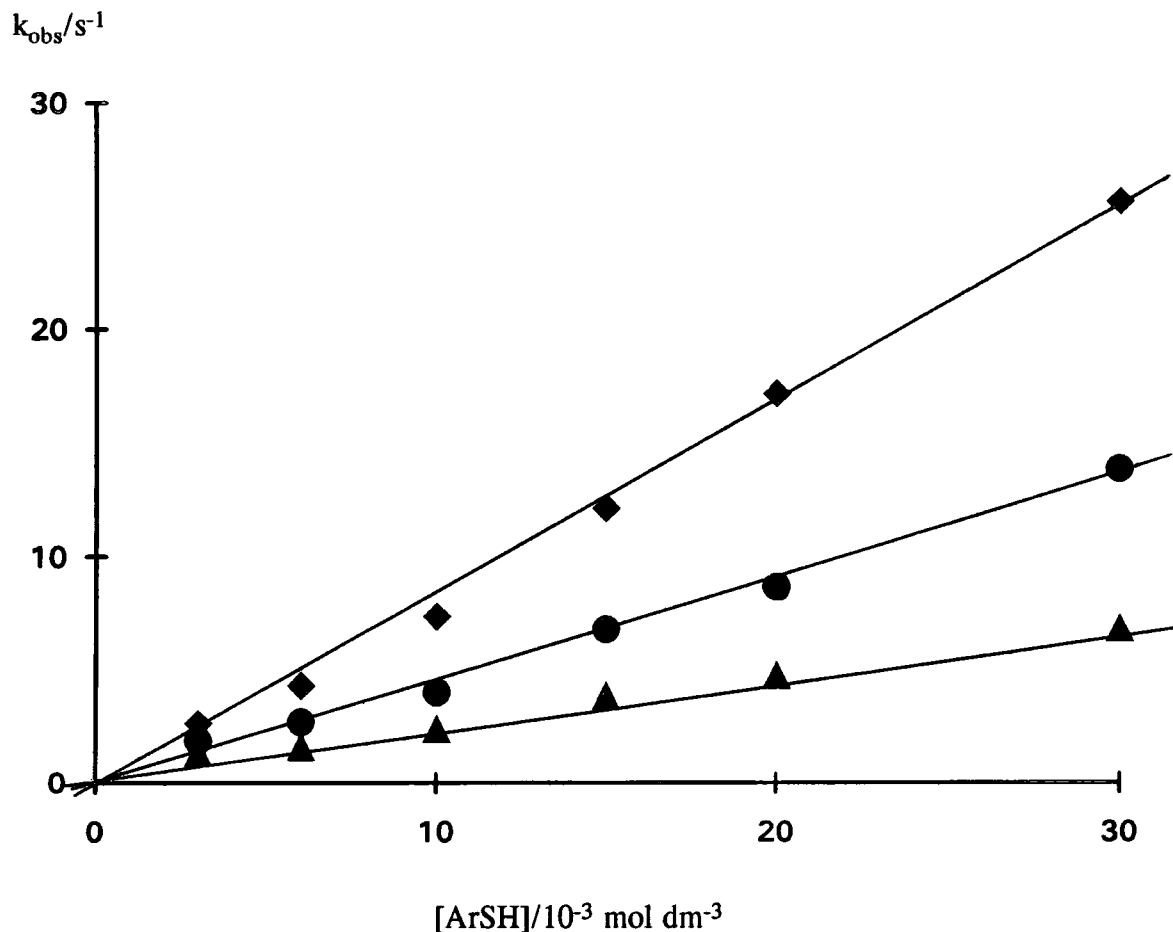
Kinetic data for the nitrosation of 2-mercaptopyridine by nitrous acid
($1 \times 10^{-4} \text{ mol dm}^{-3}$) in the presence of varying $[\text{H}^+]$

[thiol]/ $10^{-3} \text{ mol dm}^{-3}$	[H ⁺]/ mol dm^{-3}		
	0.1	0.05	0.025
3	2.65 ± 0.09^a	1.87 ± 0.07	1.37 ± 0.02
6	4.31 ± 0.12	2.68 ± 0.09	1.63 ± 0.05
10	7.36 ± 0.21	3.98 ± 0.12	2.41 ± 0.09
15	12.1 ± 0.3	6.78 ± 0.23	3.86 ± 0.11
20	17.2 ± 0.4	8.66 ± 0.26	4.76 ± 0.13
30	25.6 ± 0.5	13.8 ± 0.3	6.84 ± 0.18

^aMeasured pseudo-first order rate constant, k_{obs} (s^{-1})

Figure 4.7

Plot of k_{obs} against $[\text{ArSH}]$ for the nitrosation of 2-mercaptopyridine by nitrous acid ($1 \times 10^{-4} \text{ mol dm}^{-3}$) in the presence of varying $[\text{H}^+]$



◆ = $0.1 \text{ mol dm}^{-3} \text{ H}^+$; ● = $0.05 \text{ mol dm}^{-3} \text{ H}^+$; ▲ = $0.025 \text{ mol dm}^{-3} \text{ H}^+$.

The gradient of each line produces a second order rate constant which, when divided by the appropriate acid concentration, allows k_3 (third order rate constant, equation 4.2) to be calculated.



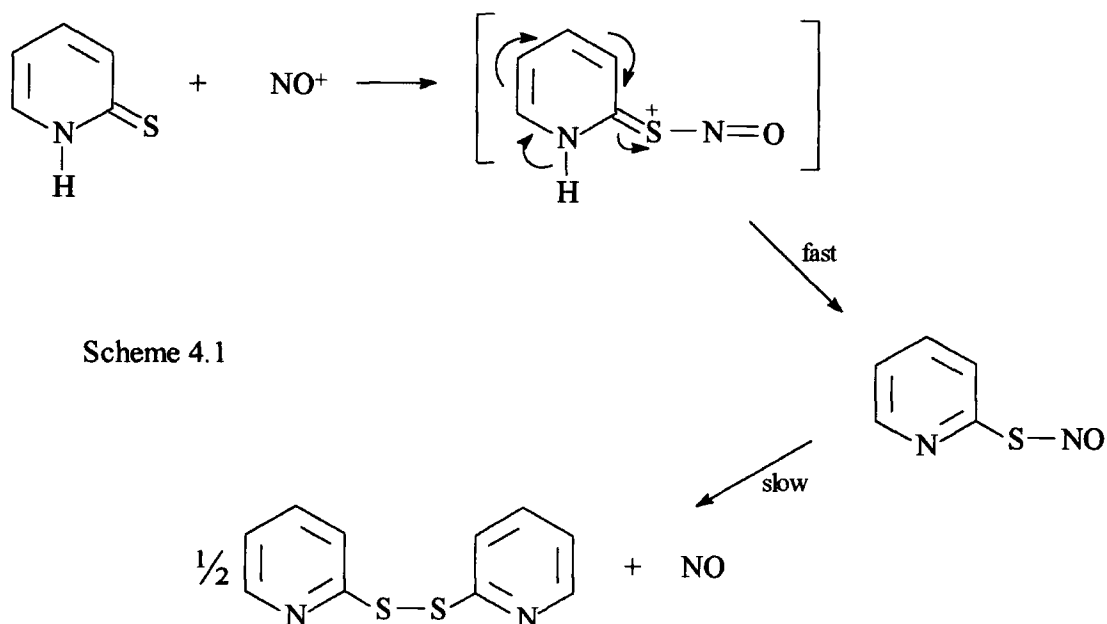
Table 4.9 indicates the k_3 values obtained at various acidities for the nitrosation of 2-mercaptopyridine.

Table 4.9

Third order rate constant (k_3) values for the reaction of 2-mercaptopyridine with nitrous acid ($1 \times 10^{-4} \text{ mol dm}^{-3}$) at three different acidities

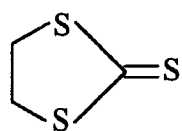
$[\text{H}^+]/\text{mol dm}^{-3}$	$k_3/\text{mol}^{-2} \text{ dm}^6 \text{ s}^{-1}$
0.1	8760 ± 260
0.05	9000 ± 400
0.025	8400 ± 320

An average for k_3 taken from these results is $8720 \pm 320 \text{ mol}^{-2} \text{ dm}^6 \text{ s}^{-1}$. The rate constant for the analogous S-nitrosation of thiourea is $6960 \text{ mol}^{-2} \text{ dm}^6 \text{ s}^{-1}$ at 25°C^{15} which is taken to be that of the encounter controlled reaction between the reagent (NO^+ or H_2NO_2^+) and the thiourea molecule. It appears that the aromatically derived 2-mercaptopyridine when nitrosated produces an unstable S-nitrososulfonium ion ($\text{Ar}=\text{S}^+-\text{NO}$) which is observable at high concentrations as a transient orange colour. This species can rapidly undergo the loss of a proton which leads to formation of an S-nitrosothiol, $\text{Ar}-\text{S}-\text{NO}$ (scheme 4.1).

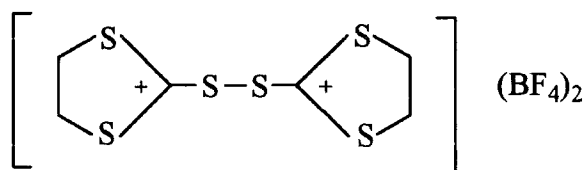


Scheme 4.1 also suggests that the final reaction products after $\text{Ar}-\text{S}-\text{NO}$ decomposition are nitric oxide and the corresponding disulfide. Doyle *et al*¹⁶ and Blankespoor *et al*¹⁷ have noted that the nitrosation of 1,3-dithiolan-2-thione (4.10)

utilising nitrosonium tetrafluoroborate produced 2,2'-dithiobis-(1,3-dithiolanium) ditetrafluoroborate (4.11) and nitric oxide almost exclusively.

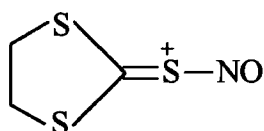


4.10

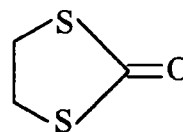


4.11

This is an example of the oxidation of a thiocarbonyl compound to a stable dication. It has also been observed that the intermediate structure (4.12) can undergo nitrosative exchange of sulfur for oxygen generating 1,3-dithiolan-2-one (4.13) in small yield.



4.12



4.13

Urea has additionally been detected as a product following the nitrosation of thiourea¹⁸. Having determined the kinetics of S-nitrosation for 2-mercaptopyridine it is now instructive to consider how heterocyclic and aromatic S-nitrososulfonium ions could decompose in varying media as a function of copper ion concentration.

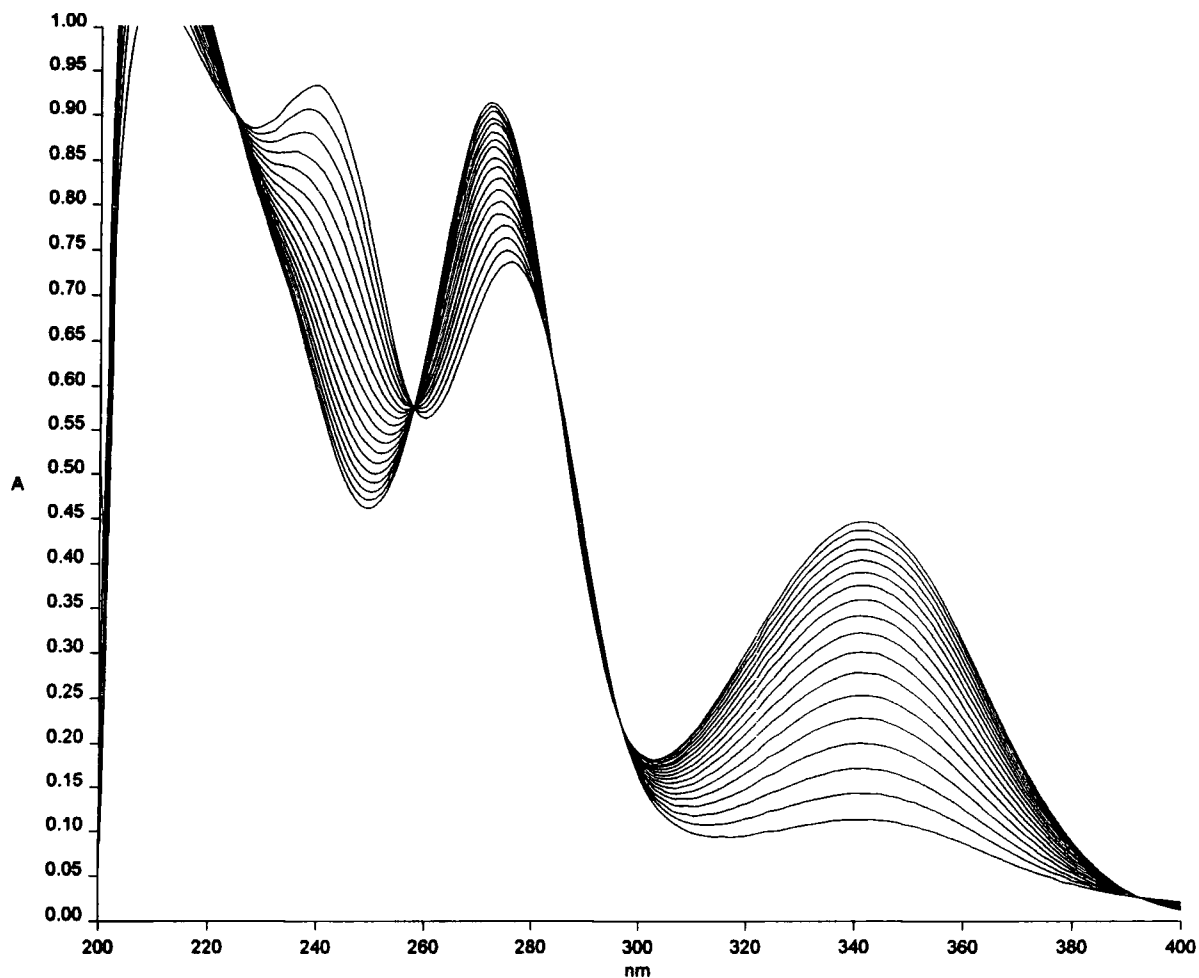
4.3.3.2 Reaction in pH 7.4 Buffer

The decomposition profiles of S-nitrosated 2-mercaptopyridine and 2-mercaptopyrimidine were recorded at physiological pH at differing wavelengths. An increase in absorbance at 340nm was noted for the former compound (figure 4.8) when $1.25 \times 10^{-4} \text{ mol dm}^{-3}$ S-nitrosated 2-mercaptopyridine was placed in pH 7.4 buffer in the absence of added copper(II) ions. The reaction had reached completion

in ten minutes and on repetition with added Cu^{2+} an increase in first order rate constant was noticeable (table 4.10).

Figure 4.8

Traces showing the absorbance increase at 340nm for the decomposition of S-nitrosated 2-mercaptopyridine ($1.25 \times 10^{-4} \text{ mol dm}^{-3}$) in pH 7.4 buffer



Scans acquired every thirty seconds.

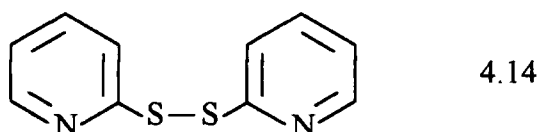
Table 4.10

Kinetic data for the decomposition of S-nitrosated 2-mercaptopyridine ($2.5 \times 10^{-4} \text{ mol dm}^{-3}$) in the presence of added Cu^{2+} , pH 7.4 buffer

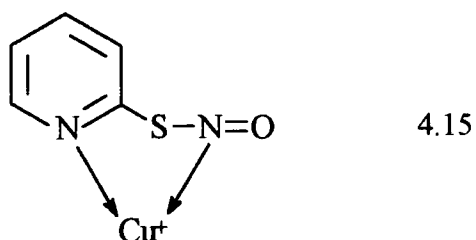
$[\text{Cu}^{2+}]/10^{-6} \text{ mol dm}^{-3}$	$k_{\text{obs}}/10^{-3} \text{ s}^{-1}$
0	3.17 ± 0.02
0.1	3.39 ± 0.06
0.5	3.88 ± 0.07
0.9	4.08 ± 0.08
10	4.20 ± 0.13
15	4.32 ± 0.13
20	4.94 ± 0.12
30	5.66 ± 0.18

$$k_2 = 780 \pm 50 \text{ mol}^{-1} \text{ dm}^3 \text{ s}^{-1}$$

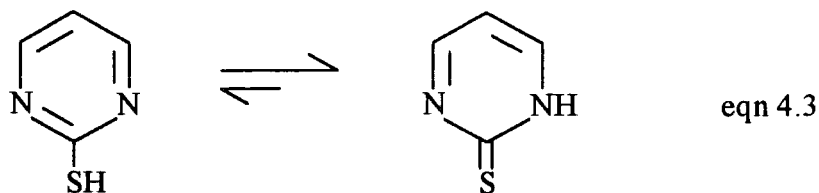
There is also an apparent decrease in absorbance at 240nm and an increase at 270nm (figure 4.8) with isosbestic points at 393nm, 296nm, 286nm, 260nm and 226nm. Aldrithiol-2™ (2,2'-dipyridyl disulfide, 4.14) was purchased from Sigma-Aldrich Co. Ltd. and a uv/visible spectrum of this material indicated a peak at 281nm with no absorbance maximum at 340nm.



It can therefore be deduced that the disulfide has not been formed in this instance. Indeed, it appears as if the thione has been regenerated as the product spectrum shows great coincidence with the mercapto precursor. A moderate reactivity towards Cu^+ is observed ($k_2 = 780 \pm 50 \text{ mol}^{-1} \text{ dm}^3 \text{ s}^{-1}$) suggesting good coordination between the -SNO group and ring nitrogen with copper(I) (4.15).



2-mercaptopyrimidine is also known to exist as the thione tautomer (equation 4.3)¹⁹ in solution and was nitrosated under similar conditions using acidified sodium nitrite.



An absorbance increase at 277nm was observed with an isosbestic point at 264nm, reaction kinetics being followed at the former wavelength. The decomposition was investigated in the presence of Cu^{2+} ions at pH 7.4 (table 4.11).

Table 4.11

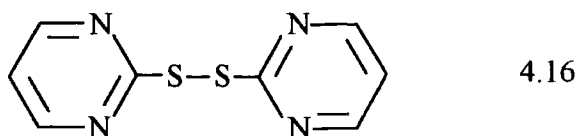
Kinetic data for the decomposition of S-nitrosated 2-mercaptopyrimidine ($1.6 \times 10^{-4} \text{ mol dm}^{-3}$) in the presence of added Cu^{2+} , pH 7.4 buffer

$[\text{Cu}^{2+}]/10^{-7} \text{ mol dm}^{-3}$	$k_{\text{obs}}/10^{-3} \text{ s}^{-1}$
0	9.67 ± 0.22
2.0	10.0 ± 0.1
4.0	10.3 ± 0.1
8.0	11.6 ± 0.3
20	14.6 ± 0.6

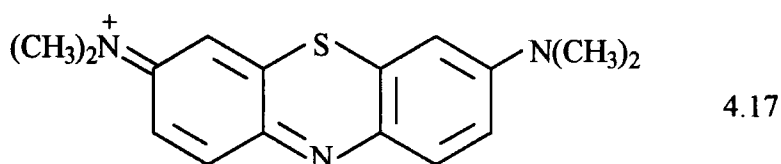
$$k_2 = 2570 \pm 100 \text{ mol}^{-1} \text{ dm}^3 \text{ s}^{-1}$$

A clear dependence of first order rate constant on $[\text{Cu}^{2+}]$ is apparent. Brown and Heffernan²⁰ have calculated electron densities at the nitrogen atoms in pyridine and pyrimidine and concluded that the density present on pyridine is greater. There are however two such nitrogens available in 2-mercaptopyrimidine, meaning that there are potentially two binding sites which could provide coordination points for Cu^+ , leading to a rate constant more than three times greater for nitrosated 2-mercaptopyrimidine.

In an attempt to deduce the reaction products at pH 7.4 the relevant disulfide (4.16) was synthesised according to the method of Miller *et al*²¹ by oxidation of the thiol precursor.



Many techniques are available which will oxidise a thiol to a disulfide including treatment with methylene blue (4.17)²², sodium chlorite²³ and alkaline KI/I₂²⁴, the latter procedure being utilised in this instance.



1.12g of 2-mercaptopyrimidine was dissolved in 20ml 1 mol dm⁻³ NaOH and chilled in ice. 10ml aqueous 1 mol dm⁻³ iodine solution containing 5.07g potassium iodide was subsequently added rapidly with constant stirring. After fifteen minutes an orange precipitate formed which was filtered and dried in a vacuum desiccator. The yield based on weight of product = 75.2%. Elemental analysis for the disulfide requires C = 43.24%, H = 2.70% and N = 25.22%. Obtained: C = 43.51%, H = 2.64% and N = 24.98%.

Melting point = 134-135°C, literature²⁴ = 139-140°C.

¹H NMR (Me₂SO-d₆): δ 7.38 (t, 2H), 8.71 (d, 4H).

The molar extinction coefficient of 2,2'-dipyrimidyl disulfide in pH 7.4 buffer was measured to be 19,400 ± 180 mol⁻¹ dm³ cm⁻¹ and 18,400 ± 140 mol⁻¹ dm³ cm⁻¹ in 0.05 mol dm⁻³ sulfuric acid, which compares well with a literature value of 19,000 mol⁻¹ dm³ cm⁻¹ in the latter medium²⁵. An absorbance peak is present at 236nm for the synthesised solid which is not observable during reaction with Cu⁺ at pH 7.4, implying that again

the disulfide is not formed under these conditions. It now became important to determine the nitrogenous decomposition product from these compounds having demonstrated the reformation of thione on reaction with copper(I).

4.3.3.3 Use of a Nitric Oxide Electrode to Detect Reaction Products

Detection of nitric oxide by a specific electrode designed solely for this purpose is the most direct method of measuring NO concentrations both *in vitro* and *in vivo*. Several differing types of electrode have been manufactured, which vary in terms of detection limits and suitability for usage in biological systems. Malinski and Taha²⁶ have developed a carbon fibre microelectrode that is modified with an electropolymerised film of nickel(II) porphyrin polymer. A negatively charged layer of Nafion[®] prevents interference by both nitrite and nitrate ions, with the metalloporphyrin catalysing the oxidation of NO to NO⁺. The current that is generated is measured and after calibration this electrode can be employed for the *in vivo* determination of nitric oxide in single arterial endothelial cells. Between 10nM and 300µM NO can be detected in this manner. The only significant drawback in this approach is the extensive modification procedure required, particularly if electrode regeneration is desirable. To this end, Pariente *et al*²⁷ designed a Nafion[®] coated polycrystalline platinum electrode modified with cellulose acetate, which minimises electrode fouling from non-specific adsorption of proteins typically found in cellular environments. However, this has led to a lack of sensitivity as only micromolar levels of nitric oxide can be determined by this electrode.

A commercially available NO electrode was purchased from World Precision Instruments. This too is based on a platinum system which features a disposable steel jacket and membrane across the electrode tip (making it nitrite blind), which has a diameter of 2mm. The manufacturers claim detection limits to be 1nM to 20µM, but the robust character and size prevents accurate placement in relation to individual cells in cellular preparations. Such an electrode has not been widely used in the analysis of S-nitrosothiols. S-nitrosated 2-mercaptopyridine (2×10^{-5} mol dm⁻³) was reacted at

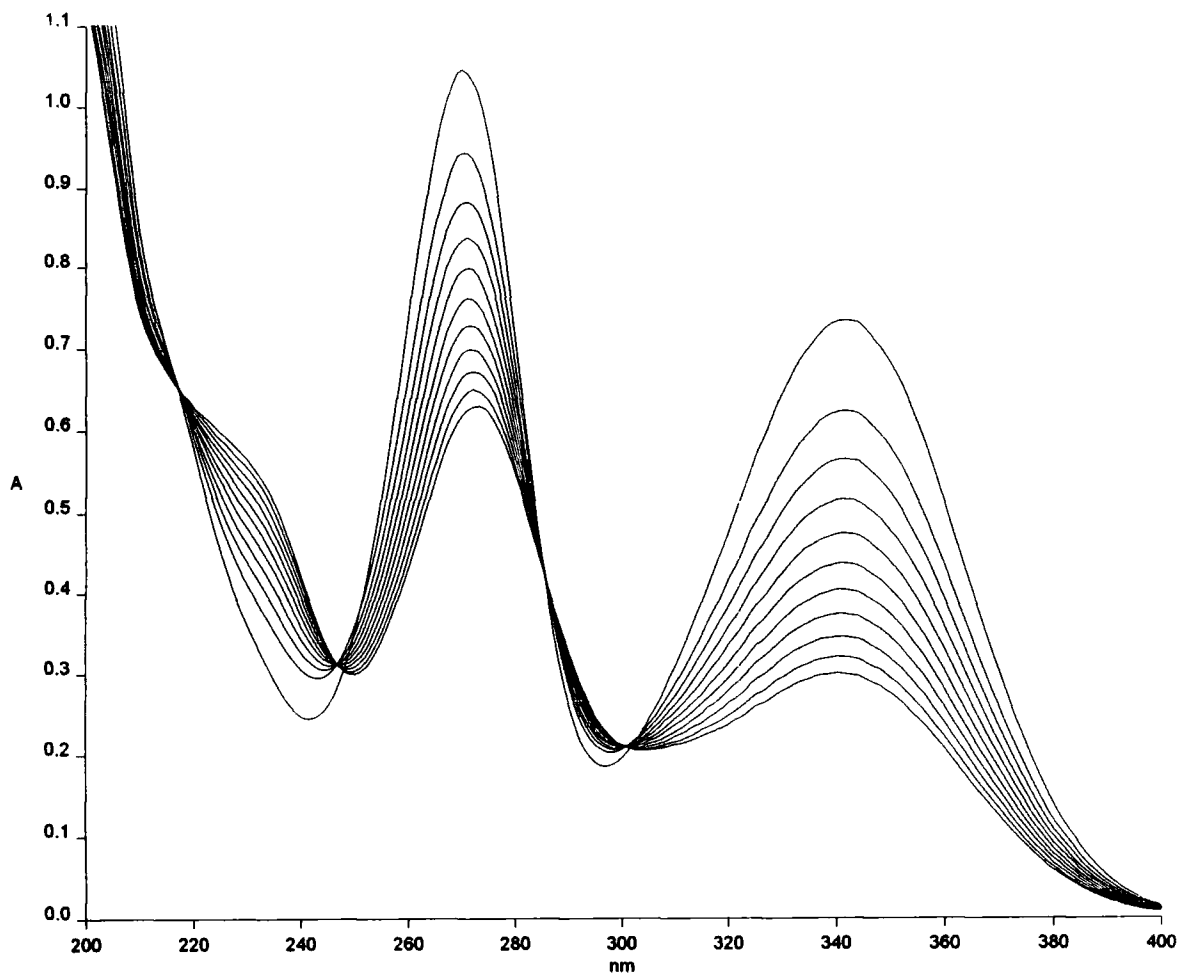
pH 7.4 with Cu^{2+} ($2 \times 10^{-5} \text{ mol dm}^{-3}$) in the presence of the NO electrode, after calibration had been performed (see Chapter Six). The reaction was slow, proceeding over fifteen or twenty minutes until a maximum current (reflecting nitric oxide generation) was reached. The amount of NO detected represented 21% of the quantity of nitrosothiol reacted. On repetition of this experiment twice, 22% and 22% nitric oxide was observed in solution. When S-nitrosated 2-mercaptopyrimidine was used as the substrate 33% NO was generated. As the reaction took place over a period of several minutes, the nitric oxide formed initially would become oxidised to nitrite as it is virtually impossible to remove all traces of oxygen from the system, despite thorough purging with nitrogen gas. It is clear that NO and thione are the major reaction products when these aromatic S-nitrosated thiols are allowed to decompose under physiological conditions in the presence of copper(II).

4.3.3.4 Reaction in Distilled Water

S-nitrosated 2-mercaptopyrimidine was allowed to decompose in distilled water both in the absence and presence of added copper(II). A much slower reaction took place than that which occurred at physiological pH with an absorbance decrease at 340nm apparent (figure 4.9).

Figure 4.9

Traces showing the absorbance decrease at 340nm for the decomposition of S-nitrosated 2-mercaptopyridine ($1 \times 10^{-4} \text{ mol dm}^{-3}$) in distilled water



Scans acquired every ten minutes.

The uv/visible spectrum after twenty-four hours was compared with that of 2,2'-dipyridyl disulfide and found to be extremely similar, suggesting that the solvent used may determine the observed products. Cu^{2+} was introduced to the nitrosated thione and reaction catalysis observed (table 4.12).

Table 4.12

Kinetic data for the decomposition of S-nitrosated 2-mercaptopyridine ($2.5 \times 10^{-4} \text{ mol dm}^{-3}$) in the presence of added Cu^{2+} , distilled water

$[\text{Cu}^{2+}]/10^{-5} \text{ mol dm}^{-3}$	$k_{\text{obs}}/10^{-4} \text{ s}^{-1}$
1.0	5.93 ± 0.13
2.0	8.06 ± 0.22
3.0	10.9 ± 0.2
4.0	13.2 ± 0.3
5.0	16.5 ± 0.3

$$k_2 = 26 \pm 1 \text{ mol}^{-1} \text{ dm}^3 \text{ s}^{-1}$$

The catalytic influence of copper ions is not as strong as is seen at pH 7.4 but it would appear that a spontaneous reaction takes place which can be affected by the copper(II) ion concentration. This is at variance with experimental evidence collected for aliphatic S-nitrosothiols which show that Cu^{2+} has to be available for decomposition to occur¹. A check was made that adding 2-mercaptopyridine to copper(II) at pH 7.4 and in distilled water could generate cuprous ion. It was discovered that between 85% and 90% Cu^+ could be trapped by neocuproine and that this reduction took place instantaneously. It has been previously documented²⁸ that "in general, heterocyclic thioamides reduce copper(II) salts to copper(I)". Similar behaviour was exhibited by S-nitrosated 2-mercaptopyrimidine (table 4.13).

Table 4.13

Kinetic data for the decomposition of S-nitrosated 2-mercaptopyrimidine ($2.5 \times 10^{-4} \text{ mol dm}^{-3}$) in the presence of added Cu^{2+} , distilled water

$[\text{Cu}^{2+}]/10^{-5} \text{ mol dm}^{-3}$	$k_{\text{obs}}/10^{-3} \text{ s}^{-1}$
1.0	3.11 ± 0.11
2.0	4.07 ± 0.12
3.0	4.74 ± 0.12
4.0	5.43 ± 0.14
5.0	6.14 ± 0.17

$$k_2 = 75 \pm 3 \text{ mol}^{-1} \text{ dm}^3 \text{ s}^{-1}$$

The second order rate constant is three times as great for this species as for the analogous 2-mercaptopyridine derivative, which may result from the presence of two nitrogen atoms available to bind Cu(I). A peak at 236nm for the reaction product is in keeping with the formation of 2,2' dipyrimidyl disulfide under these conditions.

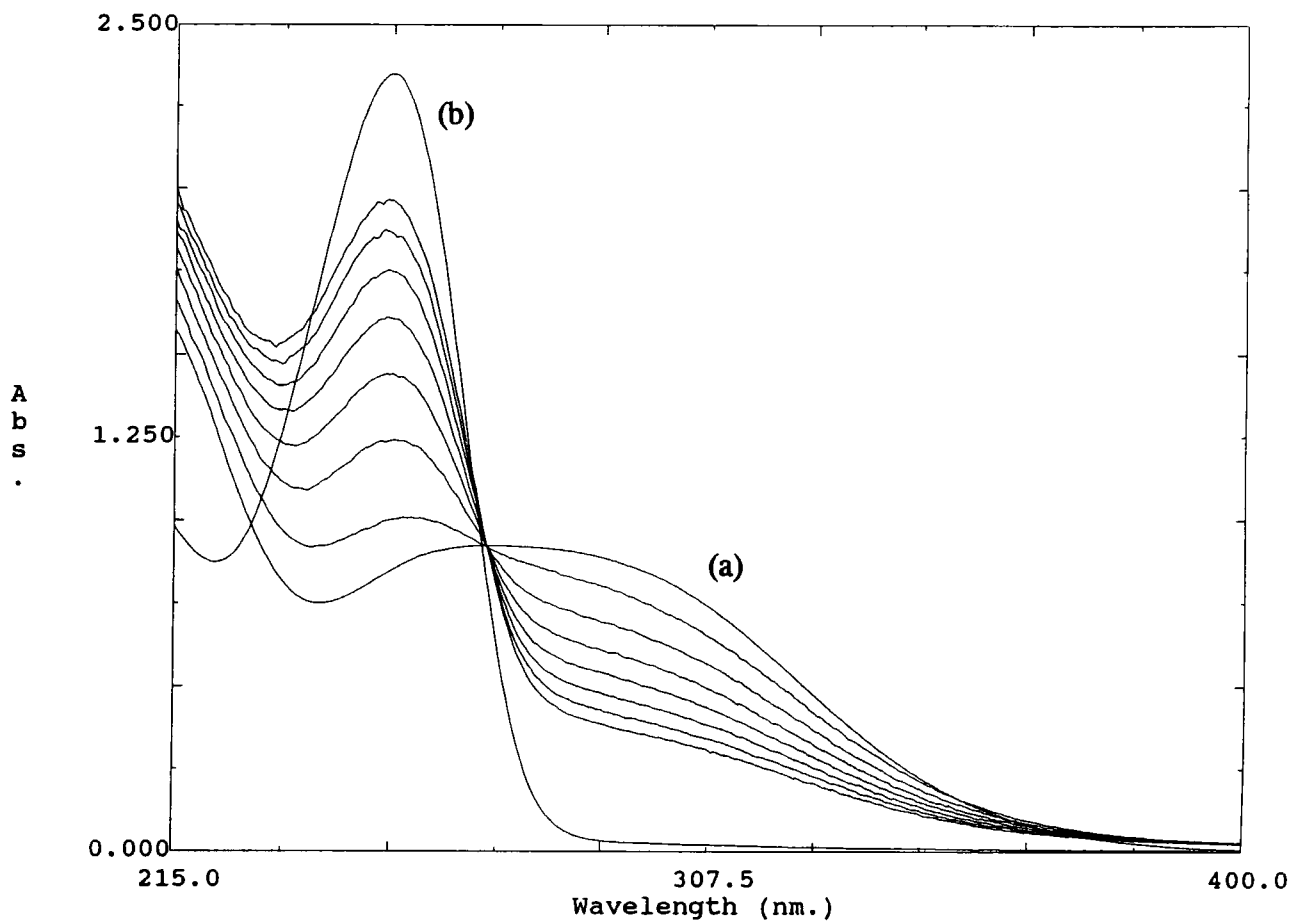
4.3.4 S-Nitrosated 2-mercaptoimidazole and Related Derivatives

4.3.4.1 Reaction in pH 7.4 Buffer

The decomposition of S-nitrosated 2-mercaptoimidazole ($2.5 \times 10^{-4} \text{ mol dm}^{-3}$) in the presence of Cu^{2+} was initially followed spectrophotometrically by measuring the increase in absorbance at 252nm due to product formation. The nitrosated thione showed a broad ultraviolet absorbance with $\lambda_{\text{max}} = 276\text{nm}$ ($\epsilon = 3870 \text{ mol}^{-1} \text{ dm}^3 \text{ cm}^{-1}$) due to the overlap of heterocyclic and -SNO chromophores. On reaction with added copper ions ($3 \times 10^{-5} \text{ mol dm}^{-3}$) at pH 7.4, a clearly defined isosbestic point at 268nm appeared along with a new peak at 252nm (figure 4.10). This could be attributed to reformation of the parent thione during a time period of thirty minutes. A spectral comparison of authentic 2-mercaptoimidazole (existing as the thione)²⁸ with the observed reaction product showed great similarities. A clear dependence of reaction rate on $[\text{Cu}^{2+}]_{\text{added}}$ was apparent (tables 4.14 and 4.15) for both S-nitrosated 2-mercaptoimidazole and its 1-methyl derivative.

Figure 4.10

Traces showing the absorbance increase at 252nm for reaction of S-nitrosated
2-mercaptoimidazole ($2.5 \times 10^{-4} \text{ mol dm}^{-3}$) in the presence of added Cu^{2+}
($3 \times 10^{-5} \text{ mol dm}^{-3}$)



(a) initial spectrum; (b) authentic 2-mercaptoimidazole

Scans acquired every three minutes.

Table 4.14

Kinetic data for the decomposition of S-nitrosated 2-mercaptoimidazole ($2.5 \times 10^{-4} \text{ mol dm}^{-3}$) in the presence of added Cu^{2+} , pH 7.4 buffer

$[\text{Cu}^{2+}]/10^{-5} \text{ mol dm}^{-3}$	$k_{\text{obs}}/10^{-4} \text{ s}^{-1}$
0.5	4.82 ± 0.11
1.0	5.40 ± 0.12
2.0	7.80 ± 0.15
3.0	10.7 ± 0.2
4.0	12.1 ± 0.3
5.0	14.4 ± 0.4

$$k_2 = 22 \pm 1 \text{ mol}^{-1} \text{ dm}^3 \text{ s}^{-1}$$

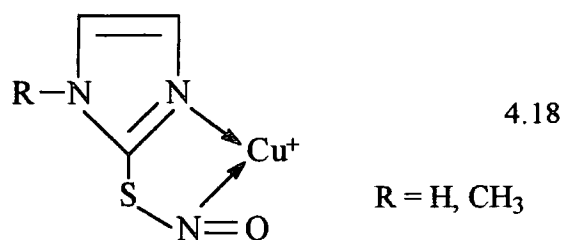
Table 4.15

Kinetic data for the decomposition of S-nitrosated 1-methyl-2-mercaptoimidazole ($2.5 \times 10^{-4} \text{ mol dm}^{-3}$) in the presence of added Cu^{2+} , pH 7.4 buffer

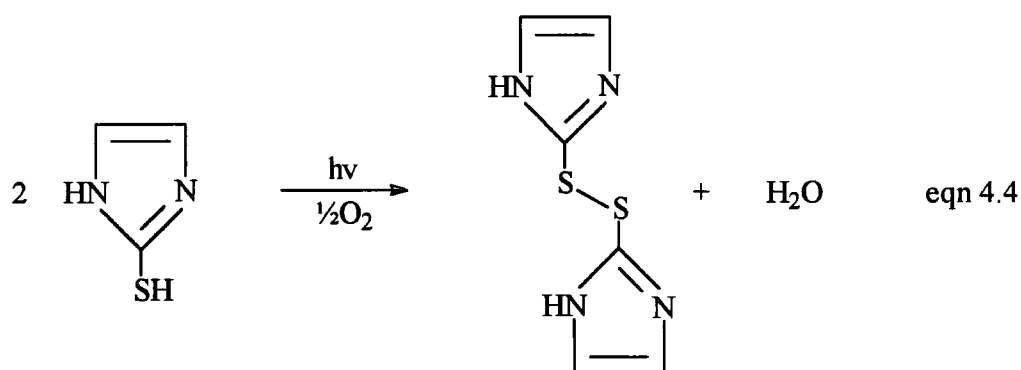
$[\text{Cu}^{2+}]/10^{-5} \text{ mol dm}^{-3}$	$k_{\text{obs}}/10^{-4} \text{ s}^{-1}$
1.0	8.55 ± 0.24
2.0	11.2 ± 0.3
3.0	13.1 ± 0.3
4.0	15.0 ± 0.3
5.0	17.5 ± 0.4
6.0	19.3 ± 0.4

$$k_2 = 21 \pm 1 \text{ mol}^{-1} \text{ dm}^3 \text{ s}^{-1}$$

Nitric oxide was detected as described previously in reasonable yield (55% from S-nitrosated 2-mercaptoimidazole, 59% from the 1-methyl derivative). The second order rate constant is found to be extremely similar for both of these substrates. It may have been expected that the presence of an electron donating methyl group may increase the reactivity of the latter compound due to an increased electron density on nitrogen, but this may be counteracted by possible steric effects associated with a more bulky substituent hindering Cu^+ chelation. The possible reactive intermediate can be represented as overleaf (4.18).



An extremely useful method which cleanly generates the required disulfide in good yield is subjecting the thiol to various kinds of radiation^{29,30}. Prolonged exposure to ultraviolet light was employed in this instance. 1×10^{-4} mol dm⁻³ 2-mercaptoimidazole in pH 7.4 buffer was irradiated with a deuterium lamp for 48 hours in the dark. The resulting solution had no characteristic absorbance maximum above 210nm and so the disulfide can therefore be discounted as being the denitrosation reaction product (eqn 4.4).

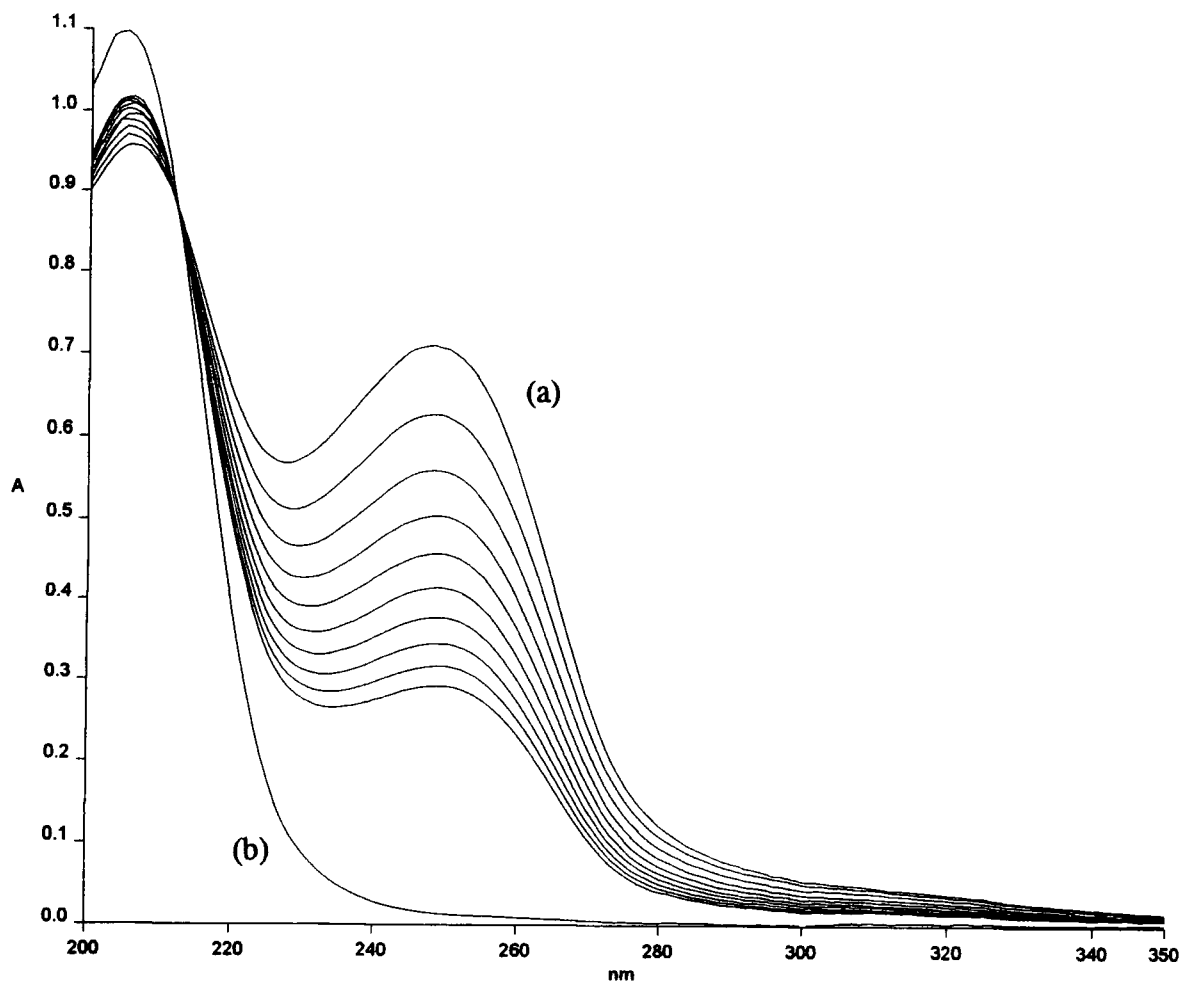


4.3.4.2 Reaction in Distilled Water

The stability of both compounds in distilled water was studied both in the absence and presence of Cu²⁺ ions. It became apparent that each nitrosated thiol decomposed very slowly in this medium in a reaction that formed the corresponding disulfide (figure 4.11) where 1.25×10^{-4} mol dm⁻³ S-nitrosated 2-mercaptoimidazole was monitored for sixty-six hours.

Figure 4.11

Traces showing the absorbance decrease at 250nm for the decomposition of S-nitrosated 2-mercaptoimidazole ($1.25 \times 10^{-4} \text{ mol dm}^{-3}$) in distilled water



(a) scan obtained after seventy minutes; (b) scan obtained after sixty-six hours.

Scans acquired every twenty-five minutes.

The product spectrum is extremely reminiscent of that obtained by ultraviolet radiation of 2-mercaptoimidazole. As the reaction took a long time to reach completion it was not possible to use the nitric oxide specific electrode as a diagnostic tool as any NO produced would become oxidised to nitrite. The effect of adding copper(II) was examined at 270nm following the decrease in [S-nitrosated thiol] (tables 4.16 and 4.17).

Table 4.16

Kinetic data for the decomposition of S-nitrosated 2-mercaptoimidazole
($2.5 \times 10^{-4} \text{ mol dm}^{-3}$) in the presence of added Cu^{2+} , distilled water

$[\text{Cu}^{2+}]/10^{-5} \text{ mol dm}^{-3}$	$k_{\text{obs}}/10^{-5} \text{ s}^{-1}$
0	8.57 ± 0.11
1.0	8.56 ± 0.11
2.0	8.51 ± 0.11
3.0	8.55 ± 0.11
4.0	8.53 ± 0.11
5.0	8.54 ± 0.11

$$k_2 = 0 \text{ mol}^{-1} \text{ dm}^3 \text{ s}^{-1}$$

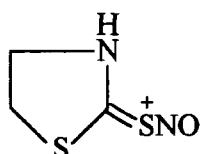
Table 4.17

Kinetic data for the decomposition of S-nitrosated 1-methyl-2-mercaptoimidazole
($2.5 \times 10^{-4} \text{ mol dm}^{-3}$) in the presence of added Cu^{2+} , distilled water

$[\text{Cu}^{2+}]/10^{-5} \text{ mol dm}^{-3}$	$k_{\text{obs}}/10^{-4} \text{ s}^{-1}$
0	1.46 ± 0.01
1.0	1.45 ± 0.01
2.0	1.47 ± 0.01
3.0	1.45 ± 0.01
4.0	1.47 ± 0.01
5.0	1.42 ± 0.01

$$k_2 = 0 \text{ mol}^{-1} \text{ dm}^3 \text{ s}^{-1}$$

It can be seen that Cu^{2+} has no effect on the rate of decomposition of these nitrosothiols in distilled water, which contrasts with the behaviour noted at pH 7.4. The S-nitrosated adduct derived from the sulfur and nitrogen heterocycle 2-mercaptothiazoline (4.19) also showed similar kinetics (table 4.18).



4.19

Table 4.18

Kinetic data for the decomposition of S-nitrosated 2-mercaptothiazoline ($1.5 \times 10^{-3} \text{ mol dm}^{-3}$) in the presence of added Cu^{2+} , distilled water

$[\text{Cu}^{2+}]/10^{-5} \text{ mol dm}^{-3}$	$k_{\text{obs}}/10^{-5} \text{ s}^{-1}$
0	7.88 ± 0.06
1.0	7.96 ± 0.04
2.0	8.13 ± 0.06
3.0	8.78 ± 0.09
4.0	7.80 ± 0.07

$$k_2 = 0 \text{ mol}^{-1} \text{ dm}^3 \text{ s}^{-1}$$

EDTA was added to the decomposition of S-nitrosated 2-mercaptothiazoline ($1.5 \times 10^{-3} \text{ mol dm}^{-3}$) to see if any reaction inhibition was discernible. Table 4.19 indicates that any trace metal ion chelation by EDTA had no effect on the rate of nitrosothiol breakdown suggesting that a copper ion independent process is prevailing.

Table 4.19

Kinetic data for the decomposition of S-nitrosated 2-mercaptothiazoline ($1.5 \times 10^{-3} \text{ mol dm}^{-3}$) in the presence of EDTA, distilled water

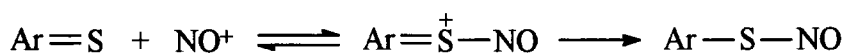
$[\text{EDTA}]/10^{-5} \text{ mol dm}^{-3}$	$k_{\text{obs}}/10^{-5} \text{ s}^{-1}$
0	7.88 ± 0.21
1.0	8.02 ± 0.32
3.0	8.11 ± 0.31
5.0	7.91 ± 0.27
10	8.39 ± 0.28

On adding a solution of 2-mercaptoimidazole to copper(II) in the presence of neocuproine, a peak at 453nm immediately formed when undertaken at pH 7.4 which indicated the almost quantitative formation of Cu^+ . However, on repeating this in distilled water, copper(I) was slowly generated over twenty minutes suggesting that the thione does not act as a particularly good reductant in this medium. This may

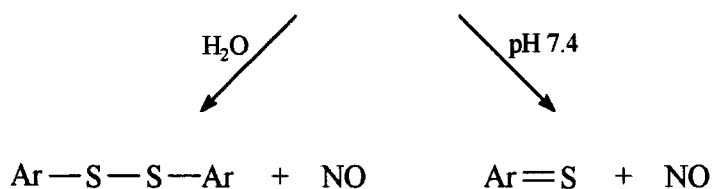
help to explain the lack of observed copper ion catalysis when S-nitrosated 2-mercaptoimidazole decomposes in aqueous solution.

4.4 Mechanism of Heterocyclic and Aromatic S-Nitrosated Decompositions

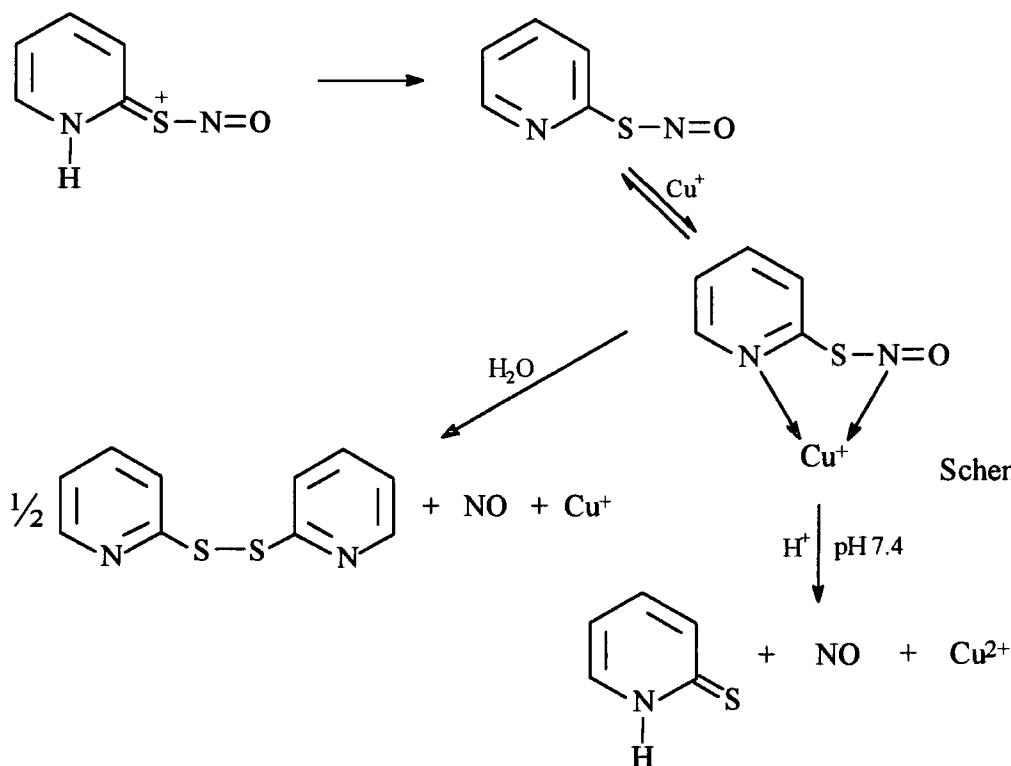
On the basis of experimental data gathered for a number of S-nitrosated heterocyclic and aromatic thiols it is possible to propose the following mechanism for their breakdown in differing media (scheme 4.2), where Ar=S represents the relevant thione tautomeric form.



Scheme 4.2



In both solvents nitric oxide is generated along with the appropriate disulfide in distilled water and thione at pH 7.4. For the specific case of S-nitrosated 2-mercaptoimidazole, the situation can be expressed as described in scheme 4.3.



It is likely that at physiological pH redox cycling of copper takes place as marked catalysis of S-nitroso decomposition occurs, reforming the thione. However, in distilled water it is evident that as the disulfide is observed, copper(I) may stay in this form once produced and enhance homolytic S-N bond cleavage. In the absence of copper ions spontaneous reaction takes place which is only catalysed by added Cu^{2+} for certain species. This appears to be dependent on the reductive ability of the thione in distilled water with respect to copper(II) \rightarrow copper(I). At present it is unclear as to why different mechanisms (and products) prevail under different conditions but it is important to re-examine the possibility of copper ion catalysis in the decomposition of S-nitrosated substrates such as thiourea.

4.5 Conclusion

This chapter has demonstrated that the copper ion catalysed decomposition pathway of S-nitrosothiols can be extended to nitrosated heterocyclic and aromatic thiols which exist predominantly in the thione form. However, it is apparent that the reaction medium has a great bearing on the observed products. Such S-nitrosated thiols have little use therapeutically as nitric oxide donor compounds but are mechanistically of great interest. S-nitrosothiols which have a similar structure to SNAP (SNCP and SNCC) show promising NO production characteristics and have undergone small-scale clinical testing with respect to their vasodilatory properties. A vast array of thiol precursors have now been nitrosated and their behaviour under physiological conditions studied, leading to a detailed understanding of their stability (or lack of).

References

1. S.C. Askew, D.J. Barnett, J. McAninly and D.L.H. Williams, *J. Chem. Soc., Perkin Trans. 2*, 1995, 741.
2. B. Roy, A. du Moulinet d'Hardemare and M. Fontecave, *J. Org. Chem.*, 1994, **59**, 7019.
3. H.A. Moynihan and S.M. Roberts, *J. Chem. Soc., Perkin Trans. 1*, 1994, 797.
4. P.C. Jocelyn, *Biochemistry Of The -SH Group*, Academic Press, 1972, 10.
5. H. Rheinboldt, *Ber.*, 1926, **59**, 1311.
6. H.S. Tasker and H.O. Jones, *J. Chem. Soc.*, 1909, **95**, 1910, 1917.
7. A.R. Hudson and D.L.H. Williams, unpublished observations.
8. D.J. Barnett, Ph.D. thesis, University of Durham, 1994.
9. B.J. Hathaway, *Comprehensive Coordination Chemistry*, Pergamon, 1987, 594.
10. W.L. Baker, *Arch. Biochem. Biophys.*, 1987, **252**, 451.
11. S.H. Laurie, E.S. Mohammed and D.M. Prime, *Inorg. Chim. Acta*, 1981, **56**, 135.
12. J. McMurry, *Organic Chemistry*, Second Edn., Brooks/Cole, 1988, 935.
13. A. Albert and G.B. Barlin, *J. Chem. Soc.*, 1959, 2384.
14. J. Crossland, J.F. Mitchell and G.N. Woodruff, *J. Physiol.*, 1966, **182**, 427.
15. P. Collings, K. Al-Mallah and G. Stedman, *J. Chem. Soc., Perkin Trans. 2*, 1975, 1734.
16. M.P. Doyle and D.M. Hedstrand, *J. Chem. Soc., Chem. Commun.*, 1977, 643.
17. R.L. Blankespoor, M.P. Doyle, D.M. Hedstrand, W.H. Tamblyn and D.A. Van Dyke, *J. Am. Chem. Soc.*, 1981, **103**, 7096.
18. K.A. Jørgensen, A.B.A. Ghattas and S.O. Lawesson, *Tetrahedron*, 1982, **38**, 1163.

19. J.R. Marshall and J. Walker, *J. Chem. Soc.*, 1951, 1004.
20. R.D. Brown and M.L. Heffernan, *Aust. J. Chem.*, 1956, **9**, 83.
21. W.H. Miller, R.O. Roblin and E.B. Astwood, *J. Am. Chem. Soc.*, 1945, **67**, 2201.
22. G.W. Schrauzer and J.W. Sibert, *Arch. Biochem. Biophys.*, 1969, **130**, 257.
23. K. Ramadas, N. Srinivasan, N. Janarthanan and R. Pritha, *Org. Prep. Proc. Int.*, 1996, **28**, 352.
24. E. Klingsberg and D. Papa, *J. Am. Chem. Soc.*, 1949, **71**, 2373.
25. J.P. Danehy, V.J. Elia and C.J. Lavelle, *J. Org. Chem.*, 1971, **36**, 1003.
26. T. Malinski and Z. Taha, *Nature*, 1992, **358**, 676.
27. F. Pariente, J.L. Alonso and H.D. Abruña, *J. Electroanal. Chem.*, 1994, **379**, 191.
28. E.W. Ainscough, E.N. Baker, A.G. Bingham and A.M. Brodie, *J. Chem. Soc., Dalton Trans.*, 1989, 39.
29. G.E. Woodward, *Biochem. J.*, 1933, **27**, 1411.
30. P. Markakis and A.L. Tappel, *J. Am. Chem. Soc.*, 1960, **82**, 1613.

Chapter 5

Thiolate Ion Induced S-Nitrosothiol Decompositions

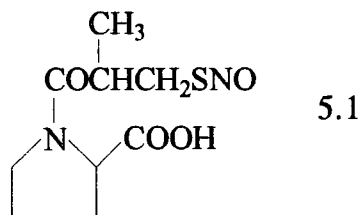
Chapter 5: Thiolate Ion Induced S-Nitrosothiol Decompositions

5.1 Introduction

On examination of the chemical and biological literature, the role of thiols in the decomposition of S-nitrosothiols both *in vitro* and *in vivo* has yet to be clearly defined. The influence of N-acetylpenicillamine on the stability of SNAP and penicillamine on the reactivity of S-nitrosopenicillamine is discussed in sections 2.5.1 and 2.5.2. It is clear from these results that a very small quantity of thiol ($\sim 1\mu\text{M}$) will have a substantial effect on the copper(I) ion catalysed denitrosation pathway¹. Previously published research on this subject has been both contradictory and irreproducible. As an example, two reports^{2,3} claim that thiol compounds such as N-acetylpenicillamine will enhance the rate of S-nitrosothiol decomposition *in vitro* generating the corresponding disulfide and nitric oxide. However, Feelisch *et al*⁴ proposed that L-cysteine will stabilise S-nitrosocysteine in solution in a concentration dependent manner. These inconsistencies can now be explained by considering the possible magnitude of chelation and reduction of Cu^{2+} by thiolate, whose presence as a consequence of the reversibility of S-nitrosothiol formation⁵ is essential for reaction.

Interestingly, very little attention has been focused on the behaviour of S-nitrosothiols in an environment which can be deemed analogous to that of biological systems. S-nitrosogluthathione (GSNO) has been detected in airway lining fluid at a concentration of $0.25\mu\text{M}$ ⁶ and S-nitrosocysteine at $0.3\mu\text{M}$ in plasma⁷. As mentioned in section 4.1, glutathione exists at levels approaching the millimolar scale within mammalian cells and thus is present in at least a several hundred fold excess over any S-nitrosothiol present. It therefore seemed of interest to examine the stability of various nitrosothiols in the presence of their thiol precursors at a much higher concentration than has been previously considered. The well-documented transnitrosation reaction (section 1.4.5) will not be significant under these conditions as the same thiol as its nitroso derivative is utilised. Some nitrosothiols which are

unreactive (even at high copper(II) ion concentrations, such as S-nitrosocaptopril, 5.1) have been studied kinetically with a large excess of captopril present⁸.



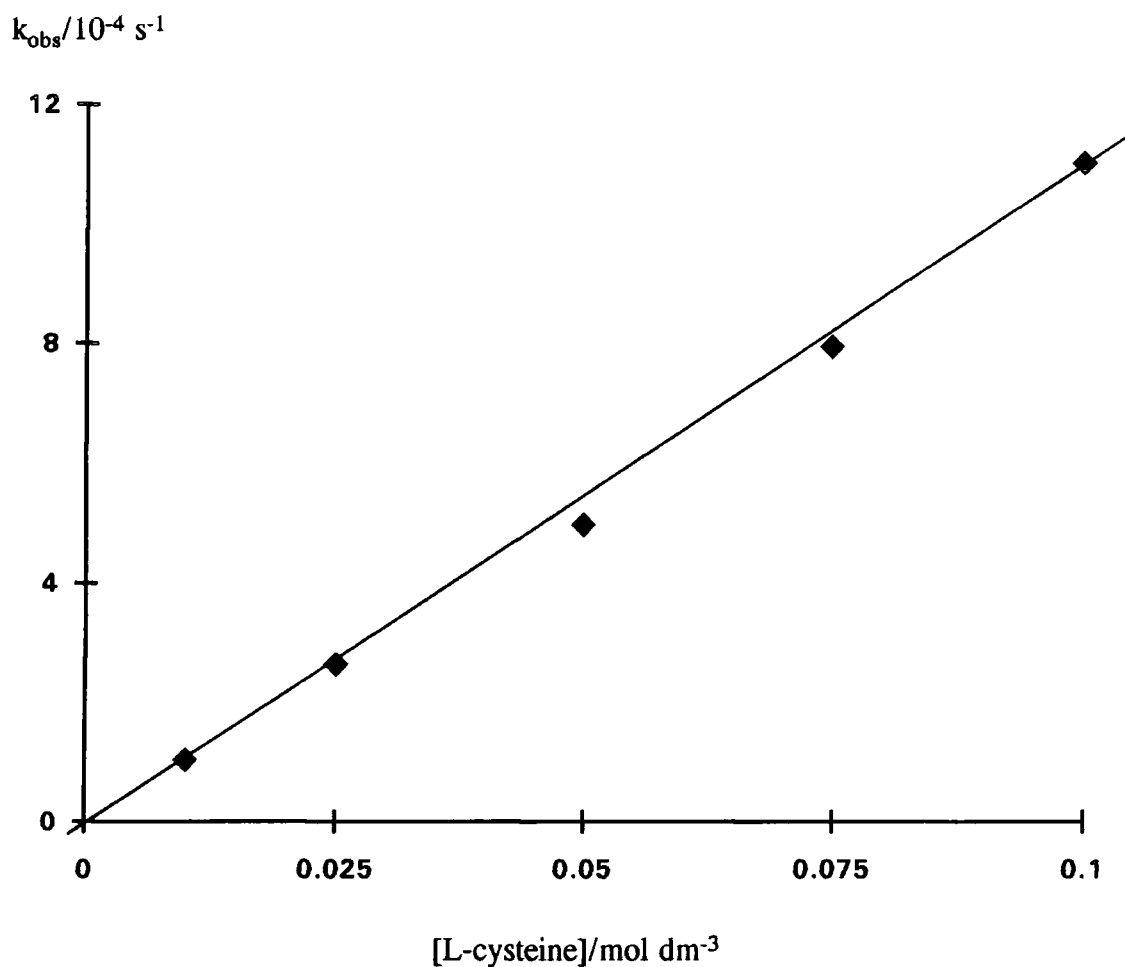
Complete decomposition was apparent with a direct relationship between the amount of thiol added and the rate of reaction. The generality of this process had to be determined along with a thorough product analysis which should allow a tentative reaction mechanism to be postulated.

5.2 Structure/Reactivity Studies

The decomposition of S-nitrosocysteine (RSNO, generated *in situ* via the nitrosation of L-cysteine (RSH) with an equimolar amount of acidified sodium nitrite) was followed spectrophotometrically at 340nm both in the presence and the absence of RSH at pH 7.4. Each kinetic experiment was performed with $[RSH] \gg [RSNO]$ (typically ten to a hundred fold excess) such that pseudo-first order conditions prevailed. Excellent first order traces ensued at each RSH concentration used, allowing k_{obs} to be calculated in every case. A plot of k_{obs} against $[RSH]$ proved to be linear (figure 5.1) which showed the reaction to be first order in thiol.

Figure 5.1

Plot of k_{obs} against [L-cysteine] for the thiol induced decomposition of S-nitrosocysteine ($1 \times 10^{-3} \text{ mol dm}^{-3}$), pH 7.4



The rate equation for this reaction can be expressed below (equation 5.1).

$$\text{Rate} = k_2[\text{RSNO}][\text{RSH}] \quad \text{eqn 5.1}$$

At these concentrations $[\text{RSH}] \gg [\text{RSNO}]$ and thus the concentration of thiol can be assumed to remain constant throughout the reaction, hence equation 5.2 exists.

$$\text{Rate} = k_{\text{obs}}[\text{RSNO}] \quad \text{eqn 5.2}$$

Therefore, k_{obs} is equal to $k_2[\text{RSH}]$ with the second order rate constant being obtained from the gradient of figure 5.1. The term representing the portion of the

rate due to spontaneous thermal decomposition of RSNO would be seen as a positive intercept on plots such as figure 5.1. Clearly this is negligibly small. This experiment was repeated under identical conditions except for the addition of 1×10^{-4} mol dm⁻³ EDTA to each run. The results are summarised in table 5.1.

Table 5.1

Kinetic data for the decomposition of S-nitrosocysteine (1×10^{-3} mol dm⁻³) in the presence of added L-cysteine and the presence/absence of EDTA (1×10^{-4} mol dm⁻³)

[L-cysteine]/mol dm ⁻³	$k_{\text{obs}}/10^{-4} \text{ s}^{-1}$	
	EDTA	no EDTA
0.01	1.19 ± 0.02	1.04 ± 0.01
0.025	2.58 ± 0.02	2.66 ± 0.02
0.05	5.40 ± 0.05	4.97 ± 0.05
0.075	8.27 ± 0.08	7.94 ± 0.08
0.1	11.4 ± 0.1	11.0 ± 0.1

In the presence of EDTA - $k_2 = (1.11 \pm 0.01) \times 10^{-2} \text{ mol}^{-1} \text{ dm}^3 \text{ s}^{-1}$

In the absence of EDTA - $k_2 = (1.07 \pm 0.01) \times 10^{-2} \text{ mol}^{-1} \text{ dm}^3 \text{ s}^{-1}$

It is clear from this kinetic data that k_{obs} is hardly affected by the introduction of the metal ion chelator EDTA, suggesting that copper ion (or indeed any ionic species adventitiously present) does not influence the reaction profile. This means that a very different mechanism must account for the decomposition of nitrosothiols which is copper ion independent. The obtained k_2 value of $0.0111 \text{ mol}^{-1} \text{ dm}^3 \text{ s}^{-1}$ at 25°C in the presence of EDTA is consistent with that recently quoted by Komiyama *et al*⁹ ($0.0310 \text{ mol}^{-1} \text{ dm}^3 \text{ s}^{-1}$ at 37°C) for the same reaction. In order to check the generality of this reaction, several other S-nitrosothiol/thiol systems were investigated in a similar way (tables 5.2 - 5.8). All reactions were carried out in pH 7.4 buffer with the exception of S-nitrosotriphenylmethanethiol/triphenylmethanethiol which was performed in dimethylsulfoxide.

Table 5.2

Kinetic data for the decomposition of S-nitrosogluthathione ($1 \times 10^{-3} \text{ mol dm}^{-3}$) in the presence of added glutathione, pH 7.4

[glutathione]/mol dm ⁻³	$k_{\text{obs}}/10^{-4} \text{ s}^{-1}$
0.01	0.964 ± 0.009
0.025	1.54 ± 0.01
0.05	2.77 ± 0.02
0.075	4.15 ± 0.04
0.1	5.44 ± 0.05

$$k_2 = (5.50 \pm 0.07) \times 10^{-3} \text{ mol}^{-1} \text{ dm}^3 \text{ s}^{-1}$$

Table 5.3

Kinetic data for the decomposition of S-nitrosopenicillamine ($1 \times 10^{-3} \text{ mol dm}^{-3}$) in the presence of added penicillamine, pH 7.4

[penicillamine]/mol dm ⁻³	$k_{\text{obs}}/10^{-3} \text{ s}^{-1}$
0.01	3.12 ± 0.03
0.025	6.72 ± 0.03
0.05	12.9 ± 0.1
0.075	19.6 ± 0.2
0.1	26.3 ± 0.2

$$k_2 = (2.62 \pm 0.02) \times 10^{-1} \text{ mol}^{-1} \text{ dm}^3 \text{ s}^{-1}$$

Table 5.4

Kinetic data for the decomposition of S-nitrosocysteine ethyl ester ($1 \times 10^{-3} \text{ mol dm}^{-3}$) in the presence of added cysteine ethyl ester, pH 7.4

[cysteine ethyl ester]/mol dm ⁻³	$k_{\text{obs}}/10^{-4} \text{ s}^{-1}$
0.05	6.47 ± 0.07
0.075	8.58 ± 0.09
0.0875	9.62 ± 0.09
0.1	10.5 ± 0.1
0.125	12.5 ± 0.1

$$k_2 = (8.01 \pm 0.11) \times 10^{-3} \text{ mol}^{-1} \text{ dm}^3 \text{ s}^{-1}$$

Table 5.5

Kinetic data for the decomposition of S-nitrosocaptopril ($1 \times 10^{-3} \text{ mol dm}^{-3}$) in the presence of added captopril, pH 7.4

[captopril]/mol dm ⁻³	$k_{\text{obs}}/10^{-4} \text{ s}^{-1}$
0.003	1.08 ± 0.01
0.006	2.12 ± 0.03
0.01	3.30 ± 0.03
0.0169	5.22 ± 0.06
0.025	7.12 ± 0.07

$$k_2 = (2.73 \pm 0.12) \times 10^{-2} \text{ mol}^{-1} \text{ dm}^3 \text{ s}^{-1}$$

Table 5.6

Kinetic data for the decomposition of S-nitrosocysteamine ($1 \times 10^{-3} \text{ mol dm}^{-3}$) in the presence of added cysteamine, pH 7.4

[cysteamine]/mol dm ⁻³	$k_{\text{obs}}/10^{-4} \text{ s}^{-1}$
0.01	1.47 ± 0.01
0.025	3.29 ± 0.04
0.05	5.85 ± 0.06
0.075	8.73 ± 0.08
0.1	12.1 ± 0.1

$$k_2 = (1.19 \pm 0.01) \times 10^{-2} \text{ mol}^{-1} \text{ dm}^3 \text{ s}^{-1}$$

Table 5.7

Kinetic data for the decomposition of S-nitroso-2-N,N-diethylaminoethanethiol ($1 \times 10^{-3} \text{ mol dm}^{-3}$) in the presence of added 2-N,N-diethylaminoethanethiol, pH 7.4

[2-N,N-diethylaminoethanethiol]/mol dm ⁻³	$k_{\text{obs}}/10^{-4} \text{ s}^{-1}$
0.01	1.91 ± 0.01
0.025	4.85 ± 0.05
0.05	12.1 ± 0.2
0.075	19.8 ± 0.2
0.1	27.1 ± 0.4

$$k_2 = (2.91 \pm 0.05) \times 10^{-2} \text{ mol}^{-1} \text{ dm}^3 \text{ s}^{-1}$$

Table 5.8

Kinetic data for the decomposition of S-nitrosotriphenylmethanethiol*
(1×10^{-3} mol dm $^{-3}$) in the presence of added triphenylmethanethiol

[triphenylmethanethiol]/mol dm $^{-3}$	$k_{\text{obs}}/10^{-5}$ s $^{-1}$
0.0048	5.66 ± 0.07
0.01	8.84 ± 0.09
0.0121	10.1 ± 0.1
0.0166	12.5 ± 0.2
0.0196	15.4 ± 0.3

$$k_2 = (6.33 \pm 0.03) \times 10^{-3} \text{ mol}^{-1} \text{ dm}^3 \text{ s}^{-1}$$

* Measured in dimethylsulfoxide.

The structural formula of each S-nitrosothiol studied and the second order rate constant, k_2 calculated for the reaction with thiol is summarised in table 5.9. It is evident from these results that the k_2 values are all of a similar order of magnitude (that is, it does not appear to be easy to define a relationship between S-nitrosothiol structure and reactivity). This is in direct contrast to the copper(I) catalysed decomposition mechanism where bidentate coordination is required for effective reaction (table 5.10).

The thiol induced reaction is clearly much slower than the corresponding cuprous ion promoted process. The tertiary compound S-nitrosopenicillamine is significantly more reactive than the other nitrosothiols studied (table 5.9). Such materials containing two α -carbon methyl groups are known to exhibit an enhanced reaction rate with respect to copper ion catalysed nitrosothiol decomposition (section 1.4.3.1), due to the "gem-dimethyl effect". It may be that the increased electronic density upon the sulfur atom and steric considerations significantly influence the reactivity of such a compound. Further tertiary and secondary S-nitrosothiols need to be studied in the presence of their corresponding thiols to verify this theory.

Table 5.9

Values of k_2 for the thiol induced decomposition of S-nitrosothiols, pH 7.4

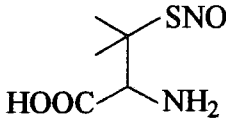
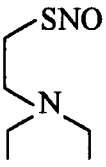
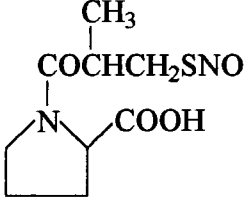
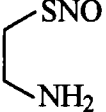
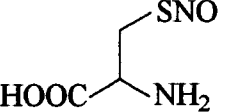
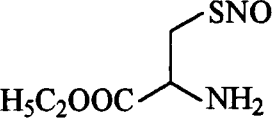
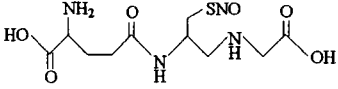
S-nitrosothiol/thiol	Structure	$k_2/10^{-4}$ $\text{mol}^{-1} \text{dm}^3 \text{s}^{-1}$
S-nitrosopenicillamine/penicillamine		2620 ± 20
S-nitroso-2-N,N-diethylaminoethanethiol/ 2-N,N-diethylaminoethanethiol		291 ± 5
S-nitrosocaptopril/captopril		273 ± 12
S-nitrosocysteamine/cysteamine		119 ± 1
S-nitrosocysteine/cysteine		107 ± 1
S-nitrosocysteine ethyl ester/ cysteine ethyl ester		80 ± 1
S-nitrosotriphenylmethanethiol/ triphenylmethanethiol (measured in dimethyl sulfoxide)	Ph_3CSNO	63 ± 1
S-nitrosogluthathione/gluthathione		55 ± 1

Table 5.10

k_2 values for the decomposition of S-nitrosocysteine and S-nitrosocysteine ethyl ester in the presence of Cu^{2+} (rate = $k_2[\text{Cu}^{2+}][\text{RSNO}]$) or respective thiol (rate = $k_2[\text{RSH}][\text{RSNO}]$), pH 7.4

S-nitrosothiol	Copper ion induced $k_2/\text{mol}^{-1} \text{ dm}^3 \text{ s}^{-1}$	Thiol induced $k_2/10^{-4} \text{ mol}^{-1} \text{ dm}^3 \text{ s}^{-1}$
S-nitrosocysteine	24,700 ^a	107
S-nitrosocysteine ethyl ester	270,000 ^a	80

^avalues obtained by D.J. Barnett, Ph.D. thesis, University of Durham, 1994.

5.3 Product Detection

5.3.1 Detection of Nitrite

Having kinetically monitored the reaction between S-nitrosothiols and an excess of thiol at physiological pH it became necessary to perform a thorough analysis of the products generated. The Griess test (section 3.2.4) provides a convenient and sensitive method of detecting the presence of any nitrite ions in solution. The required extinction coefficient at 540nm was calculated to be $46,000 \pm 760 \text{ mol}^{-1} \text{ dm}^3 \text{ cm}^{-1}$ and the appropriate solutions of sulfanilamide and N-1-naphthylethylenediamine added to the following reactions. $0.001 \text{ mol dm}^{-3}$ S-nitrosocysteine was introduced to L-cysteine in the concentration range $0.01 - 0.1 \text{ mol dm}^{-3}$ and allowed to react until complete nitrosothiol decomposition was observed (ten hours). After a further six hours 1ml of each reactant solution was analysed for the possible nitrite content in the usual manner by measuring the absorbance at 540nm following azo dye formation. The results obtained are tabulated overleaf (table 5.11).

Table 5.11

Percentage NO_2^- detected after the reaction between S-nitrosocysteine
($0.001 \text{ mol dm}^{-3}$) and L-cysteine, pH 7.4

[L-cysteine]/ mol dm^{-3}	Absorbance _{540nm}	% NO_2^-
0	0.835	91
0.01	0.318	34
0.025	0.121	13
0.05	0.068	7
0.075	0.054	6
0.1	0.050	5

In the absence of added L-cysteine, almost quantitative production of nitrite is observed, which could be predicted as the copper(I) catalysed mechanism will prevail. However, on introducing 0.01 mol dm^{-3} thiol the amount of NO_2^- detected drops to 34% and continues to fall until only 5% can be seen at $[\text{L-cysteine}] = 0.1 \text{ mol dm}^{-3}$. This is in complete contrast to the situation which exists when S-nitrosothiols react with copper ions¹⁰ but is in keeping with a recent report published by Singh *et al*¹¹ who noted a similar trend when studying the reaction between GSNO and glutathione under similar conditions. Nitrite is probably formed via the oxidation of nitric oxide in aerobic solutions but is certainly not the major nitrogenous product to be generated when $[\text{thiol}]:[\text{nitrosothiol}] = 10:1$ and greater. The question that has to be answered now relates to the nature of the other nitrogenous product(s) that are present after reaction completion.

5.3.2 Detection of Ammonia

Another observation made by Singh *et al*¹¹ is that ammonia can be detected as a product during the reaction of glutathione with GSNO. This interesting discovery prompted the purchase of a standard NH_3 diagnostic kit from Sigma-Aldrich Co. Ltd. to analyse possible ammonia levels in the S-nitrosocysteine/L-cysteine system. The principles behind this method are based on a kinetic technique first devised in 1974¹² to determine $[\text{NH}_3]$ in blood plasma (typically $6.5 - 35 \mu\text{M}$). The reductive amination

of 2-oxoglutarate is performed using the enzyme glutamate dehydrogenase (GLDH) and coenzyme reduced nicotinamide adenine dinucleotide phosphate (NADPH) according to equation 5.3.



eqn 5.3

In the presence of an excess of NADPH and 2-oxoglutarate the reaction becomes pseudo-first order. This means that the rate of reaction will only be dependent on $[\text{NH}_3]$ and the activity of GLDH. However, the activity of glutamate dehydrogenase originally present in plasma samples is small compared to the amount introduced so that the reaction rate is effectively only dependent on the ammonia concentration.

The reaction is followed spectrophotometrically at 340nm by monitoring the absorbance due to NADPH before and after the addition of GLDH, which causes coenzyme oxidation proportional to the sample ammonia concentration¹³. For each reaction between L-cysteine (0.01 mol dm^{-3} - 0.1 mol dm^{-3}) and S-nitrosocysteine ($0.001 \text{ mol dm}^{-3}$) a blank and a test solution were set up in the following manner. To the blank cuvette 1.0ml ammonia assay solution (containing 2-oxoglutarate and NADPH) was added to 0.1ml distilled water and allowed to equilibrate for three minutes at 25°C. The test cuvette was similarly prepared with 0.1ml reaction solution. After the required time period had elapsed the absorbance of each sample at 340nm was measured and 0.01ml GLDH introduced. The final absorbances were recorded after a further five minutes and ammonia concentrations calculated using equations 5.4 - 5.5.

$$\Delta A = \text{initial absorbance (340nm)} - \text{final absorbance(340nm)} \quad \text{eqn 5.4}$$

$$\text{Test ammonia concentration} = (\Delta A_{\text{test}} - \Delta A_{\text{blank}}) \times 30.3 \quad \text{eqn 5.5}$$

($\mu\text{g/ml}$)

The factor 30.3 can be derived as in equation 5.6.

$$30.3 = \frac{1.11 \times 17}{6.22 \times 0.1}$$

eqn 5.6

1.11 = volume of liquid in cuvette (ml)

17 = RMM of ammonia

6.22 = millimolar absorptivity of NADPH at 340nm

0.1 = volume of sample (ml)

Thus, it is possible to calculate the concentration of any ammonia that has been generated and express it as a percentage of the nitrogen that could be formed from the decomposition of S-nitrosocysteine (table 5.12).

Table 5.12

Percentage NH₃ detected after the reaction between S-nitrosocysteine (0.001 mol dm⁻³) and L-cysteine, pH 7.4

[L-cysteine]/mol dm ⁻³	$\Delta A_{\text{test}} - \Delta A_{\text{blank}}$	%NH ₃
0	0.004	0.7
0.01	0.315	56
0.025	0.448	80
0.05	0.459	82
0.075	0.467	83
0.1	0.478	85

The opposite effect to that seen for nitrite concentration is observed as increasing [L-cysteine] leads to more ammonia being detected. Table 5.13 summarises the results obtained for NO₂⁻ and NH₃ analysis of the S-nitrosocysteine/L-cysteine reaction which are shown graphically in figure 5.2.

Table 5.13

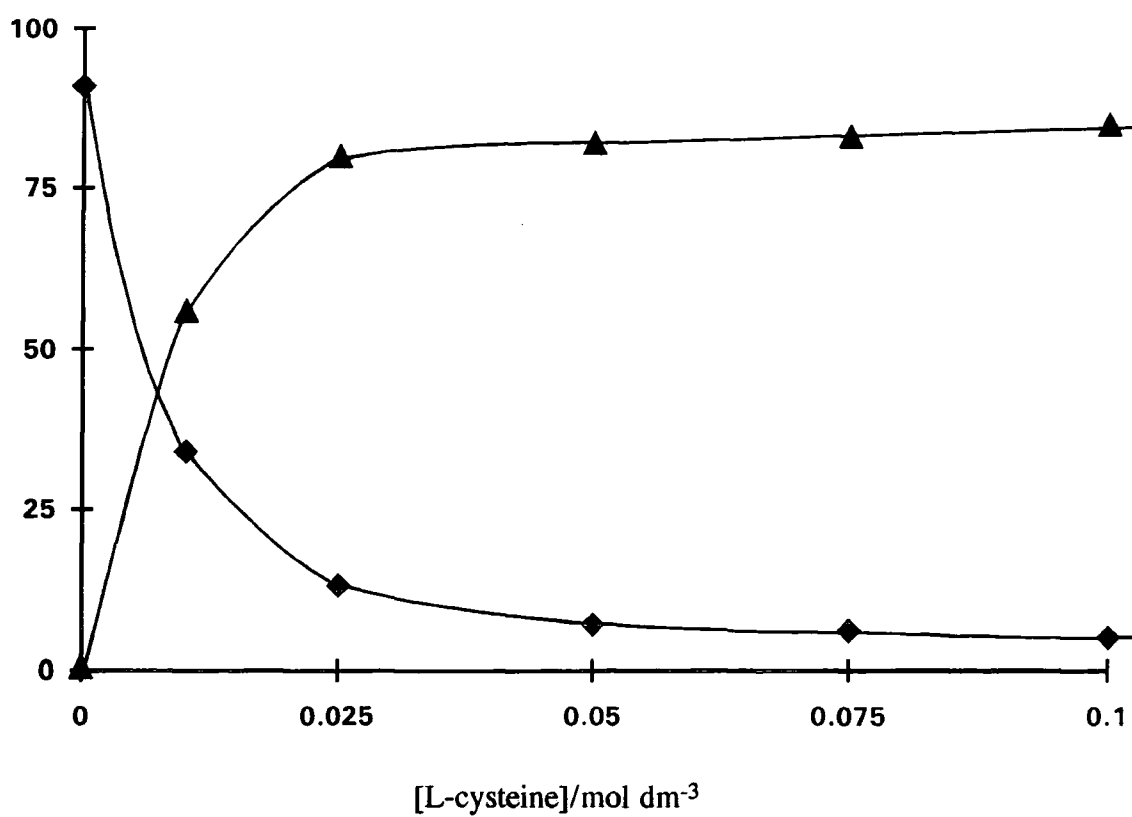
Variation of the nitrite and ammonia content in the reaction products for the L-cysteine induced decay of S-nitrosocysteine ($0.001 \text{ mol dm}^{-3}$), pH 7.4

[L-cysteine]/mol dm ⁻³	%NO ₂ ⁻	%NH ₃	%N detected
0	91	0.7	92
0.01	34	56	90
0.025	13	80	93
0.05	7	82	89
0.075	6	83	89
0.1	5	85	90

Figure 5.2

Plot of [thiol] against %NO₂⁻ and %NH₃ as products of the reaction between L-cysteine and S-nitrosocysteine, pH 7.4

%NO₂⁻ or %NH₃



◆ = NO₂⁻ ▲ = NH₃

Clearly around 90% of the nitrogen derived from S-nitrosocysteine can be accounted for by the detection of nitrite and ammonia. However, there is still a small percentage whose origin is unknown which has not been determined.

5.3.3 Detection of Nitrous Oxide and Disulfide

Nitrous oxide (N_2O) has been detected under aerobic conditions when GSNO is reacted with glutathione¹¹, using a GC-MS closed system. This is the only analytical procedure which can realistically be used to study the production of this gas. Between 1% and 3% N_2O was formed when the glutathione concentration was varied, despite reports that nitrous oxide is a major reaction product in the reaction of thiols with S-nitrosothiols¹⁴. Glutathione disulfide (GSSG) was the only product detected by HPLC in the GSNO/glutathione system, as measured both aerobically and anaerobically¹¹. It will be necessary in the future to undertake further experimental product analysis in order to quantify nitrous oxide and disulfide levels for the reaction of S-nitrosocysteine with L-cysteine.

5.4 Reaction under Anaerobic Conditions

In order to probe the reaction mechanism further, experiments were performed in the absence of oxygen and product analysis undertaken. Anaerobic conditions were attained by chemical deaeration of all buffer and distilled water components by the following technique. To 100ml solution 2mg glucose oxidase, 1mg catalase and 0.18g glucose were introduced and left for one hour at 37°C¹⁵. Nitrite and ammonia levels were recorded in an analogous fashion to that described previously (sections 5.3.1 - 5.3.2) for the reaction between 0.001 mol dm⁻³ S-nitrosocysteine and varying L-cysteine concentrations (table 5.14).

Table 5.14

Variation of the nitrite and ammonia content in the reaction products for the anaerobic L-cysteine induced decay of S-nitrosocysteine ($0.001 \text{ mol dm}^{-3}$), pH 7.4

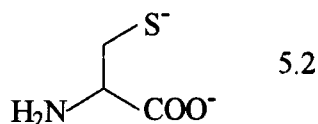
[L-cysteine]/mol dm ⁻³	%NO ₂ ⁻	%NH ₃	%N detected
0	92	0	92
0.01	26	7	33
0.025	15	35	50
0.05	12	49	61
0.075	6	55	61
0.1	7	70	77

It can be seen that in the absence of oxygen similar trends are observed as aerobically in that on increasing [L-cysteine], the amount of nitrite detected decreases and the quantity of ammonia increases. However, a big difference is that quantitative nitrogenous detection could not be achieved at any thiol concentration. This suggests that nitrous oxide is a much more significant product anaerobically, as noted previously¹¹. It would appear that N₂O becomes formed at the expense of ammonia, and that oxygen has a big influence on the ratio of the reaction products generated. The second order rate constant, k_2 was measured and calculated to be $(1.17 \pm 0.02) \times 10^{-2} \text{ mol}^{-1} \text{ dm}^3 \text{ s}^{-1}$ which is almost identical to that observed aerobically, leading to the conclusion that although the amount of NO₂⁻ and NH₃ vary according to the oxygen concentration, the rate of reaction does not.

5.5 Possible Reaction Mechanism

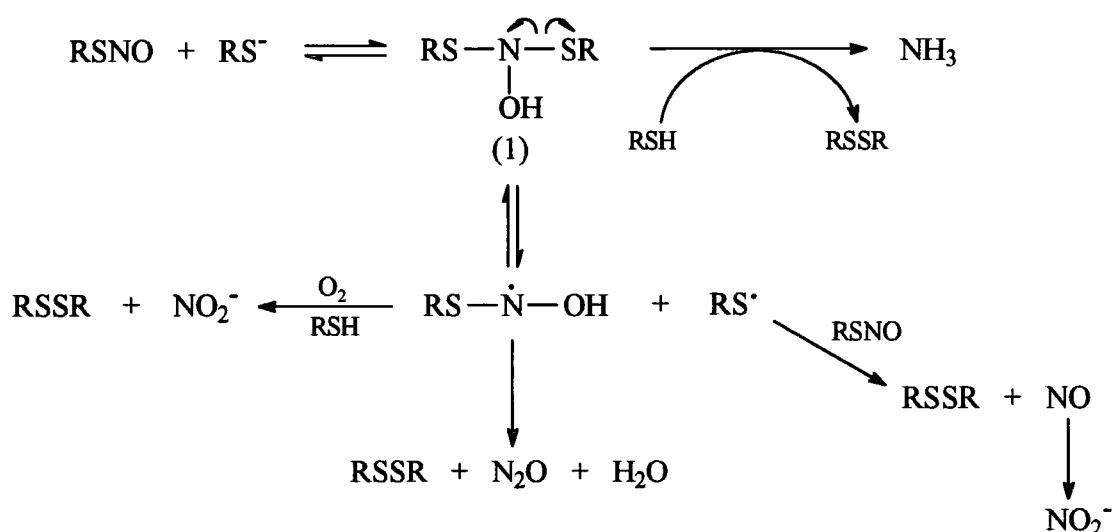
A thorough investigation into the potential pH dependence of this reaction has recently been undertaken¹⁶. Second order rate constants were calculated for the S-nitrosocysteine/L-cysteine system at various pH values ranging from 1.03 to 13.29. A significant pH dependence in k_2 was apparent with the value observed at pH 13.29 nearly thirty times greater than that at pH 1.03. A sudden increase in the magnitude of k_2 is observable above pH 8.0 which presumably can be related to a role for RS⁻

(in this case L-cys⁻) as the thiol will become deprotonated. It is proposed that the dianion derived from L-cysteine (5.2) may effect S-nitrosocysteine decomposition).



Product analysis has additionally shown that a basic pH will promote nitrite formation, whereas an acidic pH is more favoured for ammonia production.

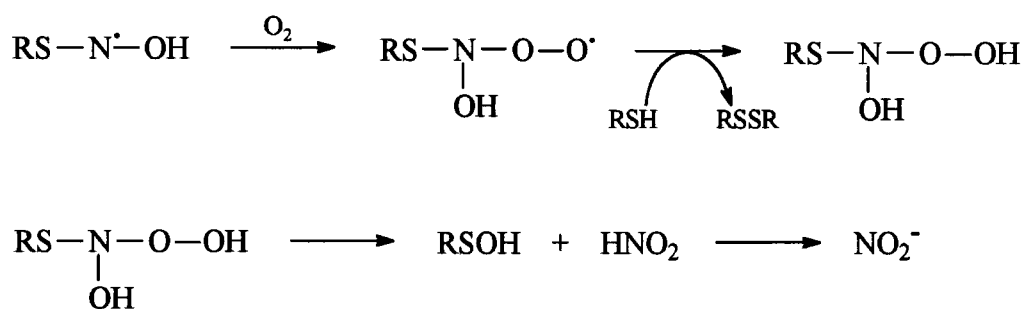
Any postulated reaction mechanism has to take into account all of the experimental data previously described, in terms of kinetics and product formation. A possible outline for reaction is shown in scheme 5.1¹¹.



Scheme 5.1

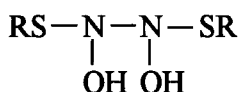
The initial step observed is that of nucleophilic thiolate ion (RS⁻) attack at the nitrogen atom of the S-nitroso functionality. This explains the reactivity of S-nitrosopenicillamine, as an enhanced electron density at the sulfur atom of this compound negates attack of RS⁻ at S, yet the thiolate ion derived from penicillamine will react increasingly rapidly with the corresponding nitrosothiol. It would be expected that similar tertiary thiols will behave in an analogous fashion when reacted with the appropriate RSNO species. The primary reaction intermediate is therefore an N-hydroxysulfenamide (1) which can react with excess thiol to produce ammonia as a

detected material, possibly via a series of thiol conjugates¹¹. This pathway will be favoured at high [RS⁻] and accounts for the greater yield of NH₃ noted when thiolate is present in a hundred-fold excess over S-nitrosothiol. Disulfide is additionally generated by this step. However, homolytic S-N bond fission may take place in the N-hydroxysulfenamide molecule which produces a thiyl (RS[•]) and N-hydroxyl (RS-N[•]-OH) radical. Both of these species can react further in solution depending on the amount of oxygen available within the system. Under normal aerobic conditions a direct interaction between O₂ and RS-N[•]-OH forms an alternative radical (scheme 5.2) which will react with thiol to eventually produce nitrite and disulfide.

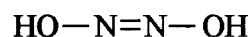


Scheme 5.2

In comparison, RS-N[•]-OH can dimerise forming a dihydroxyhydrazine (5.3) which is unstable and will decompose via hyponitrous acid (5.4) to eliminate nitrous oxide. Schultz *et al*¹⁷ have described the interaction between N-nitrosamines and L-cysteine in great detail, and have noted both N₂O and NH₃ as products.



5.3



5.4

It is clear therefore that when oxygen is not present (anaerobic conditions) the pathway forming N₂O will be favoured, explaining the incomplete detection of nitrogenous material in the absence of O₂. Another route must exist which will generate NO₂⁻ anaerobically. This is the reaction of thiyl radical with S-nitrosothiol

manufacturing the appropriate disulfide and nitric oxide which will slowly become oxidised to nitrite over a long period of time due to small traces of oxygen being present. Theoretically, if the system was completely devoid of O_2 , NO could be detected as a product directly. The mechanism described by scheme 5.1 can also be used to interpret the observed pH results¹⁶. At low pH values where RSH is the predominant species, a greater proportion of the N-hydroxysulfenamide can be converted into NH_3 . In contrast, at alkaline pH more N-hydroxyl and thiyl radicals will be produced, leading to higher nitrite concentrations. Hence, a scheme has been formulated which will hopefully be studied in greater detail with regard to product analysis over the forthcoming months.

5.6 Conclusion

In summary, it has been established that the major product formed during the reaction between S-nitrosothiols and corresponding thiols is ammonia, and not nitric oxide as may have been expected. The mechanism is proposed to be independent of the transition metal ion concentration, revealing a new angle on the chemistry of S-nitroso species. A similar reactivity rate is exhibited by many of the compounds studied with a pronounced "gem-dimethyl effect" apparent concerning S-nitrosopenicillamine. When the *in vivo* concentrations of S-nitrosothiols and thiols are considered the reaction may have significance within biological fluids as an alternative decomposition pathway for RSNO species. However, it perhaps has less interest related to it as NO is not a major product, although small quantities are generated as a consequence of thiyl radicals interacting with nitrosothiols. More work is currently in progress within this laboratory relating to the stability of S-nitrosothiols in the company of various thiols.

References

1. A.P. Dicks, P. Herves Beloso and D.L.H. Williams, *J. Chem. Soc., Perkin Trans. 2*, 1997, 1429.
2. E.A. Kowaluk and H-L. Fung, *J. Pharm. Exp. Ther.*, 1990, **255**, 1256.
3. S. Oae, D. Fukushima and Y.H. Kim, *J. Chem. Soc., Chem. Commun.*, 1977, 407.
4. M. Feelisch, M.T. Poel, R. Zamora, A. Deussen and S. Moncada, *Nature*, 1994, **368**, 62.
5. P. Herves Beloso and D.L.H. Williams, *J. Chem. Soc., Chem. Commun.*, 1997, 89.
6. A.R. Butler and P. Rhodes, *Anal. Biochem.*, 1997, **249**, 1.
7. J.S. Stamler, unpublished observations.
8. H.R. Swift, Ph.D. thesis, University of Durham, 1996.
9. T. Komiyama and K. Fujimori, *Bioorg. Med. Chem. Lett.*, 1997, **7**, 175.
10. J. McAninly, D.L.H. Williams, S.C. Askew, A.R. Butler and C. Russell, *J. Chem. Soc., Chem. Commun.*, 1993, 1758.
11. S.P. Singh, J.S. Wishnok, M. Keshive, W.M. Deen and S.R. Tannenbaum, *Proc. Natl. Acad. Sci., USA*, 1996, **93**, 14428.
12. H.C. van Anken and M.E. Schiphorst, *Clin. Chim. Acta*, 1974, **56**, 151.
13. W.E. Neeley and J. Phillipson, *Clin. Chem.*, 1968, **34**, 1868.
14. J.W. Park, *Biochem. Biophys. Res. Commun.*, 1988, **152**, 916.
15. A.C.F. Gorren, A. Schrammel, K. Schmidt and B. Mayer., *Arch. Biochem. Biophys.*, 1996, **330**, 219.
16. A.P. Munro and D.L.H. Williams, to be published.
17. U. Schulz and D.R. McCalla, *Can. J. Chem.*, 1969, **47**, 2021.

Chapter 6

Experimental Details

Chapter 6: Experimental Details

6.1 Experimental Techniques

6.1.1 Ultraviolet/Visible Spectrophotometry

All ultraviolet/visible spectra were obtained from solutions in quartz cuvettes of 1cm path length at 25°C on either a Perkin-Elmer Lambda 2, Perkin-Elmer Lambda 12 or Shimadzu UV-2101PC spectrophotometer. The same three instruments were generally used to measure reaction kinetics at fixed wavelengths. For more rapid reactions ($t_{1/2} \geq 2\text{ms}$) a stopped-flow technique was used (section 6.1.2).

All kinetic measurements were made under pseudo-first order conditions. The observed rate constants were calculated from the noted absorbance change as a function of time at a specific wavelength (usually 340nm). The absorbance/time data from each spectrophotometer were transferred to an Epson AX2 personal computer and utilised in a software program designed for rate constant calculation (Enzfitter). This program allowed the calculation of observed rate constants, k_{obs} , which was based on the following derivation.

For a first order kinetic process (equation 6.1), the rate of formation of B or the removal of A can be expressed by equation 6.2.



$$-\frac{d[A]}{dt} = \frac{d[B]}{dt} = k_{\text{obs}}[A] \quad \text{eqn 6.2}$$

Integration of equation 6.2 gives an expression for the observed first order rate constant, k_{obs} (equation 6.3).

$$\ln[A]_0 - \ln[A]_t = k_{\text{obs}}t \quad \text{eqn 6.3}$$

(where $[A]_0$ and $[A]_t$ are the concentrations of species A at times $t = 0$ and $t = t$ respectively).

Using the Beer-Lambert law ($A = \epsilon cl$, where A is the absorbance, ϵ is the molar extinction coefficient, c is the concentration and l the path length), and assuming the latter to be 1cm, the expression of the absorbance at $t = 0$ and $t = t$ can be derived (equations 6.4 and 6.5).

$$A_0 = \epsilon_A[A]_0 \quad \text{eqn 6.4}$$

$$A_t = \epsilon_A[A]_t + \epsilon_B[B]_t \quad \text{eqn 6.5}$$

As $[B]_t = [A]_0 - [A]_t$, substituting for $[B]_t$ into equation 6.5 gives-

$$A_t = \epsilon_A[A]_t + \epsilon_B[A]_0 - \epsilon_B[A]_t \quad \text{eqn 6.6}$$

At the end of reaction, $t = \infty$ and $[B]_\infty = [A]_0$, so-

$$A_\infty = \epsilon_B[A]_0 \quad \text{eqn 6.7}$$

Substituting into equation 6.6-

$$A_t = \epsilon_A[A]_t + A_\infty - \epsilon_B[A]_t, \text{ thus}$$

$$[A]_t = \frac{(A_t - A_\infty)}{(\epsilon_A - \epsilon_B)} \quad \text{eqn 6.8}$$

Similarly, at time $t = 0$ -

$$A_0 = \epsilon_A[A]_0 \quad \text{eqn 6.9}$$

Hence, subtracting equation 6.7 from equation 6.9-

$$(A_0 - A_\infty) = \epsilon_A[A]_0 - \epsilon_B[A]_0, \text{ and}$$

$$[A]_0 = \frac{(A_0 - A_\infty)}{(\epsilon_A - \epsilon_B)} \quad \text{eqn 6.10}$$

Substituting equations 6.8 and 6.10 into equation 6.3 yields-

$$k_{\text{obs}} = \frac{1}{t} \ln \frac{(A_0 - A_\infty)}{(A_t - A_\infty)} \quad \text{eqn 6.11}$$

Rearranging gives-

$$\ln(A_t - A_\infty) = -k_{\text{obs}}t + \ln(A_0 - A_\infty) \quad \text{eqn 6.12}$$

Therefore, a plot of $\ln(A_t - A_\infty)$ against t should be linear with a slope of $-k_{\text{obs}}$. The infinity values A_∞ , were determined after a period of ten half lives and the disappearance of absorbance followed for at least two half lives.

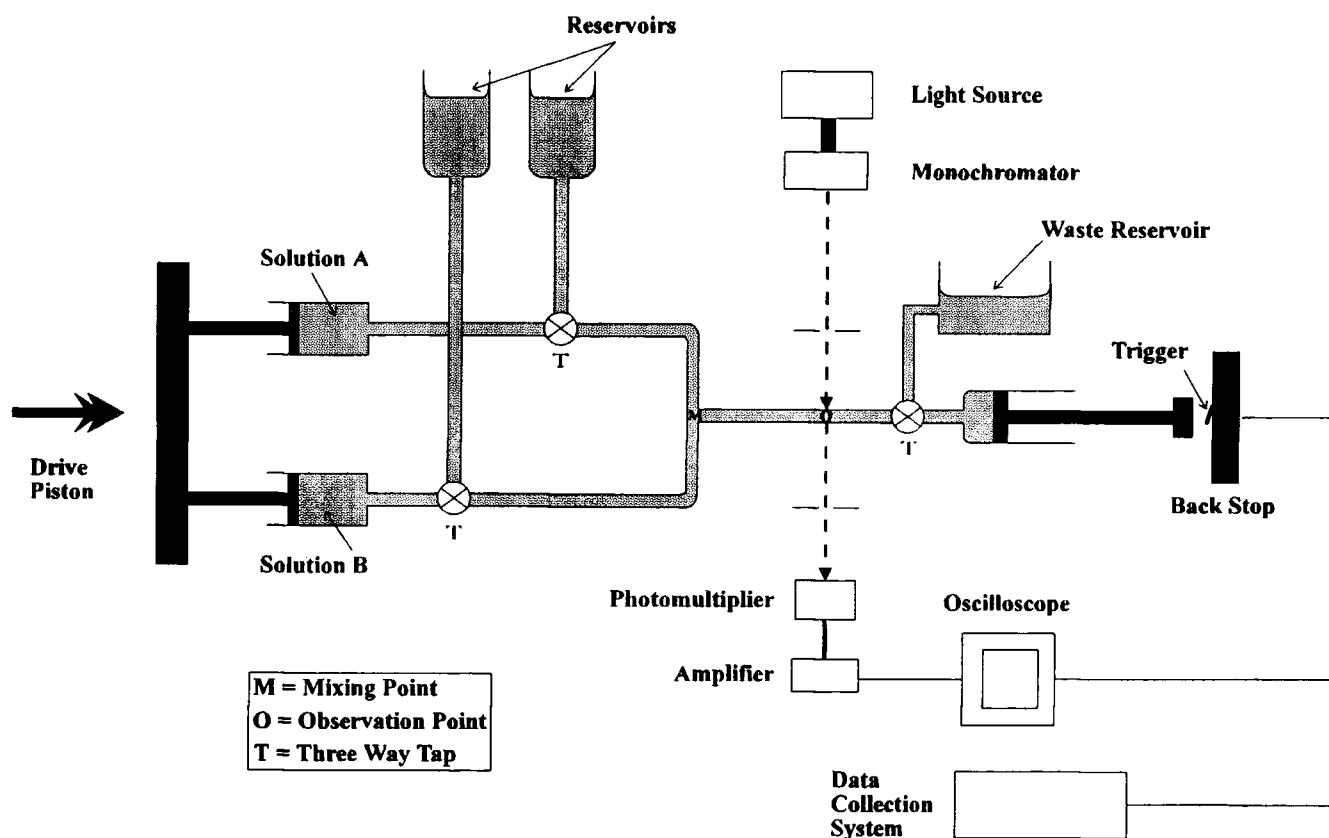
6.1.2 Stopped-Flow Spectrophotometry

For the determination of rate constants of reactions too fast to measure by conventional machines an Applied Photophysics Stopped-Flow spectrophotometer and a Hi-Tech Scientific SF-3L Stopped-Flow spectrophotometer were used. The experimental apparatus is shown schematically in figure 6.1. All reactions were carried out under pseudo-first order conditions. The two solutions to be reacted, A and B, are stored in reservoirs and drawn into two identical syringes so that equal volumes are mixed. The syringes are simultaneously compressed (either manually or by using a compressed air supply) with reactant mixing taking place at point M extremely rapidly ($< 1\text{ms}$). The mixture then flows into a thermostatted 2mm path length quartz cell at point O, which causes the plunger of the third syringe to hit a stop, with a cessation in the solution flow. The acquisition of absorbance/time data from the reaction is triggered by the stop being hit. The observation of reaction is maintained by passing a beam of monochromatic light of the appropriate wavelength (usually 340nm) through the cell by fibre optic cable. The light is passed through a

photomultiplier and the change in voltage measured due to a change in absorbance of the solution is recorded. Software on the computers that run the stopped-flow machines are capable of transforming voltage/time data into absorbance/time data and can also calculate the observed rate constants.

Figure 6.1

Schematic diagram of a stopped-flow spectrophotometer



6.2 pH Measurements

All pH measurements were carried out using a Jenway 3020 digital pH meter which was accurate to ± 0.02 pH units. The pH meter was calibrated over the range pH 4.0 to 7.0 or pH 7.0 to 10.0 depending on the solution to be measured.

6.3 Nitric Oxide Electrode Calibration

A World Precision ISO-NO nitric oxide specific electrode was used to measure NO production in aqueous solution. Calibration was carried out with ascorbic acid (0.1 mol dm^{-3}) and sodium nitrite ($2.5 \times 10^{-3} \text{ mol dm}^{-3}$) stock solutions. As the diffusion of NO across the membrane is temperature dependent, all solutions were thermostatted at 25°C prior and during reaction. The electrode was zeroed in the ascorbic acid solution with only the tip (10mm) below the surface. In order to create an anaerobic environment, nitrogen was bubbled through the system which removed the majority of any oxygen present. Upon electrode stabilisation the solution was stirred vigorously and the appropriate nitrite solution injected. A calibration curve of current (nA) against concentration of NO generated (μM) was constructed, making the assumption that nitric oxide was produced quantitatively. Following this, the S-nitrosated species under scrutiny was analysed in a similar manner.

6.4 Reagents

All reagents used for synthetic and kinetic purposes were of the highest grade commercially available. Generally, S-nitrosothiols were produced *in situ* as described using acidified sodium nitrite and a variety of thiols which were purchased commercially, except for SNAP (section 2.2) which was synthesised as a stable green solid and stored in a refrigerator. The potassium dihydrogenphosphate (KH_2PO_4 , 0.15 mol dm^{-3}) and sodium chloride used to prepare pH 7.4 buffer solutions were purchased commercially and used as supplied. The perchloric acid solutions used for nitrosation were prepared by dilution of concentrated perchloric acid which had been standardised using standard sodium hydroxide solution and phenol red as an indicator.

6.5 Analysis

Analysis of human serum albumin and buffer solutions for trace quantities of cupric ions were carried out on a Perkin-Elmer 5000 atomic absorption spectrophotometer by Miss J. Magee. Elemental analysis was performed on samples using a Carlo Erba elemental analyser by Mrs J. Dostal.

Appendix

Research Colloquia, Seminars, Lectures and Conferences

The Board of Studies in Chemistry requires that each postgraduate research thesis contains an Appendix listing-

- A. All research colloquia, seminars and lectures arranged by the Department of Chemistry and by the Durham University Chemical Society during the period of the author's residence as a postgraduate student;
- B. All research conferences attended and papers presented by the author during the period when research for the thesis was carried out;
- C. Details of the postgraduate induction course.

**A. Colloquia, Lectures and Seminars from Invited Speakers Organised by the
Durham University Chemistry Department, 1994 - 1997**

(*denotes lectures attended)

- * 05.10.94 Prof. N.L. Owen, Brigham Young University, Utah, USA
Determining Molecular Structure - the INADEQUATE NMR way
- * 19.10.94 Prof. N. Bartlett, University of California, USA
Some Aspects of Ag(II) and Ag(III) Chemistry
- * 02.11.94 Dr. P.G. Edwards, University of Wales, Cardiff
The Manipulation of Electronic and Structural Diversity in
Metal Complexes - New Ligands
- 03.11.94 Prof. B.F.G. Johnson, Edinburgh University
Arene-metal clusters
- 09.11.94 Dr. G. Hogarth, University College, London
New Vistas in Metal-imido Chemistry
- * 10.11.94 Dr. M. Block, Zeneca Pharmaceuticals, Macclesfield
Large-scale Manufacture of ZD-1542, a Thromboxane
Antagonist Synthase Inhibitor
- * 16.11.94 Prof. M. Page, University of Huddersfield
Four-membered Rings and β -Lactamase
- * 23.11.94 Dr. J.M.J. Williams, University of Loughborough
New Approaches to Asymmetric Catalysis
- 07.12.94 Prof. D. Briggs, ICI and University of Durham
Surface Mass Spectrometry
- * 11.01.95 Prof. P. Parsons, University of Reading
Applications of Tandem Reactions in Organic Synthesis
- 18.01.95 Dr. G. Rumbles, Imperial College, London
Real or Imaginary Third Order Non-linear Optical Materials
- * 25.01.95 Dr. D.A. Roberts, Zeneca Pharmaceuticals
The Design and Synthesis of Inhibitors of the Renin-
angiotensin System
- 01.02.95 Dr. T. Cosgrove, University of Bristol
Polymers do it at Interfaces

- 08.02.95 Dr. D. O'Hare, University of Oxford
Synthesis and Solid-state Properties of Poly-, Oligo- and
Multidecker Metallocenes
- * 22.02.95 Prof. E. Schaumann, University of Claustal, Germany
Silicon- and Sulfur-mediated Ring-opening Reactions of
Epoxide
- * 01.03.95 Dr. M. Rosseinsky, University of Oxford
Fullerene Intercalation Chemistry
- 22.03.95 Dr. M. Taylor, University of Auckland, New Zealand
Structural Methods in Main-group Chemistry
- 26.04.95 Dr. M. Schroder, University of Edinburgh
Redox-active Macrocyclic Complexes - Rings, Stacks and
Liquid Crystals
- * 04.05.95 Prof. A.J. Kresge, University of Toronto, Canada
The Ingold Lecture - Reactive Intermediates - Carboxylic-acid
Enols and Other Unstable Species
- 11.10.95 Prof. P. Lugar, Frei University of Berlin, Germany
Low Temperature Crystallography
- 13.10.95 Prof. R. Schmiltzer, University of Braunschweig, Germany
Calixarene-Phosphorus Chemistry - A New Dimension in
Phosphorus Chemistry
- * 18.10.95 Prof. A. Alexakis, University Pierre et Marie Curie, Paris,
France
Synthetic and Analytical Uses of Chiral Diamines
- * 25.10.95 Dr. D.M. Davies, University of Northumbria
Chemical Reactions in Organised Systems
- * 01.11.95 Prof. W. Motherwell, University College London
New Reactions for Organic Synthesis
- 03.11.95 Dr. B. Langlois, University Claude Bernard-Lyon, France
Radical Anionic and Pseudo Cationic Trifluoromethylation
- * 08.11.95 Dr. D. Craig, Imperial College, London
New Strategies for the Assembly of Heterocyclic Systems
- * 15.11.95 Dr. A. Sella, University College London
Chemistry of Lanthanides with Polypyrazoylborate Ligands

- 17.11.95 Prof. D. Bergbreiter, Texas A&M University, USA
Design of Smart Catalysts, Substrates and Surfaces from Simple Polymers
- * 22.11.95 Prof. I. Soutar, University of Lancaster
A Water of Glass? Luminescence Studies of Water-soluble Polymers
- 29.11.95 Prof. D. Tuck, University of Windsor, Ontario, Canada
New Indium Coordination Chemistry
- 08.12.95 Prof. M.T. Reetz, Max Planck Institut, Mulheim, Germany
Perkin Group Regional Meeting
- * 10.01.96 Dr. B. Henderson, University of Waikato, New Zealand
Electrospray Mass Spectrometry - A New Sporting Technique
- 17.01.96 Prof. J.W. Emsley, University of Southampton
Liquid Crystals - More than Meets the Eye
- * 24.01.96 Dr. A. Armstrong, University of Nottingham
Alkene Oxidation and Natural Product Synthesis
- * 31.01.96 Dr. J. Penfold, Rutherford Appleton Laboratory, Didcot
Soft Soap and Surfaces
- * 07.02.96 Dr. R.B. Moody, University of Exeter
Nitrosations, Nitrations and Oxidations with Nitrous Acid
- 12.02.96 Dr. P. Pringle, University of Bristol
Catalytic Self-Replication of Phosphines on Platinum(0)
- * 14.02.96 Dr. J. Rohr, University of Gottingen, Germany
Goals and Aspects of Biosynthetic Studies on Low Molecular Weight Natural Products
- 21.02.96 Dr. C.R. Pulham, University of Edinburgh
Heavy Metal Hydrides - an Exploration of the Chemistry of Stannanes and Plumbanes
- * 28.02.96 Prof. E.W. Randall, Queen Mary & Westfield College, London
New Perspectives in NMR Imaging
- * 06.03.96 Dr. R. Whitby, University of Southampton
New Approaches to Chiral Catalysts - Induction of Planar and Metal Centred Asymmetry
- 07.03.96 Dr. D.S. Wright, University of Cambridge
Synthetic Applications of Me₂N-p-Block Metal Reagents

- * 12.03.96 Prof. V. Balzani, University of Bologna, Italy
RSC Endowed Lecture - Supramolecular Photochemistry
- 13.03.96 Prof. D. Garner, University of Manchester
Mushrooming in Chemistry
- * 30.04.96 Dr. L.D. Pettit, Chairman, IUPAC Commission of Equilibrium
Data pH-metric Studies using Very Small Quantities of
Uncertain Purity
- 09.10.96 Prof. G. Bowmaker, University of Auckland, New Zealand
Coordination and Materials Chemistry of the Group 11 and
Group 12 Metals - Some Recent Vibrational and Solid State
NMR Studies
- * 16.10.96 Prof. Ojima, State University of New York, USA
Silylformylation and Silylcarbocyclisations in Organic Synthesis
- * 22.10.96 Prof. L. Gade, University of Würzburg, Germany
Organic Transformations with Early-Late Heterobimetallics -
Synergism and Selectivity
- 22.10.96 Prof. B.J. Tighe, University of Aston
Synthetic Polymers for Biomedical Application - Can We Meet
Nature's Challenge?
- * 23.10.96 Prof. H. Ringsdorf, Johannes Gutenberg-Universität, Mainz,
Germany
Perkin Centenary Lecture - Function Based on Organisation
- * 29.10.96 Prof. D.M. Knight, Department of Philosophy, University of
Durham
The Purpose of Experiment - A Look at Davy and Faraday
- 30.10.96 Dr. P. Mountford, University of Nottingham
Recent Developments in Group IV Imido Chemistry
- 12.11.96 Prof. R.J. Young, UMIST
New Materials - Fact or Fantasy?
- * 13.11.96 Dr. G. Resnati, University of Milan, Italy
Perfluorinated Oxaziridines - Mild Yet Powerful Oxidising
Agents
- * 19.11.96 Prof. R.E. Grigg, University of Leeds
Assembly of Complex Molecules by Palladium-Catalysed
Queueing Processes
- 20.11.96 Prof. J. Earnshaw, Department of Physics, Belfast
Surface Light Scattering - Ripples and Relaxation

- 03.12.96 Prof. D. Phillips, Imperial College, London
A Little Light Relief
- * 04.12.96 Prof. K. Muller-Dethlefs, University of York
Chemical Applications of Very High Resolution ZEKE
Photoelectron Spectroscopy
- * 11.12.96 Dr. C. Richards, University of Wales, Cardiff
Stereochemical Games with Metallocenes
- 15.01.97 Dr. V.K. Aggarwal, University of Sheffield
Sulfur Mediated Asymmetric Synthesis
- 16.01.97 Dr. S. Brooker, University of Otago, New Zealand
Macrocycles - Exciting yet Controlled Thiolate Coordination
Chemistry
- 22.01.97 Dr. N. Cooley, BP Chemicals, Sunbury
Synthesis and Properties of Alternating Polyketones
- * 05.02.97 Dr. A. Haynes, University of Sheffield
Mechanism in Homogeneous Catalytic Carbonylation
- * 06.02.97 Prof. B. Bartlett, University of Southampton
Immobilisation of Enzymes in Electrochemically Polymerised
Films
- * 18.02.97 Prof. Sir J. Black, Sir James Black Institute
My Dialogues with Medicinal Chemists
- 19.02.97 Prof. B. Hayden, University of Southampton
Reaction Dynamics and Fuel Cells
- * 25.02.97 Prof. A.G. Sykes, University of Newcastle
The Structure, Properties and Design of Blue Copper Proteins
- 26.02.97 Dr. A. Ryan, UMIST
Making Hairpins from Rings and Chains
- * 04.03.97 Prof. C.W. Rees, Imperial College, London
Some Very Heterocyclic Chemistry
- 05.03.97 Dr. J. Staunton, FRS, University of Cambridge
Tinkering with Biosynthesis - Toward a New Generation of
Antibiotics
- 11.03.97 Dr. A.D. Taylor, Rutherford Appleton Laboratory, Didcot
Neutron Scattering

* 19.03.97 Dr. K. Reid, University of Nottingham
Probing Dynamical Processes with Photoelectrons

B. Conferences Attended

- 1) 5th European Symposium on Organic Reactivity, Santiago de Compostela, Spain, 16-21 July 1995.
Poster presented- "The Effect of Thiols on the Copper Catalysed Nitric Oxide Formation From S-Nitrosothiols".

- 2) Royal Society of Chemistry 6th International Meeting on Reaction Mechanisms, University of Kent at Canterbury, England, 9-12 July 1996.
Poster presented- "Copper Catalysed Nitric Oxide Formation From S-Nitrosothiols using Protein-Bound Cu^{2+} Sources".

- 3) Postgraduate Winter School on Organic Reactivity - WISOR VI, Bressanone, Italy, 10-17 January 1997.
Poster presented- "The Effect of Thiols on Copper Catalysed Nitric Oxide Formation From S-Nitrosothiols".

- 4) Royal Society of Chemistry Organic Reaction Mechanisms Group
Annual seminars attended-
 - i) Merck, Sharp and Dohme, Harlow, September 1995.
 - ii) Astra Charnwood, Loughborough, September 1996.
 - iii) Glaxo-Wellcome, Stevenage, September 1997.

C. First Year Induction Course, October 1994

The course consists of a series of one hour lectures on the services available in the department.

- 1) Introduction, research resources and practicalities
- 2) Safety matters
- 3) Electrical appliances and hands-on spectroscopic services
- 4) Departmental computing
- 5) Chromatography and high pressure operations
- 6) Elemental analysis
- 7) Mass spectrometry
- 8) Nuclear magnetic resonance spectroscopy
- 9) Glassblowing techniques

